Cascade Fault Detection and Diagnosis for the Aluminium Smelting Process using Multivariate Statistical Techniques

Nazatul Aini Abd Majid

A thesis submitted in partial fulfillment of the requirements for the degree of Doctor of Philosophy in Chemical and Materials Engineering,

The University of Auckland, 2011.

ABSTRACT

Real-time fault detection and diagnosis for the aluminium electrolysis process is difficult to perform because the process measurements are dynamic, multivariate and limited. This problem motivates the use of multivariate statistical techniques, particularly Principal Component Analysis (PCA) and Partial Least Square (PLS), in this research. The objective of this research is to design and develop a new PCA/PLS based system for aluminium smelting process that can detect and diagnose faults effectively. As a result of the development of the new system, the main research question is: Does a system based on PCA and PLS, effectively detect and diagnose faults in aluminium smelting process?

In order to address the above question, the research involved several steps. A taxonomy of aluminium process fault detection and diagnosis systems was first identified with four key elements: techniques, knowledge, usage frequency and mode of results. Pilot studies were then run to address selection of variables and dynamic behaviour. Finally, the new 'Cascade' fault detection and diagnosis system was developed in four stages: (1) detecting faults using Multiway-PCA (MPCA), (2) discovering abnormal patterns using MPCA, (3) diagnosing faults using MPCA and Multiway-PLS (MPLS), and (4) integrating the functions of detection and diagnosis to develop a new system. The evaluation of the new system using aluminium smelting data shows that this system is effective to detect and diagnose faults.

This research has contributed to the development of fault detection and diagnosis systems of the aluminium smelting process by investigating the application of multivariate statistical techniques. Firstly, a new design for a MPCA/MPLS based system, in which the alumina feeding cycle was treated as a batch operation, has created a new way in which to consider

the dynamics of the process during alumina feeding. Secondly, the occurrence of cascade-like patterns during anode changing has been solved by using multiple models. Thirdly, abnormal patterns based on alumina concentration versus resistance curves have been discovered. Finally, the developed fault detection and diagnosis taxonomy has enabled researchers to communicate the key elements of the system clearly. The application of this system is expected to assist operators to detect faults and diagnose anode faults, effectively.

I seek protection in Allah from the cursed shaytan

In the name of Allah, the most Beneficent, the most Merciful.

"Read in the name of your Lord who created! He has created man from a clinging clot. Read! For your Lord is the Most Gracious (One), who has taught by pen, has taught man what he has known not."

English meanings of The Qur'an [Surat al-Alaq: 1-5].

ACKNOWLEDGEMENTS

Alhamdulillah

All praise is due to Allah, the King of the worlds. There is no god but Allah. Allah is the greatest. There is no movement nor power except by Allah's will. This entire work could not have been done without His permission.

I express my deepest gratitude to my supervisor Prof. Brent Young for his careful supervision throughout the course of my PhD research work. His excellent guidance, encouragement, support and advice from the early phase of my PhD work to the final phase facilitated me not only to produce this thesis but also to produce a number of conference papers and journal articles. For this, I owe my sincere appreciation to him.

I am heartily thankful to my co-supervisors; Prof. Mark Taylor and Prof. John Chen for giving their support and expertise in the area of the aluminium smelting process and for enabling collaboration with the aluminium smelting industry. Furthermore, their many refinements to journal articles have been much appreciated.

I am extremely grateful to Marco Stam and Albert Mulder and to their company, Aldel for providing data and assisting by patiently answering my questions concerning data and operational activities.

I would like to thank the Ministry of Higher Education of Malaysia and the National University of Malaysia (UKM) for the financial support I have received through the Bumiputera Academic Training Scheme (SLAB).

I would like to express my special thanks to Dr Wei Yu for his many suggestions, Dr Pretesh Patel, Marcus Gustafsson, Pascal Lavoie, Yashuang Gao, Michel Gilbert and David Wong for their valuable explanations about the aluminium smelting process, and also to members of Industrial Information and Control Centre (I^2C^2), the Light Metal Research Centre (LMRC) and the Chemical and Materials Engineering department for their support.

I would like to thank; Dr Susan Carter and Dr Barry White from Student Learning Centre (SLC), Dr Penny Hacker and Siew Read from English Language Self Access Centre (ELSAC), Doctoral English as an Additional Language (EAL) Support Group, Malaysia-Auckland Postgraduate Student Association (MAPSA) writing group organised by Zaidah Mustaffa, for improving my academic writing. I would also like to thank Margaret Stiles for proofreading the whole thesis.

Finally, I would like to thank my dear husband Mohammed Reza for his patience, encouragement, love and prayers, my son Muhammad Ikram and my daughter Nur Nadhirah Nabihah, who was born during the course of this PhD work, for their sincere love, my parents, mak, ayah, mummy, brothers and sisters, for their support and love from a far distance, and my friends for their friendship for the sake of Allah.

Thank you very much.

Table of Contents

LIST OF FIGURES

LIST OF TABLES

THE UNIVERSITY OF AUCKLAND
SCHOOL OF GRADUATE STUDIES

Co-Authorship Form

Graduate Centre
ClockTower – East Wing
22 Princes Street, Auckland
Phone: +64 9 373 7599 ext 81321
Fax: +64 9 373 7610
Email: postgraduate@auckland.ac.nz
www.postgrad.auckland.ac.nz

This form is to accompany the submission of any PhD that contains co-authored work. **Please include one copy of this form for each part of this thesis that was co-authored.** Forms should be included in all copies of your thesis submitted for examination and library deposit (including digital submissions), following your thesis Abstract.

Please indicate the chapter/section/pages of this thesis that are extracted from a co-authored work and the title and publication details or details of submission of the co-authored work.
Section: 7.1, 7.2, 7.3.2, 7.4, 7.5.2 Details: Diagnosing faults in the aluminium smelting process by using multivariate statistical techiques, Journal of Materials Science (submitted)

Nature of contribution by PhD candidate	Main idea and main text
Extent of contribution by PhD candidate (%)	55%

CO-AUTHORS

Name	Nature of Contribution	Extent of Contribution (%)
Brent R. Young	Part of idea, advice, enrichment, editing	20%
Mark P. Taylor	Enrichment and editing	10%
John J.J. Chen	Enrichment and editing	10%
Wei Yu	Enrichment and editing	5%

Certification by Co-Authors

The undersigned hereby certify that:
- the above statement correctly reflects the nature and extent of the PhD candidate's contribution to this work, and the nature of the contribution of each of the co-authors; and
- the PhD candidate was the lead author of the work and wrote the text.

Name	Signature	Date
Brent R. Young	B. R. Young	14/4/11
Wei Yu	wei yu	14/4/11
Mark P. Taylor	MP	18/4/11
John J.J. Chen	John Chen	18/4/11

THE UNIVERSITY OF AUCKLAND
SCHOOL OF GRADUATE STUDIES

Co-Authorship Form

Graduate Centre
ClockTower – East Wing
22 Princes Street, Auckland
Phone: +64 9 373 7599 ext 81321
Fax: +64 9 373 7610
Email: postgraduate@auckland.ac.nz
www.postgrad.auckland.ac.nz

This form is to accompany the submission of any PhD that contains co-authored work. **Please include one copy of this form for each part of this thesis that was co-authored.** Forms should be included in all copies of your thesis submitted for examination and library deposit (including digital submissions), following your thesis Abstract.

Please indicate the chapter/section/pages of this thesis that are extracted from a co-authored work and the title and publication details or details of submission of the co-authored work.
Section: 6.1, 6.2, 6.3 Details: Multivariate statistical Monitoring of the Aluminium Smelting Process, computers and chemical engineering (2011), doi: 10.1016/j.compchemeng.2011.03.001

Nature of contribution by PhD candidate	Main Idea and Main text
Extent of contribution by PhD candidate (%)	60

CO-AUTHORS

Name	Nature of Contribution	Extent of Contribution (%)
Brent Young	Part of Idea, advice, enrichment, editing	20
Mark Taylor	Enrichment and editing	10
John Chen	Enrichment and editing	10

Certification by Co-Authors

The undersigned hereby certify that:

- the above statement correctly reflects the nature and extent of the PhD candidate's contribution to this work, and the nature of the contribution of each of the co-authors; and
- the PhD candidate was the lead author of the work and wrote the text.

Name	Signature	Date
Brent R. Young	B.R. Young	14/4/11
Mark Taylor		18/4/11
John chen	John Chen	18/4/11

THE UNIVERSITY OF AUCKLAND
SCHOOL OF GRADUATE STUDIES

Co-Authorship Form

Graduate Centre
ClockTower – East Wing
22 Princes Street, Auckland
Phone: +64 9 373 7599 ext 81321
Fax: +64 9 373 7610
Email: postgraduate@auckland.ac.nz
www.postgrad.auckland.ac.nz

This form is to accompany the submission of any PhD that contains co-authored work. **Please include one copy of this form for each part of this thesis that was co-authored.** Forms should be included in all copies of your thesis submitted for examination and library deposit (including digital submissions), following your thesis Abstract.

Please indicate the chapter/section/pages of this thesis that are extracted from a co-authored work and the title and publication details or details of submission of the co-authored work.
Section : 6.1 and 7 3.1. Details : Aluminium Process Fault Detection by Multiway Principal Component Analysis, Control Engineering Practice, 19, 367 - 379

Nature of contribution by PhD candidate	Main idea and main text
Extent of contribution by PhD candidate (%)	50%

CO-AUTHORS

Name	Nature of Contribution	Extent of Contribution (%)
Brent R. Young	Part of idea, advice, enrichment, editing	20 %
Mark P. Taylor	Enrichment and editing	10 %
John J.J. Chen	Enrichment and editing	10 %
Marco Stam	Giving operational information	5 %
Albert Mulder	Giving operational information	5 %

Certification by Co-Authors

The undersigned hereby certify that:

- the above statement correctly reflects the nature and extent of the PhD candidate's contribution to this work, and the nature of the contribution of each of the co-authors; and
- the PhD candidate was the lead author of the work and wrote the text.

Name	Signature	Date
B.R. Young	B.R. Young	14/4/11
Mark Taylor		18/4/11
John Chen		18/4/11
Marco Stam		27/4/11
Albert Mulder		21/4/11

CHAPTER 1: INTRODUCTION

The application of multivariate statistical techniques in detecting and diagnosing faults within the aluminium smelting process has been investigated in this thesis. This chapter begins by briefly describing the three key areas in the investigation: the aluminium smelting process, fault detection and diagnosis, and the multivariate statistical techniques to be employed in the fault detection and diagnosis system. The aim, objective and motivation are then given, followed by the description of the problem and research questions. Finally, the research methodology and the organization of the thesis are presented.

1.1. Research background

A new multivariate system for detecting and diagnosing faults for the aluminium smelting process is urgently needed because most smelters are currently operated beyond design capacity. Detecting and diagnosing faults concurrent with, or prior to, their occurrence in a process can prevent undesirable outcomes and allow aluminium smelter plants to operate at full capacity. For example, in an aluminium smelter, the early detection of anode spikes or anode effects in operating cells can help to maintain the electrolysis process at its optimal productivity and energy efficiency (e.g. Stam et al., 2008). However, developing a real-time fault detection system has proven difficult since the process within the cells in an aluminium smelter is complex, non-linear and multivariate (e.g. Stam et al., 2008).

In an aluminium smelter, there are hundreds of aluminium reduction cells engaged in a complex electrolysis process. Figure 1.1 shows the steps in the Hall-Héroult process that are generally used for extracting aluminium metal from its oxide. Since the process is complex, it is difficult to detect and diagnose problems that occur. Furthermore, the behaviour of the electrolysis process within a cell is dynamic as it is disturbed by the important routine tasks

of alumina feeding and anode changing. Incorporating this dynamic behaviour into a fault detection and diagnosis system is crucial to revealing the signature of faults and enabling accurate and early fault detection and diagnosis.

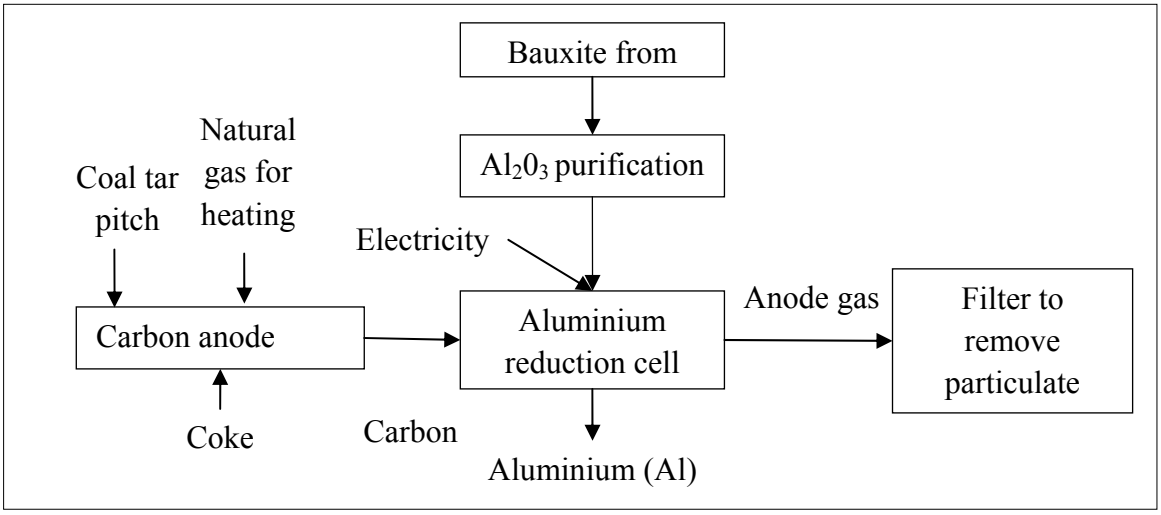

Figure 1.1: Steps in the Hall-Heroult Process for Aluminium Extraction (Pletcher and Walsh, 1990)

The challenges to developing a fault detection and diagnosis system for industrial applications are not inconsiderable, particularly in the processing of complex materials including the aluminium electrolysis process. The complexity of process dynamics, lack of adequate models and incomplete data are a few examples of the challenges to developing an effective fault detection (when a fault has occurred) and diagnostic (which fault has occurred) system (Dasha and Venkatasubramanian, 2000). The main purpose of using this system is to detect and diagnose faults that are unable to be handled adequately by a closed loop control system such as a feedback control system. Figure 1.2 shows the relationship between a feedback control system, and a fault detection and diagnosis system. In the feedback control system, the feedback controller adjusts the process control input, u, based on error values (the difference between a measured process variable, y, and a setpoint, r). This is the main function of Engineering Process Control (EPC), known as error compensation.

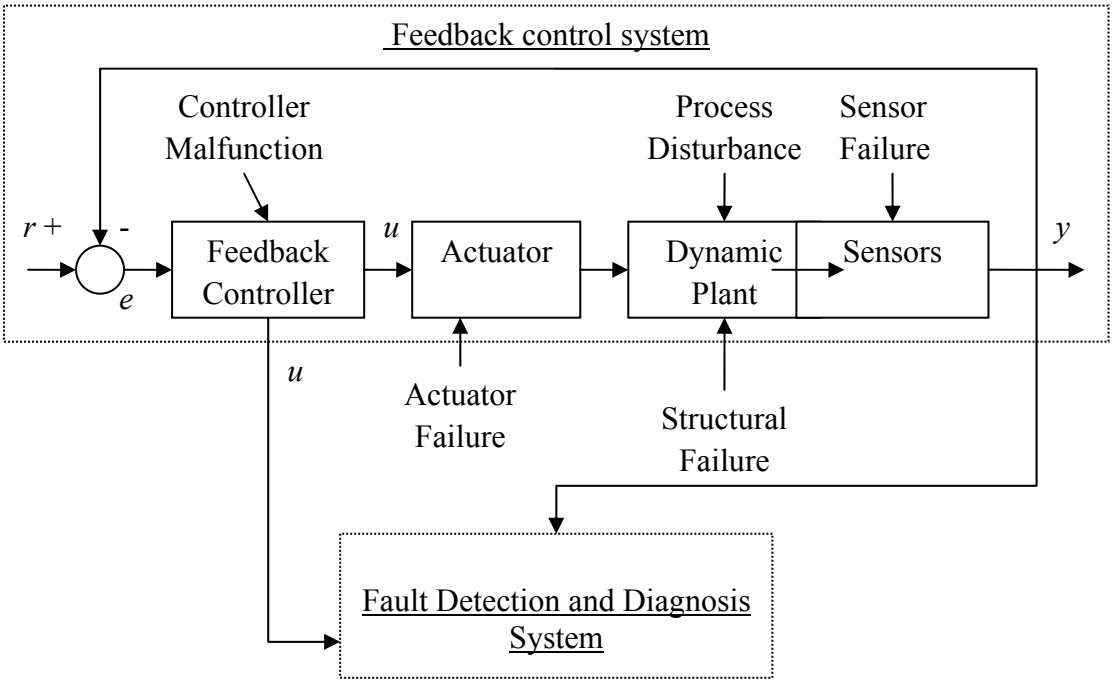

Figure 1.2: A General Control System based on Feedback with Fault Detection and Diagnosis System (redrawn from Venkatasubramanian et al., 2003c)

The objective of error compensation is to minimize the future error values in order to achieve process performance specification (Miletic et al., 2004). For example, in the error compensation for the bath height of an aluminium reduction cell, the height of the bath is controlled so as to be between 18 and 22 cm. When the bath height is very low, this error is compensated for by adding more electrolytes to the cell. However, by only using EPC, the cause of the error is still there and unexpected changes may occur without being noticed. Therefore, the fault detection and diagnosis system is used to detect and diagnose these unexpected changes in the process by utilizing some parameters from the feedback control system or other measured parameters of the aluminium smelting process.

Multivariate statistical techniques such as Principal component analysis (PCA) and Partial Least Square (PLS) are viable options for a fault detection and diagnosis system that is

suitable for complex processes with a large number of highly correlated process variables (e.g. MacGregor and Kourti, 1995). PCA/PLS is a data-based multivariate statistical method that can be used to model the normal behaviour of a process using historical data. When new data becomes available, a model developed on normal data is used as a reference set to detect faults in the new data. In fact, this is the basis of statistical process control (SPC) where the main task of SPC is monitoring a process, and when there is an alarm, corrective action is be taken by removing the cause of the alarm or fault. The main reason for using PCA/PLS in real-time detection is its capability as a data reduction method. High-dimensional data are projected onto a low-dimensional model so that it is much easier to analyse, visualize and make comparisons between the historical data and the new data from a large multivariable process.

Because it can be developed almost entirely from process data (Chiang et al., 2001), the PCA/PLS, or latent variable model, is not only very effective for fault detection and diagnosis in practice, but can also be a solution for singularity problems in the calculation of multivariate control charts, such as the Hotelling's T^2 chart, when the number of process variables is very high (Kourti, 2002, Kourti, 2005). As a result, multivariate control charts based on latent variables have been suggested for many industrial batch and continuous processes (Kourti et al., 1996). In the aluminium smelting industry, for example, PCA is used to analyse the performance of a line of operating aluminium reduction cells and to detect faults within the cells (Tessier et al., 2009), but the dynamic behaviour of the cell needs to be considered to render the monitoring system effective.

A breakthrough in the detection and diagnosis of batch processes introduced by Nomikos and MacGregor (1994) revealed an interesting approach that considers the dynamic component of

the process. In this approach, MPCA and MPLS are used to monitor the progress of batch processes by observing the variability patterns from target trajectories. In the 2000s, this approach also was utilized in monitoring variability patterns in continuous processes that included: (1) 30 sec time unit block of data for fire detection (JiJi et al., 2003), (2) the 'caster start-up' operation for steel casting processes (Zhang and Dudzic, 2006), and (3) the average daily diurnal pattern for a waste water treatment plant (Aguando and Rosen, 2008). Since the aluminium electrolysis process is a semi-continuous process, this thesis has, therefore, been designed to investigate the potential of using MPCA and MPLS for fault detection and diagnosis of the aluminium smelting process by monitoring the variability pattern from target trajectories within an alumina feeding cycle.

1.2. Research aim, objective and motivation

This research aims to demonstrate and prove the use of multivariate statistical techniques is effective in detecting and diagnosing faults in the aluminium electrolysis process. The objective of this research is therefore to design and develop a PCA/PLS based system that can be used to detect and diagnose faults effectively in the aluminium smelting process. The motivation of this work is based on the following: the use of PCA/PLS for multivariate process monitoring has recently become more widespread and practical as can be seen in the works, for examples, of the following researchers: Wise and Gallagher, 1996, Lennox et al., 1999, Wold et al., 2001, Kourti, 2002, Miletic et al., 2004, MacGregor et al., 2005, Kourti, 2005, Uraikul et al., 2007. These works have shown the potential of a PCA/PLS based system to monitor complex industrial processes. This motivates this research to develop a new fault detection and diagnosis framework based on PCA/PLS to overcome problems arising from the complexity of the aluminium smelting process.

1.3. Problem description and research questions

The complexity of the aluminium electrolysis process presents great challenges for the monitoring of this extensive energy industry. The key problem with process monitoring according to Bearne (1999), is that the aluminium electrolysis process generates a substantial quantity of data due to the large number of aluminium reduction cells. The characteristics of the data are that they are correlated, non-linear and noisy. There are also inadequacies in on-line process measurements. This situation, together with the lack of causal models, has led to difficulty for detecting operating abnormalities in a practical manner. The result of the situation is an increase in energy consumption and greenhouse gas production. The problems in detecting operating abnormalities have motivated this research to use multivariate statistical techniques to develop a new fault detection and diagnosis system. This emphasizes the origin of the main research question: Does a system based on multivariate statistical techniques, PCA and PLS, effectively detect and diagnose faults in the aluminium smelting process?

The problem of using the multivariate statistical techniques is that it is a challenge to developing a suitable fault detection system that considers the dynamic behaviour of the process during anode changing and alumina feeding. Once the problem of developing a fault detection system has been addressed, the next task is to develop an appropriate fault diagnostic tool that is compatible and easy to integrate into the fault detection tool. Thus, the main research question has been further divided into two questions:

1) Can a fault detection system that considers the dynamic behaviour of the aluminium smelting process be developed?
2) Can a fault diagnosis system which complements the fault detection system be developed?

A number of existing approaches addressed the two questions including analytical approach (Hestetun et al., 2006), expert system (Abaffy et al., 2006), neural networks (Shuiping et al., 2007) and multivariate statistical techniques (Tessier et al., 2009). However, these approaches were not capable of capturing the dynamic trends in process variables during both alumina feeding and anode changing.

1.4. Research methodology

In order to address the above research questions, the methodology of this research is described below:

1) The first step prior to designing a new system was to collect data from industry. These data were processed and analysed in order to identify whether faults could be observed from the data.
2) The second step was to review literature in three areas (aluminium smelting process, fault detection and diagnosis, multivariate statistical techniques). Knowledge from the literature was integrated based on a proposed taxonomy. Knowledge from operational experts was also integrated based on the results from one-to-one interviews, video conferencing and email communications.
3) The third step was to develop pilot studies for investigating two factors: the selection of variables, and the development of a reference set able to consider dynamic behaviour in process monitoring.
4) The fourth step was to design a new framework based on the results from the first three steps above. The new framework was divided into two parts; fault detection, and fault diagnosis.
5) The fifth step was to develop the fault detection part using MATLAB and to evaluate this part using aluminium smelting data. The first research question was addressed in this

step. Some technical issues addressed in the development of the fault detection system are:

a. Developing a multivariate system using on-line data.
b. Developing reference models that consider the dynamic behaviour of the aluminium smelting process during alumina feeding and anode changing.
c. Developing a strategy for monitoring numerous cells. Each cell has different specifications which are continually changing depending on factors such as age and temperature.

6) The sixth step was to discover knowledge related to abnormal events using a data mining tool. This part used out-of-control signals provided by the fault detection system.
7) The seventh step was to develop the fault diagnosis part using MATLAB and to evaluate this part using aluminium smelting data. The second research question was addressed in this step. Some technical issues addressed in the development of the fault diagnosis system are similar to the issues addressed in step 5.
8) The eighth step was to integrate the fault detection and diagnosis functions using MATLAB and to simulate the functions of the new system using aluminium smelting data.

The development of this new system is expected to address the main research question where the system can be used for the parallel monitoring of numerous cells and to detect and diagnose anode faults in a timely manner, thus reflecting the effectiveness of the fault detection and diagnosis system based on MPCA and MPLS.

1.5. Organization of the thesis

Chapter 1 (Introduction) shows the direction of the research from briefly describing problems in monitoring the aluminium smelting process to looking into the potential of using multivariate statistical techniques to solve these problems.

Chapter 2 (The Aluminium Smelting Process) explores the problems in monitoring the aluminium smelting process so that the system will be designed according to these problems. The variability patterns within an alumina feeding cycle are then illustrated in order to show that these patterns can be beneficial to improving fault detection and diagnosis.

Chapter 3 (Fault Detection and Diagnosis system) describes the key elements for designing a new fault detection and diagnosis system for the aluminium smelting process. These include: knowledge (variability patterns within an alumina feeding cycle), techniques (PCA and PLS), usage frequency (continuous) and mode of results (graphic and text).

Chapter 4 (Multivariate Statistical Techniques) describes the multivariate control charts based on MPCA which is the main tools to develop the fault detection system in this thesis. The general procedures for discovering abnormal patterns using PCA and for diagnosing faults using Discriminant PLS (DPLS) and MPCA, are also presented.

Chapter 5 (A New Fault Detection and Diagnosis Framework for the Aluminium Smelting Process) explains the new design of the system; it incorporates the information from these sources: analysis of real data, knowledge from literature, experts, and pilot studies. The design has been divided into three parts: (1) fault detection for identifying when a fault has

occurred, (2) knowledge discovery from databases for discovering abnormal patterns, and (3) fault diagnosis for identifying which fault has occurred using the discovered patterns.

Chapters 6 to 8 deal with the research methods. Chapter 6 (Cascade Fault Detection) describes in detail the first two parts of the design, the Cascade fault detection system and knowledge discovery from databases. This chapter covers methods, results and discussion. It will be shown that the system can detect anode faults, and abnormal patterns can be extracted by using MPCA. Chapter 7 (Cascade Fault Diagnosis) explains in detail the third part of the proposed system, the Cascade fault diagnosis system. It covers methods, results and discussion. It will be shown that the system can diagnose anode faults using MPCA and MPLS. Chapter 8 (System Integration) concentrates on the integration of the functions of detection and diagnosis in order to develop a single system.

Chapter 9 (Conclusions) gives a brief summary of the thesis, the highlights in the literature consulted and the methodology employed, the research contributions and benefits, and recommendations for possible future areas of research.

CHAPTER 2: THE ALUMINIUM SMELTING PROCESS

A production process is a process for the transformation of inputs (e.g. raw material) into outputs (e.g. finished product). For example, in the aluminium smelting process, alumina (raw material) is one of the main inputs for the production of aluminium metal (finished product). However, the process of extracting aluminium metal from its oxide, alumina, is complex. In the first section of this chapter, the aluminium electrolysis process and its faults are briefly described. The next section concentrates on the problems that lead to inefficient process monitoring. A breakthrough area for solving these problems is discussed in the final section.

2.1. Process description

One of the most important processes in the aluminium industry is the aluminium smelting process, where alumina is reduced to aluminium metal within an aluminium reduction cell. There are hundreds of aluminium reduction cells engaged in the complex electrolysis process in an aluminium smelter. For example, the Aldel Aluminium Smelter in the Netherlands (Figure 2.1) has hundreds of aluminium reduction cells (Figure 2.2).

Figure 2.1: Aldel Aluminium Smelter in the Netherlands (permission granted)

Figure 2.2: Inside the Smelter (permission granted)

Figure 2.3 shows a schematic diagram of an aluminium reduction cell in which alumina is fed into the molten cryolite-based electrolyte from point feeders and then dissolved in the electrolyte to allow for the aluminium electrolysis process to occur (Taylor, 1997). Alumina is reduced to form aluminium metal via the primary chemical reaction:

$$2Al_2O_3(diss) + 3C(s) \rightarrow 4Al(l) + 3CO_2(g) \qquad 2\text{-}1$$

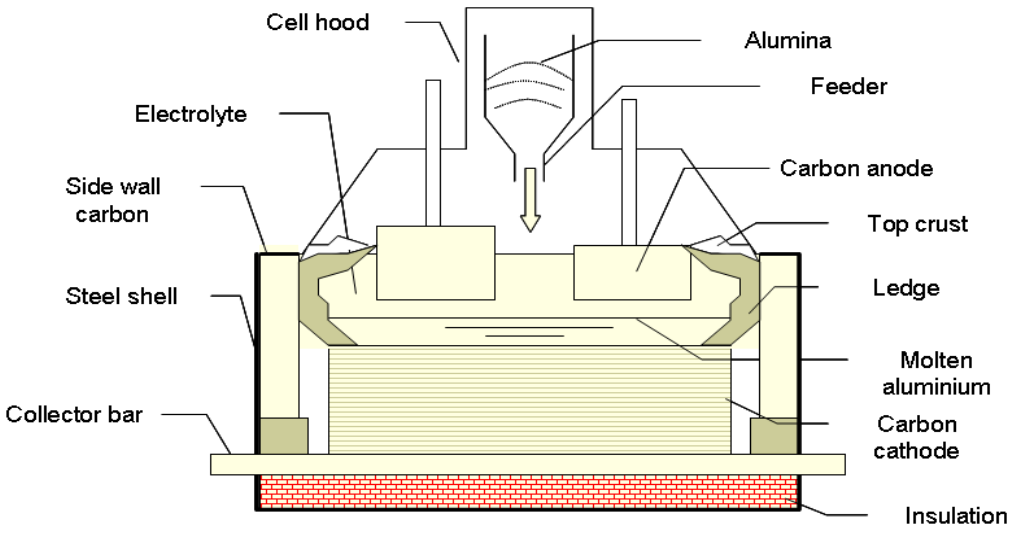

Figure 2.3: Cross Sectional Schematic Diagram of an Aluminium Reduction Cell (redrawn from Gadd, 2003)

The alumina is continuously fed into the cell to produce the molten aluminium that accumulates on the carbon cathode to form part of the cathode, and this aluminium is then tapped from the cell about once per day (e.g. Gadd, 2003). The amount of molten aluminium produced per day depends on the amperage, the control of the process, and the detection and diagnosis of faults.

2.2. Description of anode faults

An anode fault is one of the most common failures in the aluminium smelting industry. Anode spikes and anode effects are the two major examples of anode faults.

2.2.1. Anode spikes

The reason for the formation of anode spikes is still not fully understood but it is generally accepted that spikes are likely to form because of inferior anode quality or an unsatisfactory operating procedure (J. Chen, personal communication, November 14, 2009). Anode spikes cause short-circuiting between the anode and the metal because a protrusion extends from the anode, as shown in Figure 2.4. Anode spikes can cause the following to happen: (1) the current that provides energy to the cell goes directly to the molten aluminium; (2) the total resistance of the cell reduces due to short circuiting at one anode location; and therefore (3), less energy is made available to make aluminium metal as the remainder of the energy is lost as heat (e.g. A. Mulder, personal communication, December 8, 2008). Not only do these anode spikes decrease the production rate, but also, the subsequent overheating of the cell causes instability in the process. Therefore, a capability in the early detection of anode spikes is crucial in order to increase current efficiency and cell lifetime.

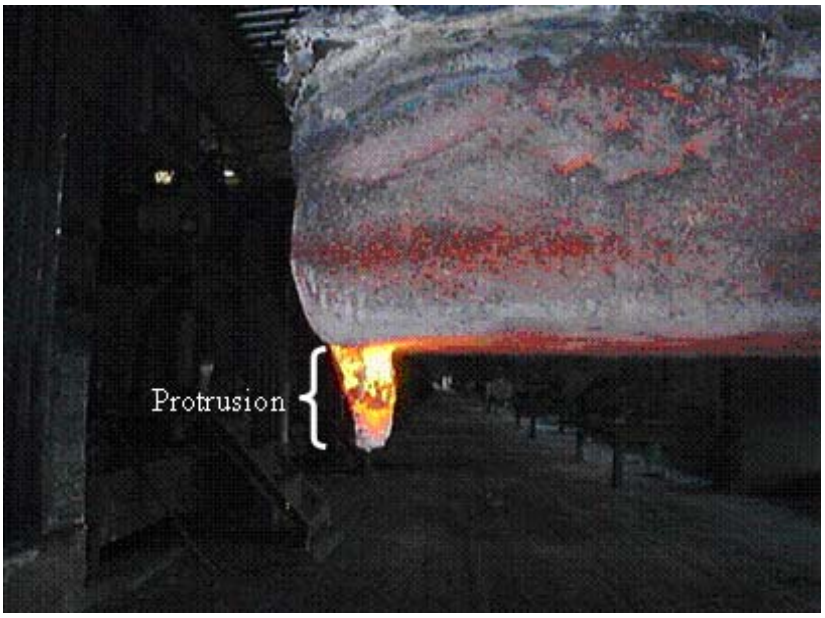

Figure 2.4: Protrusion Extended from the Working Surface of the Anode Causes Anode Spike (permission granted)

In order to detect anode spikes, the three approaches that have been proposed and applied include: (1) soft sensing based on an increase of cell temperature by more than 15°C and a decrease in alumina feeding by more than ten percent (Stam et al., 2008); (2) measuring each anode every 24 hours (M. Stam, personal communication, December 10, 2008); and (3) the fuzzy recognition methodology proposed by Shuiping and Jinhong (2006). Although the first two approaches have been applied in industry, these methods may only be able to detect anode spikes after the spiking problems have been happening for a period of time. The third approach is an integration of fuzzy mathematics and knowledge from experts but how soon in the process the faults were detected was not reported in the article. Therefore, there exists a strong need to be able to detect the occurrence of anode spikes in real-time by using existing measurements to prevent a worst case scenario for example, overheating that causes cell damage.

2.2.2. Anode effects

Anode effects happen when there is depletion of the alumina concentration within the cell. These anode effects cause a sudden increase in the cell voltage to 20-50 V, compared with its normal target value of 4.0-4.5 V. A number of approaches have been proposed for eliminating the occurrence of anode effects including: (1) fuzzy recognition (Shuiping and Jinhong, 2006); (2) feedforward neural networks (Meghlaoui et al., 1998); and (3) a fuzzy neural algorithm (Shuiping et al., 2007). The first approach needs an additional measurement such as the anode-cathode voltage which cannot be measured routinely in the typical aluminium electrolysis process. The applicability of the second and the third approaches is also limited since the neural-networks require comprehensive data. All of these methods were developed based on the established relationship between pseudo-resistance and concentration of alumina. This shows that all the approaches mentioned analysed the same dynamic pattern in the alumina feeding cycle but used differing methods for recognizing this pattern. However, none of them are particularly viable for the reasons outlined above.

2.3. Process control and problems in process monitoring

The effective use of process control does achieve benefits. Readers were reminded of this by Brisk (2005) in the article in which he also listed the benefits of the effective process control to include: safer operation, waste reduction, raw material and energy efficiency improvements, better conservation of non-renewable resources and improved economic conditions. However, effective control of an aluminium reduction cell is difficult to achieve because one of the problems arising is that there is a very low level of automation in control (Bearne, 1999). Table 2-1 shows the usual control mode for controlled and manipulated variables typically used in reduction processes where automatic control modes are not present in all the variables.

Table 2-1: Controlled and Manipulated Variables typically used for Reduction Cells (Stevens McFadden et al., 2001)

No	Controlled variable	Manipulated variable	Usual control mode
1	Bath temperature	Adjust resistance set point and/add AlF_3 or Soda	Auto Auto or Manual
2	Bath chemistry (AlF_3)	Add AlF_3 or Soda	Auto or Manual
3	Cell resistance	Beam position	Auto
4	Cell resistance rise and/or slope	Alumina feed rate	Auto
5	Bath depth	Addition/removal of bath	Manual
6	Cell resistance noise	Adjust resistance set point or action problem anodes	Auto Manual
7	Metal depth	Metal tap weight	Manual

The challenge is to develop a monitoring system that uses variables which are automatically measured and which also has an automatic control mode. These variables including cell resistance, cell resistance noise and cell resistance rise and/or slope. Thus, this thesis investigates the opportunity to improve the monitoring of the process by using these variables. Other problems that may contribute to inefficient process monitoring are: (1) highly correlated data, (2) large volume of data, (3) parameters at different frequency, and (4) dynamic behaviour. These problems are discussed below.

2.3.1. Highly correlated data

The variables indicated in Table 2-1 are highly correlated. Figure 2.5 shows the relationships between these variables. Firstly, we look at the heat balance parameters which include bath temperature, liquidus temperature and superheat. Bath temperature, the operating temperature of the cell, is the first variable in Table 2-1. The bath temperature increases when the energy input to the cell increases. Basically, the bath temperature is higher than the liquidus temperature (the temperature at which the electrolyte becomes molten). The difference between bath temperature and liquidus temperature is known as superheat (e.g. Taylor and

Chen, 2006). Superheat increases when the bath temperature increases. This can cause the protective layer of frozen electrolyte on the cell walls (ledge) to melt back into the bath and consequently change the bath chemistry (e.g. Taylor and Chen, 2006 and Stam et al., 2008).

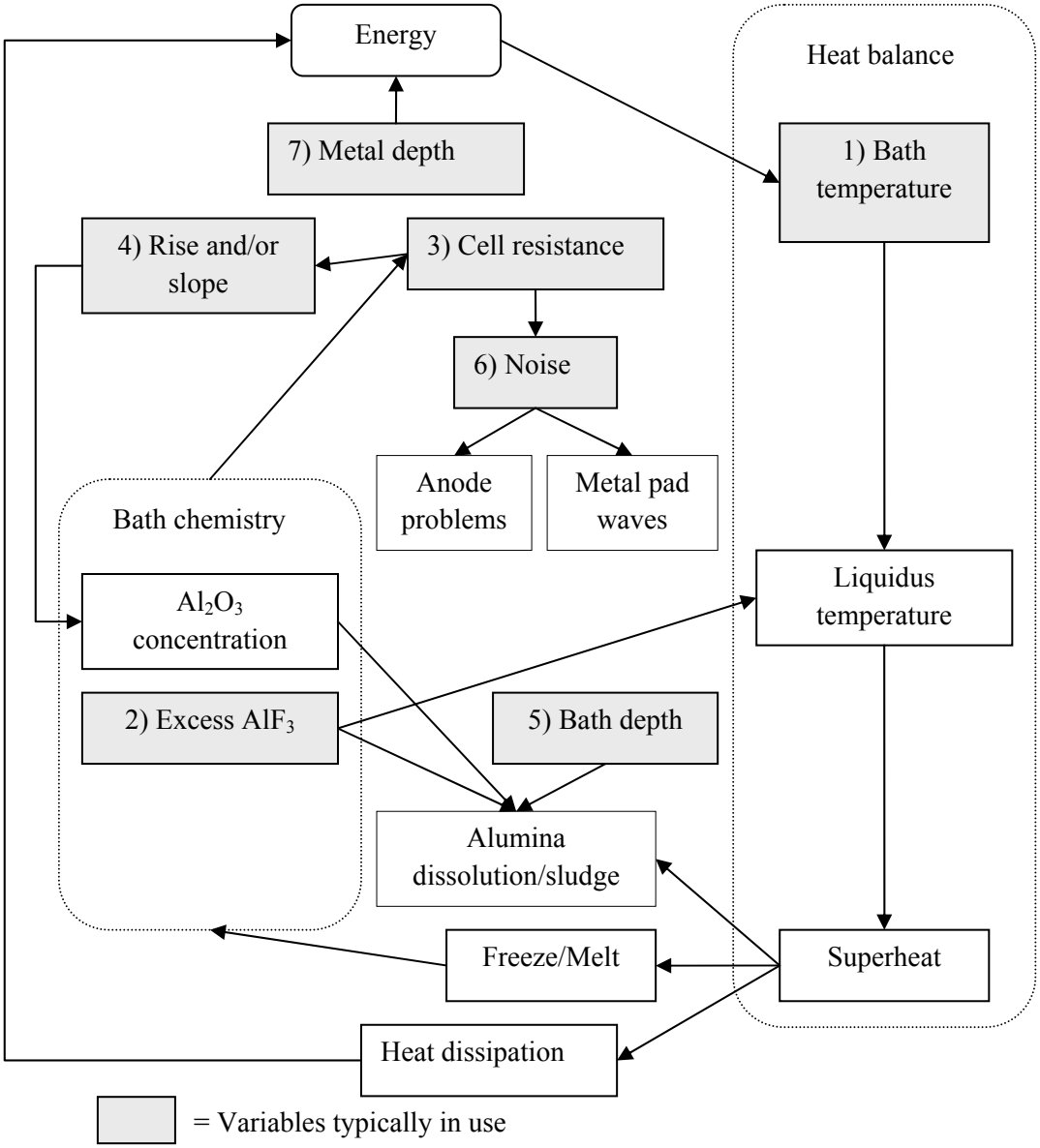

Figure 2.5: Interaction between Variables in an Aluminium Electrolysis Process (adapted from Taylor, 1997 and Stam et al., 2008)

Secondly, we look at the key bath chemistry parameters. These parameters are the constituents of the bath which are measured as; alumina concentration, excess aluminium fluoride (AlF_3), and other additives. Excess AlF_3 is the second variable in Table 2-1. A high

level of excess AlF_3 (more than 17 percent) will not only decrease the liquidus temperature but also the bath density, alumina solubility and electrical conductivity (e.g. Taylor and Chen, 2006). The changes in bath chemistry also affect cell resistance, which is the third variable in Table 2-1. The resistance can be further used to infer the changes of alumina concentration by calculating the rise and/or slope of the resistance which is the fourth variable in Table 2-1. One of the risks of a high level of alumina concentration is sludge formation. Sludge is a mixture of undissolved alumina and bath saturated with dissolved alumina (e.g. Stevens McFadden, 2005). In instances where the alumina dissolution rate is low, the alumina remains undissolved. There are many factors that cause this situation including low superheat, a high excess AlF_3 and low bath height (the fifth variable in Table 2-1). Other problems in the aluminium reduction process such as metal pad waves or anode problems can be gauged with the use of cell resistance noise (the sixth variable in Table 2-1).

Finally, we look at the changes of metal depth, the seventh variable in Table 2-1. The changes of this variable can affect the energy balance of the cell. For example, a high metal depth can cause more loss of heat (Taylor and Chen, 2006). There are other factors that also affect the energy balance such as anode changing, bath height, anode cover, superheat and metal tapping (Stam et al., 2008, and Taylor and Chen, 2006). Overall, the reaction in the cell is like that of a cycle, any changes in process variables will affect other process variables and will cause energy imbalance in the cell (Tandon, 2007). Therefore, there is a clear relationship between the variables typically used for aluminium reduction cells. Consideration of this relationship between variables in monitoring the process could prevent control errors such as false, or failed, alarms. False alarms or Type I errors mean that although the alarms are detected statistically, in reality, they do not exist. On the other hand, failed alarms or Type II errors are alarms that are not detected by statistical methods but in

reality, they do exist. By reducing these control errors, effective process monitoring can be carried out.

2.3.2. Large volume of data

In a typical aluminium smelter, there are around 200 cells which are connected in electrical series down a potline (Figure 2.6) and there are smelters with up to six potlines (Stevens McFadden, 2005). There are many process variables to be monitored throughout the smelter because of this large number of cells. This contributes to a large volume of data being monitored and stored every day in an aluminium smelter. In Aldel's Aluminium Smelter, for example, there are approximately 43 variables where each observation has an average duration of five minutes. Thus, around 12, 384 data were stored every day for each cell for these variables and, in order to save database storage space, these data were removed from the database every two weeks. Further study of these historical data such as the movement of the process from normal to abnormal events, may assist in the design of an improved fault detection system for aluminium reduction cells.

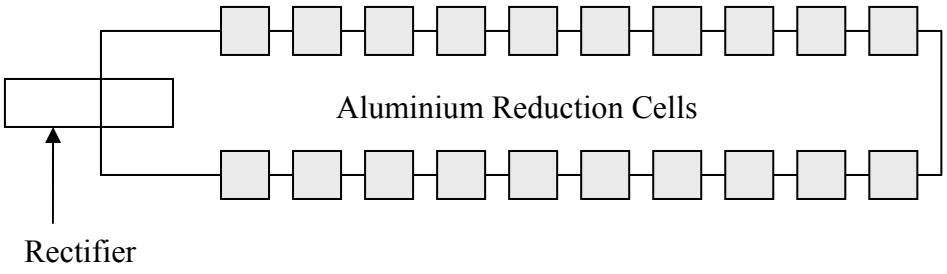

Figure 2.6: A Potline comprises a number of Cells which are Connected in Electrical Series (redrawn from Chen, 2008)

2.3.3. Parameters at different frequencies

Table 2-2 shows types of control measurements with different frequencies. Cell voltage and line current are measured continuously whereas bath temperatures are measured daily to weekly. Each measurement may contain a different fault signature. For example, temperature is a very good indicator of a spiking problem but the frequency of this measurement may

prevent the spiking problem from being detected sooner. Therefore, it is a challenge to utilize other measurements that have been recorded continuously but may lack fault signatures.

Table 2-2: Types and Typical Frequencies of Control Measurements (Bearne, 1999)

Measurement	Frequency
Widespread Use	
Cell Voltage	Continuous (automatic)
Line Current	Continuous (automatic)
Observation (Flame, Crust, Etc.)	Several times/day to daily
Bath Depth	Daily to once in two days
Metal Depth	Daily to once in two days
Tapped Metal Weight	Daily to once in two days
Bath Temperature	Daily to weekly
Bath Chemistry (AlF_3, LiF, CaF_2, $MagF_2$)	Twice per week to two weekly
Metal Purity (Fe, Si)	Daily to weekly
Cathode Voltage Drop	Weekly to annually
Alumina-Feed Dump Weight	Weekly to occasionally
Anode-Beam Position	Continuous (automatic) on some technologies
Individual Anode Currents (by Rod Voltage Drop)	Daily to weekly or on exception Continuously on one technology
Limited Use	
Crust Breaker Position	Continuous on point feeders
Aluminium-Fluoride Feed Dump Weight	On exception
Sludge/Ridge Depth	Daily (with metal height)
Sidewall Ledge Position	Twice/week
Direct Alumina Concentration	Daily
Superheat	Daily
Sidewall Temperature	Continuously
Cathode (Collector Bar) Temperature	Continuously
Sidewall Heat Flux	Continuously

2.3.4. Dynamic behaviour

The dynamic behaviour of the cell considered in this research is divided into two parts: (1) behaviour during alumina feeding and (2) behaviour during anode changing.

2.3.4.1. Behaviour during alumina feeding

In order to consider dynamic behaviour of alumina feeding, an abnormal pattern was observed based on the pattern of data within an alumina feeding cycle of a point feeder system. Alumina is fed from point feeders into a small zone within the molten cryolite-based electrolyte (Grjotheim and Welch, 1988) and then dissolved in the electrolyte for the aluminium electrolysis process to occur (Stam et al., 2008). In an electrolytic cell, alumina needs to be fed at a rate commensurate with the dissolution and reaction rate; otherwise, undesirable green-house gas may be generated and/or an unstable operation will result (Tabereaux, 2008). In modern alumina feed strategies, the amount of alumina being fed into cells is controlled based on the relationship between cell voltage in pseudo-resistance form and alumina concentration (Bearne, 1999).

The theoretical curves of this relationship at constant anode-cathode distance (ACD) are shown in Figure 2.7 where the slopes of the curves for the high ACD are different from those of the low ACD. Pseudo-resistance is a function of alumina concentration when the ACD is kept constant. Therefore, a relevant feed strategy is used to monitor the changes of the resistance in order to control the alumina concentration around an operational target (above 1% and below 3%) for avoiding anode effects or sludge formation (Heime and Esser, 2001). This feed strategy is referred to as short time interval feeding (Agalgaonkar et al., 2009) and also known as an overfeed/underfeed strategy (Bearne, 1999).

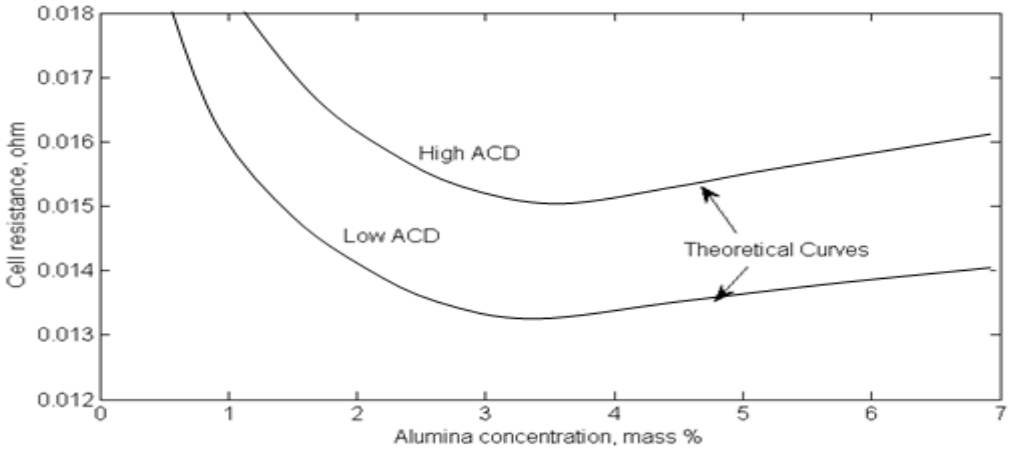

Figure 2.7: Theoretical Cell Resistance Curves versus Alumina Concentration at a Constant Anode Cathode Distance (ACD) (redrawn from Kvande, 1993)

In the overfeed/underfeed strategy, the cell is first fed at a rate higher than the rate corresponding to normal consumption of the cell (overfeed) and then, based on the changes in the pseudo-resistance slope, the feed rate is changed to underfeed (a rate lower than normal consumption). In this study, the rate corresponding to the normal consumption of the cell is given as 100%; the rates for overfeeding are 200% and 140%; and the rate for underfeeding is 70%. By using this overfeed/underfeed strategy, the pattern of resistance for the process can be predicted to have no operating abnormality. As shown in Figure 2.8, with a slope of *S1* during overfeeding, the resistance decreases from R_U to R_L. On the other hand, with a slope of *S2* during underfeeding, the resistance increases from R_L to R_U. The trajectory during overfeeding combined with the trajectory during underfeeding forms a single trajectory for an alumina feeding cycle or an overfeed/underfeed cycle. The variation of cell resistance and other variables with respect to time are monitored based on this overfeed/underfeed cycle.

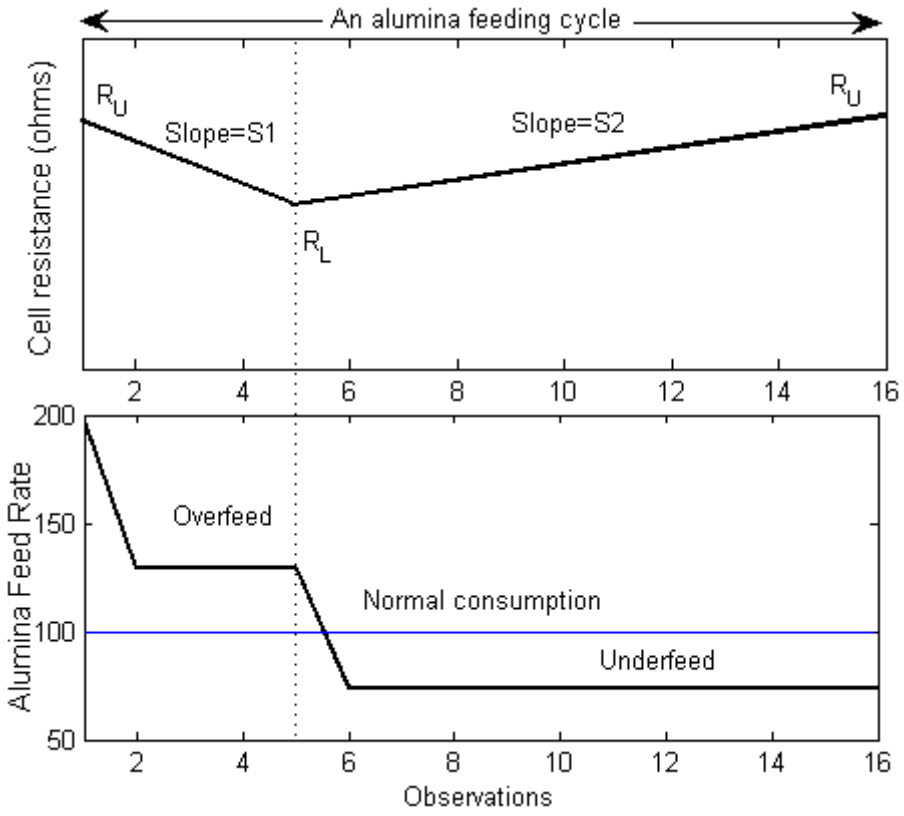

Figure 2.8: The Variation of the Cell Resistance Corresponding to the Feed Rate Changes within an Alumina Feeding Cycle (adapted from Algalgaonkar et al., 2000 and Homsi et al., 2000)

2.3.4.2. Behaviour during anode changing

While continuously observing the dynamic pattern during underfeed-overfeed cycles, the impact of the routine process task of anode changing should also be considered. In the anode changing procedure, the old anodes that have been consumed during the electrolysis process and need to be replaced by new anodes. The number of anodes in a cell is typically between 18 and 40. There are four different phases that occur during anode changing which are: (1) removal of the hood of the cell; (2) extraction of the old anode; (3) setting of a new anode; and (4) covering of the new anode with a bath/alumina mixed material (Gadd, 2003). Every phase in the anode changing procedure should have a different impact on the cell but the obvious impact is that it causes a step increase in voltage, followed by a more gradual downward trend in cell voltage. Therefore, it is crucial to develop a fault detection system

which takes account of this superimposed voltage trend so that the dynamic pattern within the underfeed-overfeed cycles can be captured effectively.

As discussed in this section, we can see that, aluminium smelting processes, by their very nature are difficult to monitor (Bearne, 1999). This was pointed out by Bearne more than a decade ago as one of the barriers to effective control of the reduction process. Highly correlated data, large volume of data, parameters at different frequency and dynamic behaviour, are some of the problems that arise in process monitoring. Considering these problems, control errors such as false alarms or failed alarms could be prevented so that effective process monitoring can be carried out.

2.4. Breakthrough for process monitoring

Although there are many problems in process monitoring, the established relationship between voltage (measured variables) and alumina concentration (unmeasured variables) analysed since 1965 via theoretical voltage/alumina concentration curves (Welch, 1965), has led to control system improvement for aluminium smelting cells. One key breakthrough for system improvement is the recognition of variability patterns and signals from the established theoretical curves and integration into an automatic control system (Taylor and Chen, 2007). This study has, therefore, been designed to further investigate the use of variability patterns within an alumina feeding cycle for detection and diagnosis of faults in the aluminium smelting process.

2.4.1. Variability patterns within alumina feeding cycles prior to anode effects

As shown in the examples in Figure 2.9, nine overfeed-underfeed cycles over a period of 11 hours were observed from cell 2022 at Aldel's smelter in the Netherlands, where each observation has an average duration of five minutes. The ninth cycle relates to an anode

effect. The changes in the cell resistance were observed in the ninth cycle. This shows the benefit of using short time interval feeding to possibly eliminate anode effects based on the rate of changes (Agalgaonkar et al., 2009). A change in the pattern in the cell voltage trace through the plot within an overfeed-underfeed cycle prior to the last cycle, may indicate problems that cause anode effects such as a blocked feeder, crust falling into the cell or low alumina dissolution (Taylor and Chen, 2007). For example, increases in resistance during overfeeding may indicate feeding problems or high alumina bulk concentration (Segatz, 2001). Therefore, there is a need to develop a model capable of finding the causes of anode effects based on the changes of the cell voltage and resistance patterns within the overfeed-underfeed cycles.

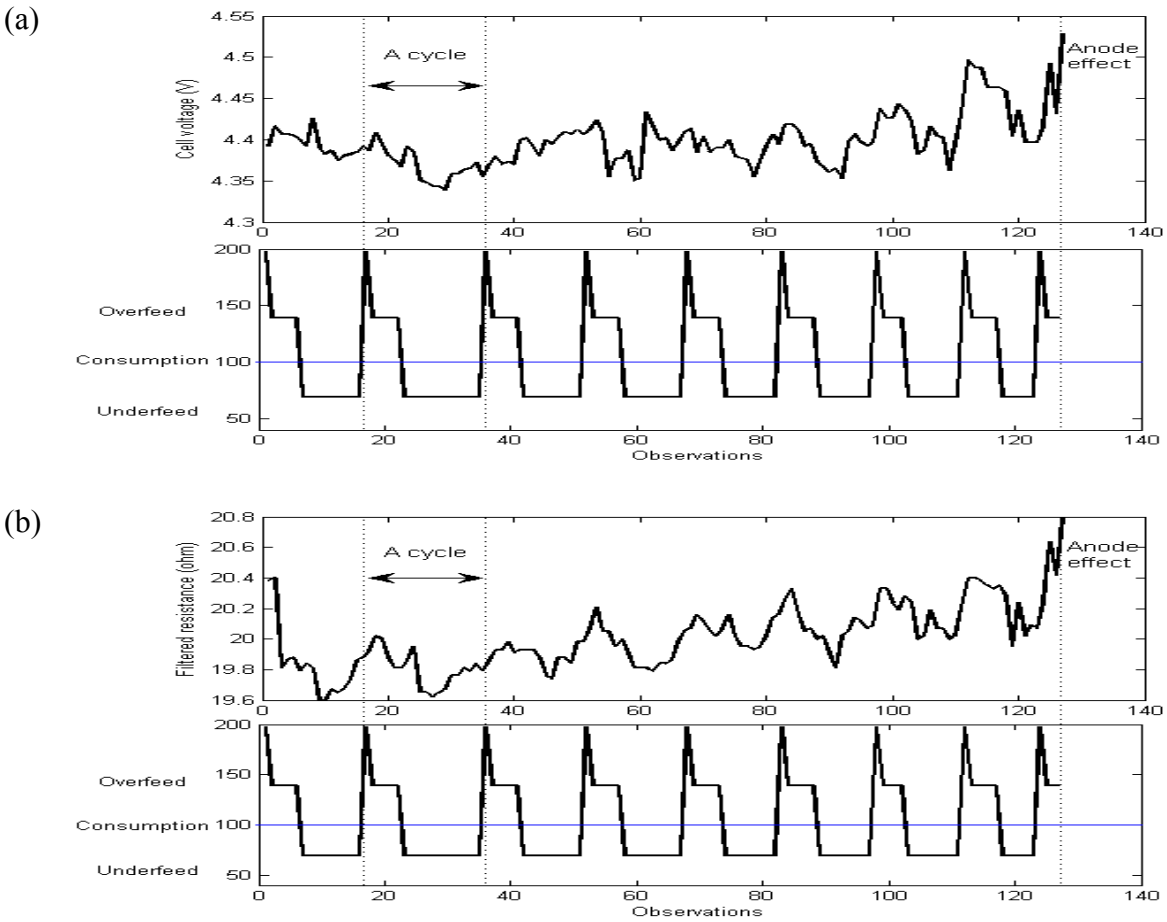

Figure 2.9: (a) Cell Voltage, (b) Cell Resistance and Feed Rate for Point Feeding that ends with an Anode Effect

2.4.2. Variability of cell voltage patterns within alumina feeding cycles with recorded anode spikes

Changes in cell voltage patterns within the overfeed-underfeed cycle may also indicate the presence of anode spikes which cause short-circuiting between the anode and the metal. These anode spikes decrease the production rate and cause subsequent overheating of the cell resulting in instability in the process. In Aldel's aluminium smelter, anode spikes are detected using: (1) soft sensing based on an increase of cell temperature by more than 15°C and a decrease in alumina feeding by more than ten percent (Stam et al., 2008) and (2) measuring process variables at each anode every 24 hours (M. Stam, personal communication, December 10, 2008). Based on these methods, the occurrences of anode spikes are recorded.

Figure 2.10 shows a series of feeding cycles from cell 2165 at Aldel where the last cycle ended with a recorded anode spike. Using the methods described above, it is difficult to ascertain when the anode spike started to occur because anode spikes may only able to be detected after spiking problems have been occurring for a period of time. Therefore, there is also a need to investigate the potential of using a statistical approach for the early detection of anode spikes by observing the changes of the variability patterns within the overfeed-underfeed cycle.

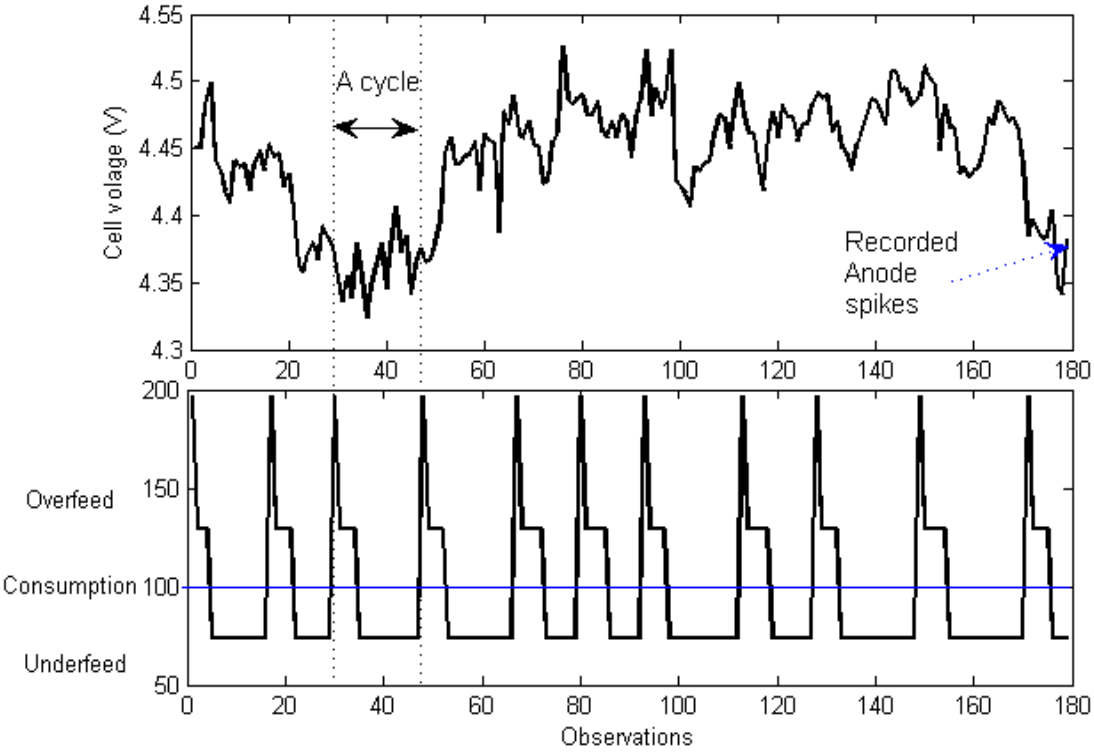

Figure 2.10: Cell Voltage and Feed Rate for Point Feeding that ends with Recorded Anode Spikes

2.5. Conclusions

Due to the problems in monitoring the aluminium smelting process, the occurrence of anode faults such as anode effects and anode spikes has been difficult to detect earlier in the process. However, monitoring the variability pattern within an alumina feeding cycle, is shown in this thesis as a potential approach for overcoming these problems. This explains the answer to the first research question which relates to the way in which the aluminium electrolysis process can be monitored effectively. This thesis posits that the occurrence of faults could be detected by monitoring abnormal patterns from the established curve using a suitable fault detection and diagnosis system.

CHAPTER 3: FAULT DETECTION AND DIAGNOSIS SYSTEM

The organizing into groups of the various fault detection and diagnosis systems of the aluminium smelting process which share similar qualities can assist in the identification of the key elements of the system. This chapter will first describe a fault detection and diagnostic taxonomy that has been developed from reviews of literature and knowledge pertaining to the aluminium smelting process. Next, the groups and elements that comprise the taxonomy are explained. Finally, the key elements of the new system for the aluminium smelting process that have been identified in this research based on the taxonomy are discussed.

3.1. A proposed taxonomy for aluminium process fault detection and diagnosis

A variety of fault detection systems for the aluminium smelting process can be found in the literature. This diversity is contributed to principally by the way in which each system utilizes the resources available by using an approach which is appropriate for the process control system in question. Investigating these systems by identifying elements that shape the systems may help us to understand the different kinds of fault detection system in the aluminium smelting process. Thus, we classified these elements in the following groups:

- Fault detection and diagnostic knowledge – What knowledge is used in the fault detection and diagnosis systems of the aluminium smelting process?
- Fault detection and diagnostic techniques – How is the system built by utilizing the knowledge?
- Usage frequency – How frequently can the system monitor the process?

- Detection mode of results – How are the results of the system are presented to the operators?

Figure 3.1 illustrates the groups and elements that create a fault detection and diagnostic taxonomy for the aluminium smelting process. The proposed taxonomy can assist in determining the various factors in developing a new fault detection and diagnosis system. The groups and elements of this taxonomy are briefly described in the following section.

3.1.1. Fault detection and diagnostic knowledge

The first group is comprised of fault detection and diagnostic knowledge. The elements of this group represent particular knowledge in the aluminium smelting process that has been used, and can be used, to develop fault detection and diagnosis systems. A brief explanation of each element is given below:

1) The first element in this group is a spectra of resistance in which the specifications of the spectra in three cases were identified for assisting in fault diagnosis. The cases are: normal cell, aluminium roll and abnormal anode (Shuiping et al., 2007).
2) Patterns of noise are the second element in this group. Three different patterns of noise were recognized, also to assist in fault diagnosis. These are bubble noise (Banta et al., 2003), short-circuiting noise and metal pad roll noise (Banta et al., 2003, Renbijun et al., 2007).

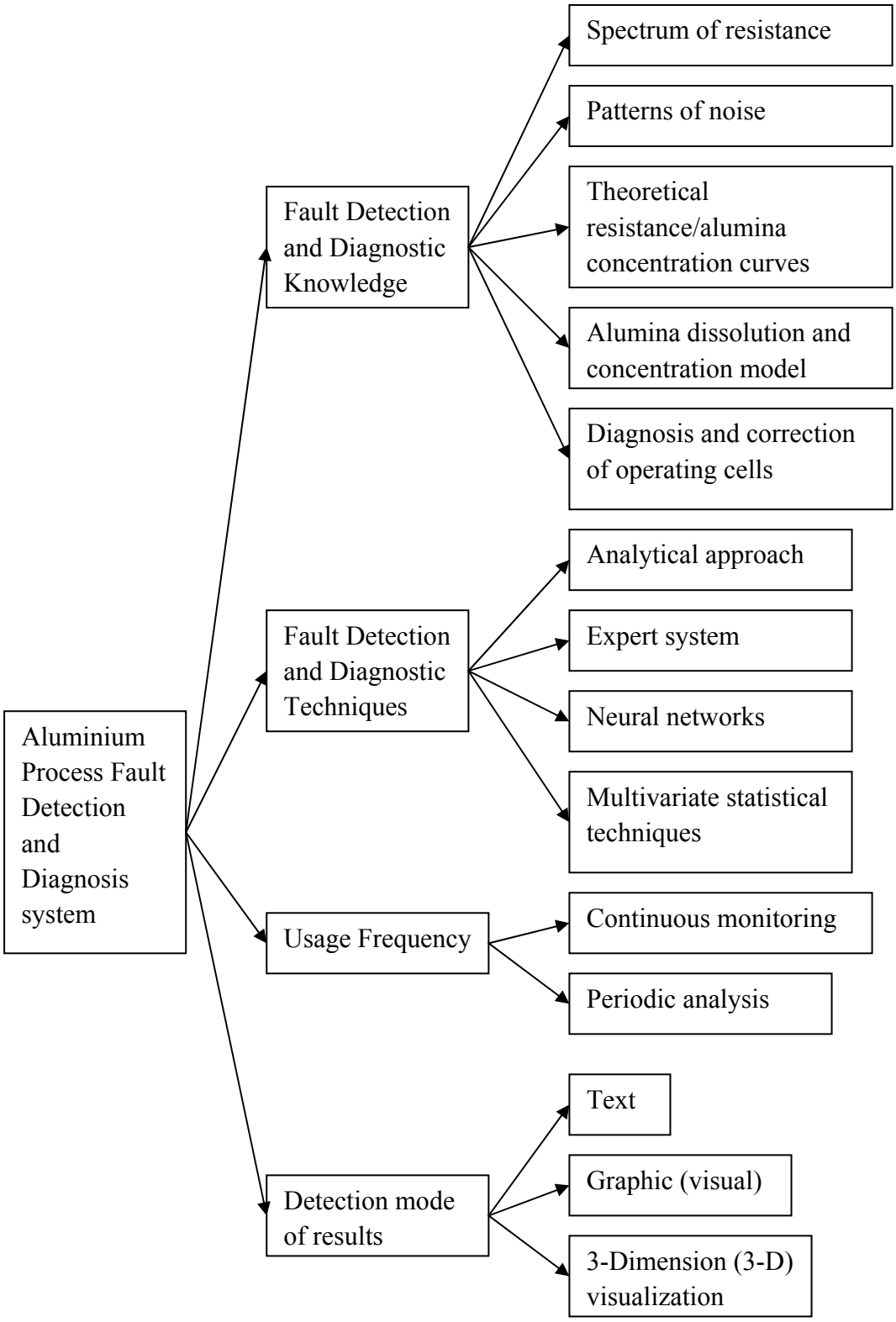

Figure 3.1: Taxonomy for Aluminium Process Fault Detection and Diagnosis

3) The third element in the group is a theoretical resistance/alumina concentration curve as illustrated in Figure 2.7 and described in detail in section 2.3.4.1. There have been other

researchers who have selected data for developing fault detection systems by using this curve as an important reference such as Yurkov et al. (2004), Nagem et al. (2009) and Meghlaoui et al. (1998):

a) The first example comes from research carried out by Yurkov et al. (2004) in which selected data which were deemed as being appropriate for analysis based on feeding cycles. These cycles were formed following the controlling of alumina feeding based on the theoretical resistance/alumina concentration curve.
b) The second example is from research by Nagem et al. 2009 in which data were divided into four regions based on the theoretical resistance/alumina concentration curve. These were: (1) lean region (low alumina concentration), (2) normal region (good operating point), (3) rich region (high alumina bulk concentration), and (4) very rich region (high alumina bulk concentration, high temperature and reoxidation phenomena).
c) The third example stems from research by Meghlaoui et al. (1998) in which two dynamic trend indicators were generated based on the theoretical resistance/alumina concentration curve.

These examples from previous research indicate that the difficulties experienced in the direct measurement of alumina concentration and the frequent measurement of important parameters, such as cell temperature; this has prompted a group of researchers to discover how to utilize existing knowledge in the development of an appropriate fault detection and diagnosis system.

4) The fourth element is a set of colour and textural features grouped according to the varying alumina content of anode cover materials. These colour and textual features were identified using multivariate image analysis techniques. These features can be used to estimate the alumina content of anode cover materials (Tessier et al., 2008a).

5) The fifth element is the diagnosis and correction of operating cells that were recorded by operators and engineers. This knowledge can be used to form a knowledge database in an expert system (e.g. Rolland et al., 1991 and Berezin et al., 2005). It can also, assist in the discovery of new knowledge for fault diagnosis, and then for validating that new knowledge by using the procedure for knowledge discovery from databases (e.g. Wang, 1999).

3.1.2. Fault detection and diagnostic methods

The development of fault detection and diagnosis systems not only involves various knowledge domains but also a variety of methods. In the taxonomy proposed here, the group pertaining to the methods to be used for fault detection and diagnosis is described as the second group. This group concerns the development of a fault detection system by using a suitable technique and utilizing specific knowledge. A brief explanation of each element is given below:

1) The first element in this group is an analytical approach because two common methods for this approach, parameter estimation and diagnostic observers were used to develop an aluminium process detection system (Hestetun et al., 2006). The approach based on a quantitative model in a well accepted taxonomy developed by Venkatasubramanian et al. (2003b) in which precise first principles or mathematical models of the process are used to model a system based on the relationship between the inputs and outputs of the process. The differences between actual system behaviour and that of the system model are then calculated and called residuals (Venkatasubramanian et al., 2003c). Figure 3.2 shows the two main stages in the model based fault detection and diagnosis (Gertler, 1998) where some of the frequently used residual generation methods are diagnostic observers, Kalman filters, and parameter estimation. These residuals are further evaluated in order to identify the occurrence of faults in the process (Gertler, 1998).

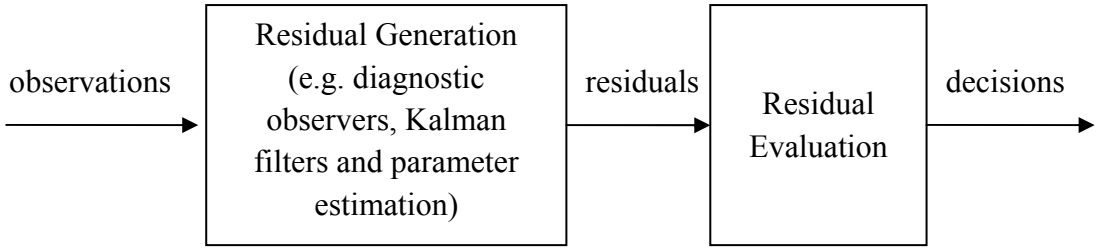

Figure 3.2: The Two Main Stages in Model based Fault Detection and Diagnosis (redrawn from Gertler, 1998)

In a fault detection system for the aluminium smelting process, an extended Kalman filter was used in order to not only estimate the alumina concentration in different sections of an aluminium reduction cell, but to also indicate an abnormal alumina distribution. A mathematical model was developed to estimate the alumina concentration. Residuals were generated from the difference between the alumina concentration expected by the system model and the actual concentration (Hestetun et al., 2006). Abnormal alumina distribution was detected when the residuals were significant. However, the residuals not only indicate abnormal events but may also indicate other sources including noise, disturbances and model errors (Gertler, 1998). This issue of robustness may limit the effectiveness of using the Kalman filter or other model-based approaches.

2) An expert system which is a process history-based approach is the second element in this group. In the process history based approach, prior knowledge is extracted from a large amount of historical data. This feature extraction can be divided into qualitative and quantitative methods as shown in Figure 3.3 (Venkatasubramanian et al., 2003b). A popular example of a qualitative method is the expert system where prior knowledge from experts is extracted to represent human knowledge in a particular domain. It is used in fault diagnosis to infer a conclusion of an out-of-control situation by combining the facts from a user with the knowledge from human experts represented in knowledge databases.

In the aluminium smelting process, knowledge relating to diagnosis and correction of operating cells was incorporated in a number of expert systems such as those of Haldris (Rolland et al., 1991), the FMFA-based expert system (Berezin et al., 2005) and the CVG Venalum potine supervisory system (Abaffy et al., 2006). In an Aluminum Electrolysis Process Expert System (AEPES)(Lu, 2002), for example, there were two subsystems; the first one incorporated more general knowledge of the aluminium reduction cell including unstable cell voltage, anode carbon quality and higher iron impurity. The second one incorporated specific knowledge including bath temperature, metal level and bath ratio. The use of expert system, however, lacks statistical inference and pattern recognition (Uraikul et al., 2007).

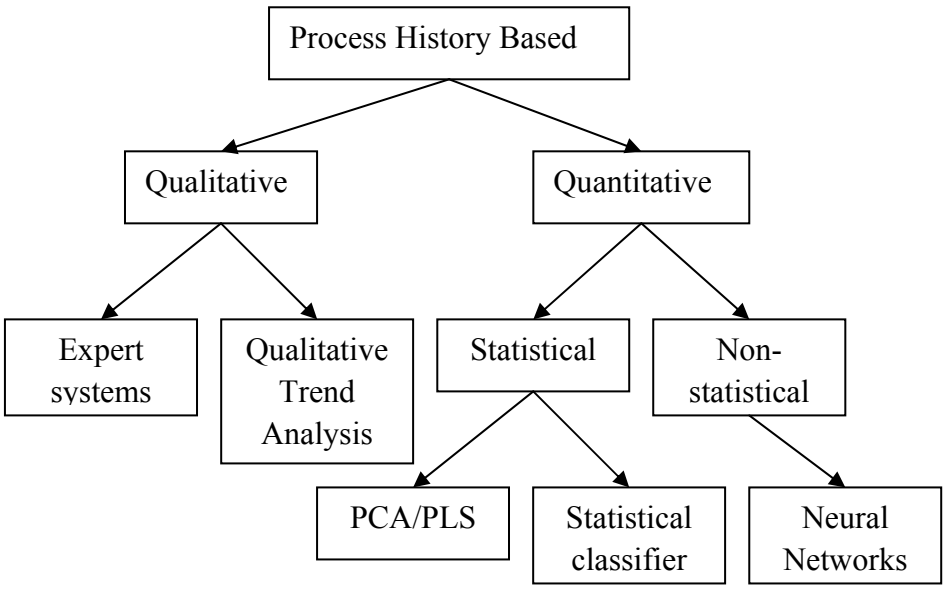

Figure 3.3: Classification of Process History-based Methods (redrawn from Venkatasubramanian et al., 2003a)

The third element in this group, neural networks, is also a process history based approach. As shown in Figure 3.3, the quantitative method can be divided into statistical and non-statistical. The use of artificial neural networks is a non-statistical approach used in fault diagnosis to recognise the received pattern of data by using a nonlinear mapping between

input (data patterns) and output (fault classes). This mapping consists of hidden neurons that are highly interconnected and arranged in layers (Uraikul et al., 2007). In the aluminium smelting process, a back-propagation neural network was used to map spectra of cell resistance and output vectors for three cases which were; normal cell, aluminium roll and abnormal anode (Shuiping et al., 2007). In addition, a feed-forward neural network was used to predict cell resistance and fast dynamic indicator (Meghlaoui et al., 1998). Both systems used simulation data to train the networks. The use of neural networks, however, lacks explanation capability (Andrews et al., 1996).

3) The fourth element in this group is the use of multivariate statistical techniques which is also a quantitative and process history based approach. Multivariate statistical techniques such as PCA and PLS are used to extract a number of latent variables from normal operating data which are retrieved from historical databases, in order to form an empirical model (Kourti, 2005, MacGregor et al., 2005). Thus, in the future, whenever the behaviour of the operation of the plant differs from the empirical model of the normal process, unexpected changes in the process can be detected (MacGregor et al., 2005). The following are examples of the use of PCA/PLS for process monitoring in materials processing including aluminium processing:
    a. A combination of PCA and Linear Discriminant Analysis (LDA) (Kano and Nakagawa, 2006) were used for monitoring the quality of iron and steel.
    b. PCA was used for monitoring the quality of copper (Wikströma et al., 1998).
    c. Multivariate image analysis was used for estimating alumina concentration on anode cover (Tessier et al., 2008a).
    d. Estimation was carried out for aluminium reduction cell performance using PLS (Tessier et al., 2008b).

e. Multivariate monitoring of aluminium reduction cells was undertaken using PCA (Tessier et al., 2009).

f. Multivariate on-line monitoring of preheating, start-up and early operation of aluminium reduction cells was investigated using PLS regression (Tessier et al., 2010).

These examples show that the multivariate techniques, PCA/PLS, have been investigated for analysis of historical data and monitoring of processes in various complex process industries because of their ability to handle, highly correlated, or large volumes, of data.

3.1.3. Detection mode of results

The fourth group in this taxonomy describes the three modes for presenting detection results: text, graphic (visual) and three-dimensional (3-D) visualization. The presentation of detection results to the operator can be more informative if the operator's needs are considered in terms of a clear visual indication in the screen design (Miletic et al., 2004). This theory is supported by research done by Harris et al. (2009) where colour and statistical graphs were incorporated in the design of a supervisory control system. The use of the colour red in this system clearly indicates when there is an alarm so that the section leader in a smelter can act accordingly.

Although many contributors to the reference literature pertaining to aluminium process fault detection cited in this taxonomy do not provide screen design in their approach, there are some articles that do provide or describe how the results are presented. Three examples are given here. Firstly, in a multivariate statistical application, for example, a 3-D visualization was used to illustrate Hotelling's T^2 statistic with a 3-D control envelope which is based on bath temperature, liquidus point and cumulative sum of alumina feed ratio (Stam et al., 2008). Secondly, a fault diagnosis system based on neural network provided its screen interface in which two modes were used: text (querying history report, spectrum analysis of cell

resistance and fault diagnosis for the cell state) and graphic (real time curve and history curve of the cell signals)(Shuiping et al., 2007). Thirdly, a supervision system for aluminium reduction cells based on mathematical models has provided its interface for five functions including real-time display and curve change for specified parameters (Shuiping and Qiuping, 2003). The state of the cells is displayed using a text box, and the temperature, the voltage, the current and the alumina concentration are displayed in charts. The user interface also consists of control boxes, such as combo boxes, and control buttons. All these examples show that a combination of text and graphic may be more effective for revealing monitoring results to the operator than solely using either text or graphic (Shuiping and Qiuping, 2003).

3.1.4. Usage frequency

The last group to be considered in this taxonomy is usage frequency where it applies to the way the fault detection and diagnosis system performs its analysis of the process. A brief explanation of each element is given below:

1) The first element in this group is one which is continuous. An online fault detection and diagnosis system monitors the process continuously by analysing continuous data from the process. The system may immediately signal abnormal events after they happen. Examples of these systems include a back propagation neural network developed by Shuiping et al. (2007) and a feed-forward neural network system developed by Meghlaoui et al. (1998).
2) Periodic analysis is the second element in this group. In an aluminium smelting process, an offline fault detection and diagnosis system periodically analyses data at a frequency ranging from daily to once in two days. This level of frequency is to enable the detection of abnormal events using bath chemistry and heat balance parameters. Some of the examples in this system include: (1) process monitoring using PCA (Tessier et al., 2009)

and (2) an analytical model for estimating alumina concentration and abnormal events (Hestetun et al., 2006).

3.2. Key elements of the new system

Based on the proposed taxonomy, the key elements of the new fault detection and diagnosis system are described below.

3.2.1. Fault detection and diagnostic knowledge

The first element of the proposed new system is the discovery of new knowledge based on the established relationship between pseudo-resistance and alumina concentration. In addition to the extraction of knowledge from the prior research of experts and the production of a theoretical resistance/alumina concentration curve through experiment, learning to identify abnormal patterns from data is one of the practical ways in which to discover fresh knowledge relating to fault detection and diagnosis. Since there is a need to develop a fault detection and diagnosis system based on the changes of cell voltage and cell resistance patterns within overfeed/underfeed cycles, ascertaining abnormal patterns within these cycles using data mining to discover new knowledge will be carried out in this thesis.

3.2.2. Fault detection and diagnostic methods

In the first element of the proposed new system, the established relationship between pseudo-resistance and alumina concentration is used as a basis for discovering new knowledge. In the second element, the established relationship is used as the basis for monitoring the process with the added use of a suitable technique. It has been interesting to note that the established relationship between pseudo-resistance and alumina concentration has become the basis for many applications from linear to non-linear models for a range of purposes such as:(1) the estimation of alumina concentration using the Kalman Filter approach (Hestetun et al., 2006); (2) the prediction of anode effects using a linear time-series model and a simple non-linear

exponential rise curve (Vajta and Tikasz, 1987), and (3) for the prediction of feed control decision variables using neural-networks (Meghlaoui et al., 1998). The strengths and weaknesses of some of these applications were discussed by Stevens McFadden et al. (2001) where an application using the neural network model has been suggested as a suitable approach for a predictive modelling task.

As discussed above, many fault detection techniques have been employed previously. The main interest of this thesis, however, is a technique that is capable of early fault detection in the industrial application of the aluminium smelting process. All of the previously mentioned applications in this research stem from analytical and knowledge-based approaches the focus of which has mainly been on the avoidance of anode effects. Less attention has been given to the use of data-driven approaches such as PCA and PLS for observing the changes of patterns within the overfeed-underfeed cycle for the detection and diagnosis of problems. Also, many researchers have used only simulated data instead of real data. Since the aluminium smelting process is complex, having many problems that require effective process monitoring (as described in section 2.3), it may be impractical to develop an accurate and explicit mathematical model of the process. Therefore, the model based methods, both quantitative and qualitative, have not been considered in this thesis.

On the other hand, there has been growing interest in using process history based approaches for fault detection of industrial applications (Venkatasubramanian et al., 2003b, Kourti, 2005). Venkatasubramanian et al. (2003a) listed three key reasons for this increasing interest, these are: (1) they are easy to put into practice, 2) little modelling effort is required and 3) little prior knowledge is needed. A number of process history-based fault diagnostic techniques have been developed for the aluminium smelting process including expert

systems, neural networks and multivariate statistical techniques (PCA/PLS). Firstly, a number of expert systems were developed for fault diagnosis (Rolland et al., 1991, Berezin et al., 2005). Due to the complexity of the aluminium smelting process, the cause of an abnormal operating pattern is often difficult to diagnose. Process engineers may interpret the abnormal pattern themselves before or while using an expert system. A computerised system that is capable of solving the persistent problem of diagnosing abnormal patterns for multiple aluminium reduction cells is needed. Furthermore, expert systems require considerable effort in order to build a knowledge based diagnosis system for a complex and large process. An existing solution for this problem has been based on neural networks (Shuiping et al., 2007). However, this requires comprehensive and excessive amounts of data, causing Shiuping et al. (2007) to use simulation data instead of real data in their study. The use of PCA and PLS is a viable option because only moderate amounts of historical data are needed. Based on this, an application of PCA was developed by Tessier et al. (2009) for monitoring the aluminium electrolysis process. However, in order for a monitoring system to be rendered effective, consideration needs to be given to dynamic cell behaviour.

Therefore, the objective of this study is to develop a new multivariate statistical framework using PCA and PLS that incorporates the dynamic behaviour of the two important events of anode changing and alumina feeding during the aluminium smelting process, for effective and timely fault detection and diagnosis. In this thesis, PCA has been chosen for the development of a fault detection system and a combination of PCA and PLS has been chosen for the development of a system for fault diagnosis. This is because these multivariate statistical techniques can address some of the problems arising in the detection and diagnosis of faults in the aluminium smelting process.

1) Firstly, PCA or PLS can handle a substantial quantity of data which is both correlated and noisy.
2) Secondly, both PCA and PLS use a non-causal model so that the lack of a causal model in the aluminium smelting process is not an issue. A causal model needs a first principles model.
3) Thirdly, multi-way PCA and multi-way PLS (extensions of PCA and PLS, respectively) are able to handle any non-linear behaviour during the process of alumina feeding.
4) Finally, PCA and PLS are effective in practice for the monitoring of the aluminium smelting process since the reference models have been mainly built from process data (Chiang et al., 2001).

Principally, the use of multivariate statistical techniques such as PCA and PLS needs to be investigated not only for the prediction of anode effects, but also for the diagnosis of problems that cause anode effects and for the early detection of anode spikes. This advanced monitoring of aluminium processing leads to a reduction in energy consumption and emission of PFCs.

3.2.3. Usage frequency

The continuous monitoring of changes of variability patterns within the overfeed/underfeed cycles is preferred in this thesis for early fault detection and diagnosis. However, the periodic analyses of data at daily and two day intervals will also be investigated in this thesis because it involves important parameters in the aluminium smelting process. This investigation was run as a pilot study as described in section 5.2.

3.2.4. Detection mode of result

Charts that can show changes of pattern against acceptable limits for operations are one of the important elements in monitoring. Information about the current process and the results of the

diagnosis that were provided in textual form were put together with the charts. In this thesis, a mixture of text and graphics incorporated with suitable colour (red and green) and user control boxes such as a combo box for selecting cells, was used instead of selecting only one mode in order to demonstrate clearly abnormal events.

3.3. Conclusions

Developing a fault detection and diagnosis system for the aluminium smelting process is a major challenge. This fault detection and diagnosis system should be able to accurately indicate abnormal situations although the process is complex and dynamic. In this chapter, a proposed taxonomy described with examples of existing systems was given. The taxonomy clearly highlights the key elements of a fault detection and diagnosis system which covers: utilization of knowledge, techniques, usage frequency and the presentation of the results.

The taxonomy has many uses including: 1) to identify the key elements that distinguish between existing systems, 2) to identify areas of improvement for the existing systems and 3) to provide an overview of the system where various techniques have been applied to detect and diagnose faults. This taxonomy has helped in the development of this thesis by identifying the gap in the existing fault detection and diagnosis systems and realizing a new approach to developing a new system that is practical, provides timely detection and diagnosis, and is easy-to-understand by operators.

CHAPTER 4: MULTIVARIATE STATISTICAL METHODS

This chapter describes multivariate statistical techniques for fault detection, knowledge discovery and fault diagnosis. First presented are the basic concept of PCA/PLS and an illustration of PCA applied to real data sets. The rest of the chapter is divided into three parts. The first part explains the use of multivariate statistical methods for fault detection. In this part, the SPC philosophy and its main tool (the control chart) is described. The rationale for using the multivariate control chart based on MPCA is also discussed. The second part briefly explains the use of multivariate statistical methods in knowledge discovery. The third part describes the use of multivariate statistical methods in fault diagnosis. This part will begin by reviewing techniques for fault diagnosis. The rationale behind the use of pre-identified abnormal regions and DPLS for aluminium smelting process is then detailed. Finally, the overview and the procedure for DPLS are presented.

4.1. Data-driven approaches: PCA and PLS

4.1.1. Basic concept of PCA

Principal component analysis or PCA is a useful statistical technique that was developed over the course of the 20th century (Holbrey, 2006). There have been thousands of applications of PCA over the years in many areas such as; psychology, education, quality control, chemistry, market research, economics, anatomy and biology (Jackson, 2003). PCA is a data reduction method that is able to project most of the important information from a large multivariable process onto a reduced dimensional PCA model. A PCA model is usually built from a few principal components. These principal components are the result of decomposing a data matrix **X** using PCA. Statistically, PCA will decompose a large data matrix **X** (K x J) comprising a number of highly correlated variables (R), into:

$$X = TP' + E = \sum_{r=1}^{R} t_r p_r' + E \quad (4\text{-}1)$$

where **X** is a two-dimensional data matrix of *J* process variables sampled over *K* time intervals. This **X** (*K* x *J*) data matrix represents the large multivariable process, whereas t_R are the *R* principal components that forms the PCA model, and **E** are assumed to be random errors (MacGregor and Kourti, 1995). The principal components are defined by the *R* loading vectors (p_R) which are the eigenvectors of **X** (*K* x *J*) and these vectors are used to transform **X** (*K* x *J*) into its *R* principal components. The number of principal components for the PCA model is lower than the number of process variables, i.e. *R* is less than *J*. The *R* loading vectors provide a direction of maximum variability in the process so that one can observe the process using the model built from a few principal components, as most of the variability in the data can be expressed in these few principal components (PCs).

Geometrically, the PCs variables are the axes of a new coordinate system obtained by rotating the axes of the original system (the *x*'s). The new axes represent the directions of maximum variability (Montgomery, 2005). These new axes are defined by the PC loading vector. PC loading vectors transform the original variables to PC variables and therefore PC loading vectors play an important role in the transformation. In Figure 4.1, for example, the first loading vector, $\mathbf{p_1}$ is in the direction of the greatest variance where most of the data is clustered along $\mathbf{p_1}$. However, less data is clustered along the second loading vector, $\mathbf{p_2}$ which is orthogonal or perpendicular to the $\mathbf{p_1}$.

Loading vectors $\mathbf{p_1}$ and $\mathbf{p_2}$ are used to transform the original data from two process variables to the first and the second PCs, respectively. As a result, scores which are the individual data points in the PC variables can be visualized in a scatter plot defined by the first and the

second PCs. This scatter plot, which is also known as a projection space, a score plot, or a reduced space, becomes the new coordinate system after the transformation. Section 4.1.3, in addition to further explaining the basic concept of PCA, illustrates and describes the main steps involved in transforming original variables to PC variables.

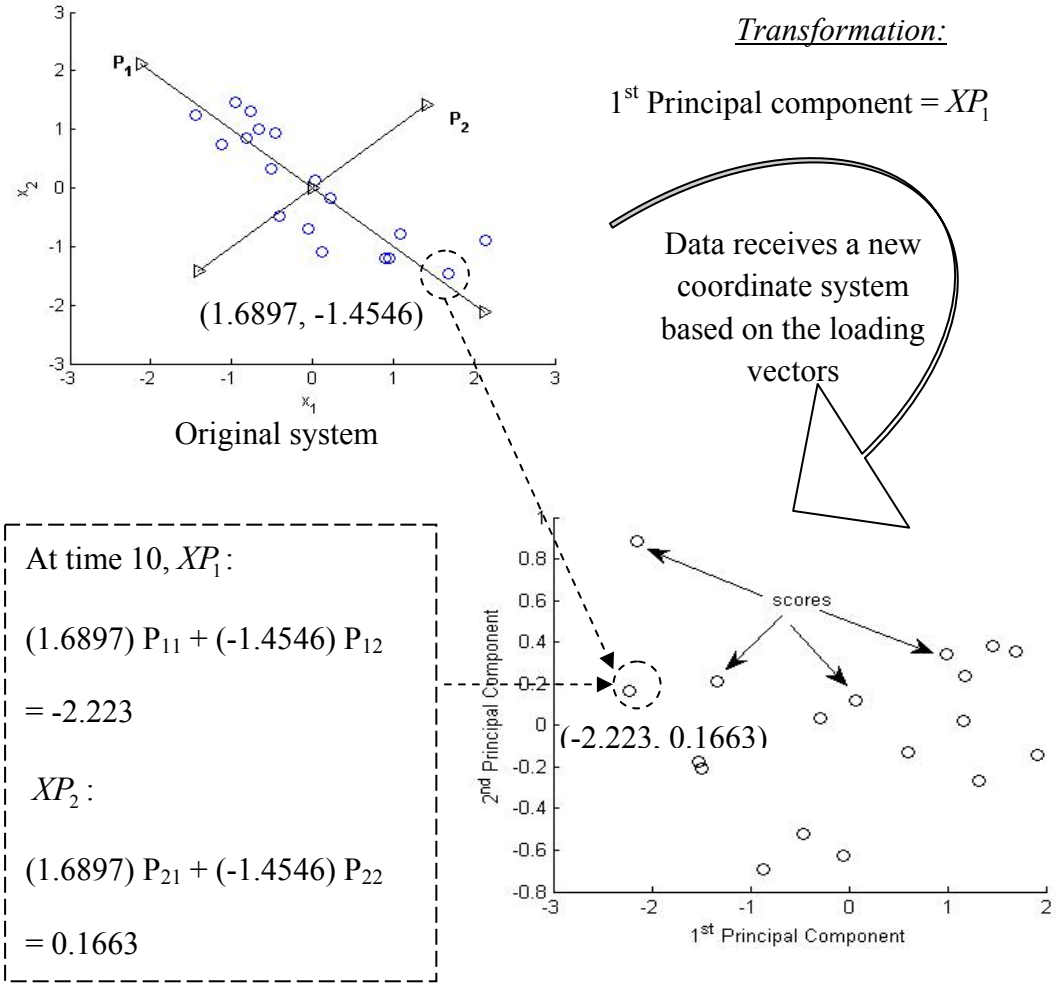

Figure 4.1: A Transformation from Original Variables to PC Variables

4.1.2. Basic concept of PLS

The difference between PCA and PLS is that PLS models the variation in the **X** and **Y** spaces while PCA only models the variation in a single space, **X** (Kourti, 2005).**Y** is a corresponding matrix of quality data. The latent variable model for **Y** space is:

$$Y = UQ' + F \tag{4-2}$$

where **U** is a matrix of latent variable scores, **Q** is a loading matrix and **F** is a residual matrix. The extracted latent variables capture variations in the process data (**X**), which are most predictive of the product quality data (**Y**), (Kourti, 2005). A robust procedure for the extraction of latent variables is NIPALS (Non-linear Iterative Partial Least Squares), developed by Wold et al. (2001). The NIPALS algorithm provides a procedure to calculate a PLS weighting matrix, **W,** by using two inputs, **X** (a set of predictor variables) and **Y** (a set of response variables). There are two phases in the use of PLS for process monitoring and this is shown schematically in Figure 4.2. In Phase I, **W** is obtained from the NIPALS algorithm. In Phase II, the **W** is then used for transforming the new data, $\mathbf{X_{new}}$, to latent variables ($\mathbf{T_{new}}$) by using equation 4-3.

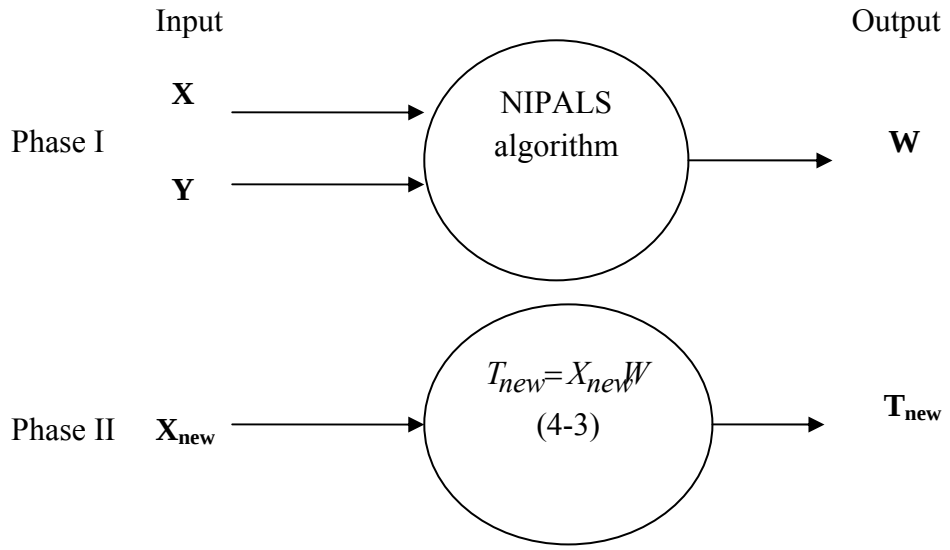

Figure 4.2: Basic Structure of PLS for Process Monitoring

The NIPALS algorithm (Wold et al., 2001) is given below.

PLS algorithm

1) Mean centre and scale **X** and **Y**
2) Set **u** equal to a column of **Y** or select a column vector, $\mathbf{u_i}$ of the matrix **Y**: $\mathbf{u=Y_i}$
3) In the **X** block:
   a) Regress columns of **X** on **u** : $\mathbf{w^T= u^TX/u^Tu}$

   b) Normalize **w** to unit length: $\mathbf{w}=\mathbf{w}/||\mathbf{w}||$
   c) Calculate the scores: $\mathbf{t} = \mathbf{X}\mathbf{w}/\mathbf{w}^T\mathbf{w}$
4) In the **Y** block:
   a) Regress columns of **Y** on t: $\mathbf{q}^T = \mathbf{t}^T\mathbf{Y}/\mathbf{t}^T\mathbf{t}$
   b) Normalize **q** to unit length: $\mathbf{q}=\mathbf{q}/||\mathbf{q}||$
   c) Calculate new **u** vector: $\mathbf{u} = \mathbf{Y}\mathbf{q}/\mathbf{q}^T\mathbf{q}$
5) Check convergence on **u**: Calculate the difference between the previous scores and current scores. If the difference |d| is larger than a predefined threshold, return to step 3.
6) **X** loadings or the column of **X** are regressed on $\mathbf{t_1}$ to give a regression vector: $\mathbf{p} = \mathbf{X}^T\mathbf{t}/\mathbf{t}^T\mathbf{t}$
7) Calculate residual matrices: $\mathbf{E} = \mathbf{X} - \mathbf{t}\mathbf{p}^T$ and $\mathbf{F} = \mathbf{Y} - \mathbf{t}\mathbf{q}^T$
8) If additional PLS dimensions are necessary then replace **X** and **Y** by **E** and **F** and repeat steps 2 to 7.

4.1.3. Illustration of PCA

The main aim of this section is to illustrate the application of PCA to real data sets from an aluminium smelter. The overall computations of PCA are relatively straightforward (Holbrey, 2006) and involve six basic steps for obtaining correlated variables, standardising data, calculating the covariance matrix, calculating the PC loading vectors, choosing the PC loading vectors and deriving the scores for PC variables. A brief explanation for each step is given below:

1) Obtaining correlated variables

Data which exhibits a moderate or high correlation is needed for PCA, because poorly correlated data will give PC variables that are similar to the original variables (Holbrey, 2006). Therefore, one of the advantages of using PCA, that is, to reduce high-dimensional data to low-dimensional data, is unlikely to be achieved. This advantage of PCA is explained further in the fifth step. Three process variables for aluminium processing $\mathbf{v_1}$, $\mathbf{v_2}$ and $\mathbf{v_3}$ (Table 4-1) are used as an illustration of PCA in this section. The process variables, excess AlF_3 ($\mathbf{v_1}$), temperature ($\mathbf{v_2}$) and liquidus ($\mathbf{v_3}$), are highly correlated so that they are suitable for using

with PCA. The strong relationship between process variables is shown in the clustering of most of the data along a line in the scatter plot in Figure 4.3.

Table 4-1: Data for Excess AlF_3, Bath Temperature and Liquidus

Observation (daily)	$\mathbf{v_1}$ [%]	$\mathbf{v_2}$ [°C]	$\mathbf{v_3}$ [°C]
1	14.47	959.00	939.27
2	13.28	960.00	942.23
3	12.08	969.00	953.19
4	11.52	977.00	959.98
5	10.96	982.00	963.76
6	10.39	980.00	960.54
7	11.28	977.50	960.27
8	12.17	957.00	942.01
9	13.06	956.00	943.24
10	13.96	953.50	942.97
11	13.12	956.00	944.17
12	12.29	966.00	952.87
13	11.46	971.00	956.58
14	11.11	976.00	961.01
15	10.77	975.00	959.44
16	11.17	980.50	967.72
17	11.58	963.00	953.00
18	11.98	961.00	953.78

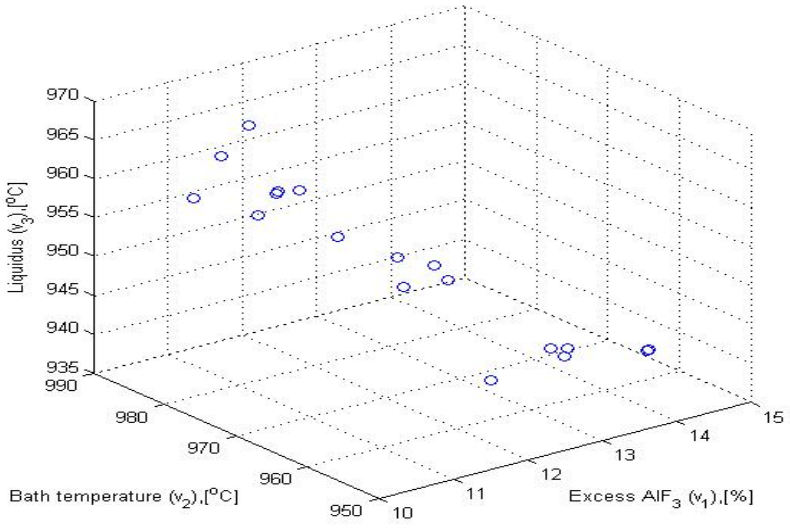

Figure 4.3: Scatter Plot of Three Process Variables showing a Strong Correlation

2) Standardising data

As the variables obtained in the first step may have several different units and the variance between those variables might be substantial, the variables are standardised by subtracting each variable by its mean and dividing by its standard deviation:

$$x_i = \frac{v_i - \mu}{\delta} \tag{4-4}$$

where $\mathbf{v_i}$ is the *i*th original variable, $\mathbf{x_i}$ is its corresponding standardised variable, μ is the mean of $\mathbf{v_i}$ and δ is the standard deviation of $\mathbf{v_i}$. The variables $\mathbf{x_1}$, $\mathbf{x_2}$ and $\mathbf{x_3}$ in Table 4-2 represent the variables $\mathbf{v_1}$, $\mathbf{v_2}$ and $\mathbf{v_3}$ in Table 4-1 after the standardisation. The scatter plot of this standardised data (Figure 4.4) has axes which differ from the scales from the scatter plot of the original data (Figure 4.3) but both scatter plots indicate a similar pattern. All the variables are dimensionless, and have mean zero and variance one.

Table 4-2: Standardised Data for $\mathbf{v_1}$, $\mathbf{v_2}$ and $\mathbf{v_3}$.

Observation (daily)	$\mathbf{x_1}$, [-]	$\mathbf{x_2}$, [-]	$\mathbf{x_3}$, [-]
1	2.1434	-0.8931	-1.5779
2	1.0910	-0.7911	-1.2401
3	0.0386	0.1276	0.0093
4	-0.4568	0.9442	0.7821
5	-0.9523	1.4546	1.2131
6	-1.4477	1.2504	0.8464
7	-0.6633	0.9952	0.8160
8	0.1210	-1.0973	-1.2658
9	0.9053	-1.1994	-1.1253
10	1.6897	-1.4546	-1.1557
11	0.9564	-1.1994	-1.0188
12	0.2231	-0.1786	-0.0272
13	-0.5102	0.3317	0.3946
14	-0.8132	0.8421	0.8999
15	-1.1162	0.7400	0.7214
16	-0.7596	1.3014	1.6649
17	-0.4030	-0.4849	-0.0128
18	-0.0463	-0.6890	0.0760

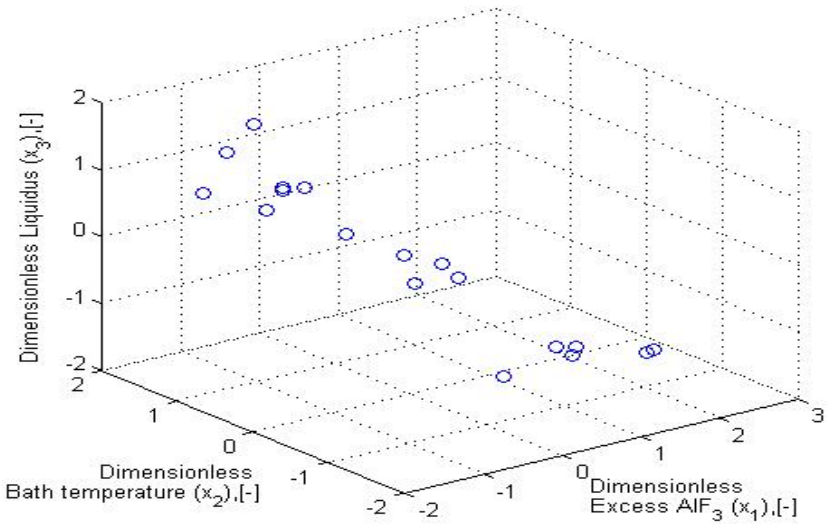

Figure 4.4: Scatter Plot of the Standardised Data

3) Calculating the covariance matrix.

The covariance matrix (**C**) is used to measure the relationship between variables. Equation 4-5 and 4-6 show the calculation to obtain a matrix **C** for three variables:

$$\mathbf{C} = \begin{pmatrix} \mathrm{cov}(x_1,x_1) & \mathrm{cov}(x_1,x_2) & \mathrm{cov}(x_1,x_3) \\ \mathrm{cov}(x_2,x_1) & \mathrm{cov}(x_2,x_2) & \mathrm{cov}(x_2,x_3) \\ \mathrm{cov}(x_3,x_1) & \mathrm{cov}(x_3,x_2) & \mathrm{cov}(x_3,x_3) \end{pmatrix} \tag{4-5}$$

where

$$\mathrm{cov}(X,Y) = \frac{\sum_{i=1}^{n}(X_i - \bar{X})(Y_i - \bar{Y})}{(n-1)} \tag{4-6}$$

After the calculation, the resulting Figure 4.5 shows that the absolute value of the correlation coefficients between $\mathbf{x_1}$, $\mathbf{x_2}$ and $\mathbf{x_3}$ in matrix **C** are above 0.8 indicating a strong correlation between them.

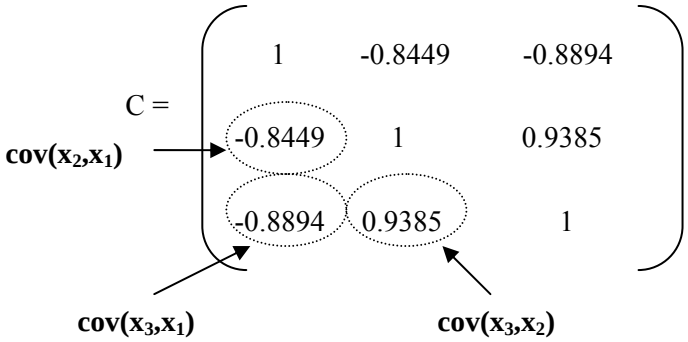

Figure 4.5: The Correlation Coefficients among Variables indicate a Strong Relationship between Them

4) Calculating the PC loading vectors

Finding the loading vectors that define the PC variables is fairly easy (Montgomery, 2005). The PC loading vectors are the eigenvectors (**P**) for the covariance matrix. Each **p** captures a different amount of variance which is represented by eigenvalues (**L**). The relationship between the matrix **C**, matrix **P** and matrix **L** can be defined as:

$$CP = LP \tag{4-7}$$

Every column in matrix **P** ($\mathbf{p_1}, \mathbf{p_{2,..,}}\ \mathbf{p_R}$) represents an eigenvector and the diagonal value for every column in matrix **L** represents its eigenvalue ($l_1, l_{2,..,}\ l_R$), respectively. The three eigenvectors, $\mathbf{p_1}$, $\mathbf{p_2}$ and $\mathbf{p_3}$ are plotted over the scatter plot, as shown in Figure 4.6. It can be seen that the third eigenvector, $\mathbf{p_3}$, shows the most intense cluster of data. Therefore, $\mathbf{p_3}$ has the largest eigenvalue, which is 2.7825, because it captures most of the variability of the data.

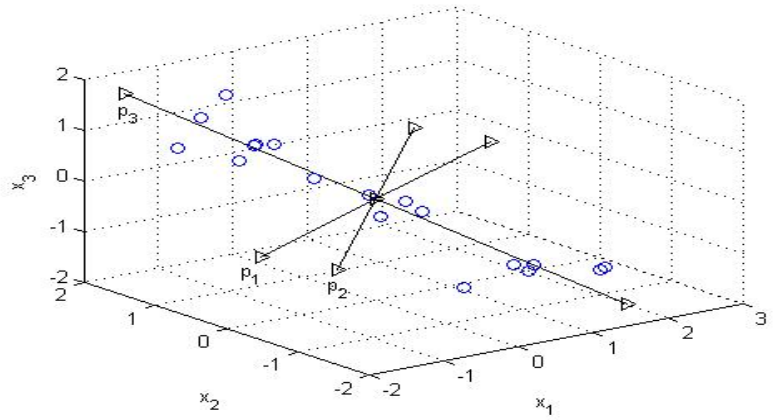

Figure 4.6: Scatter plot with eigenvectors

5) Choosing the PC loading vector and forming a feature vector

In PCA, the first PC loading vector must be based on the greatest variance. Therefore, the eigenvectors are ordered by eigenvalues, highest to lowest so that the PC loading vectors are in order of significance (Jackson, 2003). For example, as $\mathbf{p_3}$ captures the most variability of the data, $\mathbf{p_3}$ is arranged to be the first eigenvector. The number of PC loading vectors that should be retained to form the feature vector is dependent on the variance captured by the PC loading vectors. The percentage of the variance captured by every PC (EV) is calculated by using this equation:

$$EV_i = \frac{l_i}{\sum_{i=1}^{m} l_i} \times 100 \tag{4-8}$$

where $\boldsymbol{l}$ is the variance or eigenvalue, i is the selected PC loading vector and m is the number of PC loading vectors. The bar chart for the percentage of variances for the PC loading vector for the three process variables used in this section is shown in Figure 4.7.

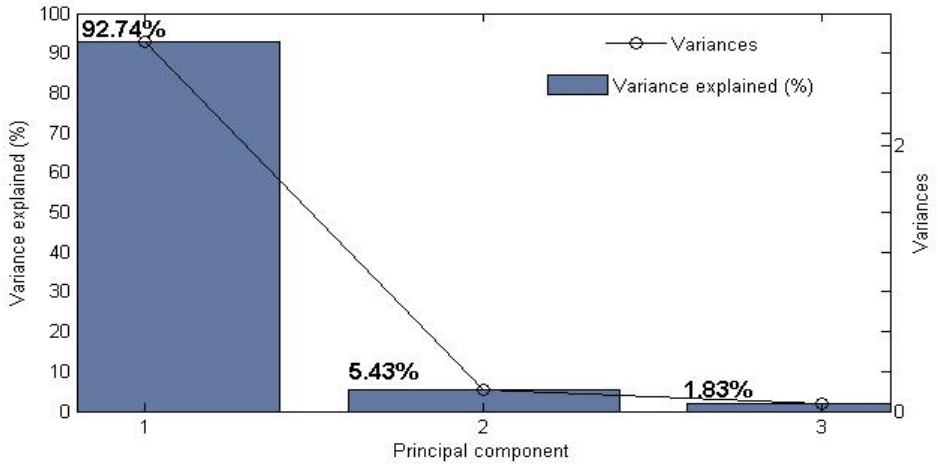

Figure 4.7: The First Two PC Loading Vectors account for 98.17 Percent of the Total Variability

Overlaying Figure 4.7 is a line plot of the variances. This line plot is a scree plot which indicates the positions of the eigenvalues from large to small. The number of PC loading vectors forming a feature vector is based on the position of an elbow which is a sharp change

in the slope that occurs in the line segments joining the points of the variances. The first PC loading vector, for example, accounts for 92.74 percent of the variance and there is a clear elbow between the first and the second PC loading vector. In this case the first PC loading vector is sufficient to explain the variance but if the first two PC loading vectors are selected, they will give a more accurate analysis as they account for 98.17 percent of the variance. Therefore, the first two PC loading vectors from matrix **P** are retained to form the feature vector Figure 4.8.

$$\text{Feature vector} = \underbrace{\begin{pmatrix} 0.2076 & -0.7972 \\ -0.5895 & -0.5644 \\ 0.7806 & -0.2142 \end{pmatrix}}_{\mathbf{P}} \quad \underbrace{\begin{pmatrix} 2.7825 \\ 0.1628 \end{pmatrix}}_{\mathbf{L}}$$

Figure 4.8: Feature Vector comprises Two PC Loading Vectors

With the feature vector, most of the variability is on a plane (flat surface) as shown in Figure 4.9. This plane represents the main pattern or feature of the data. In PCA, we are interested in analysing components that can best describe the pattern of the data. Therefore, the feature vector which now constitutes the principal components of the data is used to transform the original variables into PC variables.

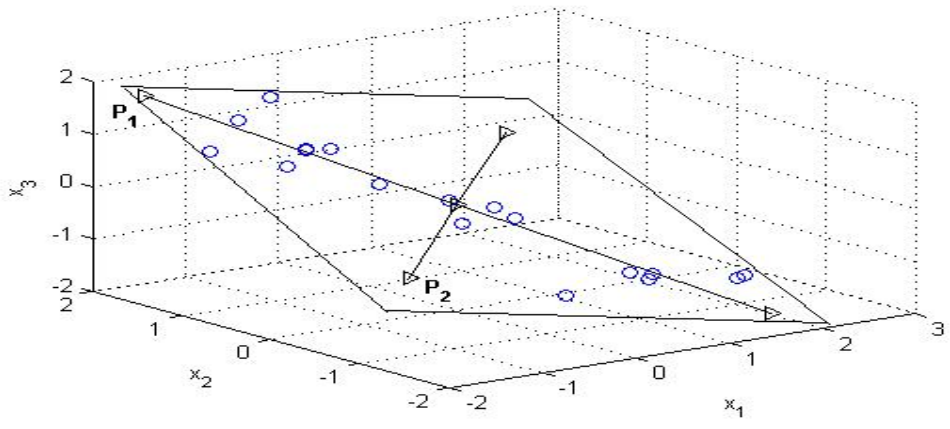

Figure 4.9: The First Two Loading Vectors are Retained

Another way to determine the number of PC is based on the 'broken stick' rule (Jolliffe, 1986). The 'broken stick' rule suggests that if a segment of unit length is randomly divided into p segments, the expected length of the kth-longest segment is:

$$g_k = \frac{1}{p}\sum_{i=k}^{p}\left(\frac{1}{i}\right) \tag{4-9}$$

As long as the proportion explained by each l_k is larger than the corresponding g_k, retain the corresponding PCs (Jackson, 2003).

6) Deriving the scores for the PC variables

Based on the selected PC loading vectors or the feature vector, original variables are transformed into PC variables. For this transformation, matrix **P** that contained the retained loading vectors is transposed so that each row in matrix **P** represents each loading vector. Figure 4.10 shows the transposed matrix **P**.

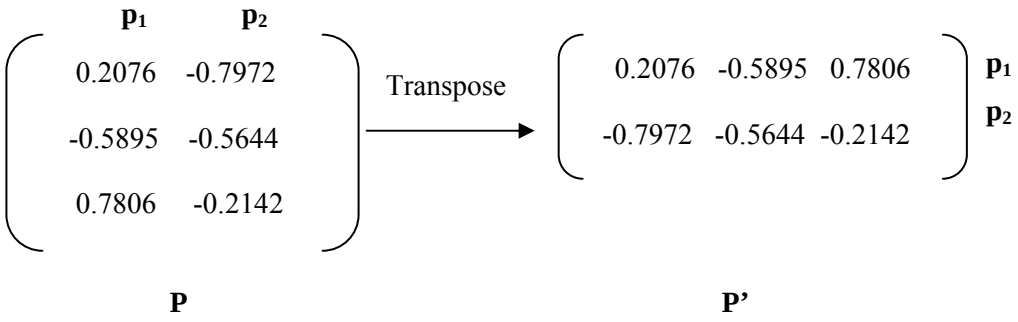

Figure 4.10: Transposed Matrix **P**

The scores (t_{ij}) then are derived by using equation 4-10:

$t_{i1}=p_{11}x_{i1} + p_{12}x_{i2} +\ldots+ p_{1p}x_{ip}$ (p_{ij} is the element in p_1)

$t_{i2}=p_{21}x_{i1} + p_{22}x_{i2} +\ldots+ p_{2p}x_{ip}$ (p_{ij} is the element in p_2)

...

$t_{ir}=p_{r1}x_{i1} + p_{r2}x_{i2} +\ldots+ p_{rp}x_{ip}$ (p_{ij} *is the element in* p_r) (4-10)

where r is the number of retained PC loading vectors, p_{ij} is the element for each loading vector, p is the number of process variables and i is the number of data points (Montgomery, 2005). Each score defined by the same loading vector forms a PC variable. The first score for the first PC variable for the three process variables used in this section with r =2 and p=3 is:

$$t_{11} = p_{11}x_{11} + p_{12}x_{12} + p_{13}x_{13}$$

$$= 0.2076\ (2.1434) + -0.5895(-0.8931) + 0.7806(-1.5779)$$

$$= -2.6576$$

The overall scores for the first PC variable ($\mathbf{t_1}$) and the second PC variable ($\mathbf{t_2}$) are shown in Table 4-3. These PC variables form the axes of the new coordinate system (Figure 4.11) and represent the most important information contained in the data.

Table 4-3: Scores for the First and Second PC Variables

Observation	t_1	t_2
1	-2.6576	-0.8666
2	-1.8037	-0.1576
3	0.0573	-0.1048
4	1.2638	-0.3363
5	2.0926	-0.3217
6	2.0402	0.267
7	1.4302	-0.2077
8	-1.4459	0.794
9	-1.867	0.1963
10	-2.477	-0.2785
11	-1.8334	0.1327
12	-0.2457	-0.0712
13	0.7126	0.1349
14	1.476	-0.0198
15	1.484	0.3176
16	2.1601	-0.4857
17	-0.0593	0.5976
18	-0.3273	0.4095

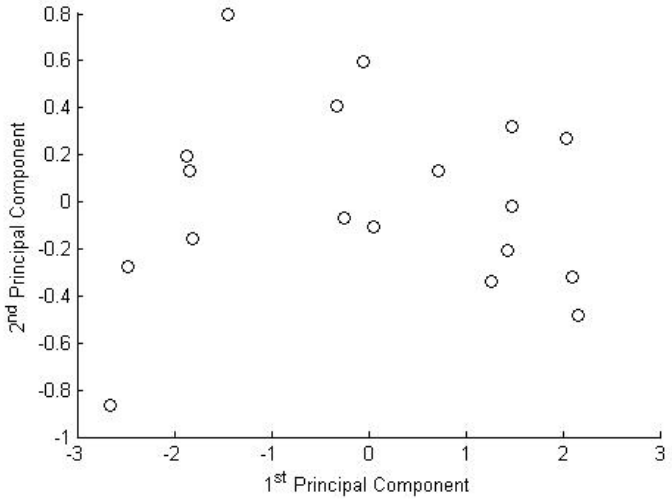

Figure 4.11: Scatter Plot for the First Two PC Variables to form a New Coordinate System

4.1.4. Conclusions

As illustrated above, using PCA, the dimension of the data was reduced and the correlations among variables were still preserved. These advantages pertaining to PCA make this technique popular in many research fields and therefore utilising those advantages in monitoring aluminium reduction cells is the main interest of this research. In this thesis, multivariate statistical methods, particularly PCA and PLS, were not only used in detecting and diagnosing faults but also in data mining to discover new abnormal patterns.

Part I: Multivariate Statistical Techniques for Fault Detection

Multivariate statistical techniques were used for fault detection by following the SPC philosophy. The philosophy behind SPC including its control charts, is given below from two perspectives. This is in order to show the changing factors from a univariate to a multivariate perspective and to highlight the importance of considering the multivariate characteristics of an aluminium reduction cell.

4.2. Statistical Process Control (SPC)

In a production process, massive amounts of data (process data and quality data) are collected and stored. These data contain variations, and the size and type of variation depends on how well the production process is being controlled. Learning the variation of manufacturing data has resulted in the development of a systematic procedure called statistical process control (SPC) for managing the process at its optimal level (Montgomery, 2005). In fact, the use of SPC as a complement to EPC is an excellent combination for process improvement because control charts based on SPC not only monitor the performance of the process over time but also remove the cause of faults as illustrated in Figure 4.12. The integration of EPC and SPC has also gained attention from researchers (Janikiram and Keats, 1998, Duffuaa et al., 2004, Montgomery, 2005). In most aluminium smelters, however, greater focus is put on EPC rather than SPC (Stam et al., 2007). There is a need to investigate further the application of SPC in monitoring aluminium reduction cells.

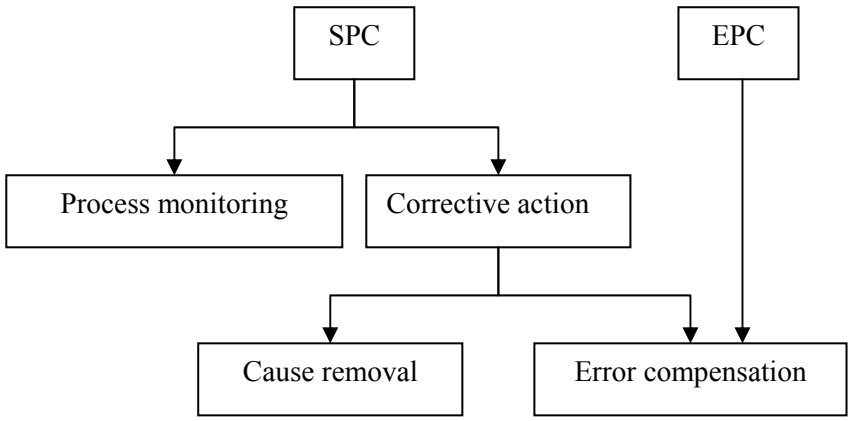

Figure 4.12: Functional combination of SPC and EPC (redrawn from Box et al.,1997)

The key idea behind SPC is to use a control chart to distinguish between two types of variation (common cause and assignable cause) so that the process can be identified as in statistical control or statistically out-of-control (Montgomery, 2005, MacGregor and Kourti, 1995). This control chart can be univariate or multivariate.

4.2.1. Univariate control chart

SPC was initiated by Walter A. Shewhart of the Bell Telephone Laboratories in the early 1920s. The first control chart proposed by Shewhart is known as the Shewhart Control Chart (Montgomery, 2005). In order to monitor a process using the Shewhart control chart, there are three phases, Phase I: data training, Phase II: model development and Phase III: monitoring new data. These phases are illustrated in Figure 4.13 where real data from an aluminium reduction cell from Aldel's aluminium smelter was used to plot the Shewhart control charts. Each phase is described below.

1) Phase I: Data training

Phase I was referred to as retrospective analysis by Montgomery (2005) and data training by Kourti (2005); the ultimate objective of the phase is to obtain in-control data or normal plant operating data by using the Shewhart control chart. These in-control data contain only common-cause variation. Common-cause variation is natural variability and an inherent part of the process (Montgomery, 2005).

2) Phase II: Model development

In order to use the Shewhart control chart for monitoring future production, the in-control data are used to develop the centre line (CL), the upper control limit (UCL) and the lower control limit (LCL) as shown in Figure 4.13 (a). The control limits are calculated using these equations (Montgomery, 2005) :

$$CL = \mu_w \tag{4-11}$$

$$UCL = \mu_w + L\sigma_w \tag{4-12}$$

$$LCL = \mu_w - L\sigma_w \tag{4-13}$$

where w is a sample statistic, μ_w is the mean of w, σ_w is the standard deviation of w and L is the distance of the control limits from the centre line, expressed in standard deviation unit (Montgomery, 2005).

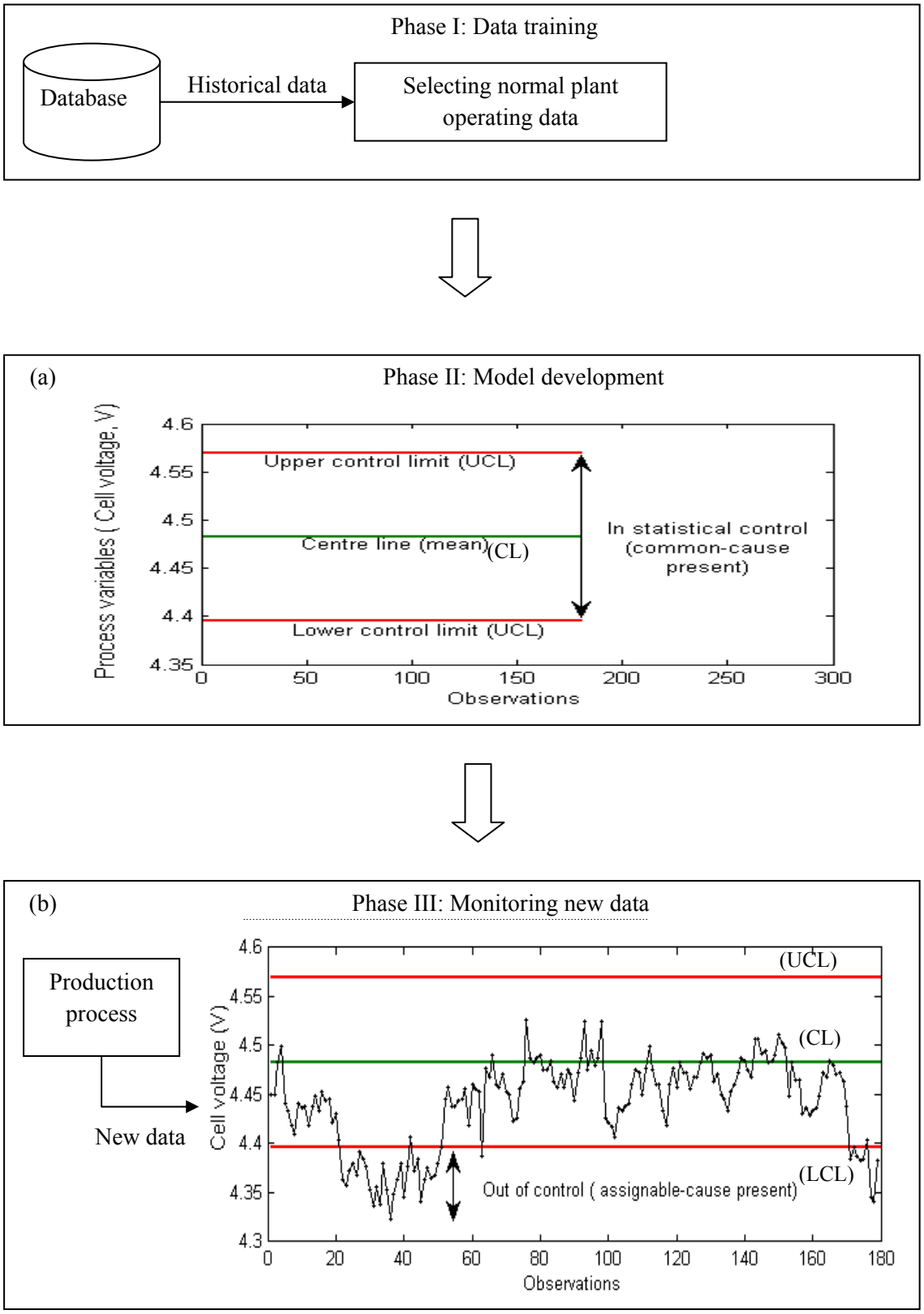

Figure 4.13: The Development of an Individual Shewhart Control Chart: (a) Control Limits of the Charts and (b) monitor New Data with Out-of-control signals

3) Phase III: Monitoring new data

After developing a control chart with control limits as shown in Figure 4.13 (a), it can then be used to monitor new data emanating from the production process. When the new data point falls between the upper and the lower control limits, the process is in a state of statistical control where only common-cause variation is present. However, when new data points violate the control limits as shown in the Shewhart control chart for cell voltage in Figure 4.13(b), the process is out-of-control. These instances of control limit violation show the presence of unusual sources of variability known as assignable causes where a cause may be assigned to the variability (Guh, 1999). Early detection, using a control chart, of this assignable cause is the main objective of SPC where this form of detection will give a signal to the process engineer to start an investigation into the causes of any the variations in the production process and to take corrective action before it is too late, thus ensuring the continued maintenance of product conformity.

4.3. Multivariate Statistical Process Control (MSPC)

The efficiency of the detection of assignable causes using control charts depends on the selected perspective, either univariate or multivariate. From a univariate perspective, each variable is monitored using a univariate control chart, either the Shewhart control chart for detecting large shifts or the cumulative sum (or cusum) and Exponentially Weighted Moving Average (EWMA) control chart for detecting small shifts (Montgomery, 2005). However, if there is more than one variable that needs to be monitored simultaneously, and if the monitored variables are highly correlated, the selection of the control chart should be based on a multivariate perspective in order to reduce failed alarms (type 2 errors). This procedure is known as Multivariate SPC (MSPC).

4.3.1. Multivariate control charts (Hotelling's T^2, MCUSUM, MEWMA)

In MSPC, the traditional control charts are extended to include Hotelling's T^2 for the Shewhart control chart, Multivariate EWMA (MEWMA) and Multivariate cusum (MCUSUM) for EMWA and cusum charts, respectively.

Figure 4.14 illustrates the MSPC environment using the Hotelling's T^2 chart where real data from six process variables from an aluminium reduction cell were used to plot the charts. The covariance matrix (**S**), the sample mean vector ($\bar{x}$) and the control limits were calculated from the in-control data obtained from Phase I. The equation for calculating the T^2 values for process monitoring is given below (Montgomery, 2005):

$$T^2 = (x - \bar{x})S^{-1}(x - \bar{x}) \tag{4-14}$$

When the number of in-control data points/samples is more 100 (m> 100), the equation to calculate the control limit is (Montgomery, 2005) :

$$UCL = \frac{p(m-1)}{m-p} F_{\alpha}, p, m - p \tag{4-15}$$

where p is the number of process variables and m is the sample number.

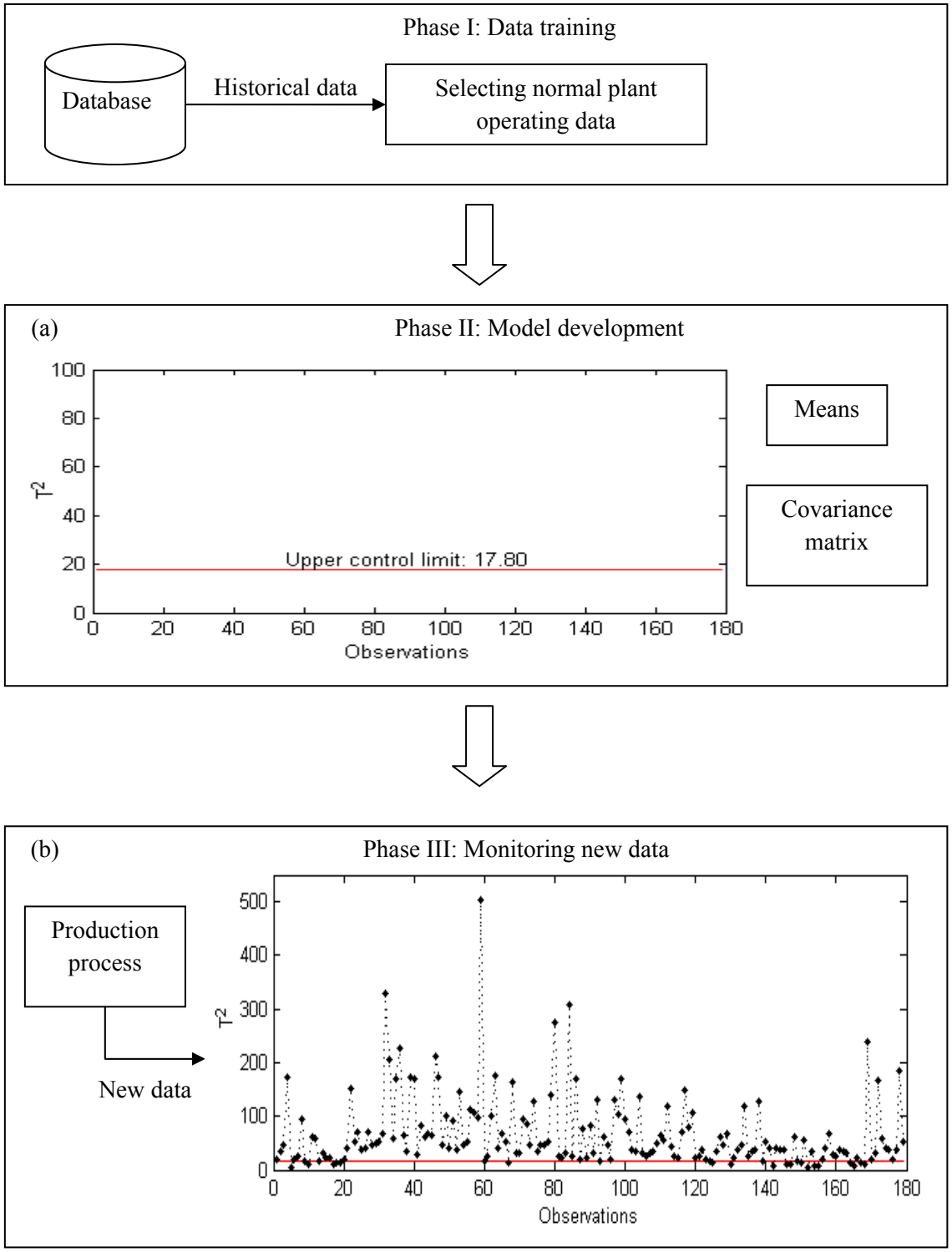

Figure 4.14: The development of the Hotelling's T^2 Chart in a MSPC Environment: (a) Control limits of the charts and (b) Monitor New data with Out-of-control signals

4.3.2. Multivariate control chart based on PCA (or latent variables)

A large number of variables (more than 10) lead to the application of the multivariate control chart based on latent variables. This chart has revolutionised MSPC since it was introduced more than 15 years ago (Kourti, 2005) because of its ability to look at the maximum variability of manufacturing data. The direction of maximum variability in which the process moves about can be revealed by using PCA or PLS and this direction is used to transform the original variables into a new set of latent variables (Montgomery, 2005). The main variability pattern can be captured by a few latent variables (the number of which is less than the number of original variables).

As illustrated in Figure 4.15, in-control data from Phase I are used to develop the reference set in Phase II which includes: means, standard deviations, eigenvectors, eigenvalues and control limits. When new data become available in Phase III, the total variance from the extracted principal components is visualised in the Hotelling's T^2 chart based on the latent variables. The rest of the variability is observed in a Squared Prediction Error (SPE) chart also known as a distance to model chart. In addition, there is an additional phase (Phase IV) in this environment where a diagnosis tool can be generated from the PCA model using a contribution plot and this phase is called fault diagnosis. Phase I, II and III will be discussed in this section. However, Phase IV will be discussed in section 4.7.1.

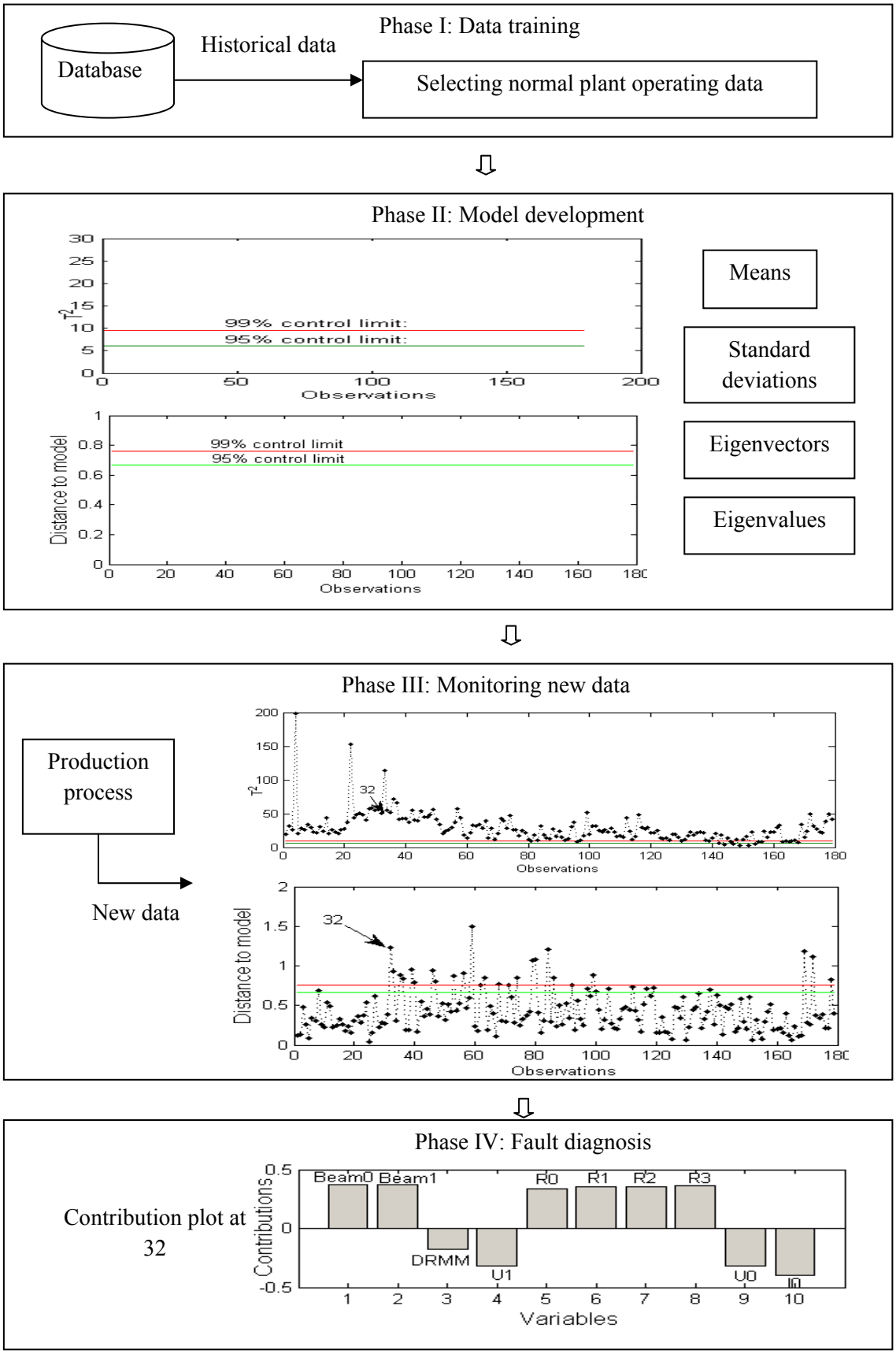

Figure 4.15 Multivariate Charts based on Latent Variables

1) Phase I: Data training

In data training, in-control data are collected from historical databases. Figure 4.16 shows the procedure to obtain in-control data. First, PCA is applied to a data matrix $\mathbf{X_{old}}$ that contains data relating to when the performance of the process has been acceptable. PC scores for $\mathbf{X_{old}}$ that move away from the main cluster in a score plot are removed. After data with large deviations has been removed, the data matrix is identified as in-control data matrix **X** and can be used to derive an empirical model (Nomikos and MacGregor, 1995b).

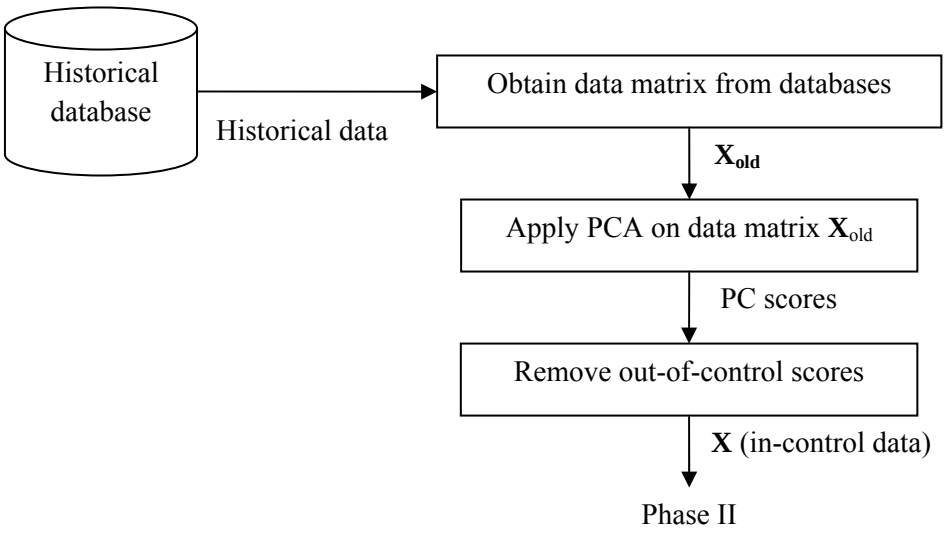

Figure 4.16: A Procedure for Data Training

2) Phase II: Model development

PCA is applied to the data matrix **X** (K x J) so that it is decomposed into **T** (K x R) and **P** (J x R) as in equation 4-1. The matrix **P**, which represents the loading matrices, its variances (s), scaling information, means and scalar limits for the Hotelling's T^2 and SPE charts, is used to form the reference distribution of in-control data, or in other words to be a guideline to monitor other data. PCA has been used to extract R latent variables from historical databases consisting of J process variables, to model most of the process variability using a value of R that is less than the value of J (Kourti, 2005).

3) Phase III: On-line process monitoring

The overall procedure for on-line process monitoring is illustrated in Figure 4.17. The four main steps of this procedure are described below.

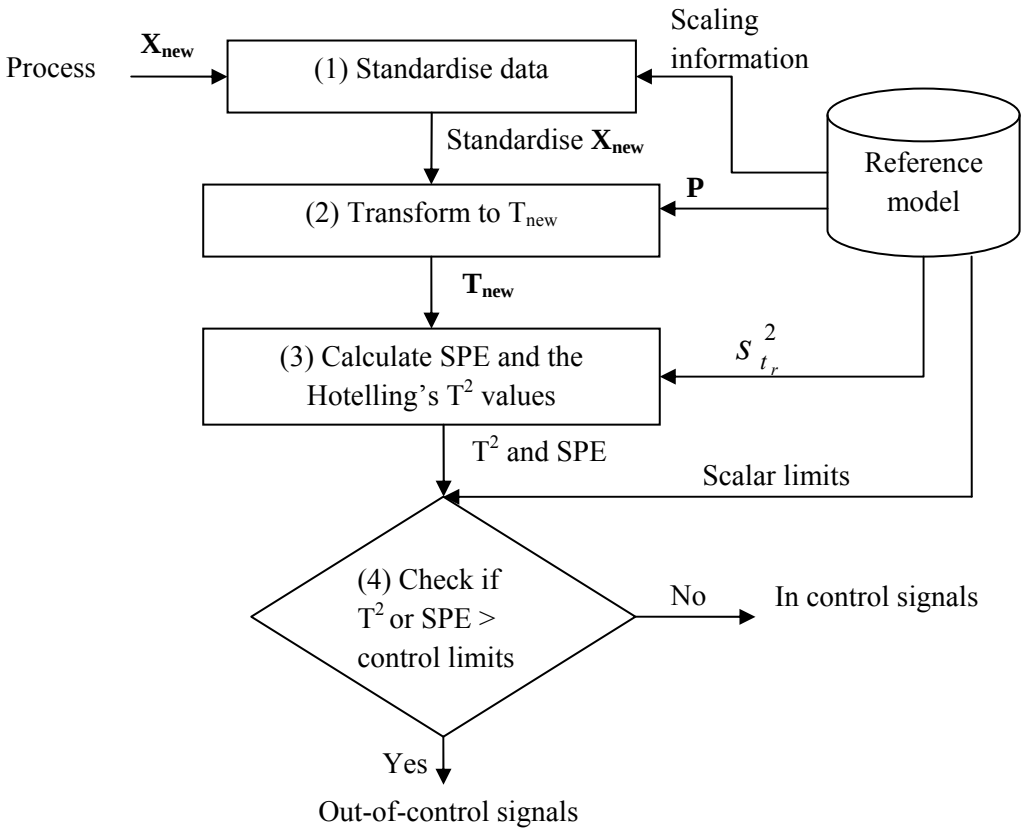

Figure 4.17: Overall Procedure for Process Monitoring

Firstly, new data $\mathbf{X_{new}}$ (1 x J) from a process are standardised using scaling information. Secondly, these data are transformed to scores, $\mathbf{T_{new}}$ (1 x R) using the $\mathbf{P}$ (J x R) from the reference set of in-control data. The equation for the transformation (Nomikos and MacGregor, 1995b) is:

$$T_{new} = X_{new} P \tag{4-16}$$

Thirdly, the scores are used to calculate T^2 to form the Hotelling's T^2 chart based on PCA and the equation to calculate the T^2 statistic (Kourti, 2005) is:

$$T^2 = \sum_{r=1}^{R} \frac{t_r^2}{s_{t_r}^2} \tag{4-17}$$

where $s_{t_r}^2$ is the estimated variance of the corresponding latent variable t_r (Kourti, 2005).

Hotelling's T^2 chart detects small shifts and deviations from the process using the reference distribution for in-control data. However, the process is monitored using the feature vector comprising only of the retained PC loading vectors (*R*). Therefore, there is a need to monitor the residual between original data and data defined by the feature vector to detect large deviation. As a result, the residual is part of the decomposition when applying PCA to a data matrix $\mathbf{X_{new}}$. The residual is given as:

$$e = X_{new} - \hat{X}_{new} \tag{4-18}$$

where

$$\hat{X} = T_{new} P' \tag{4-19}$$

(Nomikos and MacGregor, 1995b).

Squared Prediction Error (SPE) chart or also known as the Q-statistic (Jackson, 2003) is used to monitor the residual (Kourti, 2005):

$$SPE_k = \sum_{i=1}^{k} (x_{new,i} - \hat{x}_{new,i})^2 \tag{4-20}$$

Finally, abnormal events are detected when the calculated variation violates the upper control limits of T^2 and SPE statistic. The T^2 upper limits are calculated using reference data and are given by:

$$T^2_{UCL} = \frac{(n-1)(n+1)R}{n(n-R)} F_\alpha (R, n-R) \tag{4-21}$$

where *n* is the number of observations used to account for normal variation, *R* the number of components used in the model and $F_\alpha(R,n-R)$ is the critical value for an *F* distribution with

R and *n-R* degrees of freedom at the *1-α* confidence level (Nomikos and MacGregor, 1995b). The upper control limits for SPE statistics are given by:

$$Q_\alpha = \theta_1 \left[1 - \frac{\theta_2 h_o (1 - h_o)}{\theta_1^2} + \frac{z_\alpha (2\theta_2 h_0^2)^{1/2}}{\theta_1} \right]^{1/h_0} \quad (4\text{-}22)$$

where θ_m is the trace of the estimated covariance matrix of the model residuals, **V**, to the m^{th} power, for *m*=1, 2 and 3,

$$\theta_m = tr(V^m) \quad (4\text{-}23)$$

$h_0 = 1 - 2\theta_1\theta_3 / 3\theta_2^2$ and z_α is the normal variate at the $1-\alpha$ percentile and has the same sign as h_0 (Nomikos and MacGregor, 1995b).

4.3.3. Multivariate control chart based on MPCA

The PCA model for a dynamic process such as the aluminium electrolysis process should consider the dynamic behaviour of that process i.e. the time dependency in historically recorded variables of the process. However the projected data in the PCA model, namely the scores, summarise data at one point in time without taking into account the previous data values. The time histories of the process variables are not considered because each row in the data matrix **X** corresponds to the data for all the process variables at only one time instant and thus corresponds to the value of the scores. Considering previous values using time lagged data may lead to better fault detection because, not only has cross-correlation among the process variables been taken into account, but also the autocorrelation within each process variable (Ku et al., 1995).

Another way of developing multivariate dynamic data modelling, other than using time lagged data, is by using MPCA. Regular PCA is extended to MPCA by adding a third

dimension (*I*) to the, typically, two-dimensional data matrix, **X** (*K* x *J*) that as a result folds the **X** (*K* x *J)* into **W** (*I* x *J* x *K*), a 3-D data array. The third, *I* dimension depends on the dynamic pattern of the process under observation. For example, the third dimension can be: (1) a number of batches for monitoring batch processes (Nomikos and MacGregor, 1995b); (2) a number of start-up operations for monitoring process startup (Zhang and Dudzic, 2006); or (3) a number of grade-to-grade transitions for monitoring process transitions in a continuous process (Duchesne et al., 2002). All of these examples used the Multiway-PCA (extension of PCA) procedure detailed by Nomikos and MacGregor (1995b). The MPCA procedure is further described briefly as follows:

1) Phase I: Data training.

Process data organized in a three dimensional data array, **W** (*I* x *J* x *K*) (*I*=number of batches or windows, *J*=number of variables, *K*=observations gathered from a batch of data or collected from a time window), are unfolded and rearranged into a huge two-dimensional data matrix, **X**(*I* x *JK*) where the target trajectories for each process variable are derived from their average values at each time interval over the batches or windows. This way of unfolding is batch-wise where it is effective to capture variance for the duration of operations or daily patterns by taking into account all the auto- and cross-correlations among the variables (Kourti, 2003).

2) Phase II: Model development.

In order to develop a reference model for online process monitoring, **X** is first mean centred and scaled. Regular PCA is then applied to the data matrix using equation 4-1 where **T** (*I* x *R*) is a matrix of latent variables scores, **P** (*JK* x *R*) is a loading matrix for *R* latent variables and **E** is an error terms matrix (Nomikos and MacGregor, 1995b). The control limits for the multivariate control charts are also calculated (Nomikos and MacGregor, 1995b). Thus, the reference model contains crucial information for process monitoring, namely: mean-

trajectory, scaling, score vectors, loading vectors, variance and control limits for the monitoring control charts.

3) Phase III: Online process monitoring

When new data (J x K) become available from the process, the first step is to unfold the data to $\mathbf{X}_{new}$ (1 x JK). The mean-trajectory and standard deviation from the reference model are then used to mean-centre and scale $\mathbf{X}_{new}$. Finally, $\mathbf{X}_{new}$ are transformed into new scores, $\mathbf{T}_{new}$ (1 x R),using the loading vectors, $\mathbf{P}$ (JK x R), from the reference set as in equation 4-16. Any abnormalities resulting from the new scores ($\mathbf{T}_{new}$) are then detected using a score plot, Hotelling's T^2 chart and a Squared Prediction Error (SPE) chart.

a) Score plot

The movement of the new scores in the hyperplane defined by the reference model can be observed in a score plot. The changes within the operation can be investigated by observing how the transformed scores moved in the hyperplane defined by the reference model.

b) Hotelling's T^2 chart

The variations of the new scores in the hyperplane defined by the reference model are calculated using the Hotelling's T^2 statistic (also called the D statistic):

$$D = t_R{}' S^{-1} t_R I/(I-1)^2 \tag{4-24}$$

where $\mathbf{t_R}$ is the vector containing the R retained components of the model and $\mathbf{S}$ represents the covariance matrix of the R retained score vectors. Abnormal events are detected when the calculated variation violates the upper control limits of this statistic (Nomikos and MacGregor, 1995b).

c) SPE chart

The variations of the new scores, $\mathbf{T}_{new}$ out of the hyperplane defined by the reference model are based on the residual of the model which is the difference between the original

values, $\mathbf{X_{new}}$ and estimated values of the model, $T_{new}P'$. The SPE value at time interval k (k=1, 2, …, K) is calculated using equation 4-25 in order to monitor the instantaneous perpendicular distance of a batch from the model (Nomikos and MacGregor, 1995b).

$$SPE_k = \sum_{c=(k-1)J+1}^{kJ} e(c)^2 \tag{4-25}$$

The abnormal events are detected when the calculated variation violates the upper control limits for the SPE chart (Nomikos and MacGregor, 1995b).

4.4. The rationale for using multivariate control chart based on MPCA for fault detection in the aluminium smelting process

There are two main reasons for using multivariate control charts based on MPCA: (1) advanced detection capabilities of the multivariate charts and (2) research movement in the process control of the aluminium smelting process.

4.4.1. Advanced detection capabilities of the multivariate charts

The capabilities of the multivariate and univariate charts in detecting faults are summarised in Figure 4.18. The change in the perspective from univariate to multivariate is driven by the number of correlated variables that needs to be monitored simultaneously. The larger the number of monitored variables, the less effective is the fault detection using univariate charts. When the number of variables is more than ten, multivariate control charts based on latent variables have better detection capabilities than do multivariate control charts based on the extension of traditional univariate control charts. Furthermore, multivariate control charts based on latent variables (e.g. PCA and PLS) are well studied and industrial applications have been reported. For example, according to John F. MacGregor, a keynote speaker during FOCAPA 2008 in Boston USA, Fonterra in New Zealand recently installed a ProSensus

Multivariate, a software based on latent variables for analysing historical dataset, monitoring processes, diagnosing problems and many more.

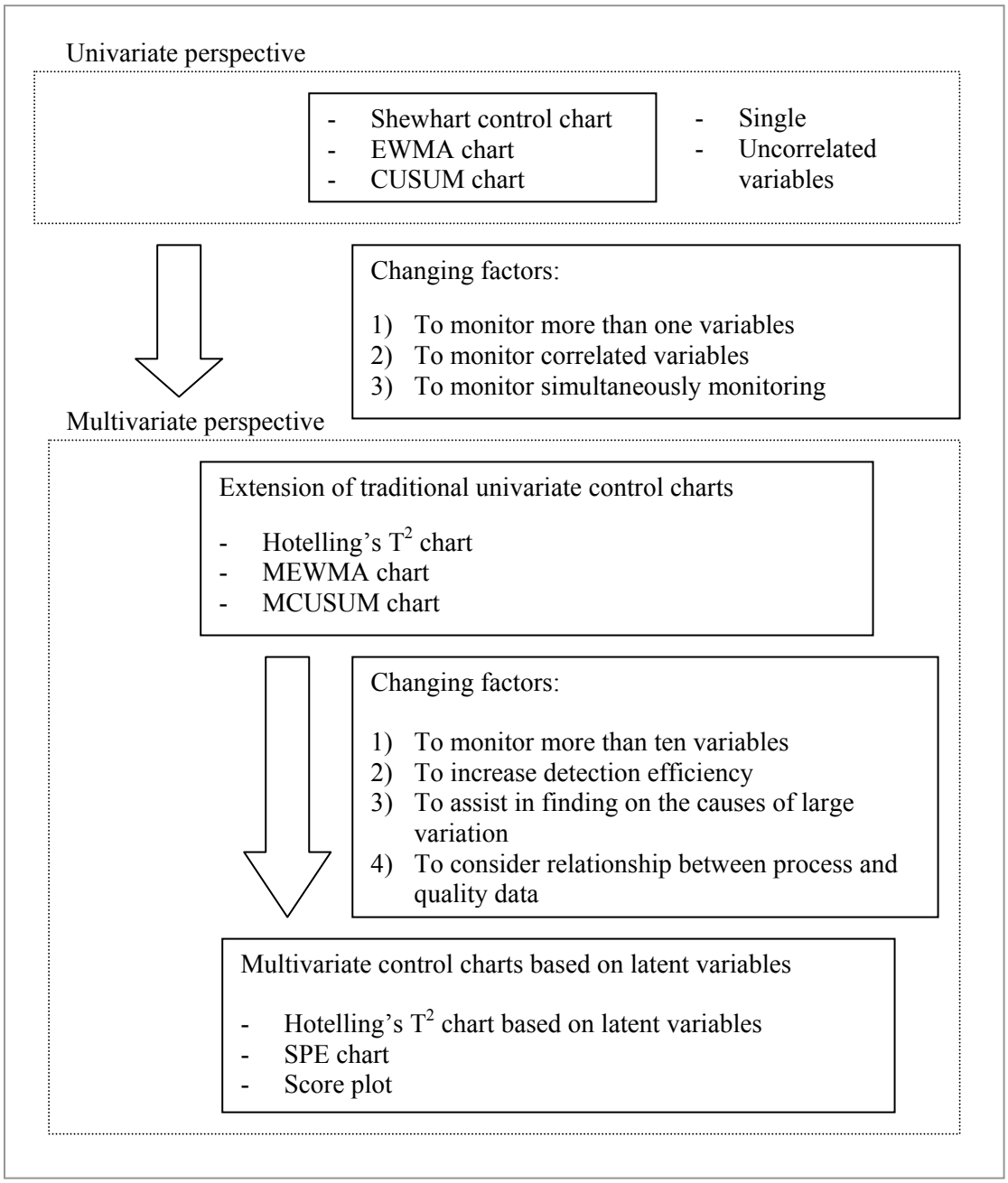

Figure 4.18: Summary of Changing Factors from Univariate to Multivariate Perspective

The main reason for using the multivariate control charts based on latent variables stated by MacGregor and Kourti (1995), who might be considered to be the leading researchers in PCA-based process monitoring, was:

> *Multivariate control charts in the projection spaces provide powerful methods for both detecting out-of-control situations, and diagnosing assignable causes, and they are applicable for both continuous and batch processes. The only requirement for applying these methods is the existence of a good database on past operations. (p.413).*

Other reasons for using a multivariate control chart based on latent variables include: (1) it can assist in finding the causes of large variation, (2) it can consider the relationship between process and quality data (e.g. PLS), and (3) it can increase detection efficiency. In terms of detection efficiency, PCA can be extended to MPCA, thus removing the dynamic component in the data. In the procedure for use of the multivariate control chart based on MPCA, the unfolding and rearranging explained in the data training phase (section 4.3.3) are the key steps for allowing target trajectories to be derived from observations gathered from a batch of data or collected from a time window. The procedure is based on research done by Nomikos and Macgregor (1995b) that explained:

> *This unfolding is particularly meaningful because, by subtracting the mean of each column of this matrix X, we are in effect subtracting the mean trajectory of each variable, thereby removing the main nonlinear and dynamic components in data. A PCA performed on these mean-corrected data is therefore a study of the variation in the time trajectories of all the variables in all batches about their mean trajectories (p.43).*

The advantage of modelling the deviations from the target trajectory was also pointed out by Kourti (2003) is converting a non-linear problem to a linear one so that it is easy to tackle with linear latent variable methods such as MPCA and MPLS. Thus, this advanced capability is one of the reasons for using multivariate control charts based on MPCA in this thesis. In fact, the MPCA procedure described in section 4.3.3 was used as a general framework in this thesis because the relationship between pseudo-resistance and alumina concentration is also non-linear and also, the variability pattern based on the curves can be observed within a defined duration (underfeed-overfeed cycle).

4.4.2. Research movement in the process control of the aluminium smelting process

Figure 4.19 shows an overview of process control strategy that might be employed for aluminium reduction cells. In this strategy, a single variable from an aluminium reduction cell is monitored using EPC and SPC approaches. The multivariate characteristics of the aluminium reduction cell (section 2.3.1 in Chapter 2) have been incorporated into some of the model-based controls for EPC (e.g. Stevens McFadden et al., 2006 and Moore and Urata, 2001) as it is recognised that multivariable characteristics are very important factors needing consideration. For example, Stevens McFadden et al. (2006) considered five process variables in their multivariable model-based controller that was made of a state estimator (Kalman filter) and an optimal state feedback controller. Thus, it can be seen that EPC in aluminium processing research is moving towards multivariable control.

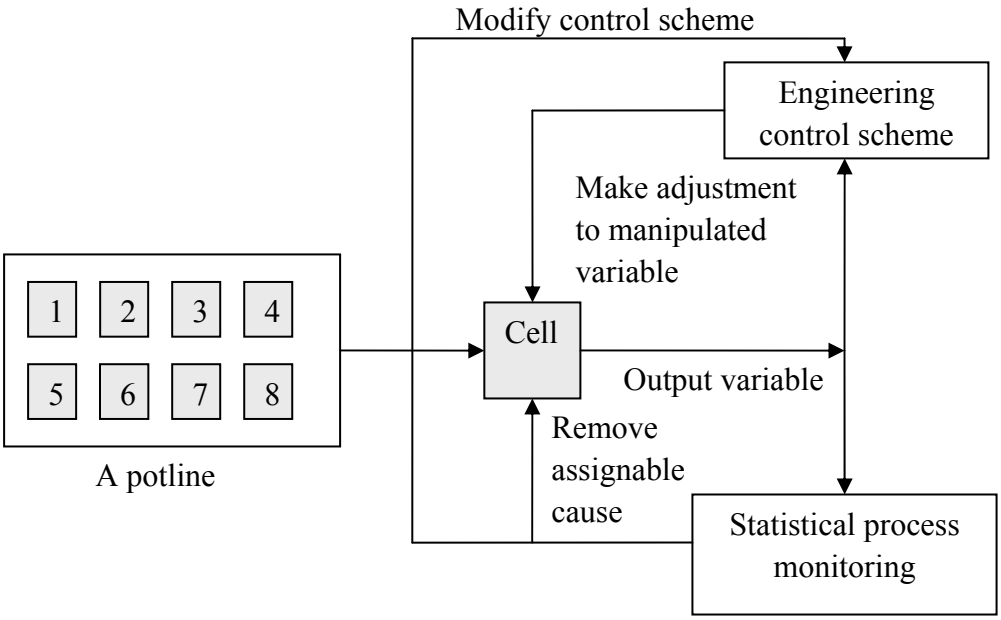

Figure 4.19: An Overview of Process Control Strategy of Aluminium Reduction Cells incorporating both EPC and SPC (adapted from Montgomery, 2005)

As EPC research is moving towards multivariable control in aluminium processing, SPC is also moving in the same direction. Stam et al. (2007) have considered multivariate characteristics in a model-based control strategy with cause removal functions, and a popular

multivariate control chart, Hotelling's T^2 chart, has been used for monitoring the aluminium electrolysis process. Hotelling's T^2 chart appears to be effective in preventing false alarms (Type I error) and failed alarms (Type II error) and particularly for monitoring the two process variables, temperature and excess AlF_3 (Chen and Taylor, 2005). Process monitoring using the Hotelling's T^2 chart is extended to three process variables where the third variable is alumina feeding (Stam et al., 2008). Process monitoring using multivariate control charts based on PCA were then used to detect faults within the cells using data from 65 variables (Tessier et al., 2009). However, there is still a lack of research in the multivariable control area for both EPC and SPC. This thesis, therefore, investigates multivariable control for SPC where control charts based on MPCA have been used in a proposed framework that incorporates the dynamic behaviour of the two important events of anode changing and alumina feeding during the aluminium smelting process.

4.5. Conclusions for Part I

Although there are many fault detection techniques, the use of multivariate control charts based on MPCA for monitoring the aluminium smelting process is the best option because the dynamic behaviour of the process is considered and the control charts are easily understood by the operators. The control charts are easy to create since they are based mainly on historical process data and the difficulty of creating an accurate mathematical model can be avoided. The key to using these MPCA-based control charts is to monitor the dynamic pattern within an alumina feeding cycle, as discussed in Chapter 2. In other words, the alumina feeding cycle is treated as a batch using MPCA.

The current focus is therefore on the investigation of producing a suitable framework on which to apply an MPCA-based fault detection system for addressing the first research question. A practical framework should be designed in order to consider the dynamic

behaviour during alumina feeding and anode changing. Every step in the process of developing the MPCA based system should be addressed, such; as selecting process variables, identifying strategies for trajectory alignment and developing reference models that explain variability patterns within feeding cycles. This will be discussed in detail in Chapter 5 and 6.

Part II: Multivariate Statistical Methods for Knowledge Discovery

4.6. Knowledge Discovery from Databases (KDD)

According to Fayyad et al. (1996), KDD is defined as "the non-trivial process of identifying valid, novel, potentially useful, and ultimately understandable patterns in data". The KDD in this thesis is aimed at discovering abnormal patterns related to abnormal events using data from historical databases. These abnormal patterns can be utilized to develop a fault diagnosis system. In order to identify these abnormal patterns, a typical procedure for KDD (Wang, 1999) was used as a guideline. This procedure is briefly given below.

A typical procedure for KDD (Wang, 1999)

1) Developing an understanding of the application domain.
2) Creating a target data set.
3) Data pre-processing and cleaning.
4) Data reduction and projection.
5) Choosing the data-mining task.
6) Choosing the data analysis algorithms.
7) Data mining.
8) Interpreting mined patterns.
9) Consolidating the discovered knowledge.

Data mining is one of the important steps in the KDD procedure. In this thesis, PCA has been used as a data mining tool by clustering scores with similar characteristics in a score plot. PCA was also used in step 4 in order to reduce and project data. The application of PCA in KDD is given in section 6.3 in Chapter 6.

Part III: Multivariate Statistical Methods for Fault Diagnosis

Multivariate statistical techniques were selected to develop a diagnosis system in this thesis. This diagnosis system is a capstone tool for an MPCA-based fault detection system. The use of PCA/PLS for detecting when a fault has occurred is now well established (Yoon and MacGregor, 2001). The PCA-based detection system has been selected for monitoring the aluminium smelting process (section 4.4) where out-of-control signals can be detected when their values exceeded the 95% or 99% control limits in the two multivariate control charts, Hotelling's T^2 and SPE charts. However, this fault detection system is less capable for diagnosing faults. This is because it uses non-causal model that has been developed from normal operating data (MacGregor et al., 2005). A diagnosis system should be used to diagnose out-of-control signals provided by the PCA-based fault detection system; this will be discussed in the following sections.

4.7. Fault diagnosis techniques

Various types of diagnostic algorithms are used to diagnose out-of-control signals provided by the PCA-based fault detection system. The diagnostic algorithms began simply by using the information from a PCA-based model. More complex diagnostic algorithms were then developed by integrating an additional tool into the existing PCA-based detection model. Figure 4.20 indicates these two separate groups where the first group is using the information from the PCA-based detection model and the second group is integrating an additional tool to the PCA-based detection model.

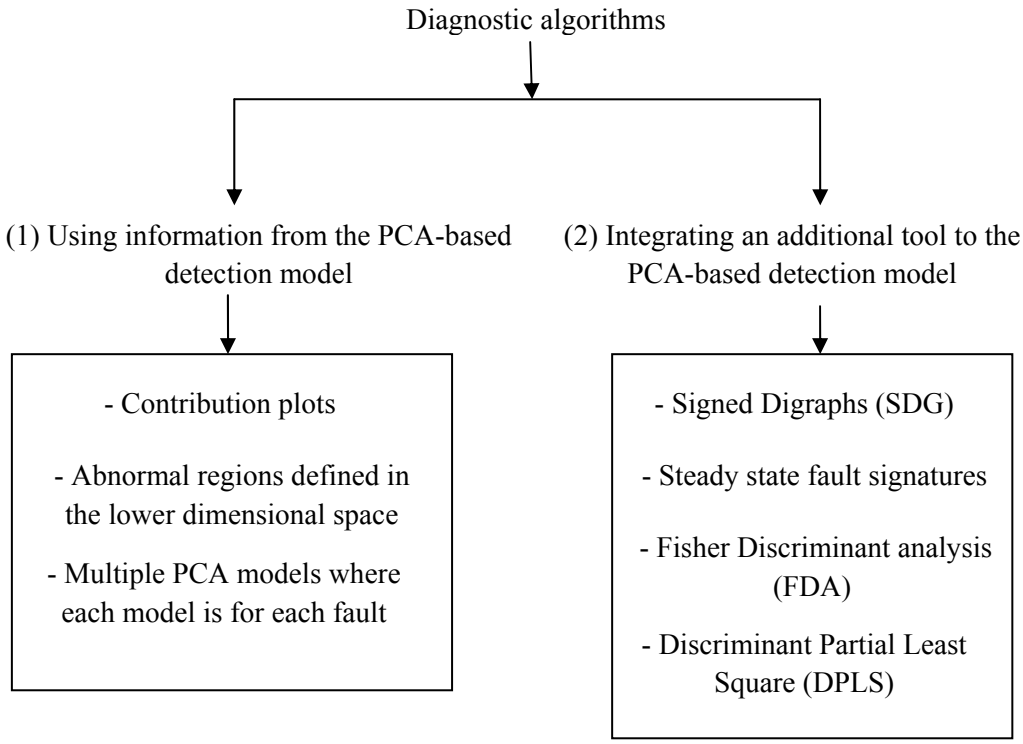

Figure 4.20: Diagnostic algorithms for Diagnosing Out-of-control signals from a PCA based Fault Detection System

4.7.1. Using information from the PCA/PLS model

In the first group, the fault diagnosis techniques using information from the PCA/PLS model include: (1) using contribution plots (Nomikos and MacGregor, 1994), (2) abnormal regions defined in the low-dimensional space (Romagnoli and Palazoglu, 2006), and (3) multiple PCA models where each model is for each fault (Raich and Cinar, 1996). A brief explanation of each approach is given below.

1) Contribution plots

With traditional SPC methods, when there is an out-of-control signal in the control chart, quality practitioners will try to diagnose an assignable cause. Multivariate charts based on PCA, however, can give more information about the assignable causes. In other words, these methods have more capability in diagnosing the sources of variation. For example, at the point when an event has been detected, the contribution of each variable to the event can be

extracted for the Hotelling's T^2 and the SPE chart from a PCA model. The contribution plot for the Hotelling's T^2 chart is given by:

$$c_j = p_{q,j}(x_{new,j} - \bar{x}_{new,j}) \tag{4-26}$$

where c_j is the contribution of the jth variable at the given observation, $p_{q,j}$ is the loading of this variable to the score of the principal component q and $\bar{x}_j$ is its mean value (Kourti, 2005). The contribution plot for the SPE chart is given by:

$$d_j = (x_{new,j} - \bar{x}_{new,j})^2 \tag{4-27}$$

where d_j is the contribution of the jth variable at the given observation (Kourti, 2005). These contribution plots do not show causal relationships. They only reveal which group of variables and which part of the plant, are related to the movement or event that occurred. However, by narrowing down the possible variables and event location in the plant, it is usually much easier for the engineer or operator to diagnose some possible reasons for the event (MacGregor et al., 2005).

2) Abnormal regions defined in the monitoring charts

Abnormal regions were defined in the monitoring charts based on the training cluster method. Figure 4.21 shows the procedure for the PCA-based diagnosis method. In data training, past data are used to build up the clusters related to abnormalities in a PCA model (Romagnoli and Palazoglu, 2006). The cluster formed in the plot can be used to detect future faults. To detect anode spikes, for example, the cluster that is formed corresponding to an anode spike in the score plot can be defined as the anode spike area. On the other hand, the area for scores related to the data without anode spikes is defined as a normal area. When new scores enter the anode spike area, an anode spike is predicted to occur in the process.

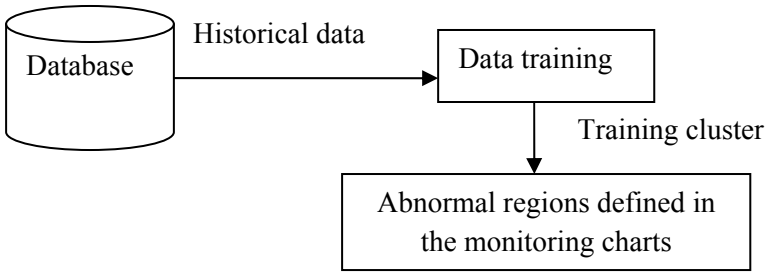

Figure 4.21: Procedure for developing Abnormal Regions defined in the Monitoring Charts

3) Multiple PCA models where each model is for each fault.

Multiple PCA models are developed where each model is for a particular fault. When there is control limit violation in the PCA model, the type of fault is identified by calculating the score and residuals tests, and the disturbance with maximum discriminant is selected as the fault which may potentially occur (Raich and Cinar, 1996).

4.7.2. Integrating an additional tool with the PCA model

In the second group, the additional tool can be further described as non-PCA based methods. The use of non-PCA-based methods integrated with the PCA-based detection model is gaining increasing interest from industrial sources. These additions have enhanced the diagnostic capability of PCA. Non-PCA-based methods include:

1) Signed Digraphs (SDG) (Vedam and Venkatasubramanian, 1999). These are used to investigate the root cause of a fault by using a cause-effect model that captures the information flow in the cause–effect relationship and also the directions of the effects (Mauryaa et al., 2004).
2) Steady-state signature. This is used to isolate a fault by comparing the fault signatures (vector of movement in both the model space and the residual space) of the new event to the corresponding fault signatures of known faults in the fault library (Yoon and MacGregor, 2001).

3) Fisher's Discriminant Analysis (FDA). This is used to classify multiple fault classes by using a set of projection vectors that maximize the scatter between the classes and minimize the scatter within each class (Chiang et al., 2000).
4) A PLS version of LDA (PLS-DA) (Wold et al., 2001) also known as DPLS (Chiang et al., 2000), has the ability to model the relationship between the process data and the class of faults so that any future fault can be predicted from the new out-of-control signals from the process.

4.8. Rationale for using multivariate statistical methods: pre-identified abnormal regions and DPLS for aluminium smelting process

There have been a number of fault diagnosis techniques that have been developed, as shown in the two separate groups in the previous sections. In this thesis, two multivariate statistical methods, selected from each group, have been used. They are: (1) pre-identified abnormal regions from group 1, and (2) DPLS from group 2.

4.8.1. Pre-identified abnormal regions from group 1

Although approaches in group 1 are less successful for diagnosing a complex fault, pre-identified abnormal regions were chosen for this thesis because they can be used to diagnose simple faults and visualise the movement of abnormal scores using a score plot. However, in this thesis, the approach was modified by using pre-identified abnormal regions defined in a new PCA fault model instead of using an existing PCA model. The boundaries for this problem area were then identified. The procedure for this approach is given in detail in section 7.3.1 in Chapter 7.

4.8.2. DPLS from group 2

DPLS method was also chosen in this thesis for fault diagnosis. Other methods from group 2 were not used because firstly, SDG has disadvantages, the major one being the generation of

false solutions (Venkatasubramanian et al., 2003a). Secondly, steady-state signatures need additional information such as the fault signatures of known faults. Finally, although FDA is superior than PCA and PLS for classification with its slightly more complex algorithm, it has been less adopted for process monitoring (Chiang et al., 2000). In fact, the research efforts in PCA/PLS based process monitoring date back more than a decade. Since the use of PCA and PLS for multivariate process monitoring is more practical and widespread, PCA/PLS was used in this thesis. However, a future study investigating the use of FDA for monitoring the aluminium smelting process would be very interesting.

In addition, DPLS method was used in this thesis for three main reasons. The first reason is that DPLS method can solve the regression problem between **X** (predictor) and **Y** (predicted) for facilitating fault diagnosis. The second reason is that DPLS method has been found to be effective for a small-scale classification problem (Chiang et al., 2000) as in this study there were only four unnatural patterns of operating abnormalities in need of classification. Lastly, the fault detection system that provides the out-of-control signals is based on a data driven approach. The use of DPLS in fault diagnosis, which also uses multivariate statistical methods, results in a coherent approach in the overall system, especially for pre-processing data. The details of DPLS will be described in the following section.

4.9. DPLS

DPLS is a data reduction method that can be used to discriminate a block of process data (**X**) into a block of pre-identified faults (**Y**). The covariance between block **X** and **Y** for each extracted latent variable or component is maximised using DPLS (Chiang et al., 2000). The overview of DPLS by comparing to other PLSR applications is given in the beginning of this sub section. The procedure of DPLS for fault diagnosis is then presented.

4.9.1. Overview of DPLS

DPLS or PLS-DA is an extension of PLS-regression (PLSR) (Wold et al., 2001). The ability of PLSR to solve regression problems in a chemical processes enables many applications of PLSR to be used in different areas in process control, such as in process monitoring, predicting product quality and in fault diagnosis. The summary of each perspective is shown in Figure 4.22.

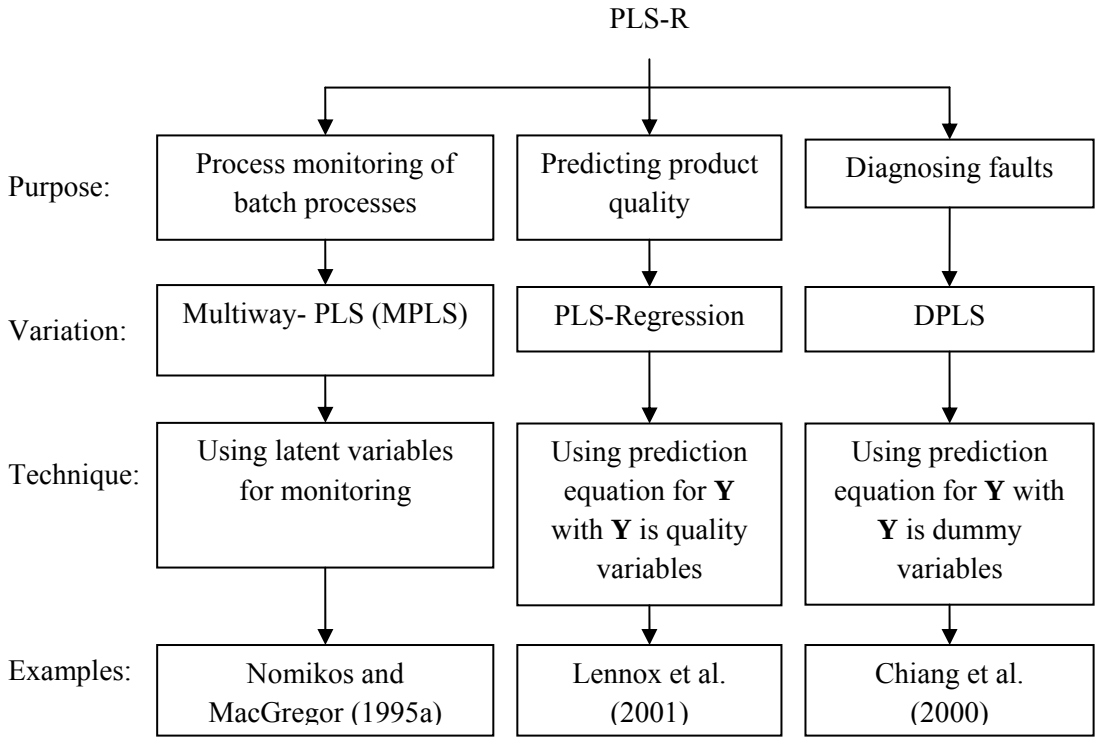

Figure 4.22: The use of PLS in Process Control

Firstly, in the process monitoring of batch processes, Multi-way PLS (MPLS) is used for extracting principal components from a three-way data array. These principal components are the most predictive of product quality and they are used for monitoring the process (e.g. Nomikos and MacGregor, 1995a). Secondly, in the prediction of product quality, PLS-R can be used to solve the regression problem between **X** (process variables) and **Y** (quality variables) so that the quality of the product can be predicted using a PLS-R model (e.g. Lennox et al., 2001). Thirdly, in diagnosing faults, DPLS extracts latent variables that have

maximum discriminatory ability so that it can be used to solve the regression problem between **X** (process variables) and **Y** (class of faults). This is different from the PCA system where the extracted latent variables have maximum variance in the process. Therefore, in fault diagnosis, DPLS has more power than PCA.

4.9.2. DPLS procedure for fault diagnosis

DPLS's overall procedure for fault diagnosis is shown schematically in Figure 4.23. The procedure for using DPLS for fault diagnosis can be divided into three phases: data training, model development and on-line fault diagnosis. A brief explanation of the phases is given below.

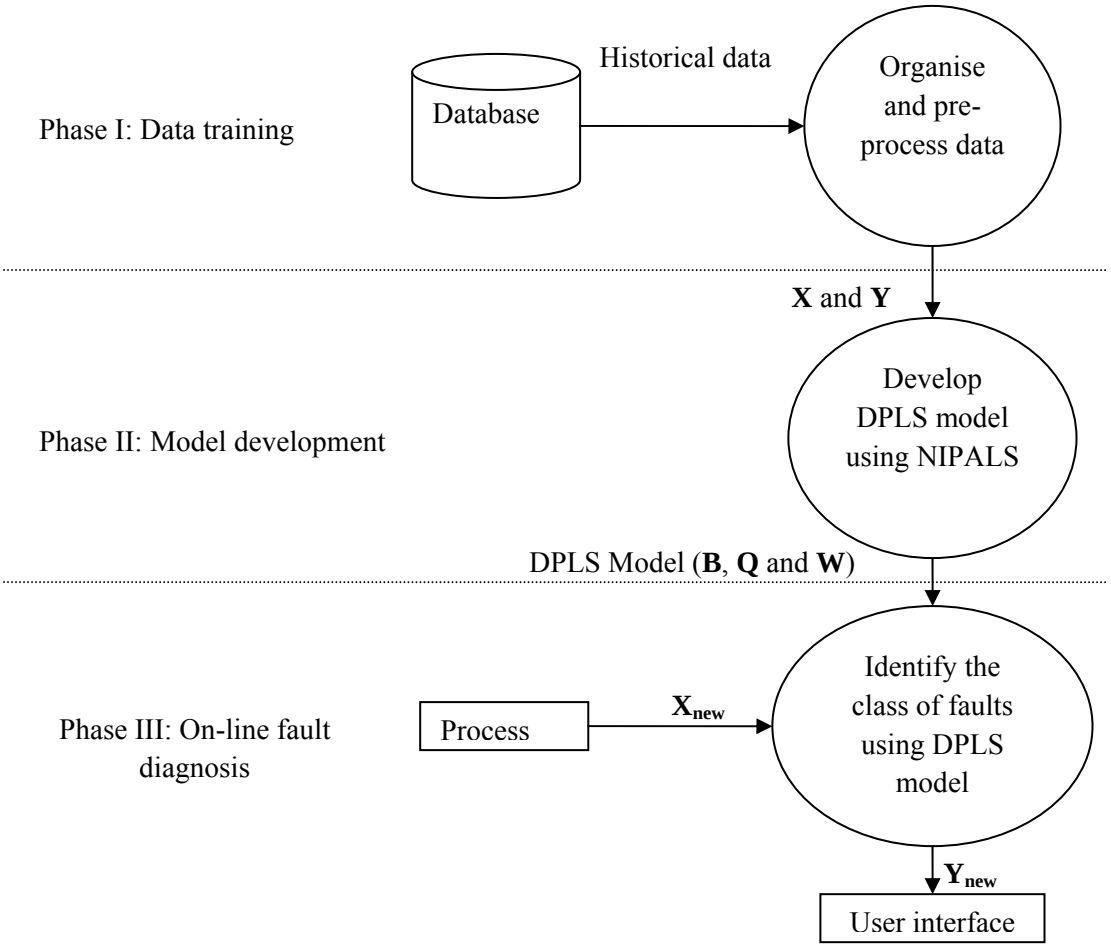

Figure 4.23: Basic Structure of DPLS for Fault Diagnosis

1) Phase I: Data training

Past data are collected according to pre-identified faults and organised into **X** (*J* x *K*) where *J* is number of process variables and *K* is number of observations. The class of faults (**Y**) are defined according to the organisation of data in **X**. If the past data is organised into a 3-D data array, two steps, unfolding and rearranging the 3-D data array to a 2-D data matrix, are applied here. In fact, this is the concept of Multiway-PLS (MPLS). The data matrix **X** is then pre-processed to mean centred and scaled the data.

2) Phase II: Model development

The DPLS model is developed using the NIPALS algorithm, a robust procedure for extracting latent variables from **X** and **Y**. The basic idea of this algorithm is to estimate parameters by forming new variables called X-scores and denoted by **t** (Wold et al., 2001). These X-scores are used as predictors of **Y** (Wold et al., 2001) because DPLS is a data decomposition method that maximises the covariance between the fault predictor (**X**) and predicted class of faults (**Y**) (Chiang et al., 2000). The NIPALS algorithm developed by Wold et al. (2001) is explained below.

<u>PLS algorithm</u>

1) Mean centre and scale **X** and **Y**
2) Set u equal to a column of **Y** or select a column vector, u_i of the matrix **Y**: $\mathbf{u=Y_i}$
3) In the X block:
   a) Regress columns of X on u : $\mathbf{w^T= u^TX/u^Tu}$
   b) Normalize w to unit length: $\mathbf{w=w/||w||}$
   c) Calculate the X-scores: $\mathbf{t = Xw/w^Tw}$
4) In the Y block:
   a) Regress columns of Y on t: $\mathbf{q^T= t^TY/t^Tt}$
   b) Normalize q to unit length: $\mathbf{q=q/||q||}$
   c) Calculate new u vector: $\mathbf{u = Yq/q^Tq}$
5) Check convergence on u: Calculate the difference between the previous scores and current scores. If the difference $|d|$ is larger than a predefined threshold, then return to step 3.

6) **X** loadings or the column of **X** are regressed on t_1 to give a regression vector: $\mathbf{p} = \mathbf{X}^T\mathbf{t}/\mathbf{t}^T\mathbf{t}$
7) Normalize **p** to unit length: $\mathbf{P}=\mathbf{p}/||\mathbf{p}||$
8) Normalize **t** to unit length: $\mathbf{T}=\mathbf{t}/||\mathbf{t}||$
9) Normalize **w** to unit length: $\mathbf{w}=\mathbf{w}/||\mathbf{w}||$
10) Find regression coefficient for inner relation: $\mathbf{B}=\mathbf{u}^T\mathbf{t}/\mathbf{t}^T\mathbf{t}$
11) Calculate residual matrices: $\mathbf{E_h}=\mathbf{E_{h-1}}-\mathbf{tp}^T$; $\mathbf{X}=\mathbf{E_h}$ and $\mathbf{F_h}=\mathbf{F_{h-1}}-\mathbf{b_h t_h q_h}^T$; $\mathbf{Y}=\mathbf{F_h}$
12) If additional PLS dimensions are necessary then replace **X** and **Y** by **E** and **F,** and go to steps 2.

This NIPALS algorithm is slightly different than the algorithm presented in section 4.1.2 in which a procedure to calculate a regression coefficient (**B**) by using two inputs, **X** (a set of predictor variables) and **Y** (a set of response variables) is provided. In this algorithm, the **X** is a matrix of process data and **Y** is a matrix of class labels. These **X** and **Y** matrices are decomposed as in equation 4-1 and 4-2. One of the advantages of using PLS is that the relationship between the class of data and the process data is modelled so that **Y** is the class of the faults for the future process data.

3) Phase III: On-line fault diagnosis

When new data $\mathbf{X_{new}}$ (1 x *J*) is detected as having an abnormality, the first step is to transform $\mathbf{X_{new}}$ to $\mathbf{T}_{new}$ as in equation 4-3. The DPLS model developed in Phase II is then used to diagnose the new data using:

$$Y = T_{new} BQ^T + F \tag{4-28}$$

where **B** is the regression matrix (Chiang et al., 2000). If MPLS is applied earlier in the data training, the new data will be $\mathbf{X_{new}}$ (1 x *JK*) so that variability pattern within a defined duration can be observed. Finally, the result which is the class of faults is shown to the end user via a user interface.

4.10. Conclusions for Part III

Since the relationship between pseudo-resistance and alumina concentration has been considered in selecting a fault detection technique, a capstone fault diagnosis system should also consider this relationship. Thus, in order to address the second research question, the pre-identified abnormal regions approach using the MPCA model, and classification using DPLS and the concept of MPLS, have been selected. This means by using these approaches, the alumina feeding cycle is also treated as a batch in order to observe the variability pattern within an alumina feeding cycle for fault diagnosis. This will be discussed in detail in Chapter 5 and 7.

CHAPTER 5: A NOVEL FAULT DETECTION AND DIAGNOSIS FRAMEWORK FOR THE ALUMINIUM SMELTING PROCESS

The novelty of this framework is that the use of MPCA and MPLS provides not only an indication as to whether the aluminium smelting process is in statistical control, but also enables the causes of out-of-control events to be known. This chapter will first describe the crucial design steps for this framework. One of the steps, the running of the pilot studies, is then explained in detail. Finally, the proposed framework is presented.

5.1. Important steps in the design of the framework

The design of the novel framework was developed following three important steps:
(1) processing and analysis of data from industry, (2) integration of knowledge received both from literature and operational experts, and (3) development of pilot studies.

5.1.1. Processing and analysis of data from industry

In the course of the study it was advantageous to have access to real-data from an aluminium smelting processing plant, Aldel's aluminium smelter. These data were not only continuous five minutes averaged sampled data, but also process data obtained at a frequency of once every two days and quality data at a frequency of once daily. The amount of process data received from the industry was quite large since the data were from a number of cells, more than ten, and also from various time periods, within the years of 2007, 2008 and 2009. The availability of real-data has directed this thesis to focus on using a data-driven approach which is a process history based method. The rationale for using this method has been discussed in section 3.2.2 of Chapter 3.

After obtaining real data from industry, the next step was to analyse the data in order to investigate whether faults could be observed from the data. Preliminary data analysis was done, such as using EWMA and Hotelling's T^2 charts. Process data with and without anode faults were used in this analysis. Firstly, the result obtained from using Hotelling's T^2 charts is shown in Figure 5.1. From the figure, it can be seen that darker points fall within Hotelling's T^2 control ellipse. These darker points represent cell 91 so that this cell can be identified as a normal cell whereas cell 87 is an abnormal cell. A cell is recognised as normal (normal cell) when the performance of the cell is acceptable, that is, having no recorded faults. A cell is considered to be abnormal (abnormal cell) when there one or more faults occur in it. Abnormal cells should have a higher percentage of impurities than normal cells while having a lower degree of current efficiency.

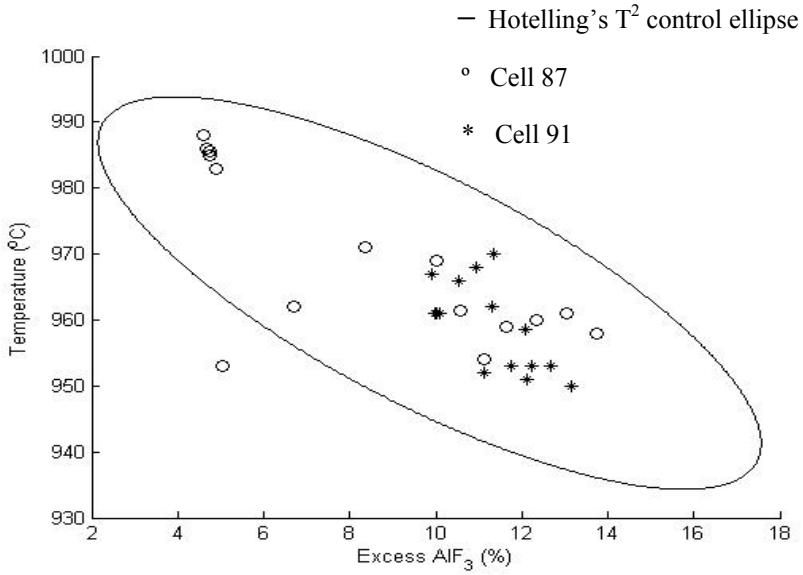

Figure 5.1: Comparison between Cell 87 (Abnormal Cell) and Cell 91 (Normal Cell)

The results obtained from using the EWMA chart are shown in Figure 5.2. In this figure, the voltage and alumina shot for normal and abnormal cells are compared, showing that the data for the normal cell are within the control limits for both voltage and alumina shot. This

illustrates that faults are observable from the data. Therefore, data without faults were used to develop reference models for fault detection. Data with recorded faults were used to develop reference models for fault diagnosis.

(a) Cell 87

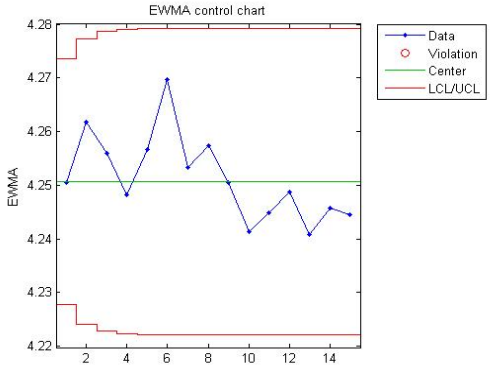

EWMA chart for voltage

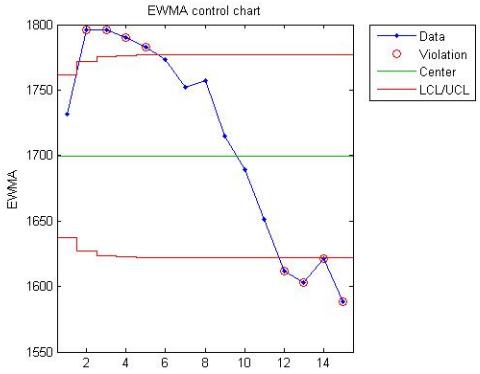

EWMA chart for alumina shot

(b) Cell 91

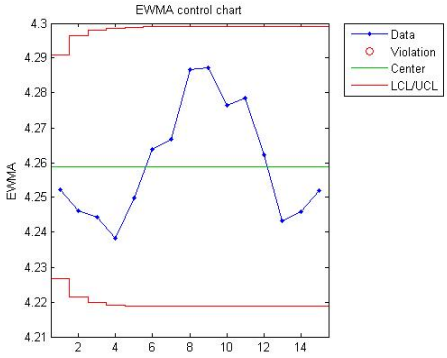

EWMA chart for voltage

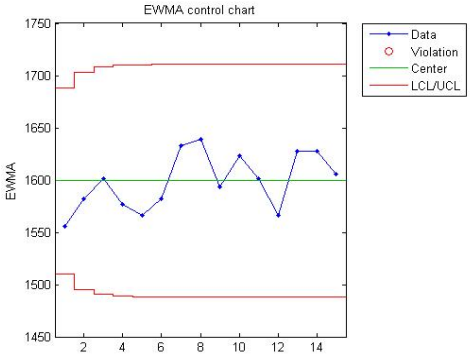

EWMA chart for alumina shot

Figure 5.2: Results for Cells: (a) 87 and, (b) 91

5.1.2. Integration of knowledge received from literature and operational experts

In the process of designing the novel framework for the fault detection and diagnosis system, firstly, knowledge from the literature were integrated based on the proposed fault detection and diagnosis system taxonomy (section 3.1). By referring to this taxonomy, the most important elements of the proposed system as discussed in section 3.2 are seen to be that:

- The knowledge domain is theoretical resistance/alumina concentration curves.
- The fault detection techniques are a statistical multivariate approach based on MPCA and MPLS.
- The usage frequency is continuous.

- The modes of interaction with operators are those of text and graphic.

Secondly, knowledge and advice from operational experts such as process engineers and operators were also integrated into the proposed system. The knowledge from the process engineers who have worked in aluminium smelters were received by:

1) One-to-one interviews

A one-to-one interview with a technical manager in an aluminium smelter helped to identify some important operational issues including: mechanism of anode spikes, detection of anode spikes in real-time operations, patterns of data observed from the operator screen and the accuracy of the proposed system in the detection of anode faults. In addition, one-to-one interviews and discussions with process engineers from the Light Metal Research Centre have enhanced the researcher's understanding, both theoretically and practically, of the process, particularly behaviour during alumina feeding and the importance of looking at feeding events in order to detect abnormal events (M. Taylor, P. Patel, M. Gustafsson, and P. Lavoie, personal communications, 2009).

2) Video conferencing

A video conference with the technical manager and operation engineer assisted in the identification of the most important elements for implementing the system in the smelter. This includes the analysis of further case studies to validate the proposed system, the identification of sources that are needed to run the system and the development of a system able to analyse data in real-time (P. Lavoie, M. Stam and A. Mulder, personal communications, September 23, 2009).

3) Email communication

Much of the communication with experts from the industry was by email. Many issues regarding the development of the system were solved using email, these included; multiple faults detection, impact of anode changing, impact of feeding control and collection of data from industry (M. Stam and A. Mulder, personal communications, 2008 - 2010).

5.1.3. Development of pilot studies

The main objective of the pilot studies was to address the problems identified in monitoring the aluminium reduction cells. The problems were: (1) parameters measured at a variety of frequencies (section 2.3.3) and (2) dynamic behaviour (section 2.3.4). In order to deal with these problems, two factors for effective monitoring have been recognized. The first factor is the selection of variables which depend on the type of variable and the selected sampling frequency. Since variables are sampled at different frequencies, an investigation was needed in order to identify which variables should be selected in the effective monitoring of the process. The investigation was run in two pilot studies; pilot study 1 used daily data and pilot study 2 used continuous data.

The second factor in the design of an effective monitoring process was the development of a reference set for process monitoring that would be capable of considering dynamic behaviour. The behaviour of the electrolysis process within the cell is dynamic as it is disturbed by the vital routine tasks of alumina feeding and anode changing as described in section 2.3.4 in Chapter 2. Incorporating this dynamic behaviour into a fault detection system was critical to the revealing of the signature of the faults and to enable accurate and early fault detection. An alternative way of modelling the process was investigated in order to develop a reference model suitable for monitoring the aluminium electrolysis process. Thus, pilot study 1 investigated the variation between cells so that the number of cells was used as the third dimension in the formation of the 3-D data array for MPCA methodology. Pilot study 2 investigated the use of a moving data window in monitoring the process.

The two pilot studies will now be described in more detail.

5.2. Pilot study 1: MPCA for monitoring daily data for a number of cells

Pilot study 1 examined not only the ability of MPCA to monitor daily data but also the significance of forming a data set using a number of cells as the third dimension. This pilot study includes three phases: (1) data training, (2) model development, and (3) process monitoring.

5.2.1. Phase I: Data training

Two main steps in data training were the selection of variables and the formation of a data set as outlined below.

1) Selection of variables

The first step in data training was to select variables for process monitoring. Variables were to be taken at a sampling frequency of daily, to once every two days. The variables were divided into two: process and quality variables. Seven process variables were chosen because of the correlation between variables. Table 5-1 shows the correlation coefficient among the seven variables: liquidus, excess AlF_3, temperature, alumina (Al_2O_3) shot, bath height, metal height and superheat. Although the correlation coefficients for bath height and metal height were low, they were included because they might contain valuable information for fault detection.

Table 5-1: Correlation Coefficients for Process Variables

	Liquidus	ExcessAlF_3	Temperature	Al_2O_3 shot	Bath Height	Metal height	Superheat
Liquidus	1	-0.938	0.862	-0.151	0.233	-0.230	-0.599
ExcessAlF_3	-0.938	1	-0.816	0.159	-0.232	0.250	0.550
Temperature	0.862	-0.816	1	-0.257	0.314	-0.206	-0.110
Al_2O_3 shot	-0.151	0.159	-0.257	1	-0.137	-0.014	-0.103
Bath height	0.233	-0.232	0.314	-0.137	1	-0.311	0.040
Metal height	-0.230	0.250	-0.206	-0.014	-0.311	1	0.125
Superheat	-0.599	0.550	-0.110	-0.103	0.040	0.125	1

Focussing on quality variables, Table 5-2 compares three quality variables: (1) percentage of impurities for iron (Fe), (2) percentage of impurities for silicon (Si), and (3) current efficiency, for both normal and abnormal cells. However, the comparison, as shown in Table 5-2, indicates that there were some abnormal cells that have lower percentage of impurities and a higher current efficiency. Therefore, this thesis focuses on using only process variables, instead of quality variables, for process monitoring.

Table 5-2: Impurities and Current Efficiency between Normal Cells and Abnormal Cells

Normal cells			
Cells	Impurity content (%)		Current efficiency (%)
	Fe	Si	
6	0.0557	0.0361	103.8145
8	0.0636	0.0292	102.3922
15	0.0685	0.0284	102.8968
Total	0.0626	0.0312	103.0345
Abnormal cells			
Cells	Impurity content (%)		Current efficiency (%)
	Fe	Si	
2	0.0716	0.0291	104.6588
3	0.0662	0.0468	107.5631
16	0.0654	0.0358	104.9310
Total	0.0677	0.03724	105.7176

2) Forming a data set

The second step in data training was to form a data set of normal data using a number of cells as the third dimension, $\mathbf{W}(I \times J \times K)$, in which I is number of cells, J is seven process variables and K has a duration of 15 days. If one superimposes all the scores for 41 cells onto the same score plot, it can be clearly seen in Figure 5.3 that most of the scores are clustered into one region or main cluster, and some of the scores are outside the main cluster and thus are out-of-statistical-control signals. Thus, by using the 3-D data array, the vast amount of

data in a potline can be organised based on its cell number so that the data are managed as a group of cells and any abnormal cells in a potline can be easily identified.

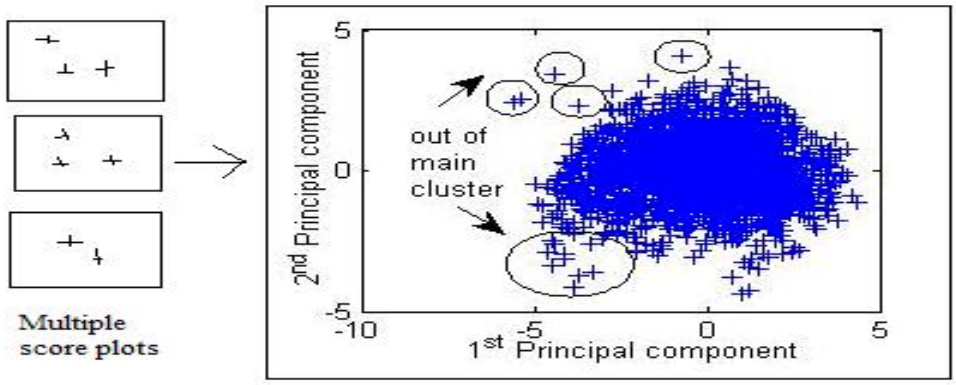

Figure 5.3: Scores for Multiple Score Plots can be visualized by projecting all the Scores to a Score Plot

Abnormal cells are identified by an investigation of the values calculated for the cells in the score plot, Hotelling's T^2 chart and the SPE chart. The combination of three charts (score plot, Hotelling's T^2 chart and the SPE chart) is important in monitoring the variation between cells. After removing abnormal cells, the data set, **W** (29 x 7 x 15), was used to develop a reference model.

5.2.2. Phase II: Model development

The 3-D data matrix, **W**, was unfolded into a 2-D data matrix. Data were arranged side by side in a sequence based on time in a data window. This produced a huge 2-D data matrix with each row representing each cell. Each row then contained 15 days data for *J* process variables. PCA was applied to the new 2-D data matrix and transformed each row into scores. Every score summarised the information for each cell.

5.2.3. Phase III: Process monitoring

In order to monitor the process using the developed reference model, real data sets for 43 cells were used. Some cells were out of the distribution of normal cells. As shown in Figure

5.4, the abnormal cells, cell 46 for example, was out of the control limits in the score plot (Figure 5.4) and in the Hotelling's T^2 charts (Figure 5.5).

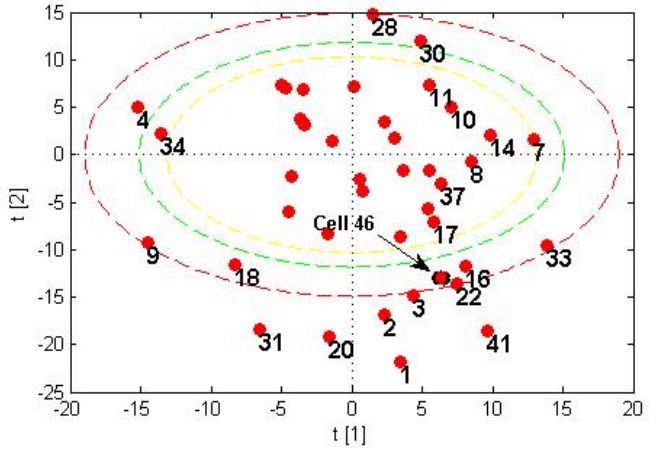

Figure 5.4: Cell 46 out of the 95% Confidence Limit

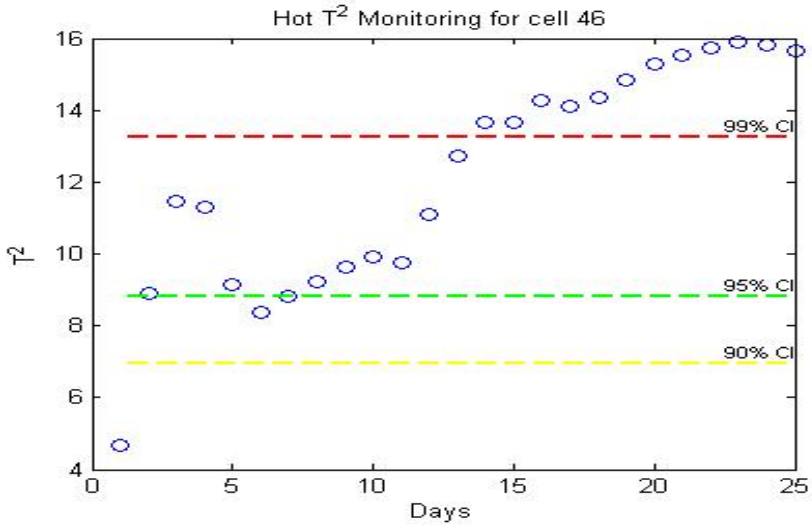

Figure 5.5: Hotelling's T^2 Chart for Cell 46

5.2.4. Conclusions

The results of this pilot study show that by applying MPCA to a data set where the third dimension is the number of cells, cells which have deviations in their process variables such as cells with anode effects can be detected. However, it is difficult to detect early faults using daily data because the faults might have been happening for a period of time. Furthermore, in terms of finding the causes of deviation in the monitoring charts, continuous five minute

averaged sampled data might be better used instead of daily data to diagnose problems because there are many variations that contribute to deviations, even in one day (Taylor and Chen, 2006).

5.3. Pilot study 2: MPCA for monitoring continuous data using a moving data window

Based on the reason outlined above in pilot study 1, continuous five minute averaged sampled data were used in pilot study 2. Pilot study 2 examined not only the ability of MPCA to monitor these data but also the impact of forming a data set using a number of data windows as the third dimension. This pilot study includes three phases: (1) data training, (2) model development, and (3) process monitoring.

5.3.1. Phase I: Data training

1) Selecting variables

The process variables selected for this pilot study are shown in Table 5-3.

Table 5-3: Process Variables used for Process Monitoring

X1	Beam movement for machine 1
X2	Beam movement for machine 2
X3	Ratio of alumina feeding
X4	Noise
X5	Operational voltage
X6	Filtered resistance for feeding 1
X7	Filtered resistance for feeding 2
X8	Filtered resistance for feeding 3
X9	Resistance
X10	Amperage
X11	Filtered resistance for feeding 4

2) Forming a data set

In order to monitor a continuous process without a known and distinct operational pattern over a defined duration, MPCA can also be employed by using the number of data windows as the third dimension (*I*). For example, it could be used during an operation without the start-up of a continuous process, or continuous process transitions from grade to grade. In this pilot study, process data collected every few seconds and averaged over each five minute period were monitored based on the moving data window concept. These data windows were formed from *J* variables which were sampled between two process events: anode changing and tapping. To develop the data windows, the data were first scaled by subtracting the means of the variables and dividing by their standard deviations as proposed by Chen and McAvoy (1994). Then windows with length *K* and width *J* were moved forward, sample by sample, along the scaled samples to form the data windows. The data window formed for each window movement contained *K*x*J* data points which included the data point at the current sampling time (*T*) and the *K*-1 previous data points. All the data windows formed were stacked together making a 3-D data array, **W** (*K* x *J* x *I)*, where *J* was the number of process variables, *K* was the number of time intervals and *I* was the number of data windows. This **W** (*K*x*J*x*I)* was able to capture the dynamics of the process as the previous data were loaded together with the current data in each data window.

5.3.2. Phase II: Model Development

In order to show how previous data were used with MPCA, the four steps using a data sample are illustrated in Figure 5.6 and the steps were:

1) Setting a data window

The data window contained 60 minutes of data or 12 samples from all process variables.

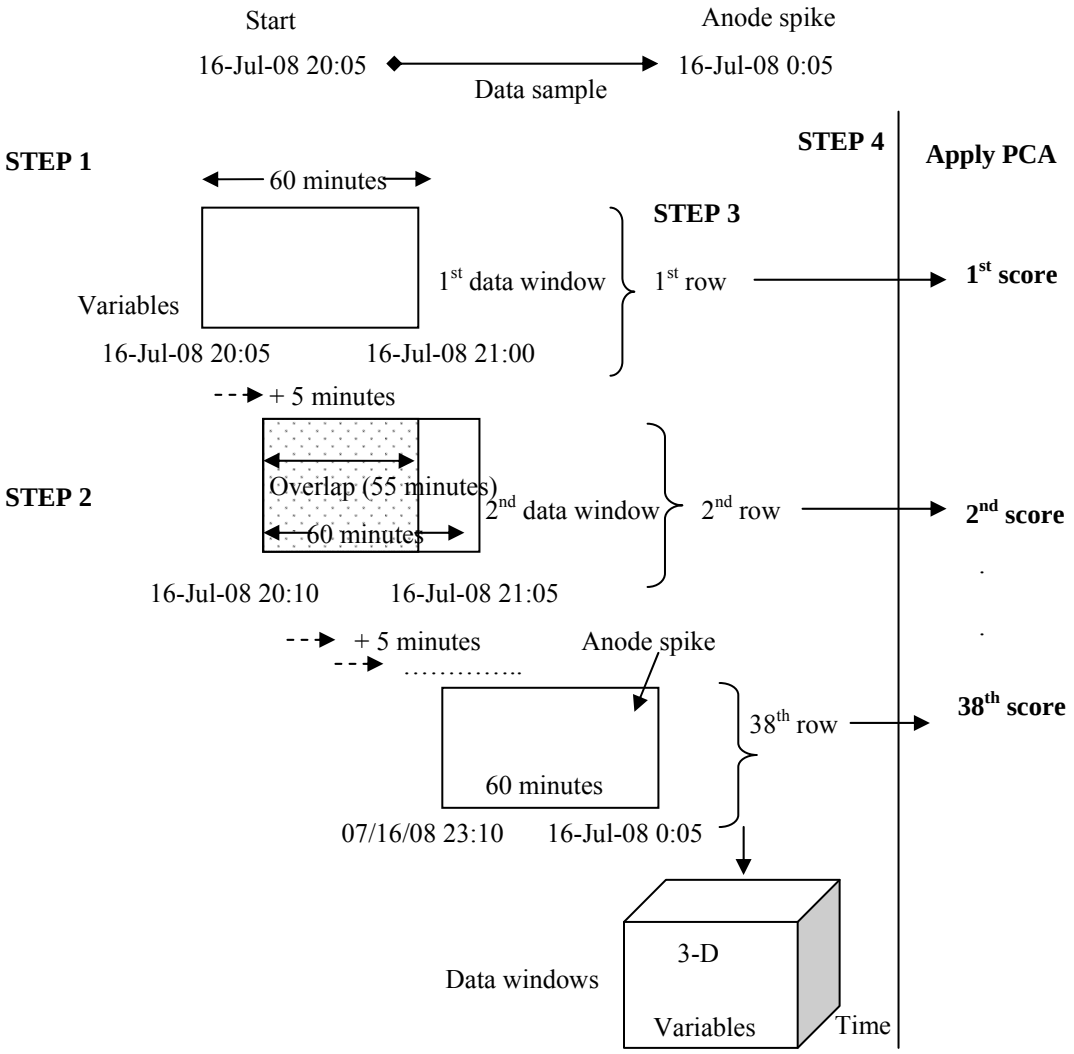

Figure 5.6: Steps in using a Moving Data Window method for MPCA based Process Monitoring

2) Moving the data window

The data window was moving forward to another five minute period and this was recorded as another data window. The data window continued to move until the last of the samples was reached. For example, after the first data window, the data window moved for another five minute period to form the second data window. The later data window had 11 previous samples with one current sample. Thus 11 samples overlapped in each data window. Finally, 38 data windows were produced in this example and the data then was a 3-D data array.

3) Unfolding 3-D data array

The 3-D data array was unfolded into a 2-D data matrix by arranging data side by side in one row in a sequence based on time in a data window. This produced a huge 2-D data matrix

with each row representing each data window. Each row then contained data for 12 samples or one hour for *J* process variables.

4) Applying PCA

PCA was applied to the new 2-D data matrix and transformed each row into scores. Every score summarised information for 12 samples or one hour for *J* process variables.

5.3.3. Phase III: Process monitoring

In this section, the aim is to show the movement of the new scores in the principal score space during process monitoring. Since an anode effect and an anode spike are two different faults with different mechanisms, it was expected that both faults would cluster in different locations in the chart. Three data sets for three different events: (1) with anode spikes, (2) with an anode effect and (3), without unknown abnormalities, were used to show the movement of the new scores. The results and discussion for analysing these data sets are outlined below.

1) Results

All the scores for the first two principal components for the three different events are shown in Figure 5.7 (a), (b) and (c). The scores for the three different events moved from A, to B, to C and to D. This shows a similar trend of scores for these events.

(a) Anode spikes

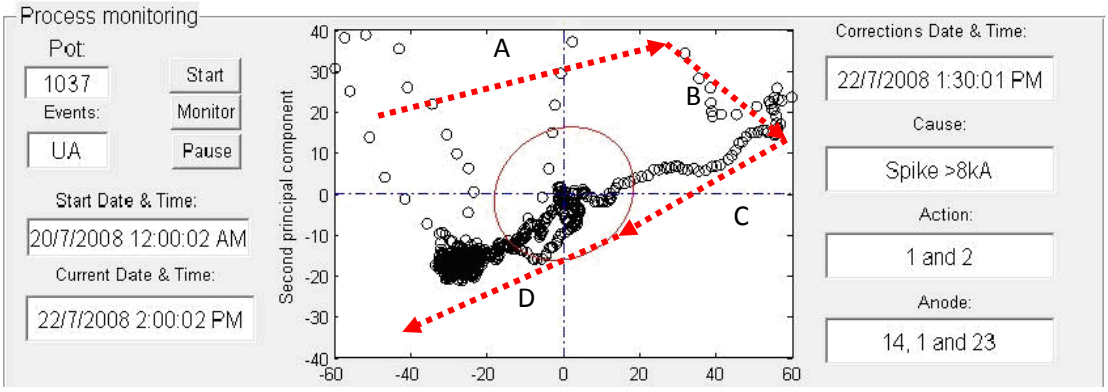

(b) An anode effect

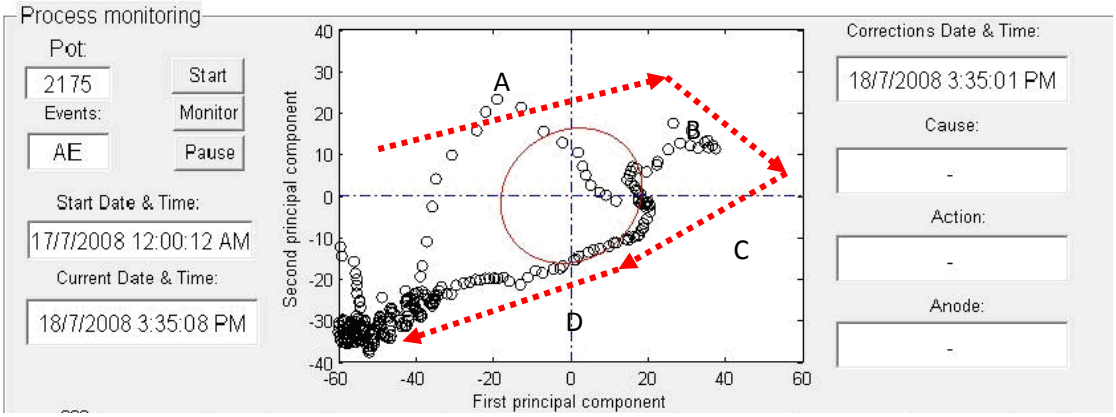

(c) Without unknown abnormalities

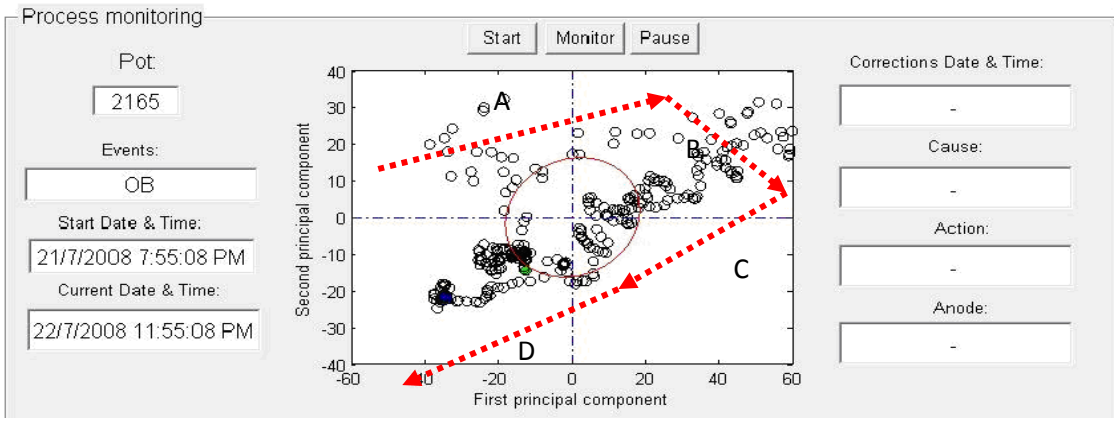

Figure 5.7: Results of applying the Moving Data Window method to the Three different events: (a) Anode Spikes, (b) an Anode Effect, and (c) without Unknown Abnormalities

2) Discussion

The MPCA model developed in this pilot study only captured the major trend of the data. As can be seen in Figure 5.7, after anode changing, the scores moved from A, to B, to C and to D. These A, B, C and D areas form an anode changing cycle. Obviously, more scores were in

area D. This shows the MPCA model used in this pilot study was insensitive to the occurrence of anode spikes and anode effects because the scores for the different events followed the anode changing cycle. Thus, it was hard to discriminate the occurrence of abnormalities.

The reason why the MPCA model was insensitive to the abnormal events is because the dynamic behaviour of the cell during anode changing was not considered. In fact, the dynamic behaviour during alumina feeding was also not considered because in an anode changing cycle, there are also a number of alumina feeding cycles. As a comparison, Kourti et al. (1995) considered the dynamic pattern during batch operation by monitoring the deviation of process data from the mean-trajectory of a complete batch. However, in this pilot study, new data were monitored based on the same trajectory whether the data were in area A, B, C or D. As a result, by using the same mean trajectory for all cycles, the PCA based method may not effectively remove the non-linear behaviour of the cells.

5.3.4. Conclusions

The fault detection and diagnosis system was not entirely effective in this pilot study because we used the same mean trajectory for the whole anode changing cycle. Since the data windows were formed based on a moving window, as described above, the detection was not based on a distinct pattern in the underfeed-overfeed cycle. Furthermore, the same established trajectory in a data window was used, including through the anode changing cycle, thus making it possible for an incorrect detection and diagnosis. Therefore, there is a need to improve the application of the MPCA by: (1) incorporating the dynamic pattern in the alumina feeding cycle as it has the potential to detect faults; and (2) incorporating the behaviour of the cell during anode changing as it can decrease Type I errors (false positives).

5.4. The novel framework: Cascade Fault Detection and Diagnosis system

5.4.1. Novelty of the framework

The first novelty of the framework is the utilisation of MPCA and MPLS where the alumina feeding cycle was treated as a batch for fault detection and fault diagnosis of aluminium smelting process, respectively. This approach was developed by utilizing information from chapter 2, 3 and 4 that addresses research question 1 and 2, respectively. An effective method for monitoring the aluminium electrolysis process is by observing the variability pattern within a feeding cycle (Chapter 2 and 3). Treating the alumina feeding cycle as a batch using MPCA is one of the practical methods to develop a fault detection system that considers the dynamic behaviour of the process (Chapter 4). This system can be complemented by a fault diagnosis system based on MPLS in which the alumina feeding cycle was also treated as a batch (Chapter 4). In fact, incorporating the dynamic pattern in the underfeed-overfeed cycle has been recognised as having the potential to improve fault detection from the results in the pilot studies (section 5.1.3) and discussion with experts and process engineers (section 5.1.2). The second novelty of the framework is the incorporation of the behaviour of the cell during anode changing, as recognised in the pilot studies (section 5.3) and in discussion with process engineers (section 5.1.2). This is due to the fact that there is a succession of anode changing cycles in the aluminium smelting process. Successions of alumina feeding cycles occur inside these cycles. These alumina feeding cycles were observed continuously in a downward trend inside the anode changing cycles which is similar to a cascade-like pattern (Figure 5.8). This downward trend is influenced by the different phases in the anode changing cycle (section 2.3.4.2 in Chapter 2). Therefore, the significance of anode changing to the process data within an alumina feeding cycle was considered in developing the framework.

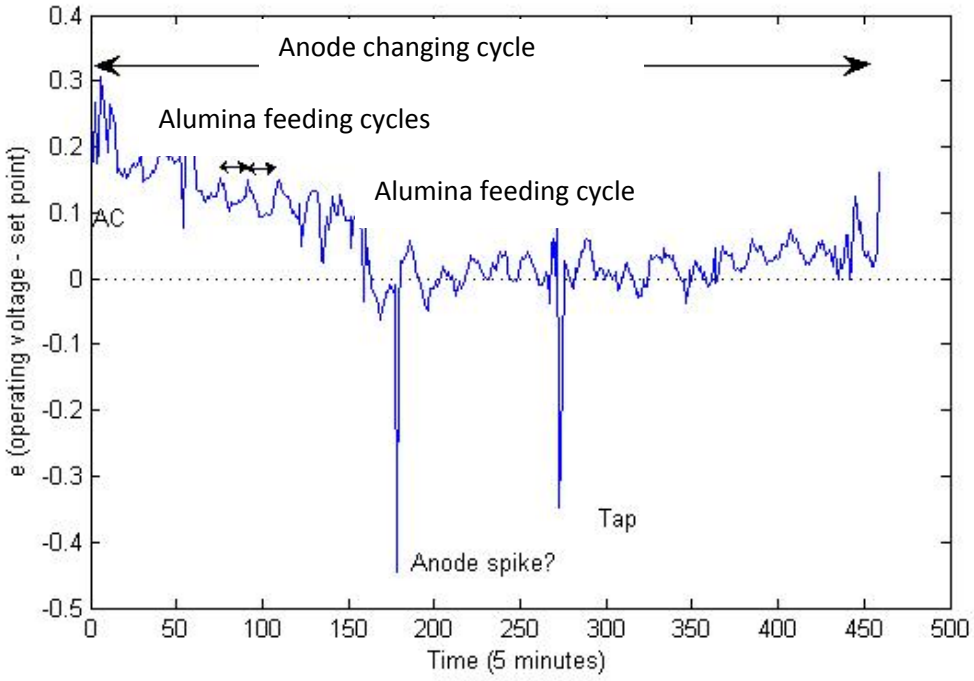

Figure 5.8: Cascade-like pattern occurs during Anode Changing

5.4.2. Cascade fault detection and diagnosis system

The Cascade fault detection and diagnosis system is divided into two main parts so that each part focuses on its specific objective, Part I for detecting faults and Part II for diagnosing faults. The key components for Part I and Part II are illustrated Figure 5.9 and Figure 5.10, respectively. In the data training phase illustrated in these figures, process data were organised in a three dimensional data array, $\mathbf{W}(I \times J \times K)$ (I=number of feeding cycles, J=process variables, K=observations in a feeding cycle) in order to treat an alumina feeding cycle as a batch. After unfolding, each row consists of process data within an alumina feeding cycle. This means the dynamic behaviour that is going to be monitored occurs within the duration of the overfeed-underfeed cycle.

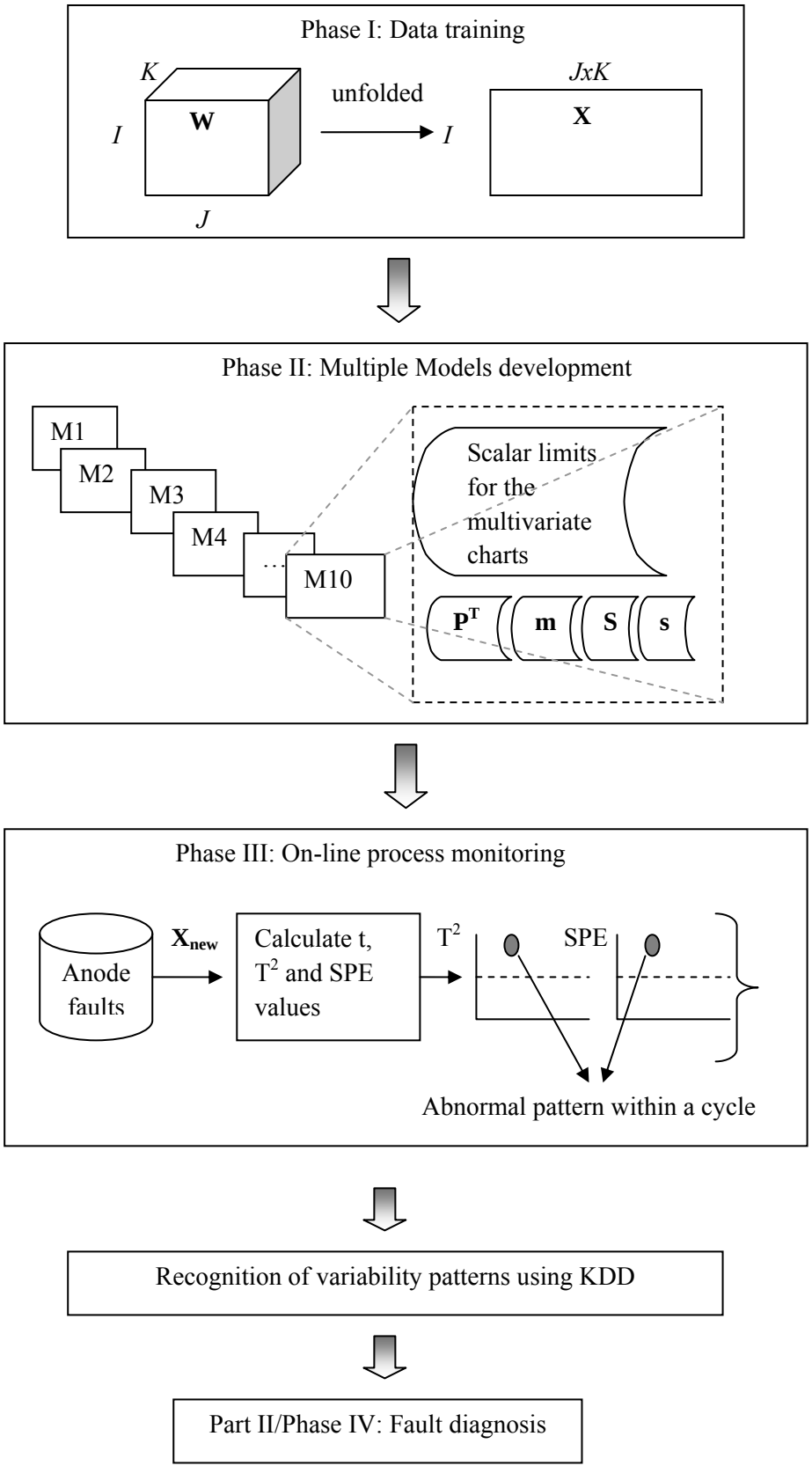

Figure 5.9: Framework for Part I: Fault Detection

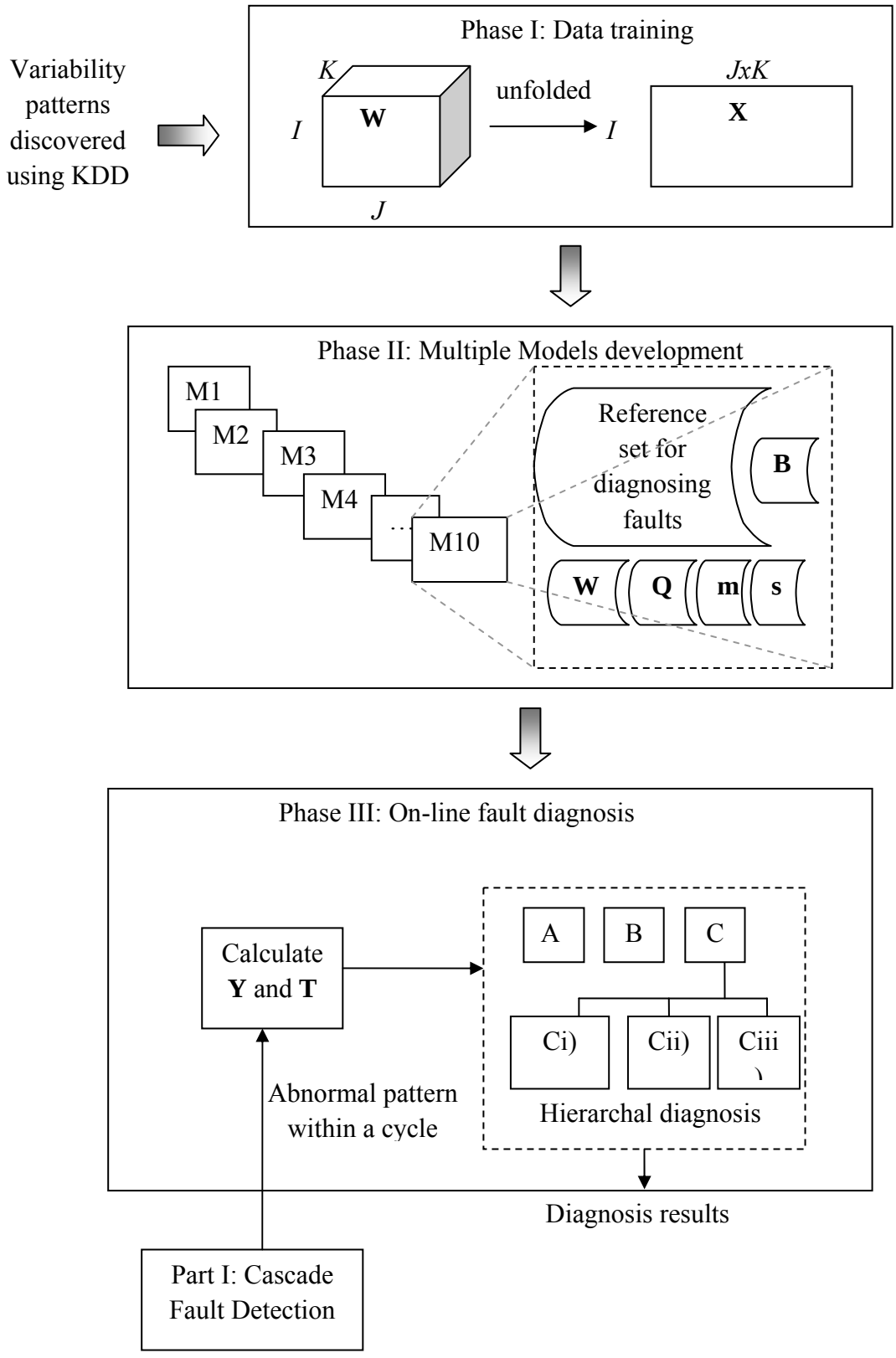

Figure 5.10: Framework for Part II: Fault Diagnosis

The fault detection system follows the general MPCA based framework by Nomikos and MacGregor (1995), as discussed in section 4.3.3 in Chapter 4, but instead of one reference model, ten reference models (M1-M10) have been designed to be developed in the multiple models development phase as shown in Figure 5.9. The fault diagnosis system (Figure 5.10) also involves the development of ten reference models and it also follows the general framework of using DPLS for fault diagnosis and MPLS for unfolding the three-dimensional data into two-dimensional data. The purpose of the development of these multiple models for fault detection and diagnosis system is for the consideration of the downward cascade-like trend in cell voltage during anode changing. In fact, this unique ability is the reason for calling this proposed system a Cascade fault detection and diagnosis system in this thesis.

In addition, in the on-line process monitoring phase for Cascade fault detection, shown in Figure 5.9, information from the reference models was used to monitor the real-time changes of data ($\mathbf{X}_{\mathbf{new}}$) within the alumina feeding cycles. The two multivariate control charts, the Hotelling's T^2 and SPE charts were used to detect the anode faults by showing out-of-control signals. Patterns related to these faults were then extracted using KDD. It was possible to relate each event with specific patterns to abnormalities. This recognition of the variability patterns is later able to facilitate fault diagnosis. In Cascade fault diagnosis as shown in Figure 5.10, the data were trained according to the variability patterns that were recognised using KDD. The out-of-signals detected by the Cascade fault detection system were diagnosed according to hierarchal modules and the results were revealed to the end user via a user interface.

5.5. Conclusions

This chapter has shown ideal framework for monitoring the aluminium smelting process. This novel framework was developed after integrating findings and knowledge from three

sources, real-data analysis, knowledge acquisition and pilot studies. The developed framework was the basis for the development of two main parts: fault detection (Part I) and fault diagnosis (Part II). Further details on the procedures and results in Part I (fault detection) will be described and discussed in Chapter 6; Part II will be discussed in Chapter 7 and the integration between Part I and Part II will be described in Chapter 8.

CHAPTER 6: CASCADE FAULT DETECTION

In order to describe the development of the Cascade fault detection system incorporating innovative features for monitoring the aluminium smelting process, this chapter begins by describing the procedure for developing the system. The evaluation of this system using real case studies and recognition the patterns of variability using KDD approach is then described. Finally, the discussion on addressing the first research question is presented.

6.1. Procedure for the Cascade fault detection system

A fault detection system was proposed to incorporate the dynamic behaviour of the cell. MPCA was adopted for this system because it is a dynamic multivariate data modelling method that can potentially capture the distinct dynamic pattern of the underfeed-overfeed cycle. In fact a number of MPCA models were developed so that the effects of anode changing were also incorporated into the fault detection system. The procedure used to develop this fault detection system is illustrated in Figure 6-1 where there are nine key steps in this procedure. These steps are described in the sections that follow based on their phases: Phase I (data training), Phase II (reference models development) and Phase III (on-line process monitoring).

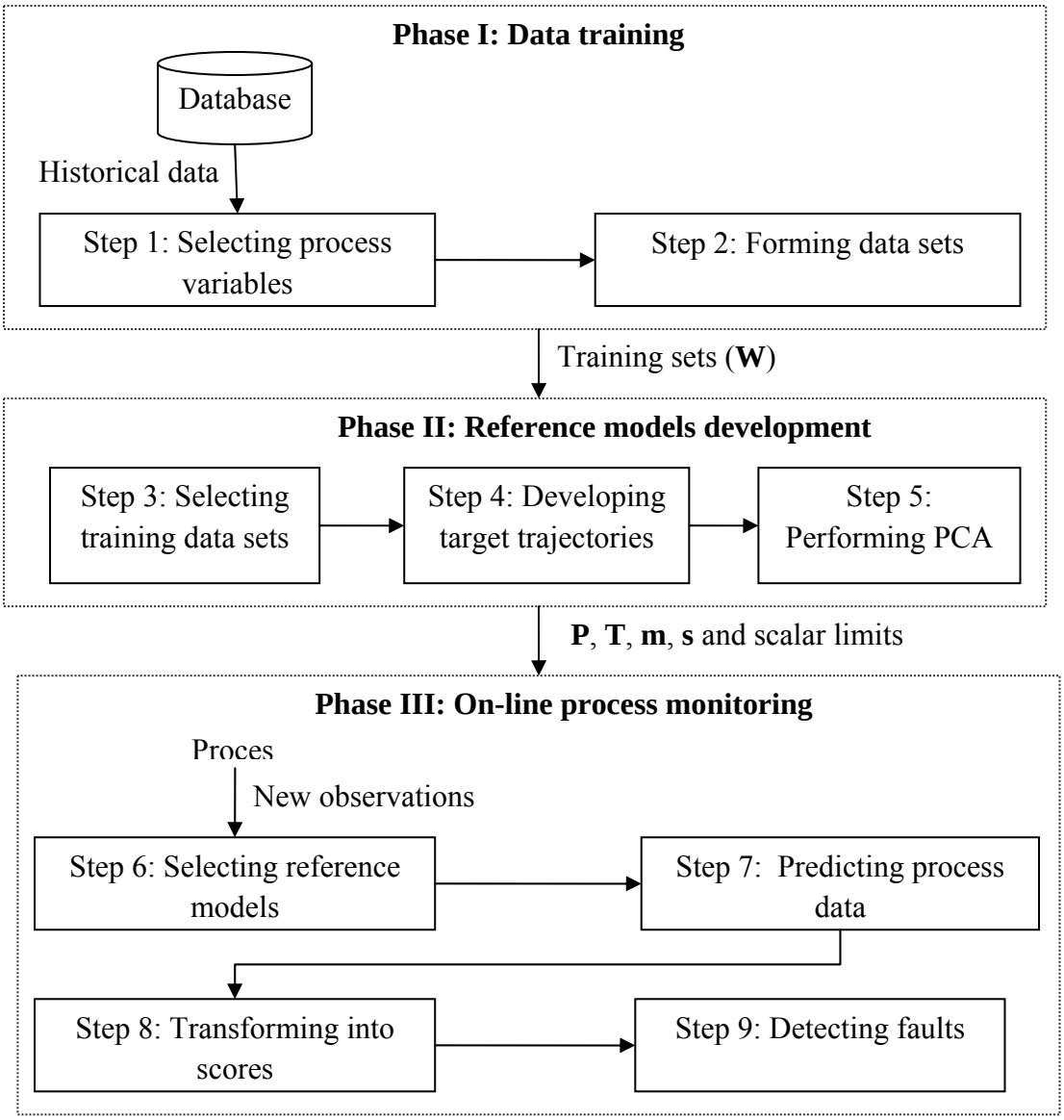

Figure 6-1: Procedure for the Cascade Fault Detection System

6.1.1. Phase I: Data training

In order to prepare a training data set, two main steps were involved: selecting process variables and forming a data set. Each step is described below.

6.1.1.1. Step 1: Selecting process variables

In an industrial aluminium smelter, there are a large number of process variables that are measured at various sampling frequencies. Cell voltage and line current are measured continuously, whereas, bath temperatures are measured daily to weekly. Each measurement may contain a different fault signature. For example, temperature is a very good indicator of a

spiking problem but the frequency of this measurement may prevent the spiking problem from being detected earlier. It is a challenge to utilize other measurements that are continuously measured but that lack fault signatures. Therefore, six process variables (J=6) that provide good information, are actually collected and are strongly linked to the dynamic process behaviour during alumina feeding were selected. These variables were (1) operational cell voltage, (2) cell voltage noise, (3) cell resistance, (4) filtered resistance 1, (5) filtered resistance 2, and (6) filtered resistance 3. The reasons for selecting these particular variables are discussed below.

The first variable, operational cell voltage, is one of the most crucial and regularly used variable in the process control of the aluminium smelting process because it is very difficult to sense a cell's temperature and alumina concentration (Agalgaonkar et al., 2009). The second variable, cell voltage noise, is the cell's voltage fluctuations. This variable is also important for fault diagnosis because several patterns of noise can be used to classify a number of abnormalities, such as in the neural network qualifier of noise developed by Berezin et al. (2003). The other four variables are used in a feed control strategy in order to maintain the alumina concentration in the cell within a narrow range. Variables 4, 5 and 6 are the results of filtering the cell resistance for three filter-time constants: (1) 60 msec (2) 1.2 sec and (3) 122.88 sec, respectively.

Over five minute periods, data samples of the six process variables were taken and averaged. However, the cells which are connected in electrical series down a potline showed a variation of values in set points due to their differences in age, temperature, electrolyte composition, anode and cathode current distributions, and many other factors. In order to monitor all the cells using a general reference set, the set points are subtracted from the process variables to

form error signals so that the deviations of each variable from its set point can be extracted and used to form a data set. The list of the process variables used for each cell in this system after pre-processing was: (1) cell voltage error, (2) cell voltage noise (no pre-processing), (3) cell resistance error, (4) filtered resistance 1 error, (5) filtered resistance 2 error and (6), filtered resistance 3 error.

6.1.1.2. Step 2: Forming a data set

In forming a data set for data training, one main issue is the trajectory synchronization /alignment because the length of all the feeding cycles (J x K) in a three dimensional data array should be equal. In practice, alumina feeding cycles have variable duration. This situation is frequently found in batch processes where there is variation in the batch length. The length of the batch and the shape of the trajectory cannot be predicted, thus requiring a trajectory alignment (Kourti, 2003). This can be addressed using two trajectory alignment approaches: (1) indicator variable (Nomikos and MacGregor, 1994) or (2) dynamic time warping (Kassidas et al., 1998). The indicator variable is the simplest approach for trajectory alignment for industrial applications (Kourti, 2005). An indicator variable must increase (or decrease) monotonically, and has the same start and end values as well as values for all batches (Kourti, 2005). When the indicator variable does not exist in a process, trajectory alignment can be achieved using a dynamic time warping approach. A well defined trajectory is selected as a reference trajectory, and all other trajectories are synchronized based on this reference trajectory using a dynamic time warping algorithm.

In the aluminium smelting process, however, an indicator variable cannot be found. The reason is that there is no variable that has the same start values as well as the same end values for all feeding cycles. The length of cycle depends on the behaviour of the cell so that there are variations in the length of the cycle. When the cell temperature is high, for example, the

resistance does not follow the pre-identified slope during underfeeding. The length during underfeeding is usually longer than normal in order to track the causes of the problem. For this reason, the number of observations for each cycle may vary in the data set.

As a result, trajectory alignment is not applied. Instead of using a well defined feeding cycle to synchronise other trajectories as in the dynamic time warping approach, two approaches were investigated: well defined alumina feeding cycles and artificially lengthened feeding cycles. Each approach is described below.

1) Well defined alumina feeding cycles. A well defined alumina feeding cycle was identified as a feeding cycle with 16 observations, (K=16) and this was possible because there are a sufficient number of feeding cycles with this length for data training. This is because, during the course of this study, alumina feeding cycles with 16 observations were found to be the most frequently occurring length when cases where no anode faults had occurred. Furthermore, the shape of trajectory of an alumina feeding cycle can be predicted ahead of time because the trajectory of the cell resistance of a normal feeding cycle decreases during overfeeding and increases during underfeeding, as described in section 2.3.4.1.
2) Artificially lengthened feeding cycles. Since the number of observations might be inconsistent for each cycle due to the varying time taken in the underfeed or overfeed periods, the number of observations for the longest cycle is used as the number of measurement, K. If the number of observations for a cycle is less than the chosen number K, the last values of the process variables in the current cycle are used to lengthen the number of observations up to the chosen number K. As a result, all the cycles will then artificially have the same number of observations. In the study, all these cycles were stacked together to form a data set which was a 3-D data array, $\mathbf{W}$ (K x J x I), where I is the number of alumina feeding cycles. For example, the artificially lengthened cycle for

an alumina feeding cycle is shown in Figure 6-2 as **W**, where observations from 19 to 40 were predicted based on the deviation of the last data point in the cycle: data point 47.

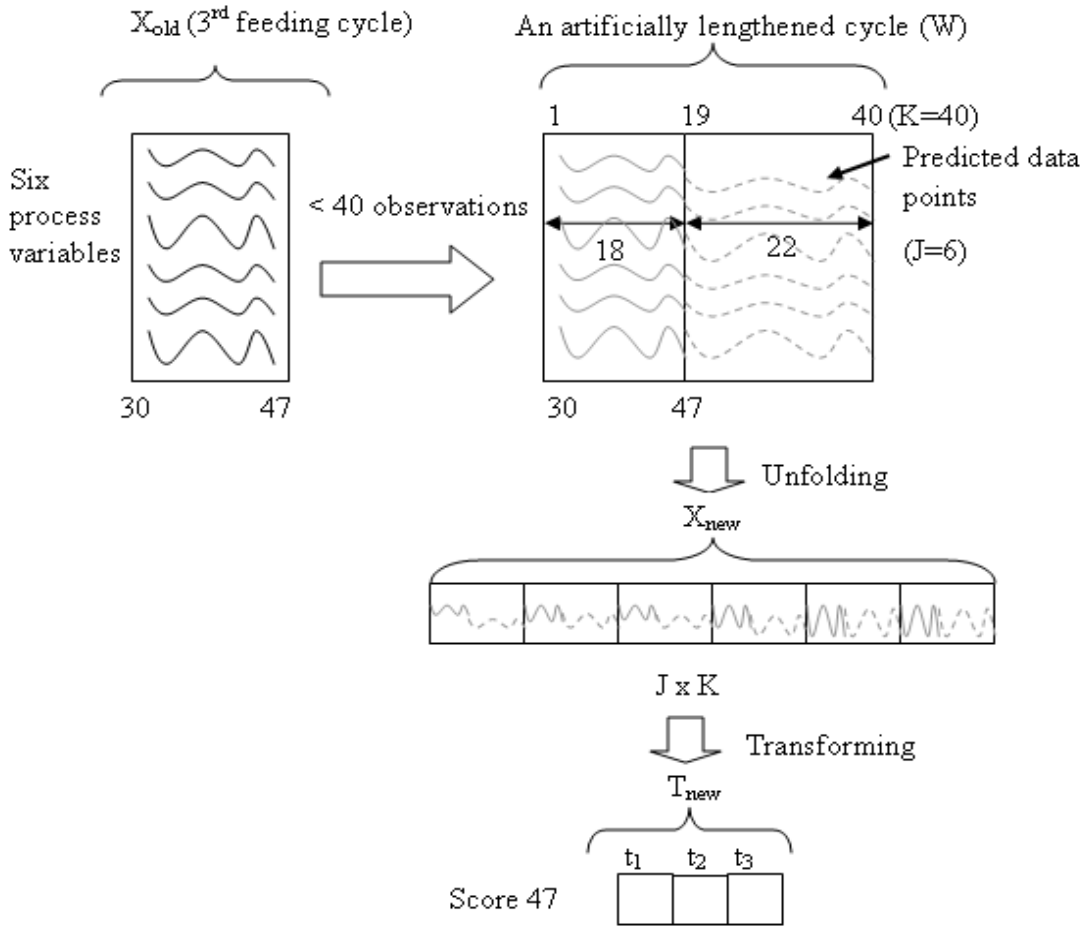

Figure 6-2: Example of an Artificially Lengthened Cycle for a Score

6.1.2. Phase II: Multiple reference models development

In order to develop reference models, three main steps were involved: selecting training data sets, developing target trajectories and performing PCA. Each step is described below.

6.1.2.1. Selecting training data sets

Multiple MPCA models were designed to be developed to incorporate the effects of anode changing on the process where the cell voltage exhibited an overall downward trend or cascade-like trend. As shown in Figure 6-3, the secondary cycle refers to the underfeed-overfeed cycle and the primary cycle refers to the anode changing cycle. These two cycles became the basis of the fault detection system where the reference trajectory for the

secondary cycle was based on the effects of the primary cycle exhibiting a downward voltage trend. In this Cascade fault detection system, a training data set was developed for every feeding cycle phase, starting from the beginning of the anode changing until the tenth secondary cycle where the downward trend ended. Thus, each data set for each feeding cycle phase was selected to develop the reference model for each phase.

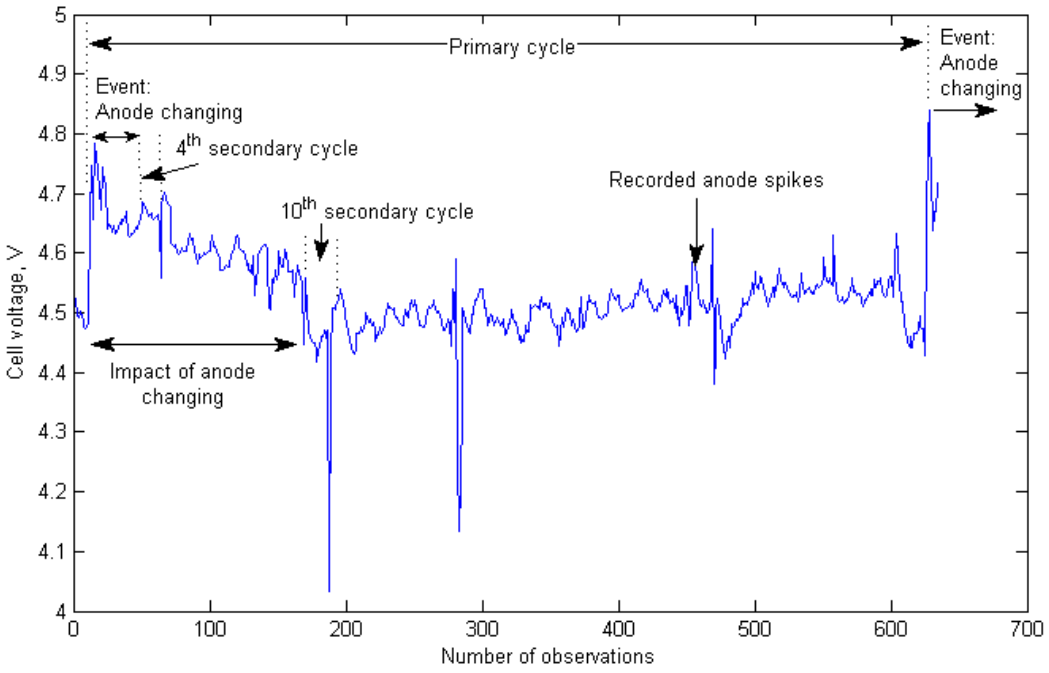

Figure 6-3: Cell voltage exhibiting a Downward Trend indicating the Impact of Anode Changing in Cell 2022

6.1.2.2. Step 4: Developing target trajectories

In order to derive target trajectories from a reference data base of normal alumina feeding cycles for developing the reference models, the training data set, $\mathbf{W}$ (I x J x K) were unfolded and rearranged into a two-dimensional data matrix, $\mathbf{X_{old}}$ (I x JK) where every row contained all observations (J x K) within a feeding cycle. The mean trajectories (m) and standard deviation (s) for each variable within an alumina feeding cycle were calculated. To allow for comparison, Figure 6-4 shows the target mean trajectory for the cell voltage for the end of Cascade phase and also the target trajectory for the beginning of Cascade phase.

These target trajectories show the dynamic behaviour of data within the overfeed-underfeed cycles. However, the trajectories for the end of Cascade phase were smoother, clearer and different than the beginning of Cascade phase as the impact of anode changing was still present in the earlier phase. Therefore, this MPCA application was called Cascade fault detection as it was designed by considering the downward Cascade trend in the data.

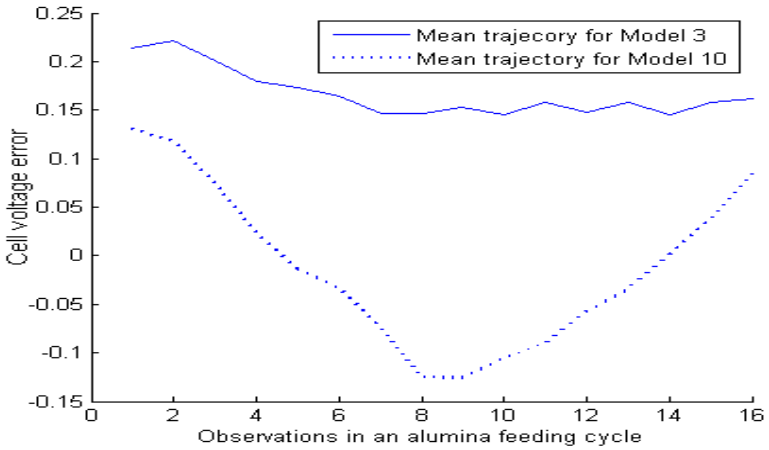

Figure 6-4: Reference Trajectory for Cell Voltage Error within an Alumina Feeding Cycle for Reference Model Number 10 (end of Cascade Phase) and 3 (beginning of Cascade Phase)

6.1.2.3. Step 5: Performing PCA

After developing the target trajectories, the unfolded data matrix was accordingly mean-centred using its mean trajectories and scaled using its standard deviation. Since each reference model has been developed based on the MPCA procedure detailed by Nomikos and MacGregor (1995b), PCA was then applied to the unfolded data matrix. The number of principal components was selected by comparing the results from some of the existing approaches, including the broken-stick rule (Jolliffe, 1986), the R statistic (Wold, 1978) and the W statistic (Krzanowski, 1987).

6.1.3. Phase III: On-line process monitoring

In on-line process monitoring, there are four key steps: selecting reference models, predicting process data, transforming new data into scores and detecting faults. Each step is described below

6.1.3.1. Step 6: Selecting a reference model

The reference model for on-line process monitoring has been selected based on the phase of the cycle, whether at the beginning (model 1-4), middle (model 5-9) or end (model 10 onwards). Each new observation at time interval k was pre-processed by subtracting the set-points and were then stacked into a new data matrix (K x J) containing all the measurements from the beginning of the alumina feeding cycle up to the time interval k. The new data matrix was then unfolded to $\mathbf{X}_{new}$ (1 x Jk).

6.1.3.2. Step 7: Predicting process data

The deviations of the new data, $\mathbf{X}_{new}$, from the target trajectories were calculated by subtracting the mean trajectories (**m**) from all measurements. These deviations were further scaled to unit variance using standard deviation (**s**). If the $\mathbf{X}_{new}$ was not complete, the future observations in an incomplete feeding cycle were anticipated by assuming that the future deviations from the mean trajectories will remain constant at their current values for the remainder of the feeding duration for time interval k (Nomikos and MacGregor, 1995b).

6.1.3.3. Step 8: Transforming new data into scores

The deviations of new process data in $\mathbf{X}_{new}$ were projected into scores by using **P** (KJ x R) loading vectors of the reference MPCA model as in equation 4-16 in Chapter 4. These loading vectors summarised the behaviour of the variables during the alumina feeding cycle. The T^2 and SPE values were then calculated as in equation 4-24 and 4-25, respectively.

6.1.3.4. Step 9: Detecting faults

Abnormal patterns within a feeding cycle were detected when the T^2 and SPE values exceeded the control limits. The variability patterns relating to faults were recognized and detected by the system through the observation of changes within the alumina feeding cycles using the multivariate control charts (Hotelling's T^2 and SPE) for later fault diagnosis.

6.2. Evaluation of the fault detection system

6.2.1. Scope and reference models

The scope of this evaluation only covers the use of the reference model number 10 which is used for monitoring the aluminium smelting process when the downward trend ended. This is because a substantial amount of data needs to be monitored during the end of the Cascade phase when compared to the beginning and the middle of the Cascade phases. The performance of Cascade fault detection system for two different trajectory alignment approaches was evaluated. The details of reference models for each trajectory alignment approach are described below:

1) Reference models using well defined alumina feeding cycles.

The main MPCA model for trajectory alignment using well defined alumina feeding cycles contains information for: (1) scaling using **m** (1 x 96) and **s** (1 x 96); (2) transforming new data using loading vectors, **P** (96 x 4); (3) calculating Hotelling's T^2 and SPE values using scores, **T** (96 x 4) and **P**; and (4) detecting out-of-control signals using scalar limits for both monitoring charts. Forty-seven of well defined alumina feeding cycles were selected and organised to form a data set for data training, **W** (47 x 6 x 16). In order to derive target trajectories from a reference data base of normal alumina feeding cycles for developing the reference model, the training set data, **W** (47 x 6 x 16) were unfolded and rearranged into a two-dimensional data matrix, $\mathbf{X}_{old}$ (47 x 96). The number of components for the

model was selected by comparing the results from the broken-stick rule (Jolliffe, 1986): R=1, the R statistic (Wold, 1978): R=1 and the W statistic (Krzanowski, 1987): R=4. Since the four components suggested by the W statistic explain around 77.19% of the total variability in the data, the number of components selected for the main model was four (R=4).

2) Reference models using an artificially lengthened cycle.

The details of the reference model for the second approach are: (1) scaling using **m** (1 x 240) and **s** (1 x 240); (2) transforming new data using loading vectors, **P** (240 x 5);

(3) calculating Hotelling's T^2 and SPE values using scores, **T** (240 x 5) and **P,** and

(4) detecting out-of-control signals using scalar limits for both monitoring charts. Ninety-seven alumina feeding cycles were selected and organised to form a data set for data training, **W** (97 x 6 x 40). Figure 6-5 shows the eigenspectrum of the first five principal components that were retained in the main module. The broken stick rule (Nomikos and MacGregor, 1995b) suggested two principal components, but five principal components were retained (R=5 in Equation 4.1) in this model in order to capture more variance (95.44% of the total variability of the data).

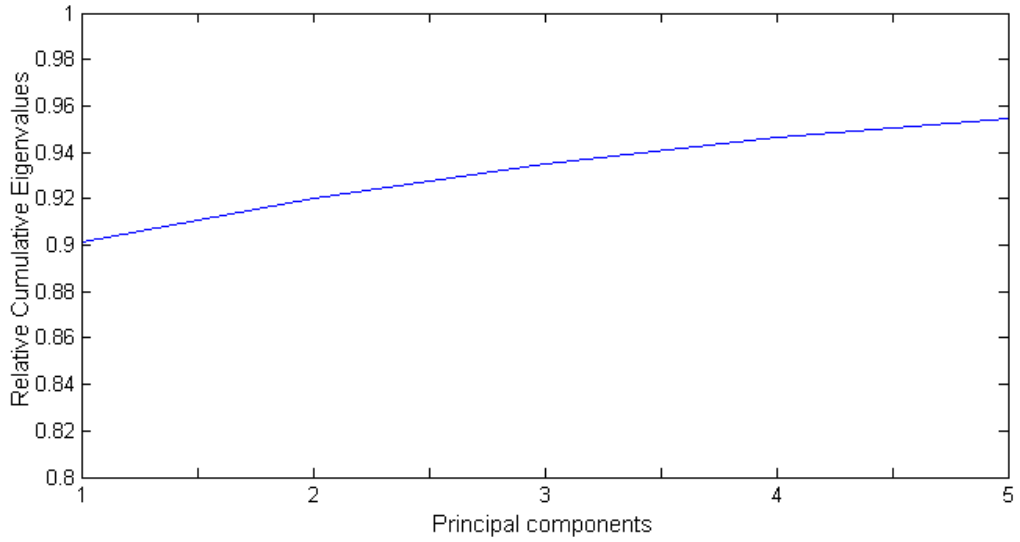

Figure 6-5: Eigenspectrum of the Principal Components for the Reference Model

6.2.2. Results and discussion

After developing the reference models, changes in patterns from the voltage/alumina concentration curves were observed using 31 data sets. These data sets containing operating data recorded from Aldel's aluminium smelter were analysed off-line. Each data set was represented by a test number and was divided into four circumstances which are: (1) hours prior to recorded anode spikes (test 1 to 7), (2) several minutes prior to recorded anode effects occurring (test 8 to 17), (3) hours prior to recorded anode effects occurring (test 18 to 27), and (4) hours without recorded anode faults (test 28 until 31). The details of the detection for each circumstance and its link with the abnormal variability pattern are given in the sections that follow.

6.2.3. Hours prior to recorded anode spikes

Each test shown in Table 6-1 and Table 6-2 contains samples from the tenth feeding cycle from an anode changing event before an anode spike was recorded by operators in the Aldel's aluminium smelter. The number of samples is denoted by the number in the bracket in the Cell column. Test 7 (cell g), for example, contains 179 observations for each process variable before a recorded anode spike. The percentages of detected events at 95% and 99% for the Hotelling's T^2 and the SPE charts were calculated separately. The first part is for scores that exceed the 95% control limit but below 99% and the second part is for scores that exceed the 99% control limit. The results in Table 6-1 and Table 6-2 show that MSPC scheme detected anode spikes for all test cells for both trajectory alignment approaches. This means that there are no missed events. Since the tests containing data associated with a specific assignable cause (anode spike) can be detected by the Cascade fault detection system, the next task is to identify the abnormal pattern associated with the anode spikes.

Table 6-1: Percentages of Samples outside 95% and 99% Control Limits, Hours Prior to Recorded Anode Spikes by using Well Defined Alumina Feeding Cycles

Test	Cell	T^2		SPE	
		> 95% &< 99%	>99%	> 95% &< 99%	>99%
1	a(164)	9.76	9.76	2.44	-
2	b(132)	10.81	17.12	2.70	1.80
3	c(292)	2.74	11.30	1.03	-
4	d(305)	8.20	15.41	0.98	-
5	e(72)	-	1.64	1.64	-
6	f(136)	7.41	60.74	0.74	7.41
7	g(179)	15.08	59.78	12.85	5.59

Table 6-2: Percentages of Samples outside 95% And 99% Control Limits, Hours Prior to Recorded Anode Spikes by using Artificially Lengthened Feeding Cycles

Test	Cell	T^2		SPE	
		> 95% &< 99%	>99%	> 95% &< 99%	>99%
1	a(164)	8.54	78.05	12.20	0.61
2	b(132)	15.79	61.65	6.77	-
3	c(292)	9.22	19.80	3.41	8.53
4	d(305)	4.90	17.97	3.27	3.27
5	e(72)	2.74	-	1.37	-
6	f(136)	0.89	86.03	2.21	25
7	g(179)	10.56	80.56	38.89	9.44

6.2.4. Several minutes prior to anode effects occurring

The MSPC scheme detected anode effects several minutes before the anode effects occurred for all test cells, as given in detail in Table 6-3 thus it can be concluded that there were no

missed events when using well defined aluminium feeding cycles as the trajectory alignment approach. However, in Table 6-4, there was one missed event when using artificially lengthened feeding cycles. Here, differences in the percentage of detection depend on the magnitude of changes in the abnormal variability pattern prior to the anode effect occurring. For test 17, for example, only one score violated the control limits and this may be because the typical task, tapping, was done in a few minutes before the anode effect occurred.

Table 6-3: Percentages of Samples outside 95% And 99% Control Limits, within 20 Minutes Prior to Anode Effect Occurring by using Well Defined Aluminium Feeding Cycles

Test	Cell	T^2		*SPE*	
		> 95% &< 99%	>99%	> 95% &< 99%	*>99%*
8	h(167-170)	-	25	-	-
9	i(377-380)	-	25	-	*25*
10	j(117-120)	-	25	-	*25*
11	k(100-103)	-	100	-	-
12	l(50-53)	-	100	50	*25*
13	o(125-127)	-	100	-	*75*
14	p(131-134)	-	75	-	*50*
15	q(423-426)	75	-	-	-
16	r(307-310)	-	50	25	*25*
17	s(255-258)	25	-	-	-

Table 6-4: Percentages of samples outside 95% And 99% Control Limits, within 20 Minutes Prior to Anode Effect occurring by using Artificially Lengthened Feeding Cycles

Test	Cell	T^2		SPE	
		> 95% &< 99%	>99%	> 95% &< 99%	>99%
8	h(167-170)	-	100	25	-
9	i(377-380)	-	25	-	25
10	j(117-120)	-	50	50	-
11	k(100-103)	-	100	-	25
12	l(50-53)	-	100	50	25
13	o(125-127)	-	75	25	25
14	p(131-134)	-	100	25	25
15	q(423-426)	-	-	-	-
16	r(307-310)	-	50	25	25
17	s(255-258)	25	-	-	-

6.2.4.1. Comparison between Cascade and 'one-time-instant' monitoring

The performance of the Cascade monitoring system in detecting anode effects was also compared with the 'one-time-instant' approach where the details of the violation of control limits for the 'one-time-instant' approach are given in Table 6-5. The one-time-instant approach monitors the deviations of the variables from their overall mean at the current time instant (Kourti, 2003). On the other hand, the Cascade monitoring system has been shown to be different from the 'one-time-instant' approach as it unfolds the three-way data array batch-wise so that the deviations of the variables over the duration of an alumina feeding cycle can be observed. Therefore, the comparison between these approaches has also been included in the off-line data testing for several minutes prior to recorded anode effects occurring in order to examine the implications of different ways of developing the model. The first one captures

the variance for the duration of the overfeed-underfeed cycle whereas the second one captures the variance for the current time instant.

When comparing the results in Table 6-3 and Table 6-5, the Cascade monitoring system using well defined alumina feeding cycles has better detectability of faults for most of the test sets. In fact, the Cascade system detected the occurrence of anode effects for Test 8 and 15 but the 'one-time-instant' approach missed to detect them. This situation shows that the Cascade monitoring system is more effective for detecting anode effects. This is because the proposed monitoring system was developed to consider the dynamic behaviour of the process during anode changing and alumina feeding.

Table 6-5: Percentages of samples outside 95% and 99% Control Limits for Several Minutes Before the Anode Effects occurring for the 'One-Time-Instant' approach

Test	Cell	T^2		SPE	
		> 95% &< 99%	>99%	> 95% &< 99%	>99%
8	h(167-170)	-	-	-	-
9	i(377-380)	-	25	-	-
10	j(117-120)	-	25	-	-
11	k(100-103)	75	25	-	-
12	l(50-53)	-	100	-	-
13	o(125-127)	-	100	-	-
14	p(131-134)	-	75	-	-
15	q(423-426)	-	-	-	-
16	r(307-310)	-	50	-	-
17	s(255-258)	-	25	-	-

6.2.5. Hours prior to anode effects occurring

The aim of this section is to search for the causes of the recorded anode effects that were shown in the previous section. As given in detail in Table 6-6 and Table 6-7, assignable causes were detected by the multivariate control charts hours prior to the anode effects occurring so that there were no missed events. Although there was evidence of assignable cause variations from the ones in the table, there is a need to identify the abnormal patterns associated with these assignable causes and also to investigate the cause that may be assigned to the variability pattern.

Table 6-6: Percentages of samples outside 95% and 99% Control Limits, Hours Prior to Anode Effects occurring for Well Defined Alumina Feeding Cycles

Test	Cell	T^2		SPE	
		> 95% &< 99%	>99%	> 95% &< 99%	>99%
18	h (166)	10.30	23.64	2.42	0.6
19	i (376)	4.26	9.04	1.06	1.06
20	j (116)	3.45	3.45	0.86	0.86
21	k (99)	16.33	9.18	-	1.02
22	l (49)	16.33	9.18	-	1.02
23	o(124)	13.82	50.41	-	-
24	p (130)	3.84	15.38	0.77	-
25	q(422)	15.09	28.30	0.47	2.83
26	r (306)	2.61	4.25	-	0.65
27	s (254)	10.30	23.64	2.42	0.6

Table 6-7: Percentages of samples outside 95% and 99% Control Limits, Hours Prior to Anode Effects occurring for Artificially Lengthened Variables

Test	Cell	T^2		SPE	
		> 95% &< 99%	>99%	> 95% &< 99%	>99%
18	h (166)	10.24	25.30	0.60	-
19	i (376)	5.32	9.31	7.98	1.86
20	j (116)	9.48	12.07	-	15.52
21	k (99)	24.49	55.10	7.14	2.04
22	l (49)	-	85.71	10.20	-
23	o(124)	8.13	19.51	0.81	-
24	p (130)	6.92	22.31	0.77	-
25	q(422)	7.78	52.83	4.71	8.25
26	r (306)	6.86	6.86	-	8.50
27	s (254)	13.39	24.80	13.39	0.79

6.2.6. Hours without recorded anode faults

Data sets for hours without anode faults were also investigated but only with the use of well defined alumina feeding cycles for alignment trajectory. Although there was evidence of control limit violation for these data (no anode faults) as shown in Table 6-8, the level of the control limit violations for the data from this circumstance were significantly less than for other circumstances (e.g. Table 6-1 and Table 6-3). Furthermore, portions of the percentage of the evidence for this circumstance (no anode faults) were related to a typical routine task, that of metal tapping. Since the percentage of the evidence related to anode faults was relatively small, this means the false alarm rates were also relatively small. This shows the ability of the Cascade fault detection system to signal clearly when anode faults were occurring and when there were no anode faults present.

Table 6-8: Percentages of Samples Outside 95% and 99% Control Limits, Hours without Recorded Anode Faults

Test	Cell	T^2		SPE	
		> 95% &< 99%	>99%	> 95% &< 99%	>99%
28	b1 (380)	1.06	2.64	1.32	-
29	b2 (445)	16.44	11.78	0.44	0.67
30	b3 (454)	6.39	11.23	0.66	-
31	b4 (484)	2.90	4.55	0.41	0.41

6.3. Knowledge discovery: recognition of the variability patterns

This knowledge discovery from database or KDD was used to recognise abnormal patterns associated with anode spikes, anode effects and the causes of anode effects. A brief explanation of each step in KDD is given below:

1) Developing an understanding of the application domain

The goal of using KDD was to recognise variability pattern of abnormal feeding cycles so that the researchers could relate between an abnormal events and a variability pattern within an alumina feeding cycle. The relevant prior knowledge that was required for the discovery of these patterns related to any alumina feeding cycles that were detected as out-of-control signals by the multivariate control charts. Also required was information concerning the relevant process information related to the abnormal events.

2) Creating a target data set

The target data set comprised of out-of-control signals detected by the fault detection system. These signals were related to pre-identified faults.

3) Data pre-processing and cleaning

Data were pre-processed by mean-centring and standardising the data using mean trajectories and standard deviations. Since the data were selected based on the out-of-control signals from

the fault detection system, the data set had been pre-processed and cleaned earlier in the fault detection system.

4) Data reduction and projection

Data were reduced and projected using information from the reference model of the Cascade fault detection system.

5) Choosing the data-mining task

Since scores were transformed from the original data using PCA, the selected data mining task was clustering the scores in a score plot according to their pre-identified class of faults.

6) Choosing the data analysis algorithms (s)

The search of abnormal pattern was done by investigating the location of scores related to abnormal events. These scores had been detected earlier as having abnormal patterns by the Cascade fault detection system. The variability patterns related to these scores were then extracted.

7) Data mining

The data mining algorithm was run after the Cascade fault detection system had detected out-of-control signals from training sets with pre-identified faults.

8) Interpreting mined patterns

The variability patterns of abnormal scores were recognised based on the trajectories of normal feeding cycles. These trajectories showed the curve of the established relationship between the resistance and alumina concentration.

9) Consolidating the discovered knowledge

The discovered knowledge was incorporated into the fault diagnosis system so that the type of fault that had occurred could be identified based on the abnormal patterns discovered using KDD approach.

The identification process, by using the above-listed steps, of abnormal patterns associated with anode spikes, anode effects and their cause, is explained further in the following sections.

6.3.1. Identification of an abnormal pattern associated with anode spikes

The abnormal pattern associated with anode spikes is recognized as a systematic pattern. A systematic pattern is defined as a series of points which are influenced by a systematic cause, so that the fluctuation of the points is predictable or systematic (Western Electric, 1958). This pattern has been recognized, in many tests in this section, as a series of high points followed by low points, as in Test 7, Test 1 and Test 4. Test 7 was recorded as the test with the highest level of detection and, as can be seen in Figure 6-6, the test in which many scores violated both the 95% and 99% control limits for both multivariate charts.

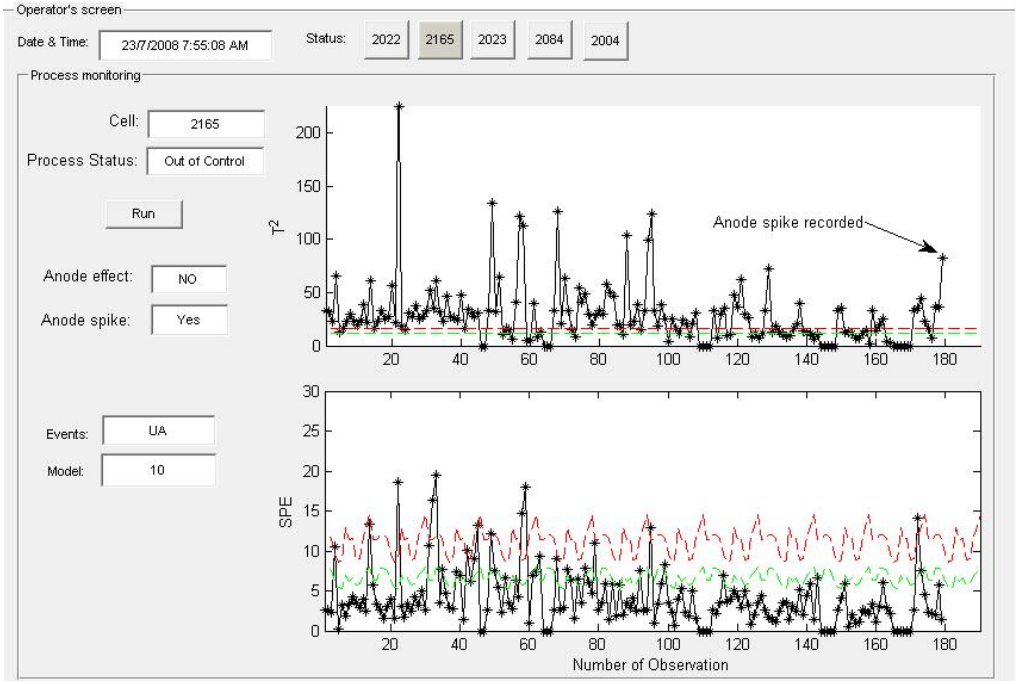

Figure 6-6: The Multivariate Control Charts for Test 7 (Cell g) for Well Defined Alumina Feeding Cycles

There were many scores that violated the control limits captured the systematic pattern within a feeding cycle, such as in Figure 6-7, for example. The abnormal variability pattern, as

shown in this figure, was identified as a systematic pattern of oscillation since it shows that high points were followed by low points. The same oscillatory pattern was also observed from other tests. For example, this pattern was observed hours before an anode spike was recorded for cell a (Test 1) and cell d (Test 4), as shown in Figure 6-8. This systematic pattern can be linked to spiking problems since it was happening hours before the recorded anode spike. It also shows the influence of the spiking problems on the data since the problems occur when an extension of an anode hits the metal, consequently affecting cell voltage.

(a)

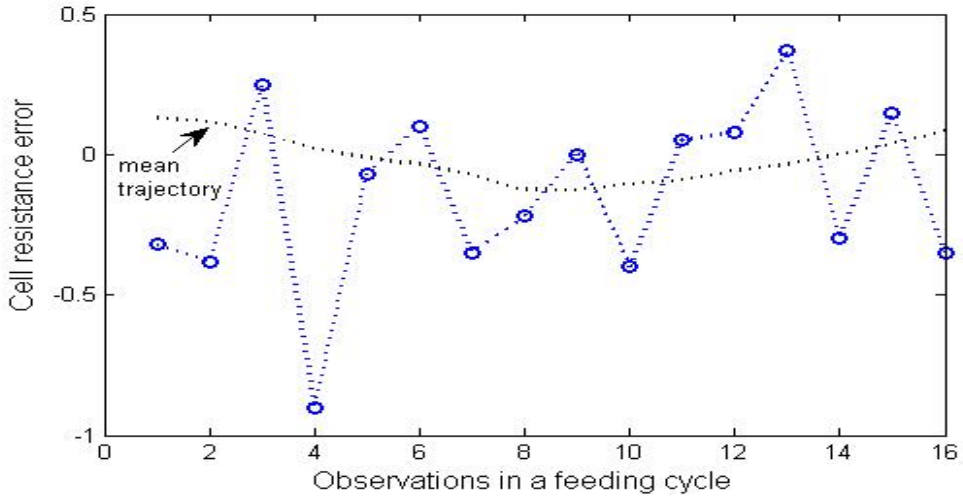

(b)

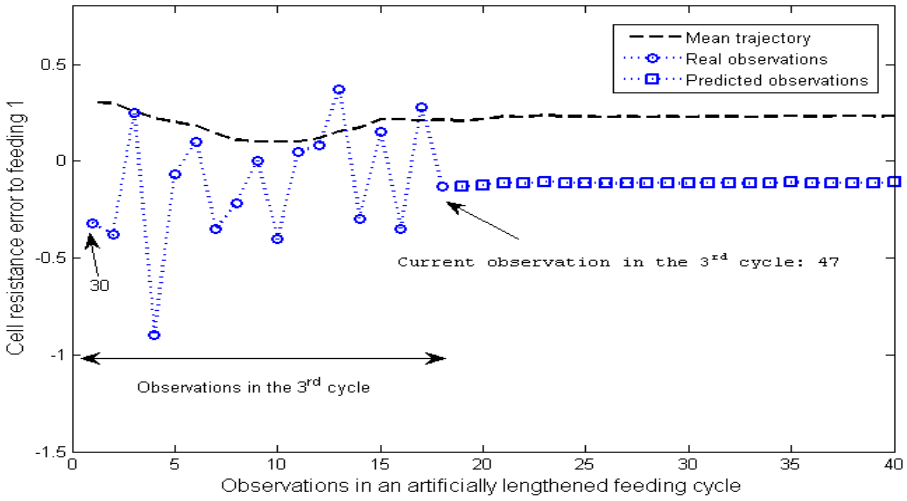

Figure 6-7: Part of the Variability Pattern for Score 47 in Test 7: (a) Well Defined Feeding Cycles and (b) Artificially Lengthened Feeding Cycles

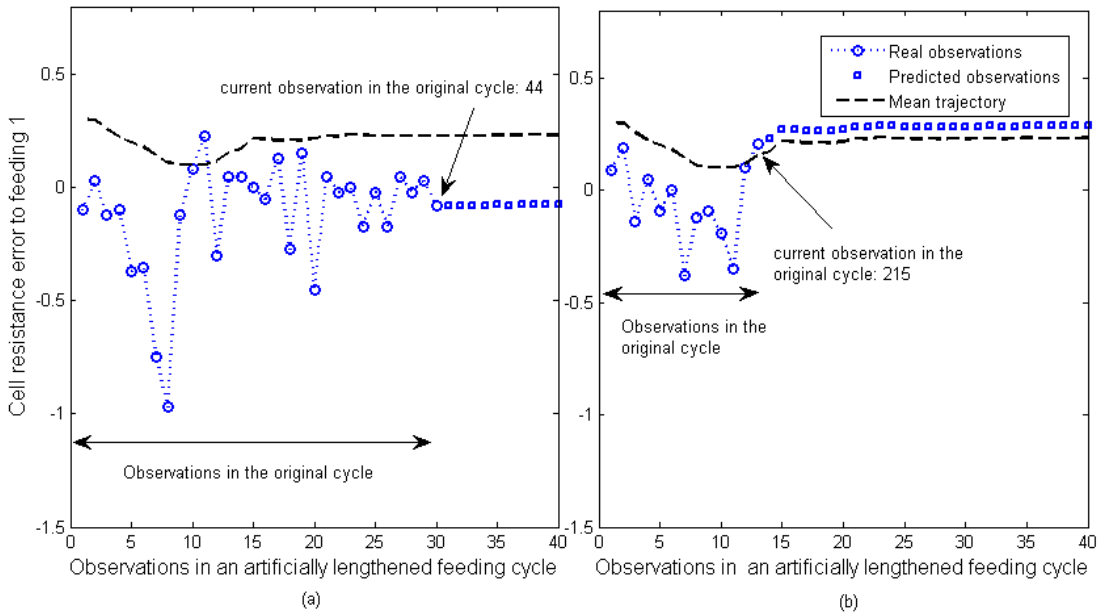

Figure 6-8: Cell Resistance Error to Feeding 1 for: (a) Score 44 for Cells a and (b) Score 215 for Cell d

6.3.2. Identification of an abnormal pattern associated with anode effects

The abnormal pattern associated with anode effects is recognised in this work as a 'large upward trend'. This abnormal pattern was recognised by the investigation of scores that violated the control limit; these scores had appeared within the 20 minutes prior to an anode effect. In Test 13, for example, within the last 20 minutes before the occurrence of an anode effect, scores appeared that corresponded to the control limit violations (Figure 6-9). Observing the variability pattern corresponding to the control limit violating scores before an anode effect, may lead to the recognition of the 'large upward trend' pattern. Figure 6-10, for example, shows a gradual shifting of the cell voltage error within the cycle that ended with an anode effect and this pattern was recognised as a 'large upward trend'.

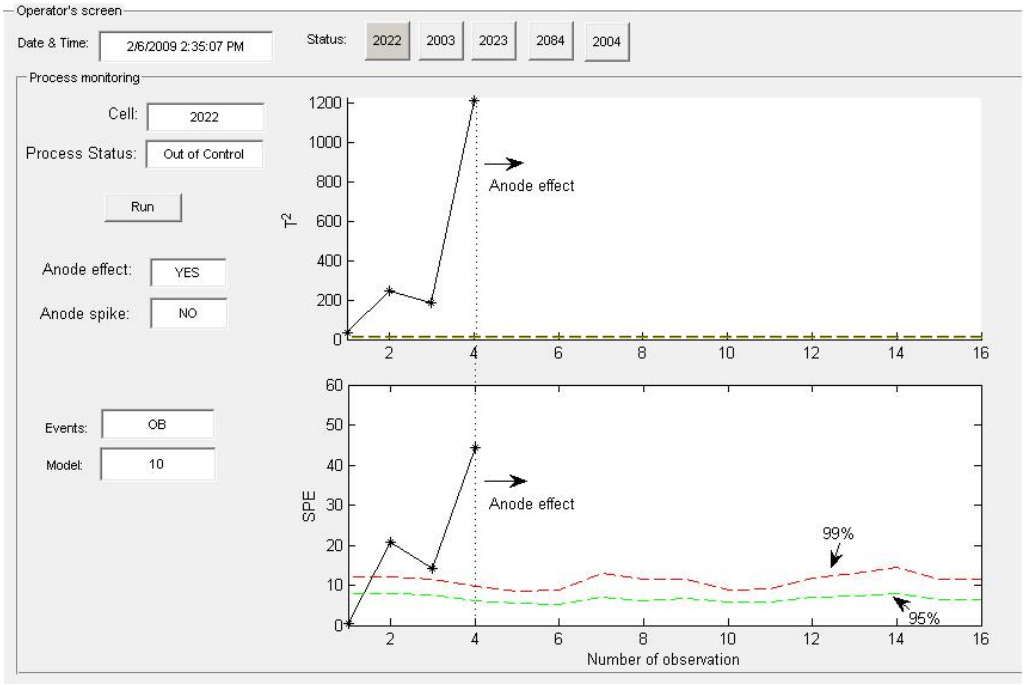

Figure 6-9: Evidence of Control Limits Violations in the Multivariate Control Charts of the Cascade Monitoring System for Test 13 for Well Defined Alumina Feeding Cycles

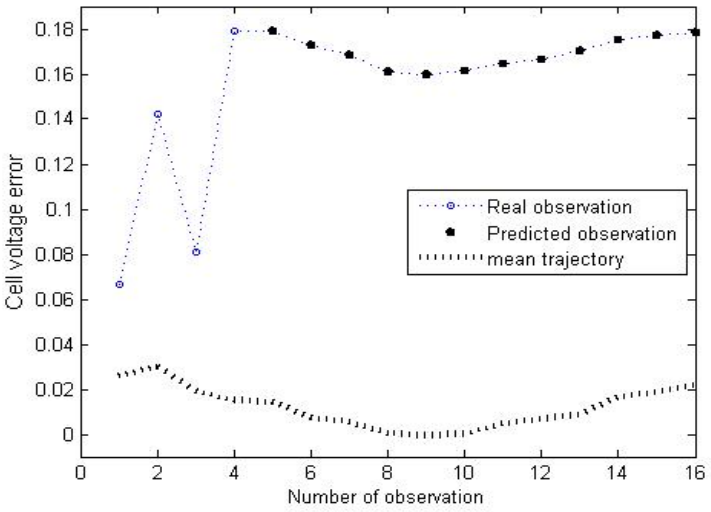

Figure 6-10: Part of Variability Patterns Captured by Scores in Test 13

6.3.3. Identification of abnormal patterns associated with assignable causes

There were two main patterns identified from the violated scores which appeared several hours prior to the occurrence of anode effects, namely: an ‘earlier upward trend during underfeeding’; and an ‘upward trend during overfeeding and underfeeding’.

6.3.3.1. 'Earlier upward trend during underfeeding'

An 'earlier upward trend during underfeeding' is defined as a point or a series of points that show a shift earlier than the upward trend of the mean trajectory. This trend was recognised after observation of the variability patterns that had been captured by the scores that had violated the control limit such as those in Test 18 and Test 21; these were in the direction of low t[1](first principal component) and t[3](third principal component) as shown in Figure 6-11.

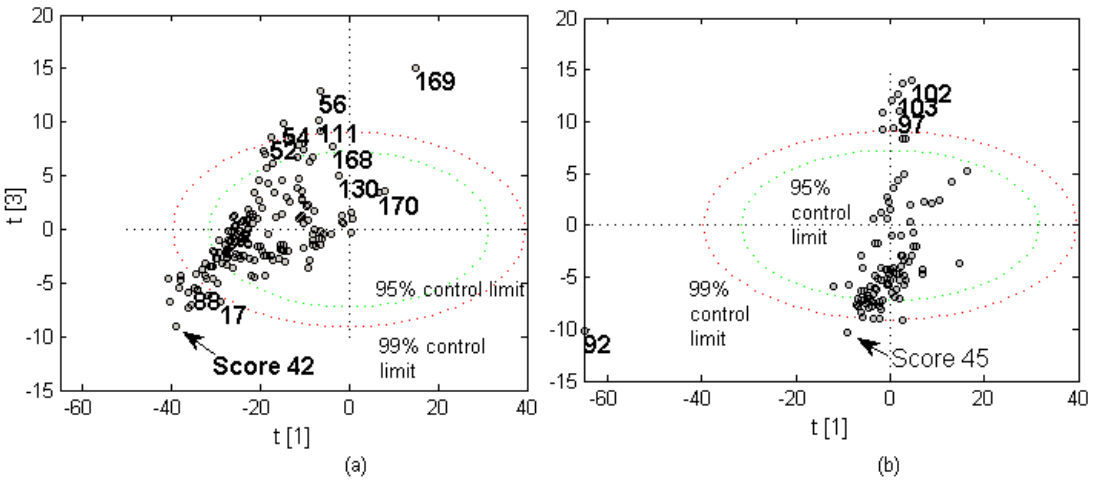

Figure 6-11: Score Plots for (a) Test 19 (cell s) and (b) Test 22 (cell v)

The variability pattern of the cell resistance error for Test 18 is shown in Figure 11. In this variability pattern, the trajectory of the test data followed the downward pattern of the mean trajectory during the overfeeding phase. However, during the underfeeding phase, there was a change at observation number 11 for Test 18 (Figure 6-12). At this point, the upward trend for the mean trajectory had not yet started. The abnormal pattern in this cycle was recognised as an 'earlier upward trend during underfeeding' because the test data had begun an upward trend that started earlier than the upward trend for the mean trajectory. This variability pattern was also observed for Test 21, as shown in Figure 11. This pattern is different from the systematic pattern associated with an anode spike and this difference can be seen in Figure 11 where the systematic pattern was superimposed.

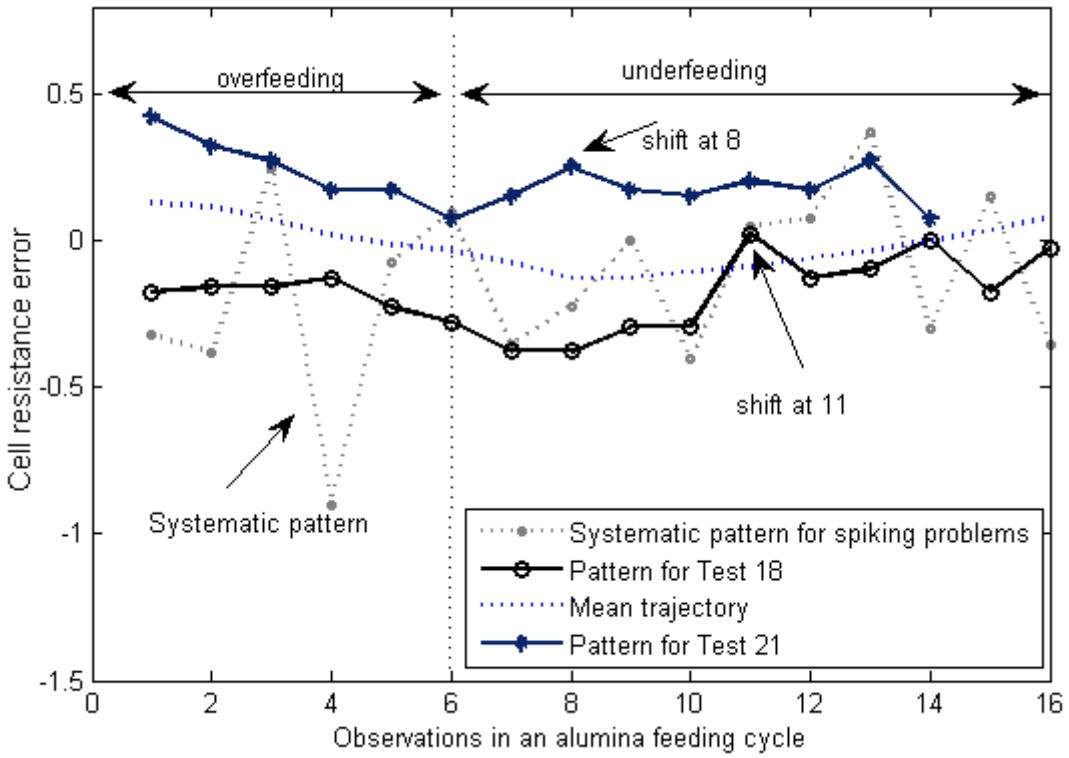

Figure 6-12: 'Earlier Upward Trend during Underfeeding' Pattern for Test 18 and 21 where the Systematic Pattern was superimposed

6.3.3.2. 'Upward shift during overfeeding and underfeeding'

An 'upward shift during overfeeding and underfeeding' is defined as one or more points shifted upward during the downward trend in overfeeding and the continuation of this pattern during underfeeding. This trend was recognised after observing the variability patterns captured by control limit violating scores such as in Test 23 and Test 27. These scores were in the direction of high values of t[1] as shown in Figure 6-13.

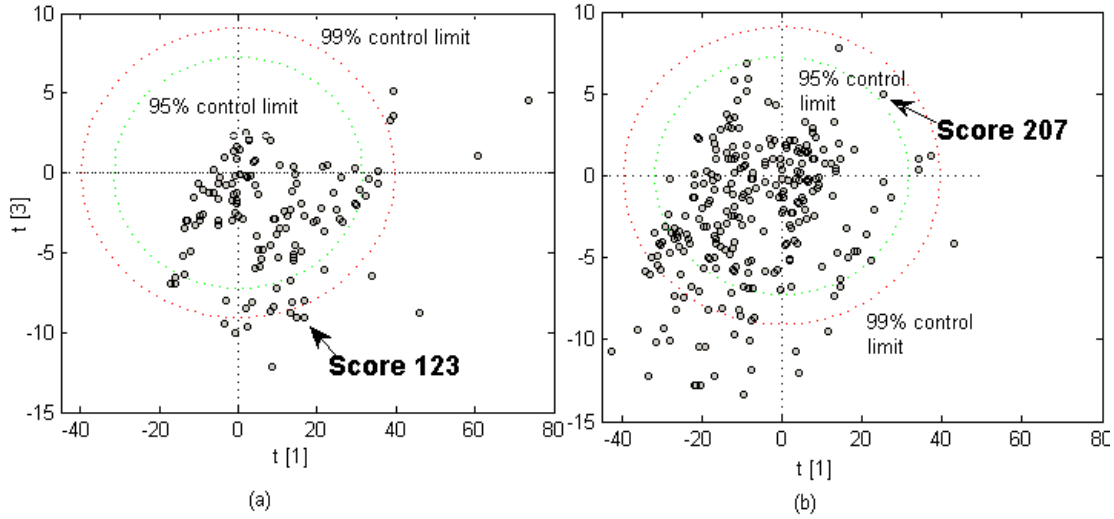

Figure 6-13: Score Plots for (a) Cell x (Test 24) and (b) Cell a2 (Test 28)

Part of the variability patterns captured by the control limit violating scores is shown in Figure 6-14 where there were upward shifts during the overfeeding and this pattern continues during underfeeding.

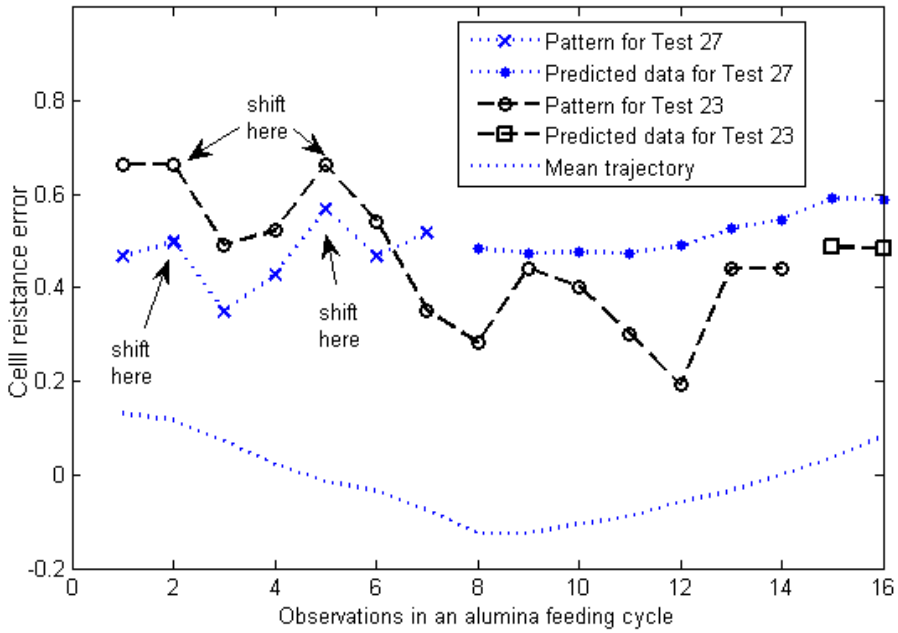

Figure 6-14: 'Upward Shift during Overfeeding and Underfeeding' Pattern for Test 23 and 27

6.3.4. Investigation of abnormal patterns to find the assignable causes

Investigations were undertaken on the assignable causes for the abnormal patterns that had been recognised several hours prior to the occurrence of anode effects. This was due to the

fact that knowledge pertaining to the causes of the occurrence of anode effects, particularly for cell h (Test 18) and cell k (Test 21) was readily available. The ‘earlier upward trend during underfeeding’ was associated with low alumina dissolution; and the ‘upward shift during overfeeding and underfeeding’ was associated with a blocked feeder.

6.3.4.1. Low alumina dissolution

The first possible cause of anode effects is low dissolution of the alumina. No unsuccessful crust breaks were recorded prior to the anode effects occurring so that, most probably, alumina was entering cell h and cell k. There was also an increase in the set point of the cell voltage six hours and 45 minutes prior to the anode effect for cell k. This may be due to the low cell temperature as this was recorded as being 953.6 °C. When the bath is at a comparatively low temperature, the back-feeding of alumina stops because the sludge becomes very viscous and does not move around. The alumina content reduces and consequently the voltage increases (M. Taylor, personal communication, May 10, 2010).

One of the indications of sludge formation is a decrease in bath temperature along with an increase in alumina additions (Stam et al., 2007). This occurred in cell v when there was a long underfeeding phase in a cycle of more than 30 observations. This cycle was followed by a shorter cycle of 11 observations. Therefore, the action taken was to increase the set point of the cell voltage in order to increase the temperature. However, the extra energy was being absorbed in the back-feeding of the sludge and less energy was available for alumina dissolution (Hyland et al., 2001).

However, for cell h, the set point of cell voltage was still the same. This is possibly because the difference between the liquidus temperature and the bath temperature was recorded as

14.4 °C. However, it is possible that the same problem of dissolution occurred in this cell as occurred in the pattern within the investigated cycle for Test 18. The pattern was similar to the pattern for Test 21 (Figure 6-12). However, the root cause of the alumina dissolution in cell h might be different from that in cell k. Poor dispersion of alumina might be the root cause of the low alumina dissolution for cell h. This problem occurs when the alumina is not fed into an 'open bath hole'. There are reasons for this problem, such as, an excess cover material build-up near the feeder, or a closed feeder hole due to the position of the bath surface relative to the crust. These reasons can only be determined by visual examination of the feeder hole itself (M. Taylor, personal communication, May 10, 2010).

6.3.4.2. Blocked feeder

The second possible cause for an anode effect is a blocked feeder or crust falling into the cell. Alumina not entering the cell (feeding problem) may cause an increase in cell voltage during overfeeding (Segatz, 2001) and this pattern matches the patterns that were recognised as an 'upward shift during overfeeding and underfeeding' as shown in Figure 6-14. This assignable cause, a blocked feeder, decreases the concentration of alumina in the bath and may cause an anode effect. Therefore, a blocked feeder or crust falling into the cell might be the possible cause of an anode effect because the variability pattern that is related to low alumina dissolution is shown in section 5.3.1(a) to have a different pattern

6.4. Discussion: addressing the first research question

Significant evidence of control limits violation in the evaluation of the system shows that faults can be detected using the proposed multivariate models. These models considered the dynamic behaviour of the process during alumina feeding and anode changing by treating an alumina feeding cycle as a batch operation and designing multiple models. The results of the evaluation of the system are further discussed as follows.

Firstly, the results show that the aluminium smelting data can be modelled using a batch process method by treating an alumina feeding cycles as a batch operation. This process data modelling contributes to the research of the following group: Jiji et al. (2003), Zhang and Dudzic (2006), Duchesne et al. (2002) and Aguando and Rosen (2008), who use the same batch process modelling method for continuous processes. This process data modelling method allows for monitoring the deviations of the continuous process from its target trajectory.

Secondly, the results also show the necessity for developing multiple models for incorporating the cascade-like pattern during anode changing. This study supports previous research that used multiple models for different operating conditions in order to build a robust monitoring system (Zhang and Dudzic, 2006). Kourti (2005) also pointed out that there is a possibility of developing multiple models if necessary e.g. depending on different grades. The robustness of the multiple model approach was assessed using data from different cells and also from different periods of plant operation in the offline data testing. The results validate that the differences in age and temperature of the cells were removed by monitoring the deviation of the process from its target (current state).

Thirdly, the results show that non-linear processes such as the aluminium smelting process can be modelled using the batch process method. Although non-linear methods are available including research by Kramer (1991) and Dong and McAvoy (1996), the results of this thesis support the statement given by Kourti (2005) that this methodology is sufficient to explain non-linear process. In this thesis, an alumina feeding cycle was treated as a batch operation and the cycles were organised in a three-dimensional data array, $\mathbf{W}$ (I x J x K). The $\mathbf{W}$ (I x J x K) were unfolded and rearranged into a two-dimensional data matrix, $\mathbf{X}_{old}$ (I x JK) where

every row contained all observations (J xK) within a feeding cycle. The data matrix **X** was mean centred by subtracting the mean of each column of this matrix. This way of subtracting the mean trajectory is actually subtracting the non-linear trajectory within an alumina feeding cycle. This is how the non-linearity in the process data is removed.

Overall, the results of the off-line data analysis address the first research question where a fault detection system that considers the dynamic behaviour of the process can be developed. Although this analysis is off-line, the aim of identifying faults can be detected in the process by using the developed models (Kourti, 2005) has been achieved in this thesis. Therefore, the decision on implementing on-line monitoring is a 'go' based on the 'go/no-go' strategy developed by Miletic et al. (2004). However, three main issues may arise in on-line monitoring: (1) changes in anode-cathode distance (ACD), (2) changes in the length of an alumina feeding cycle, and (3) availability of data free of faults.

1) Changes in anode-cathode distance (ACD)

The changes in ACD make an impact on the slopes of the curves, as shown in Figure 2.7, so that the capability of the developed model to detect future data with changing ACD is a crucial issue. However, pre-processing historical data by subtracting their set points prior to developing a PCA model as described in section 6.1.1 can address this problem. This is based on the fact that the set points are actually the target ACD. In the course of this research, after pre-processing, process data were recorded as deviation variables from their set points before the development of the reference model. Furthermore, the differences in age and temperature of the cells were also removed by monitoring the deviation of the process from its target (current state). For example, when the set point of cell voltage for the new data is increased because of the low bath temperature, the reference model for the Cascade monitoring system is still valid for the monitoring of the new data because their set points will be subtracted.

Thus, the reference model can be used for monitoring a number of cells and at different time periods of plant operation. To support this, and by way of validation, the recorded faults used in the offline data testing were from different cells and were also from different periods of plant operation.

2) Changes in the length of an alumina feeding cycle

As shown in the results section, the performances of the system using two different approaches of trajectory alignment are quite similar. Both approaches can be used to detect faults but, in some cases, the trajectory alignment approach, using well defined alumina feeding cycles, is more effective in detection than the artificially lengthened cycle approach. Thus, the issue discussed here is focused on using the well defined alumina feeding cycles approach. As described earlier, the Cascade fault detection system monitors the variability pattern within an alumina feeding cycle with 16 observations. The length of a new alumina feeding cycle which has more than 16 observations causes the system to stop monitoring until another new cycle commences. In this situation, a typical PCA model can be developed to monitor data that are recorded beyond the length of the normal cycle since it is not based on the dynamic behaviour during alumina feeding. However, the use of the 'Cascade' monitoring system is adequate for the early detection of faults since during a normal feeding cycle, the observation of the abnormal pattern focuses on the pre-identified curve. This means that although only 16 observations were monitored for each feeding cycle, the proposed variability patterns could be detected based on the changing of patterns during overfeeding or underfeeding. Cycle duration can be added as a separate variable to be monitored together with cell temperature, liquidus temperature and excess AlF_3. These three variables can assist in finding the causes of problems but were not included in the developed reference model since they are measured only once every two days and not continuous.

3) Availability of data free of faults

The main MPCA model did not follow the traditional SPC philosophy that only common cause variation should be present. The reason for this is that the collection of data, at any sampling frequency, with only common cause variation present, or freedom from faults, is almost impossible to undertake, as, currently, in an actual smelter operation, not all faults can be detected and recorded. Since anode faults are recorded in Aldel's smelter, complete with corrective action for affected anodes, the reference set for the Cascade monitoring system has been built using common-cause and assignable-cause variation with the exclusion of the variations relating to anode faults. Therefore, the development of this reference model allows for the use of multivariate control charts based on latent variables, so that any future anode fault events can be monitored using multivariate charts.

6.5. Summary and conclusions

The changes of patterns in the voltage/alumina concentration curves were observed from 31 data sets by the Cascade fault detection system and the results show:

1) The use of the Cascade fault detection system leads to early detection of an anode spike, prediction anode effects, and also to the detection of problems that may have caused anode effects.
2) Using KDD, four abnormal patterns were recognised as being associated with four different events: (1) a systematic pattern for an anode spike, (2) a 'large upward trend' for the prediction of an anode effect, (3) an 'earlier upward trend during underfeeding' for low alumina dissolution and (4), an 'upward shift during overfeeding and underfeeding' for the occurrence of a blocked feeder.
3) The reference model for detecting anode faults was constructed by using data from a range of cells and from a range of different time periods. However, the spiking problems that were recorded later, and occurred in other cells, were able to be detected by the developed model.

4) The development of the reference model with common cause and assignable cause variation appears to be an alternative solution for developing a data-based monitoring system for complex processes such as the aluminium electrolysis process.

All in all, the Cascade fault detection system appears to be an efficient tool for monitoring the changes of patterns for the detection of faults in the aluminium smelting process. The recognition of variability patterns would provide information for the development of a fault diagnosis.

CHAPTER 7: CASCADE FAULT DIAGNOSIS

In order to develop a fault diagnosis system that incorporates new features for diagnosing faults in the aluminium smelting process, the variability patterns recognised in Chapter 6 were utilized. This chapter will begin by describing the hierarchal diagnosis that involves Module I and Module II and explaining the arrangement of abnormal data from the aluminium smelting process. The procedure for Module I which is based on MPCA and DPLS-M methods is explained and the procedure for using the DPLS-M method for Module II is described. The results of the performance evaluation of the new system are then discussed. Finally, the discussion on addressing the second research question is presented.

7.1. Hierarchical diagnosis approach (Module I and II)

The Cascade fault diagnosis is based on a hierarchical diagnosis approach where the diagnosis is divided into two modules, Module I and Module II (Figure 7.1). Module I addresses the first purpose of the system which were designed to detect anode faults: an anode effect represented by a 'large upward trend' (*A*) and an anode spike represented by a systematic pattern (*B*). The abnormal patterns were diagnosed using two data driven approaches, the MPCA model, with a pre-identified abnormal region approach, and DPLS. These approaches were selected on the basis of forming a coherent approach in the system, especially for pre-processing the process data, because the existing fault detection system that provides the out-of-control signals is based on a data driven approach.

Out-of-control signals which had not been classified as *A* or *B* were identified as not having anode faults (*C*) and were further classified in Module II. This module, which is based on DPLS, was used to classify the unnatural patterns *Ci*, 'earlier upward trend during

underfeeding' (low alumina dissolution) and *Cii*, an 'upward shift during overfeeding and underfeeding' (a blocked feeder). Out-of-control signals which had not been classified as *Ci* or *Cii* were identified as having other faults (*Ciii*) and further investigation is needed to identify these faults. The main reason for adopting two modules was to make fault diagnosis more effective. If only one module was used to perform all classifications, the reference model would be more complex. Since the use of MPCA and DPLS is effective for small-scale classification problems, the unnatural patterns were divided into two modules in order to first focus on classifying anode faults and then to focus on non-anode faults that include low alumina dissolution, a blocked feeder and other faults.

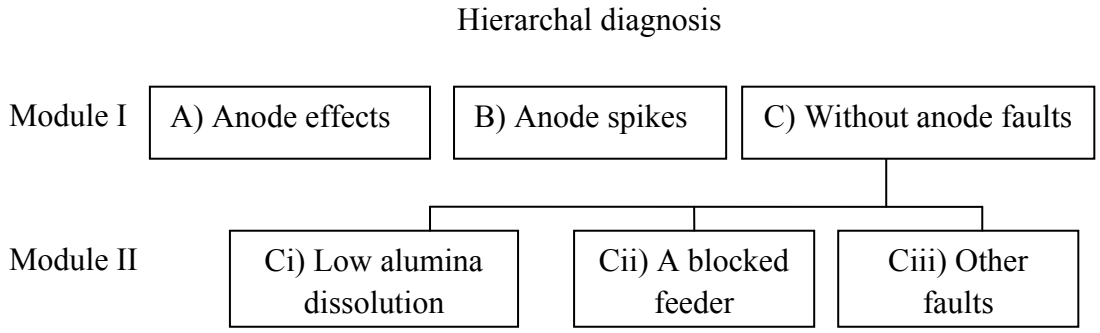

Figure 7.1: Faults for each Module in a Hierarchal Diagnosis approach

7.2. The arrangement of abnormal data from aluminium smelting process

In order to consider the dynamic pattern during alumina feeding in developing Model I and Module II, the relationship of each event with specific patterns associated with abnormality is represented by a matrix of events (**Y**) and a three-way data array of abnormal data (**X**). Each horizontal slice of the three-way data array consists of process data for an abnormal pattern within a alumina feeding cycle. This abnormal pattern was captured using *J* process variables for *K* observations within a complete feeding cycle. Feeding cycles (*I*) with different operating abnormalities were collected from a historical database and were organized into a three-way data array, **X** (*I* x *J* x *K),* by stacking the alumina feeding cycles together according to their class of faults, $\mathbf{y_a}$ (a=1,2,….*A*). The class of fault for each feeding cycle was given a

code. This code was stored as a row in an event matrix **Y** that was filled by the number one in the *a*th column and zero in the rest of the columns. Figure 7.2 illustrates an example of a three way data array with three classes of faults, y_1, y_2 and y_3, where each class contains *o*, *d* and *e* feeding cycles, respectively. The first *o* feeding cycles for the first class of fault is represented by each row in **Y** filled with 1 in the first column, and zero in the second and third columns. As a result, there is a predictor block, **X**, and a predicted block, **Y**. Thus, in the development of a fault diagnosis system, this forms the regression problem of how to relate **Y**=class of faults to **X**=their process data within an alumina feeding cycle.

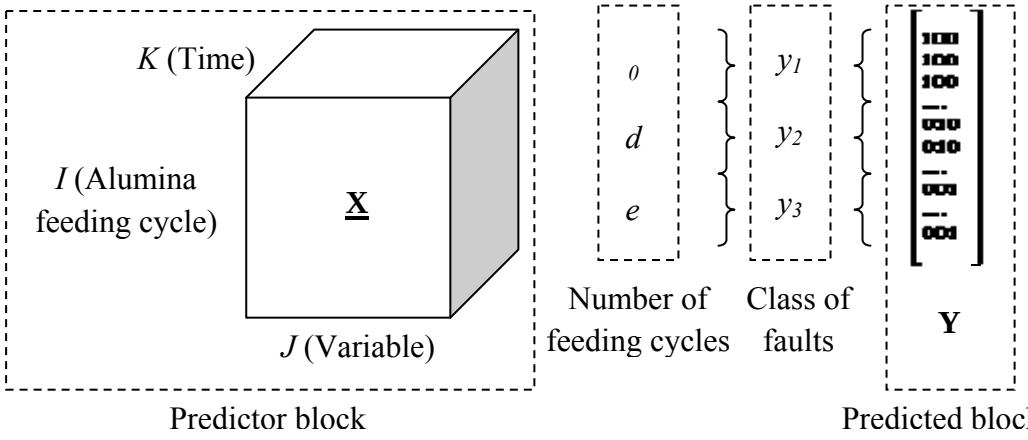

Figure 7.2: A relationship between the Three-way data array, **X**, and the matrix of Events, **Y**

7.3. Procedure for Module I (anode faults module)

In order to relate the class of faults and their process data within an alumina feeding cycle, an MPCA model with pre-identified abnormal regions was first developed by utilizing the class of faults to identify abnormal regions in a score plot. A DPLS model was then used to further diagnose missed events by modelling the relationship between the class of faults and their process data. The key is to treat the alumina feeding cycle as a batch operation using both MPCA and DPLS. The procedures for both approaches and their integration are given as follows.

7.3.1. The MPCA model with pre-identified abnormal region approach

To develop MCPA models, the MPCA procedure detailed by Nomikos and MacGregor (1995b), and as previously described in Chapter 4, was applied to the developed data set, but with some key variations in each phase.

7.3.1.1. Phase I: Data training

For the development of the reference model, a data set of past abnormal and normal operations was used, unfolded, and arranged to form a large two-dimensional data matrix, **X** (*I* x *KJ*). In order to develop this fault model, process measurements from Aldel's aluminium smelter were extracted, as described in section 6.1.1.1. These data were collected from six aluminium reduction cells involving 104 alumina feeding cycles. From these 4160 data points, a three dimensional data array, **W** (40x6x104), was formed. In the formed array **W** (40x6x104), 13 of the alumina feeding cycles were used to define a 'problem area' in the fault model as follows. The 13 feeding cycles were the 10th secondary cycle through to the 23rd secondary cycle shown in Figure 7.3, in which anode spikes were recorded in the 24th secondary cycle. Three anodes were affected in these abnormal events and the action was the changing of the anodes. The impact of these anode spikes can be seen in Figure 7.3 where, starting from the 10th secondary cycle, there was a decrease in filtered feeding resistance.

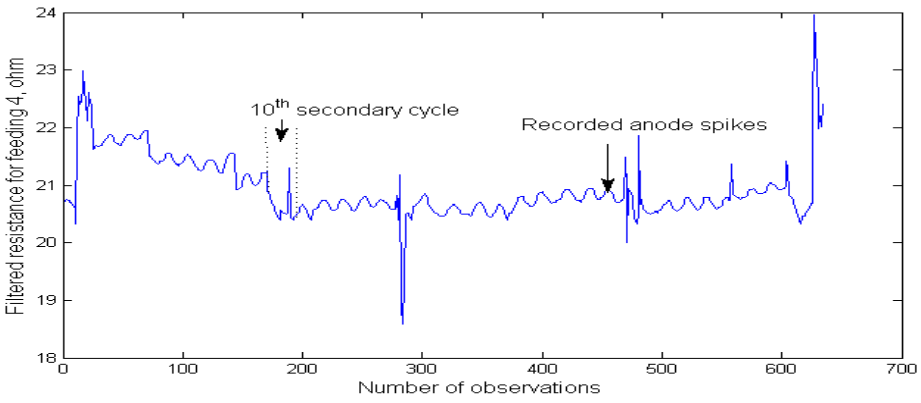

Figure 7.3: Reductions in the Filtered Resistance for Feeding 4 starting from the 10th Secondary Cycle

7.3.1.2. Phase II: Model development

The PCA decomposition of this data matrix produced the loading vectors ($\mathbf{p}_r$) that capture the direction of the variability and can explain abnormal situations via a score plot of the selected principal components plotted against each other. A 'problem area' was defined in the fault model based on a training cluster method in which past data are used to build up clusters related to abnormalities in the developed PCA model (Romagnoli and Palazoglu, 2006). This is based on the fact that data with similar characteristics, when transformed into scores, can be clustered together in a plot. Since abnormal data were used in developing the fault model, the cluster that was formed corresponded to the abnormalities in a score plot defined by the loading vectors of the reference model. This cluster of abnormalities is referred to as the 'problem area' as shown in Figure 7.4.

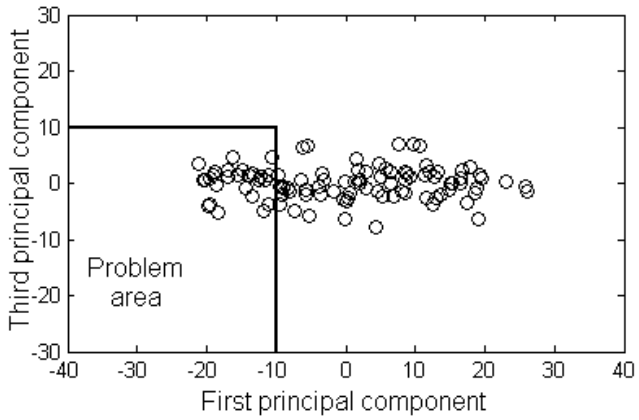

Figure 7.4: The 'Problem Area' in a Score plot

Multiple fault models have been designed to be developed in order to incorporate the effects of anode changing on the process which is a cascade-like pattern. In this thesis, fault model number ten was developed to be the reference model for detecting anode spikes because the potential for anode spikes to occur is high in this area due to the distance between anode and cathode becoming smaller. In fault model number ten, three principal components should be retained in the model. This number has been determined by the broken-stick rule. The three principal components explained about 86.75% of the total variability in the data. Figure 7.5

shows the eigenspectrum of the first five principal components. However, the first and the third principal components were selected to form the principal component score space. This is because the clusters of scores related to anode spikes and anode effects can be clearly defined in this space.

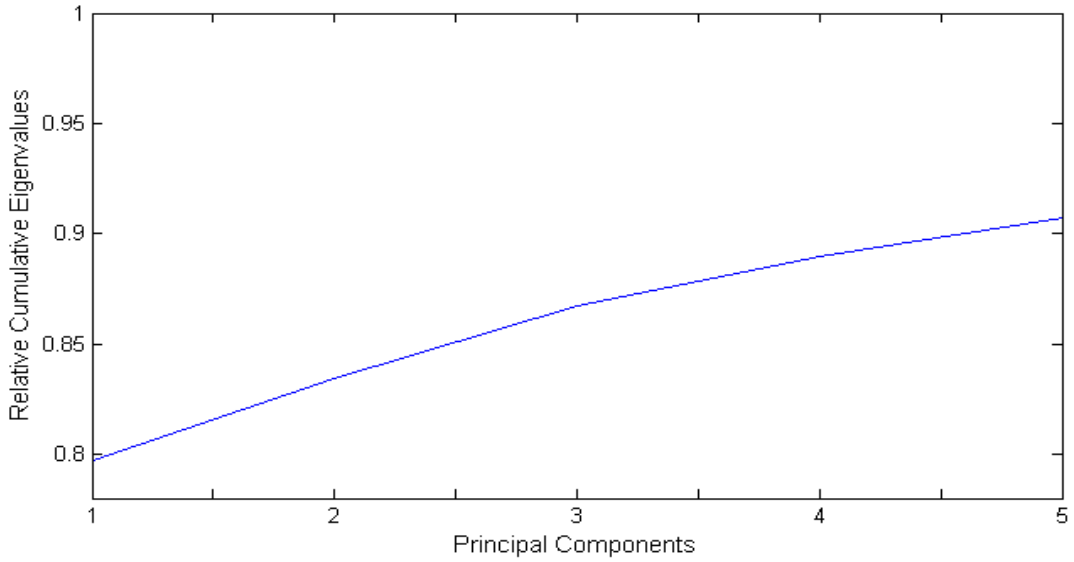

Figure 7.5: Eigenspectrum of the Principal Components for the Fault Model

The boundaries of the 'problem area' in the score space were defined according to:

$$CL_{t1} = Mean\ (PC1_{ab}) + 3\,std\ (PC1_{ab}) \quad (7\text{-}1)$$

$$CL_{t3} = Mean\ (PC3_{ab}) + 3\,std\ (PC3_{ab}) \quad (7\text{-}2)$$

where CL_{t1} is the control limit for the first principal component whereas CL_{t3} is the control limit for the third principal component. $PC1_{ab}$ is a data matrix of abnormal scores for the first principal component, whereas $PC3_{ab}$ is for the third principal component.

7.3.1.3. Phase III: Diagnosing faults

After detecting the occurrence of faults by using multivariate control charts, the faults were classified using the pre-defined abnormal regions in the lower dimensional space, a score plot

(first latent variable (t_1) versus third latent variable (t_3)). The region for spiking problems was in the direction of the low values of t_1 and t_3, whereas the region for the anode effect was in the direction of the high values of t_1 and t_3. These regions were identified based on the movement of scores related to the anode spike and anode effect in the score plot. During the anode spike, for example, the movement of scores was related to the reduction in the total resistance of the cell due to a short circuit at one anode location. As the remaining energy was lost as heat, this meant that less energy was made available to make aluminium metal (A. Mulder, personal communication, December 8, 2008).

Nevertheless, the 'problem area' in the fault model has been redefined in order to consider the process as it evolves during the alumina feeding cycles. This requires that the process is statistically under control, a requirement which is doubtful in some situations where large excursions from the normal process occur (smelting cells can exhibit such changes in state due to disruptions in energy balance and the distribution of the associated electrical current). However, in process operations, these situations are normally preceded by gradual changes in dynamic cell response, and these gradual changes are the phenomena that are detection by MPCA attempted for (M. Taylor, personal communication, November 14, 2009).

In order to detect the gradual changes, the abnormal data that were used to form the 'problem area' in the fault model, were replayed through the on-going monitoring module. In this on-going monitoring module, on those occasions when there were large deviations occurring at that moment, the remaining, unknown parts of the alumina feeding cycles were also filled with these deviation values. Therefore, the $\mathbf{X}_{\mathbf{new}}$ with these predicted data, when transformed to scores, created a new 'anode spike area' as shown in Figure 7.6. This 'problem area' was tested using two samples with no recorded anode spikes from two different cells. As shown in

Figure 7.7, the scores for these samples moved away from the 'problem area' thus validating the anode spike trajectory. In addition, Figure 7.8 shows the score space with the anode effect area for the anode effect fault model.

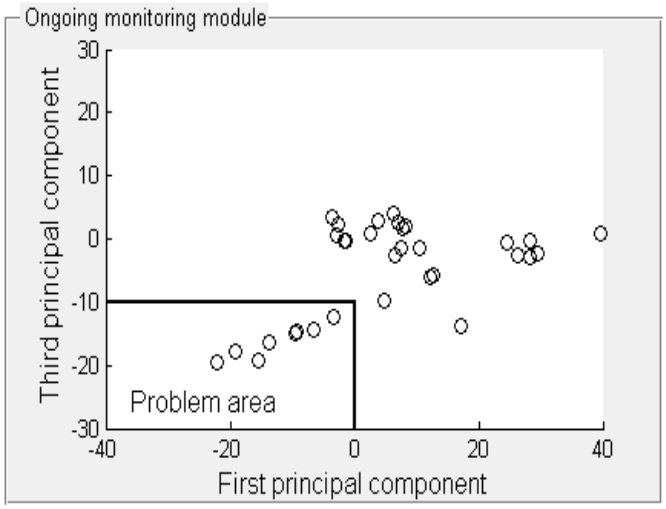

Figure 7.6: The New 'Problem Area' in a Score plot

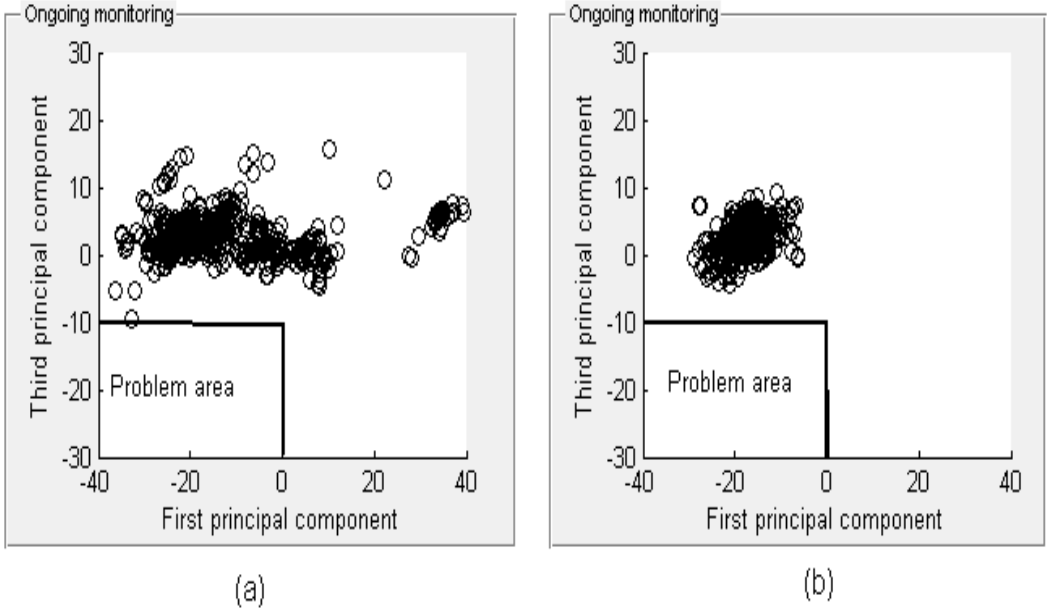

Figure 7.7: Scores for two Cells without Anode Spikes, (a) Cell 2023 and (b) Cell 2084, move away from the 'Problem Area'

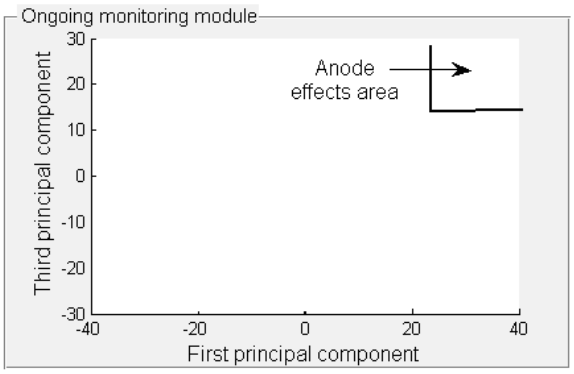

Figure 7.8: A score plot indicating an Anode Effect area

7.3.2. DPLS approach

Fault diagnosis based on DPLS was used according to the procedure described in section 4.9.2 in Chapter 4. However, in this thesis, the new statistical framework for diagnosing the aluminium electrolysis process based on DPLS is shown in Figure 7.9. The reference model (DPLS 1) developed from Phase II, was used to diagnose the out-of-control signals in Phase III. The key to success is to treat the alumina feeding cycle as a batch operation so that the main steps in MPLS, step 2 and step 3 in Figure 7.9, were applied in this framework. The reference models were designed to be developed by considering the impact of anode changing. The final output of the system was the class of fault that can be revealed to the operators via a user-friendly interface. The details of each step in developing the system are given as follows.

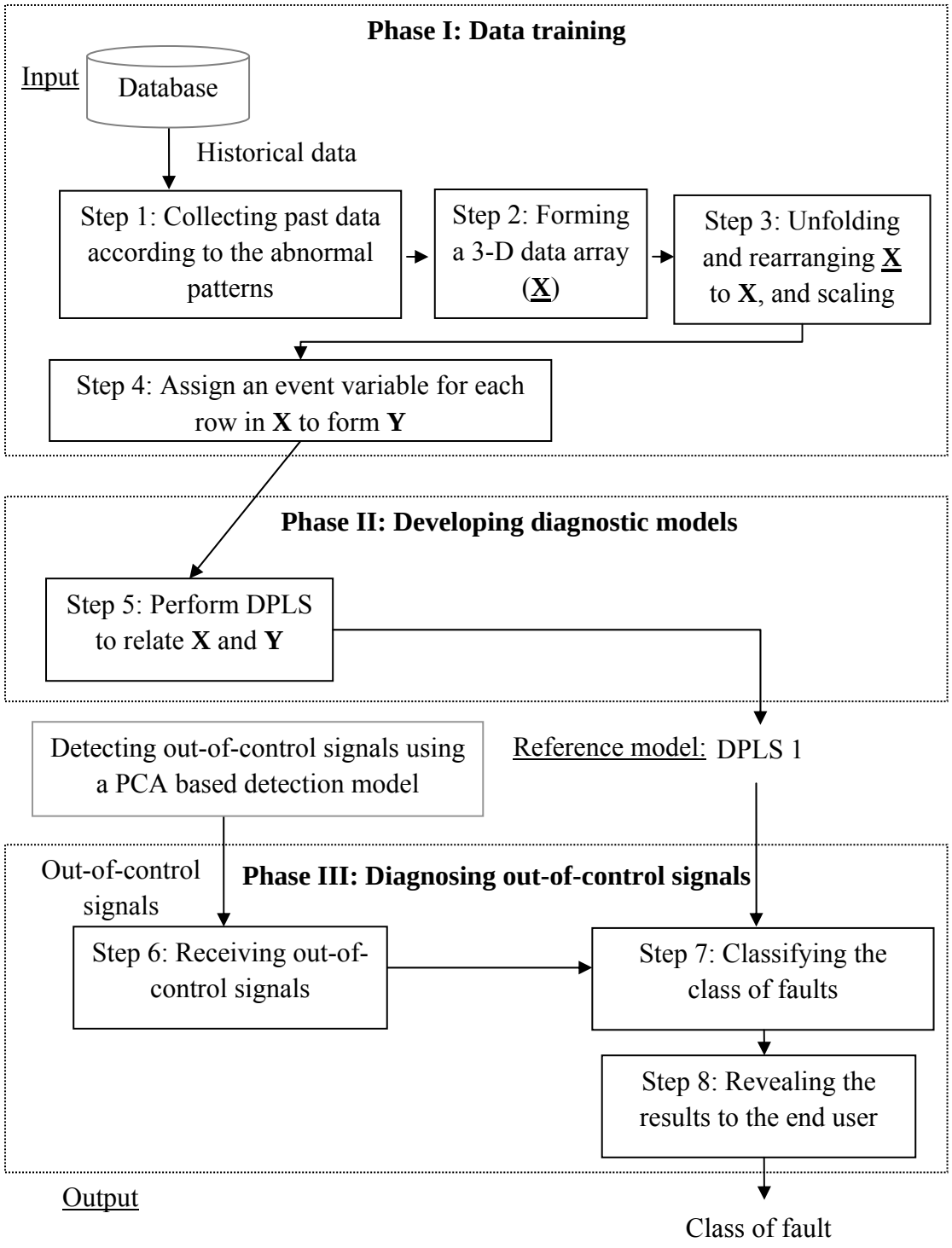

Figure 7.9: Framework of the Fault Diagnosis system using DPLS

7.3.2.1. Phase I: Data training

Step 1: When the downward trend of anode changing ended, past data or training data, were collected according to the pre-identified abnormal patterns.

Step 2: Training data were used to construct a 3-D data arrays, $\underline{\mathbf{X}}_1$, for anode faults module as shown in Figure 7.10

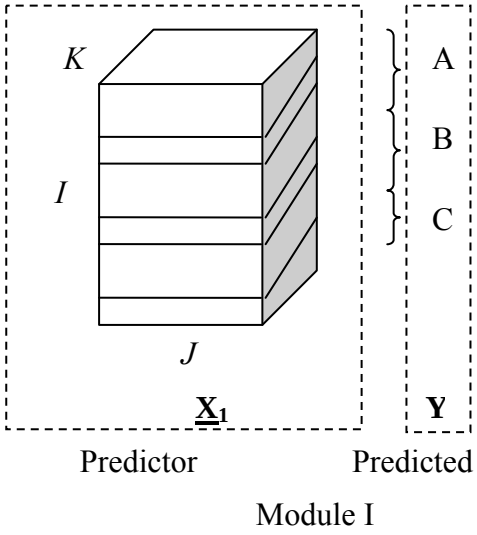

Figure 7.10: Three-dimensional data array for Module I (Anode Faults module)

Step 3: The data array ($\underline{\mathbf{X}}_1$) was unfolded and rearranged into a large 2-dimensional data matrices ($\mathbf{X}_1$) as shown in Figure 7.11.

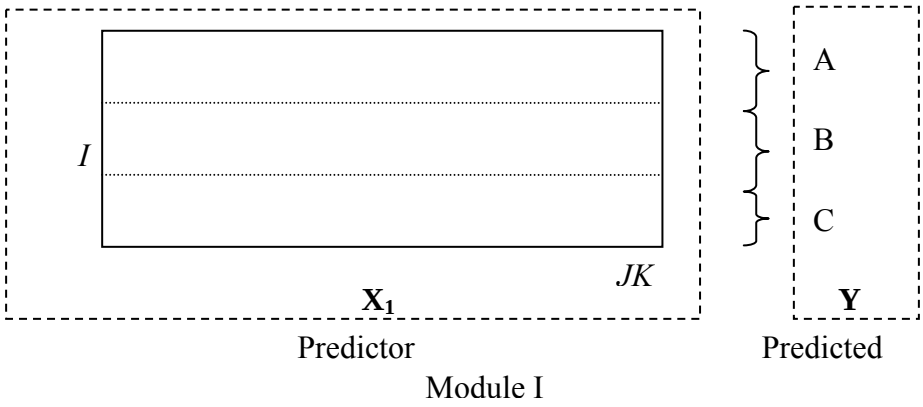

Figure 7.11: Schematic of the Unfolded Training Data, $\mathbf{X}_1$

Step 4: A unique code was assigned for each abnormal pattern as can be seen in Table 7-1 for Module I. This forms a set of event variables, $\mathbf{Y}_1$, where each row in the matrices represents the type of fault for each row in $\mathbf{X}_1$.

Table 7-1: Response Variables for Module I

Pattern	$\mathbf{Y_1}$			Class code
	1	2	3	
A	1	0	0	100
B	0	1	0	010
C	0	0	1	001

7.3.2.2. Phase II: Developing diagnostic models

Step 5: The procedure relating to DPLS was performed for modelling $\mathbf{X_1}$ with $\mathbf{Y_1}$ using the NIPALS algorithm, as described in section 4.9.2. The main parameters for these models were a weighting matrix (**W**), a regression matrix (**B**), a loading matrix (**Q**) and a residual matrix (**F**).

7.3.2.3. Phase III: Diagnosing out-of-control signals

Step 6: Out-of-control signals from the PCA based fault detection system were received in the form of an unfolded 2-D data matrix. The estimation of the future data was performed using the PCA based fault detection system.

Step 7: The class of fault for the new out-of-control signal was estimated using equation 4-28.

Step 8: The diagnostic results were revealed in the user interface of the system.

7.3.3. Integration between MPCA model with pre-identified abnormal region approach and DPLS-M approach in Module I

In Module I, variability patterns recognised from Part I and used to develop the fault diagnosis tool were based on process data within a number of feeding cycles. So a 3-D data array was used to represent these data. Therefore, extension of PCA and PLS, MPCA and MPLS, were used in order to unfold and rearrange the 3-D data array to a large two dimensional (2-D) data matrix. Following this, MPCA with pre-identified regions and DPLS

were then applied to this 2-D data matrix for the development of diagnostic models and for the classification of a number of faults. Therefore, for a DPLS based diagnostic model, a combination of MPLS and DPLS or DPLS-M was used in this research. A flow chart for Module I that integrates the MPCA model with a pre-identified 'abnormal region' approach combined with a DPLS-M approach is shown in Figure 7.12.

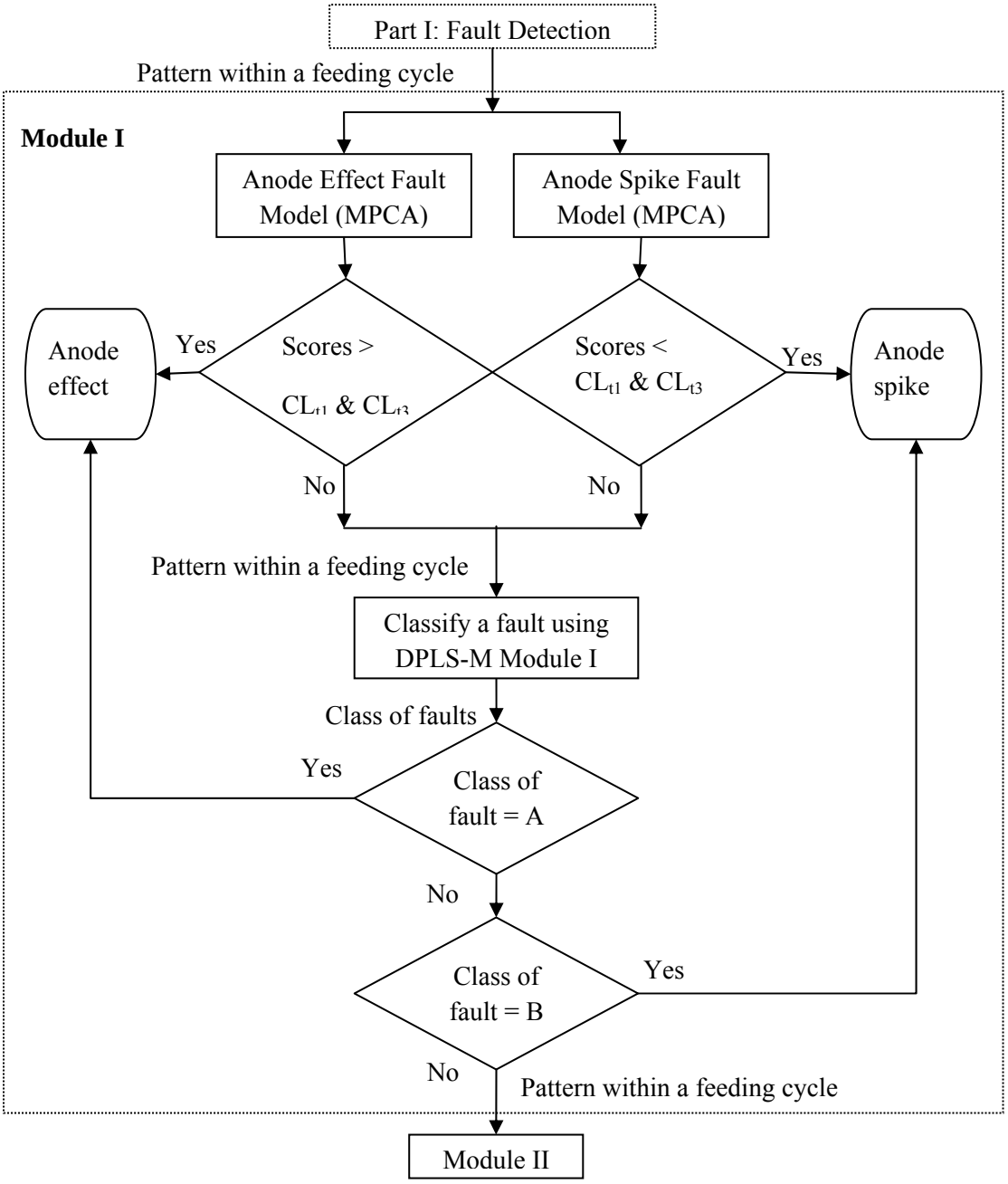

Figure 7.12: The Flowchart for Module I in Fault Diagnosis

In the flowchart for Module I (Figure 7.12), once out-of-control signals were detected in Part I, an abnormal pattern was diagnosed using the MPCA based model to detect anode faults. Following the process of diagnosis by the MPCA model in which abnormal patterns, anode faults, were not detected, it was possible to detect anode faults using the DPLS model, the reason being that, in the process of diagnosing faults in chemical processes, this model performs better than PCA. Finally, abnormal patterns for non-anode faults were diagnosed using Module II.

7.4. Procedure for Module II (non-anode faults module)

Module II was also developed according to the main steps presented in Figure 7.9. A 3-D data array for Module II is shown in Figure 7.13, a schematic of the unfolded training data, $\mathbf{X_2}$, is shown in Figure 7.14, and response variables for Module II are shown in Table 7-2.

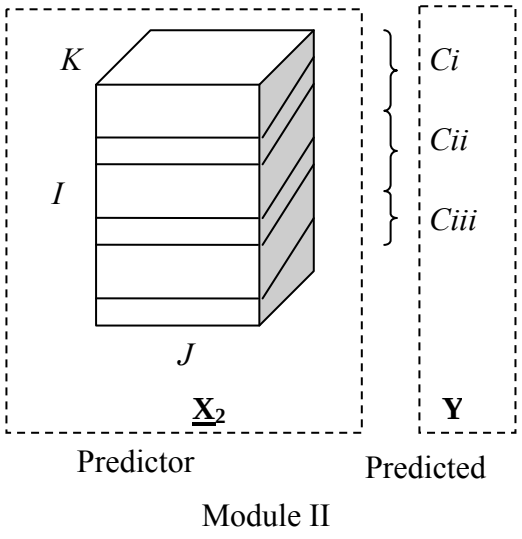

Figure 7.13: Three-dimensional data array for Module II (Non-Anode Faults module)

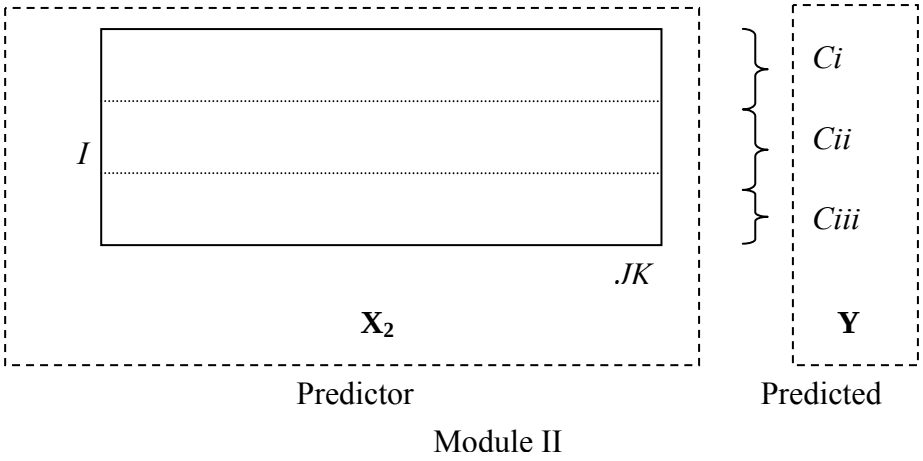

Figure 7.14: Schematic of the Unfolded Training Data, $\mathbf{X_2}$

Table 7-2: Response Variables for Module II

Pattern	**Y**			Class code
	1	2	3	
Ci	1	0	0	100
Cii	0	1	0	010
Ciii	0	0	1	001

The flow chart for Module II where the results could be low alumina dissolution, a blocked feeder or other faults, is shown in Figure 7.15. In addition, if the next out-of-control signals were classified as having an anode effect or pattern *A*, the out-of-control signals before the anode effect classified using Module II could indicate the causes of an anode effect.

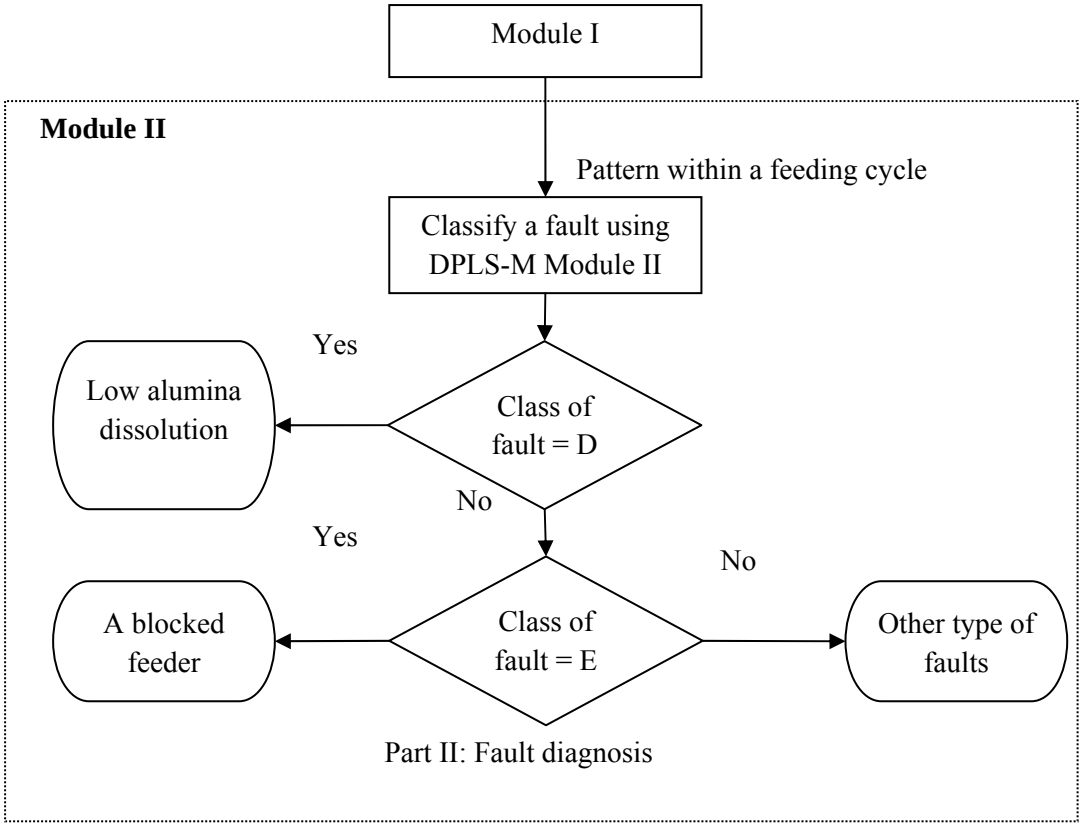

Figure 7.15: Flow Chart for Module II

7.5. Evaluation of the fault diagnosis system

7.5.1. Scope and reference models

The scope of this evaluation only covers the use of the reference model number 10 to diagnose new data from the process at the point at which the downward trend ended. This model used an artificially lengthened cycle as the trajectory alignment method. In order to develop DPLS models for Module I and II, first, training data were collected, as in Step 1, and two 3-D data arrays, $\underline{\mathbf{X}}_1$ (24 x 6 x 40) for Module I and $\underline{\mathbf{X}}_2$ (66 x 6 x 40) for Module II were constructed using these training data, as in Step 2. These data arrays were then unfolded and rearranged as in Step 3 to form data matrix $\mathbf{X}_1$ (24 x 240) and $\mathbf{X}_2$ (66 x 240). Every row in these matrices was assigned with an abnormal event code according to Table 7-1 and Table 7-2 in Step 4. Finally, as in Step 5, the DPLS procedure was applied to the first data matrix, $\mathbf{X}_1$ in order to form the first diagnostic model consisting of **W** (240 x 10), **B** (10 x 10) and **Q**

(3 x 10), whereas, the second diagnostic model built from $\mathbf{X_2}$, consisted of **W** (240 x 18), **B** (18 x 18) and **Q** (3 x 18). These diagnostic models were stored for the purpose of diagnosing the faults.

7.5.2. Results of fault diagnosis using aluminium smelting data

In order to evaluate the performance of the system during fault diagnosis, real data from Aldel's aluminium smelter were used as test data sets in this section. All test data sets were run through the PCA-based detection model to detect out-of-control signals. The diagnosis system first classified these signals using the diagnostic model from Module I in order to detect anode faults. The results for test sets for Module I are shown in subsection 7.5.2.1 where the DPLS and MPCA approaches were evaluated separately. The results for test sets for Module II are then shown in subsection 7.5.2.2.

7.5.2.1. Results for test sets for Module I

Thirteen aluminium reduction cells were used as test cells, 8 cells had anode effects and 5 cells for anode spikes. Since these test sets related to faults, the PCA based detection system detected out-of-control signals using the Hotelling's T^2 and SPE charts. The total number of these out-of-control signals received in Step 6 in Figure 7.9 is shown in the detection window in Table 7-3 and Table 7-4. These out-of-control signals were classified as in Phase III (Diagnosing out-of-control signals) for both MPCA and DPLS models. The success rate of the out-of-control signals correctly diagnosed by the system, or the diagnosis success rate, was calculated by dividing the correctly diagnosed signals (CDS) with the total number of out-of-control signals as shown in the detection window. This diagnosis success rate was used to evaluate the performance of the proposed diagnostic models.

Table 7-3: Performance Evaluation Results of the First Module for Anode Effects

Anode fault	Test	Cell	Detection window	DPLS		MPCA	
				CDS	Diagnosis success rate	CDS	Diagnosis success rate
Anode effect	1	a	4	3	0.75	-	-
	2	b	1	1	1	-	-
	3	c	2	2	1	-	-
	4	d	4	4	1	3	0.75
	5	e	3	-	-	-	-
	6	f	4	2	0.50	-	-
	7	g	2	1	0.50	2	-
	8	h	3	3	1	-	0.50
Average diagnosis success rate					0.72		0.16

Table 7-4: Performance Evaluation Results of the First Module for Anode Spikes

Anode fault	Test	Cell	Detection window	DPLS		MPCA	
				CDS	Diagnosis success rate	CDS	Diagnosis success rate
Anode spike	1	i	141	9	0.06	2	0.01
	2	j	77	31	0.40	26	0.29
	3	k	62	17	0.27	4	0.06
	4	l	2	2	1	-	-
	5	m	116	12	0.10	3	0.03
Average diagnosis success rate					0.37		0.08

The results of classifying the out-of-control signals are shown in Table 7-3 and Table 7-4 in which the DPLS based diagnosis system achieves 0.72 for the average diagnosis success rate for anode effect and 0.37 for the average diagnosis success rate for anode spikes. The proposed method produces satisfactory diagnosis results for anode effect cases. For Test

4, for example, the anode effect can be predicted 20 minutes ahead of time. However, for anode spike cases, the average diagnosis success rate is below 0.5. The reason for this is that compensatory actions were taken when the total of cell voltage was low during the spiking problem. Therefore, the systematic pattern that is related to an anode spike was difficult to observe continuously although the spiking problem remained. However, when the system diagnosed the fact that the process was undergoing an anode spike, the diagnosis time occurred at an earlier time than when the spiking problem was detected in the actual smelter. This indicates that although the diagnosis success rate below 0.50, it provides a better solution for the detection anode spikes since in real operations, an early detection of this operating abnormality is difficult to achieve.

The results also show that the DPLS model was more proficient than the PCA model for fault diagnosis during anode spikes and for the detection of anode effects. These results support the expectation that DPLS would perform better than PCA in diagnosing faults in chemical processes. The reason for this is that DPLS is a supervised approach so that the extracted latent variables capture large variations in the process data (**X**), which are most predictive of the fault classes (**Y**). Whereas, MPCA is an unsupervised approach so that the extracted latent variables only capture large variations in the process data (Chiang et al., 2000).

7.5.2.2. Results for test sets for Module II

Table 7-5 provides the results of the DPLS-M model for out-of-control signals for non-anode faults by classifying three events (*Ci*, *Cii* and *Cii*). The results show that the percentages of low alumina dissolution (*Ci*) are much higher than for the occurrence of a blocked feeder (*Cii*). In fact, most of the causes of the anode effects were attributed to low alumina dissolution. These results relating to the low alumina dissolution were validated by using additional information for cell 2139 (Test 1 in Table 7-5) where an increase in the number of

alumina shots occurred because of the low level of alumina dissolution. Furthermore, the temperature of the cell was lower than the target, 957.6 °C so that less energy is available in order to dissolve alumina.

Table 7-5: Performance Evaluation Results of the Second Module

Test	Cell	Detection window	CDS	Diagnosis success rate for low alumina dissolution	CDS	Diagnosis success rate for blocked feeder	CDS	Diagnosis success rate for other faults
1	A	31	28	0.90	-	-	3	0.09
2	B	25	24	0.96	1	0.04	-	-
3	C	12	12	1	-	-	-	-
4	D	0	-	-	-	-		-
5	E	1	-	-	1	1		-
6	F	12	11	0.92	-	-	1	0.08
7	G	38	37	0.97	1	0.02		-
8	H	22	21	0.95	1	0.05		-
Average diagnosis success rate				0.71		0.13		0.02

7.6. Discussion: addressing the second research question

The diagnosis success rate in the evaluation of the diagnosis system shows that faults can be diagnosed by using a multivariate system. This multivariate diagnosis system also considers the dynamic behaviour during anode changing and alumina feeding as does the fault detection system by treating the alumina feeding cycle as a batch operation and designing the diagnostic framework with multiple reference models. The results show that the consideration of the variability pattern within an alumina feeding cycle in modelling the system can help in diagnosing abnormal events. This also supports the finding that DPLS is effective here

because the predictive model was developed by considering the correlation among the variables (Miletic et al., 2004). Overall, the results show the ability of the proposed multivariate diagnosis system to complement the fault detection system, thus addressing the second research question. This again allows the implementation of on-line process monitoring as does the first research question (section 6.4). However, there are several issues that need to be considered in implementing this system in an actual smelter including insufficient offline fault data and the occurrence of multiple faults.

The first issue for implementing the diagnosis system in an actual smelter is the insufficiency of off-line fault data. This research focuses only on diagnosing anode faults and the causes of an anode effect. There are many other faults that could happen in the smelter. However, the types of fault diagnosed in this study were limited to the data being received from an aluminium smelter. In fact, only a small number of faults were actually recorded in detail in the smelter. Therefore, in order to extend this system for the diagnosis of other faults, the occurrence of the faults should be recorded in the smelter to enable the extraction of the abnormal pattern of the fault.

Another issue that needs to be considered is the diagnosis of multiple faults. Based on communications with a process engineer at Aldel's aluminium smelter, multiple faults do occur in this smelter. The reason is inefficiency in the detection of faults that may cause other faults to occur in sequence. This is explained further and three examples are provided. The first example is inefficient detection of low alumina dissolution that causes the formation of sludge. Because of the preferential flow characteristics of the metal, the sludge gradually forms under the point feeders directed towards the corner of the cell. This could cause anode spikes when the current of the cell goes directly to the molten aluminium because of the build

up sludge. The second example is inefficiency in detecting problems with the hardware of the alumina feeders. This can result in poor feeding which consequently causes low bath levels and high cathode resistance. The third example is compensatory control actions such as voltage and AlF_3 additions, these may add to the difficulties in fault detection. This is because these actions could change the current status of the cell so that the real problems are concealed for a particular period of time (M. Stam, personal communication, November 10, 2010). Only one fault was recorded at one time for the training data used in this system. In order to detect multiple faults, when a smelter has detected several faults at the same time, the data relating to that event should be stored so that the abnormal pattern of the event can be learnt. It is then possible to detect multiple faults by recognizing the extracted pattern.

7.7. Conclusions

A Cascade fault diagnosis system was designed to incorporate the novelty features for diagnosing the aluminium smelting process by treating alumina feeding cycle as a batch operation. The dynamic behaviour of the process during anode changing was also addressed by designing a framework with multiple reference models. The changes of patterns in the voltage/alumina concentration curves from 29 data sets detected by the Cascade fault detection system were further diagnosed by the Cascade fault diagnosis system. The evaluation results show that the use of the Cascade fault diagnosis system successfully classified four abnormal patterns based on the variation of data within an alumina feeding cycle. This system is expected to automatically assist the process engineer in an aluminium smelter in diagnosing anode faults so that the need for laborious manual work and human interference can be reduced. Since the questions about when and which fault has occurred have been addressed, the next task is to discover how to integrate the Cascade fault detection and diagnosis systems.

CHAPTER 8: SYSTEM INTEGRATION

Since the two main parts of this research, fault detection and fault diagnosis, have been described earlier in this thesis, the integration of these parts is the main concern of this chapter. The part pertaining to fault detection has been integrated with the section concerning fault diagnosis using a 'tight coupling' model and this is presented first. The graphic visualisation of the system is given in data flow diagrams. The implementation of the system is also explained. This explanation is followed by an evaluation of the whole system using illustrative examples of real case studies that were recorded in the real-world environment of an aluminium smelter. The severity of detected faults is finally discussed.

8.1. Integration of Cascade fault detection and fault diagnosis

8.1.1. Methodology of integration

In process of the integration of fault detection and fault diagnosis, two types of methodology were investigated, 'tight-coupling' and 'loose-coupling'. Figure 8.1 shows the loose-coupling model for the proposed system where the interaction between fault detection and diagnosis has been accomplished with the aid of data files. The advantages of using this model include: (1) ease of development; individual components can be developed using various forms of commercial software, (2) ease of maintenance because of the simplicity of the process of interaction using data files (Guh, 1999).

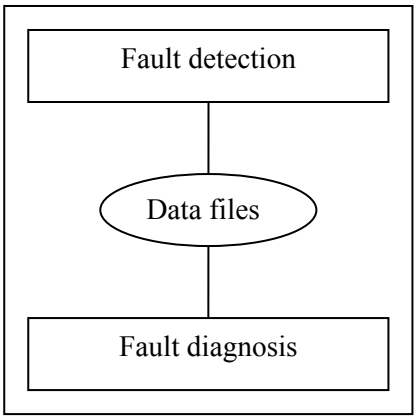

Figure 8.1 Loose-coupling Model for integrating between Fault Detection and Fault Diagnosis

In the tight-coupling model, the interaction is accomplished by using memory-resident data structures rather than by the use of data files (Figure 8.2). This is the main difference between the tight-coupling model and the loose-coupling model. Therefore, the runtime performance for the tight-coupling model is better than that of the loose-coupling model (Guh, 1999). This method of integration has been adopted in this research because both detection and diagnosis applications were developed using MATLAB 7. The idea behind developing the two parts of the investigation separately and then integrating them using an integration method was to increase the flexibility of the system for the future use. For example, if one wants to integrate an additional tool into the PCA model that is different than the existing one, the new tool can be easily integrated into the existing fault detection system. However, loose-coupling might be considered if the new tool were to be developed using an alternative environment.

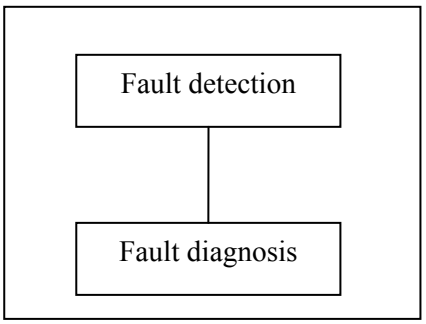

Figure 8.2: Tight-coupling Model for integrating between Fault Detection and Fault Diagnosis

8.1.2. System modelling of Cascade fault detection and diagnosis

The Cascade fault detection system was designed to detect faults: an anode effect, an anode spike and other faults (a blocked feeder and low alumina dissolution). In order to detect these faults, the system was divided into two parts. The first part identifies when a fault has occurred (fault detection) and the second part determines which fault has occurred (fault diagnosis). Data flow diagrams were further used to demonstrate the logical flow throughout the system.

The data flow data diagrams for the system are shown in Figure 8.3 to Figure 8.6. The context diagram (level 0) for the system, which is the overall view of the system, is shown in Figure 8.3. This diagram shows the data flow from the production process (external entity) to the system and then to the user (another external entity). The context diagram is decomposed into a lower level of detail, a level 1 diagram. This decomposition is shown in Figure 8.4 where the main modules within the system are fault detection and fault diagnosis. The fault detection module triggers the fault diagnosis module when abnormal events occur in the process. The related abnormal pattern is then sent to the fault diagnosis module. Each module in level 1 in Figure 8.4 is then broken down into a lower level of detail which is a level 2 diagram. The level 2 diagram for each Cascade fault detection module and Cascade fault diagnosis module is shown in Figure 8.5 and Figure 8.6, respectively.

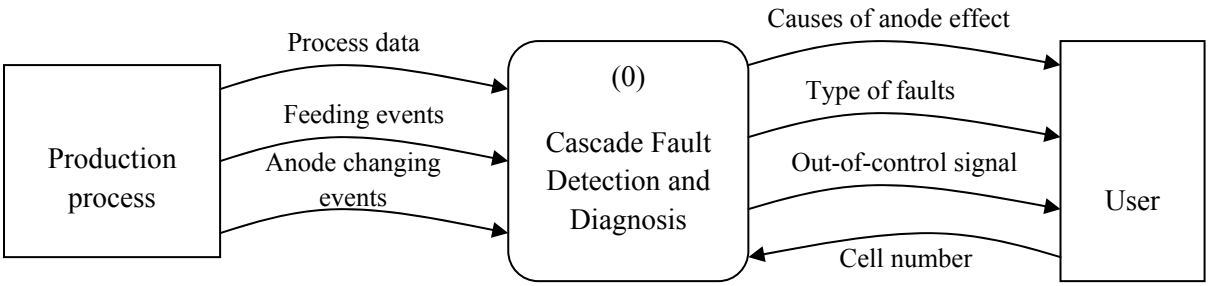

Figure 8.3: Context diagram for the Cascade Fault Detection and Diagnosis system (Level 0)

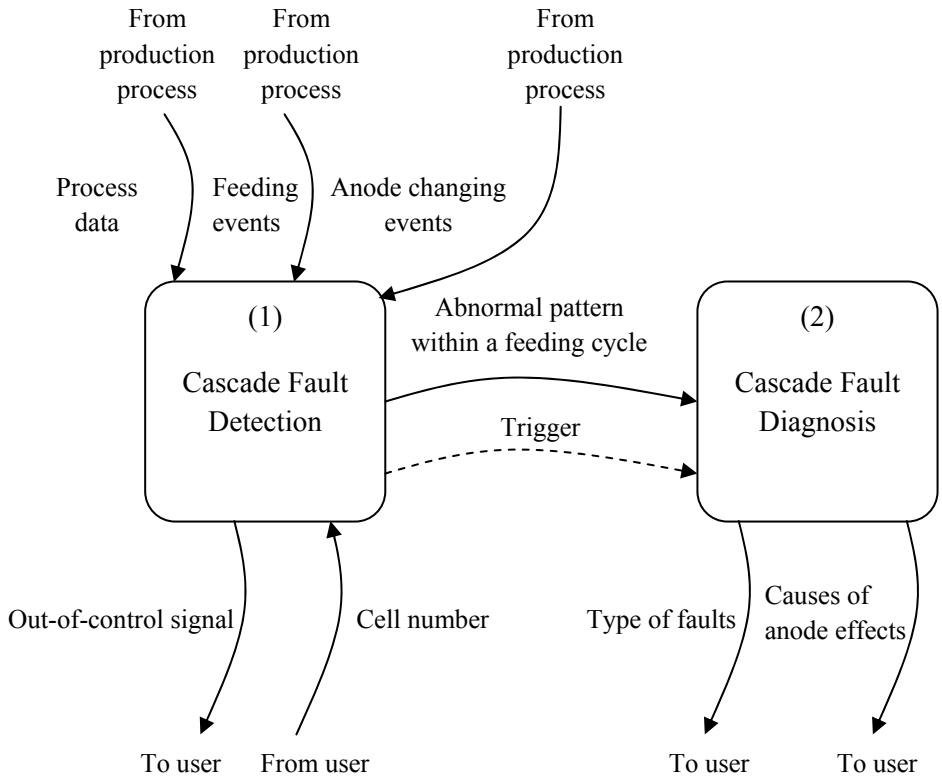

Figure 8.4: Level 1 of Cascade Fault Detection and Diagnosis

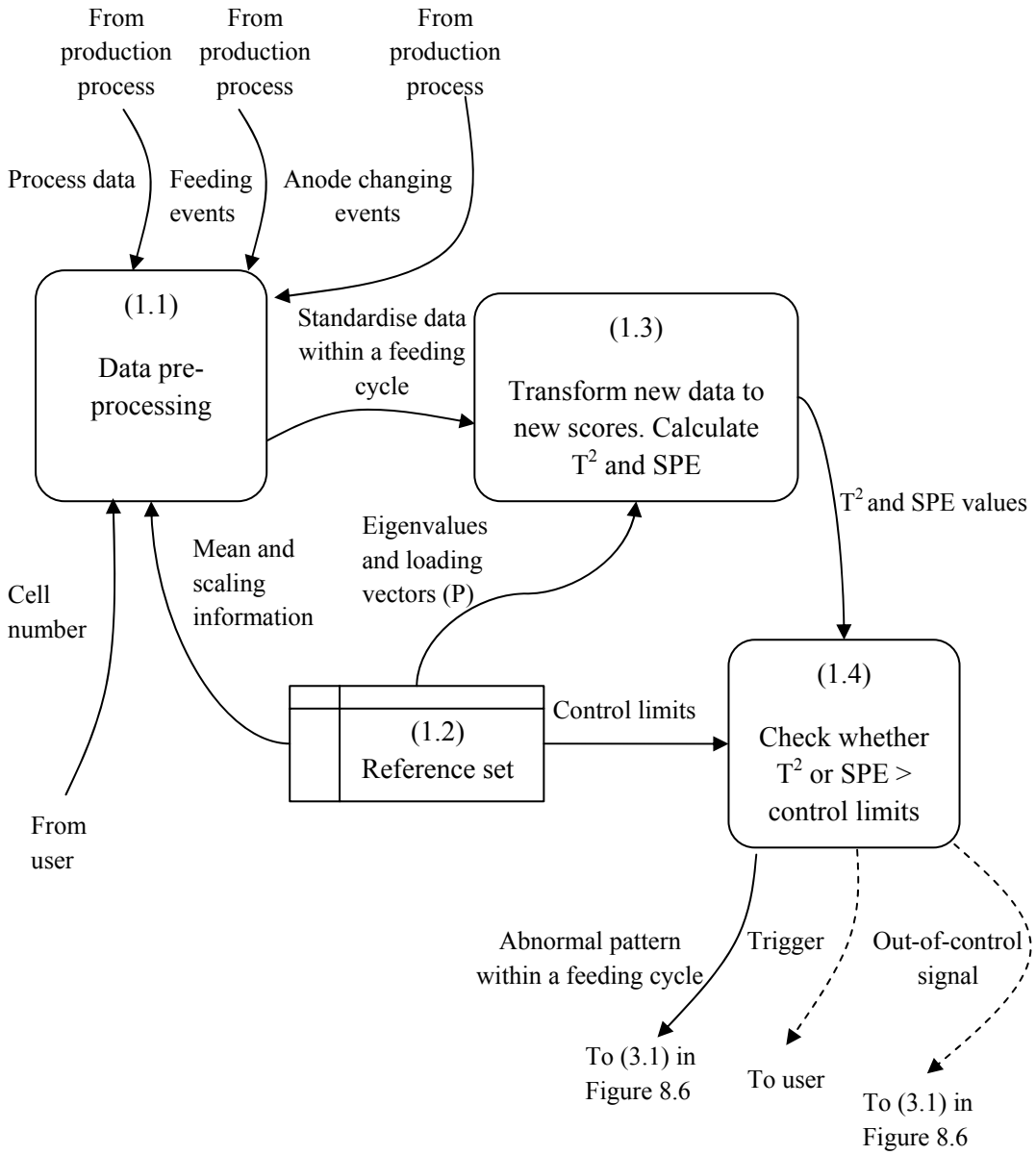

Figure 8.5: Cascade Fault Detection-Level 2

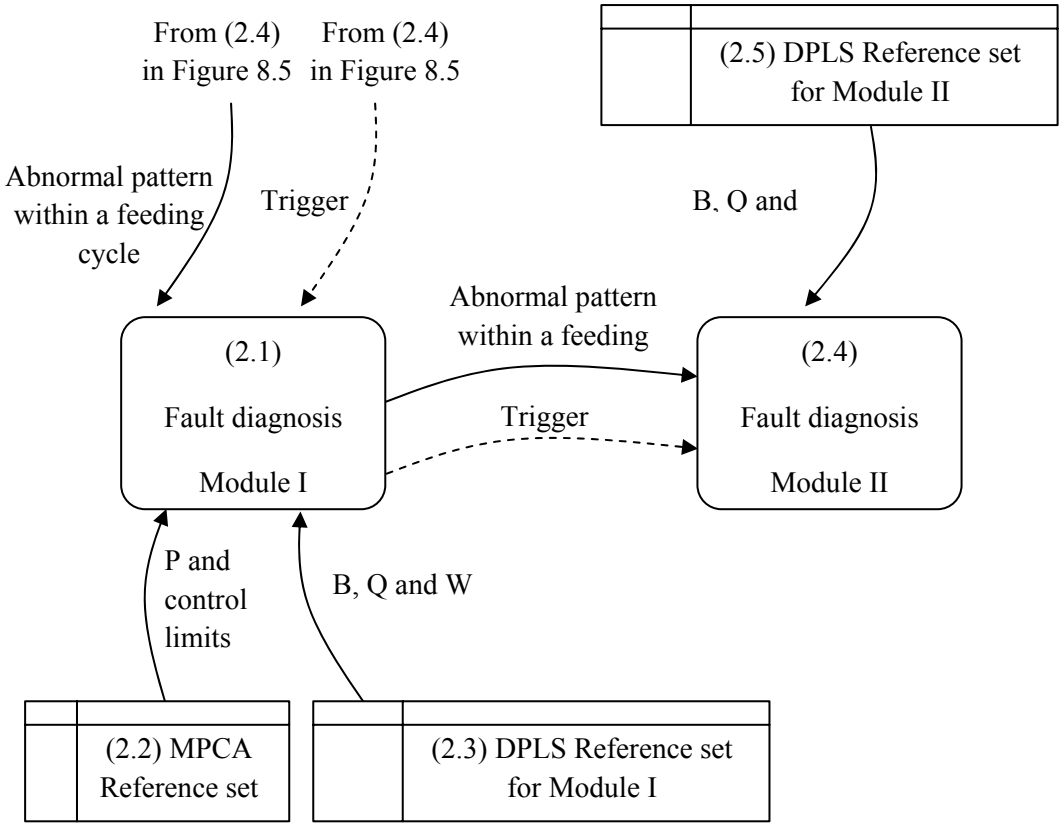

Figure 8.6: Cascade Fault Diagnosis- Level 2

8.2. Implementing the Cascade fault detection and diagnosis

In order to implement the Cascade fault detection and diagnosis system, this system was attached to the larger, existing process control system of the aluminium smelter, as illustrated in Figure 8.7. There are four main modules in this larger system and it is typically based on a real-time computer system (e.g. Burns and Wellings, 1990). In this larger system, the Cascade fault detection and diagnosis system was an additional part which, in real-time, contributed most to the detection of some particular faults.

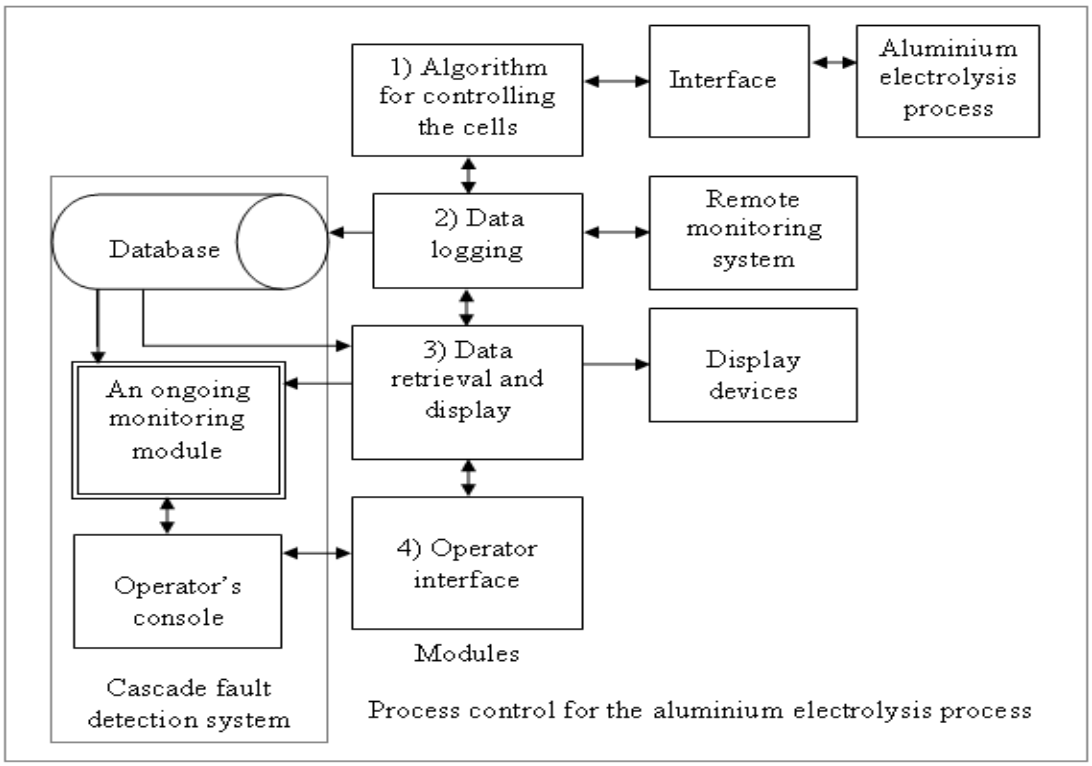

Figure 8.7: A Schematic of a Typical Real-time Process Control System for the Aluminium Electrolysis Process with a Fault Detection and Diagnosis System attached (adapted from Burns and Wellings, 1990)

The Cascade fault detection and diagnosis system was attached to the data retrieval and display module, the operator interface module and then to the database of that larger system, as shown in Figure 8.7. The inputs, such as: (1) process measurements, (2) feeding events, and (3) anode changing events, obtained from the data retrieval and display module were analysed using the on-going monitoring module that was updated in real time. The inputs became the current data points, while the previous data points were retrieved from the process plant database. It is essential that, since this system is a real-time system, the time taken for the detection system to signal the occurrence of faults based on the received data be minimal. The current status of the cell must be revealed in a timely manner to the operator and/or to the process engineer's computer screen. Information, such as the status of the cell, the current date and time, a list of suggested diagnoses and remedial or preventative actions,

is transmitted in order to assist the process engineer in making a proper decision to improve the current situation.

In order to develop the Cascade fault detection and diagnosis system, a high-level technical computing language, MATLAB, was used. The bridge between the MATLAB code and the existing system was a Microsoft Excel spreadsheet file on which all inputs and the outputs from the larger system were also stored. In addition, the graphic user interface that was built using the MATLAB code is also capable of displaying the data and the results using its own user interface, as shown in Figure 8.8.

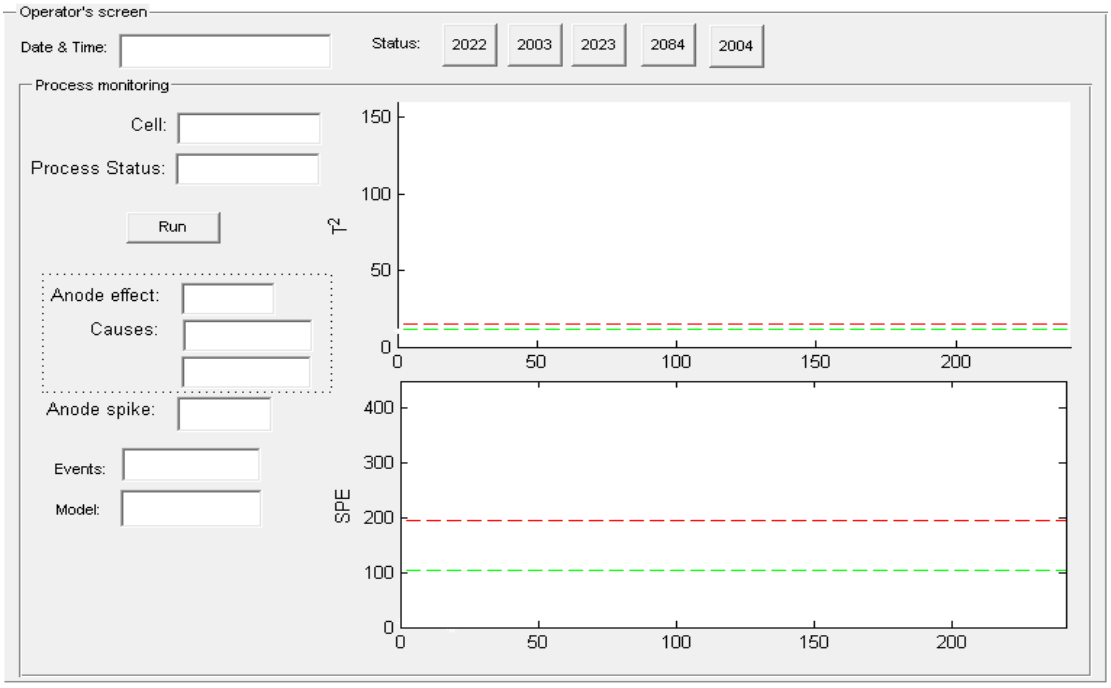

Figure 8.8: The Introduction Screen of the Cascade Fault Detection and Diagnosis System

8.3. System evaluation

The two parts of the system, fault detection and fault diagnosis, have been evaluated individually in previous chapters. In this section, case studies relating to the problems in a real-world environment have been used to evaluate the performance of the system after

integration. The aim is to validate whether, or not, the implementation of the whole system will meet the needs of the user.

Since the system was developed for real-time process monitoring, the MATLAB code of the system was written in on-line mode. Figure 8.8 shows the introduction screen of the system where the only input needed to run the simulation is the cell number. After the run button was clicked, during the monitoring process, samples were input to the program from the Excel file for the selected cell and then analysed by two separate programs. The first program is used for fault detection and the second program is used for fault diagnosis. The second program would be executed when a fault has been detected either by the T^2 chart or the SPE chart. In order to demonstrate how two abnormalities, anode spikes and anode effects, can be detected by using the Cascade fault detection system, two examples from Aldel's aluminium smelter are detailed in the examples that follow.

8.3.1. Example 1: Detection of anode spikes

An anode spike was recorded in cell 2003 in Aldel's aluminium smelter at 4.16 p.m. on 23 May 2009. One anode was affected and the remedial or preventative action was to change the anode. At the time when the anode spike was recorded by operators, it was not certain when this anode spike had begun to happen. Furthermore, at this time, the Cascade fault detection system was not implemented as an attachment to the existing process control system of the aluminium smelter. Early detection is advantageous. Therefore, in this example, an investigation was carried out to ascertain exactly how early in the Cascade fault detection system process could an anode spike be detected.

From the start of the anode change to the recording of the anode spike, the process data were stored in an Excel file. These data were retrieved in sequence from the Excel file and sent to

the Cascade system so that the results from the data could be compared to the practical application. In a real situation, the process data would be input in real time through the data acquisition system of the existing process control system. Figure 8.9 shows the logical flow from the aluminium reduction cells to the main operator's screen for the Cascade fault detection system and for the first part of Module I of Cascade fault diagnosis system which is an MPCA based fault diagnosis.

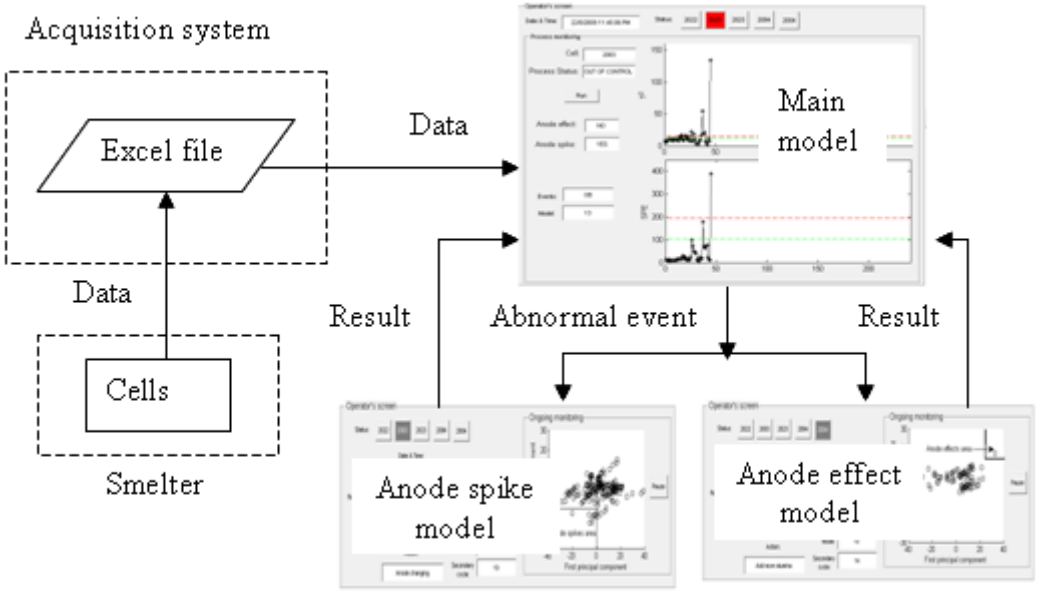

Figure 8.9: Logic Flow from Cells to the Cascade Fault Detection and Diagnosis System

Monitoring the data set revealed evidence of faults in this example where some of the Hotelling's T^2 and SPE values were above the control limits (Figure 8.10). Further analysis of these faults using the fault models (anode spike and anode effect fault models) showed that the related scores entered the anode-spike area. The operator's screen indicated this situation by a change in the colour of button for cell 2003 from green to red, the status of the process from 'IN CONTROL' to 'OUT OF CONTROL' and the status of the anode spike detection from 'NO' to 'YES'.

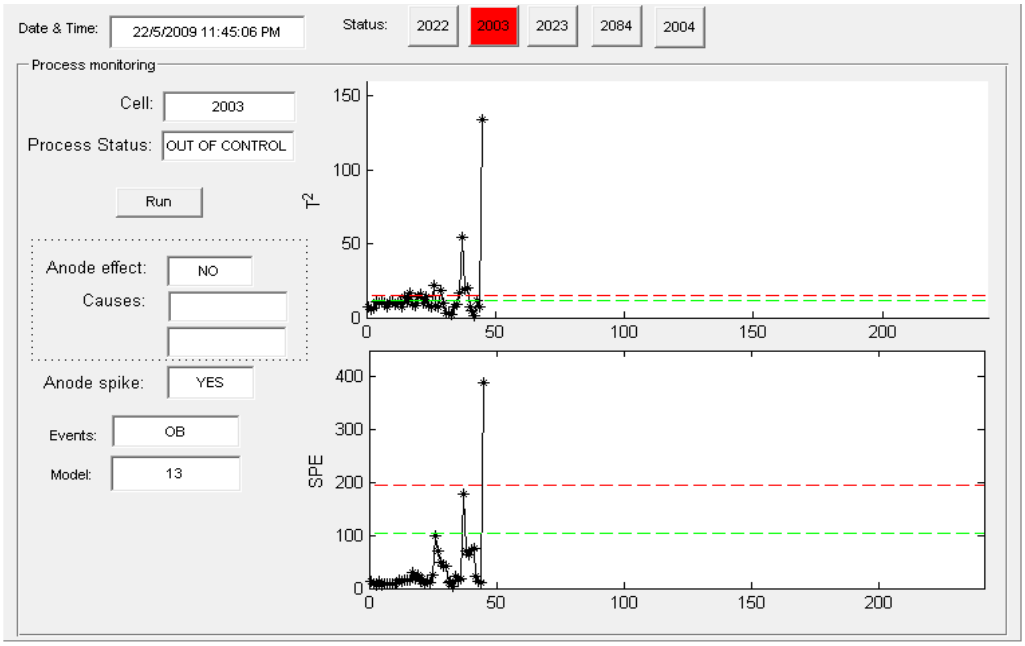

Figure 8.10: Operator Screen for Example 1 showing a Fault was detected at 11.45 pm on 22 May 2009 and the possible Fault was an Anode Spike

In this investigation, the time when the scores of the above samples entered the 'problem area' was compared with the detected time of the anode spike. There were three time periods, prior to the recorded time of the anode spike, during which scores entered the 'problem area', as indicated in Figure 8.11 for the cell voltage and Figure 8.12 for the screenshots of the anode spike model of the system.

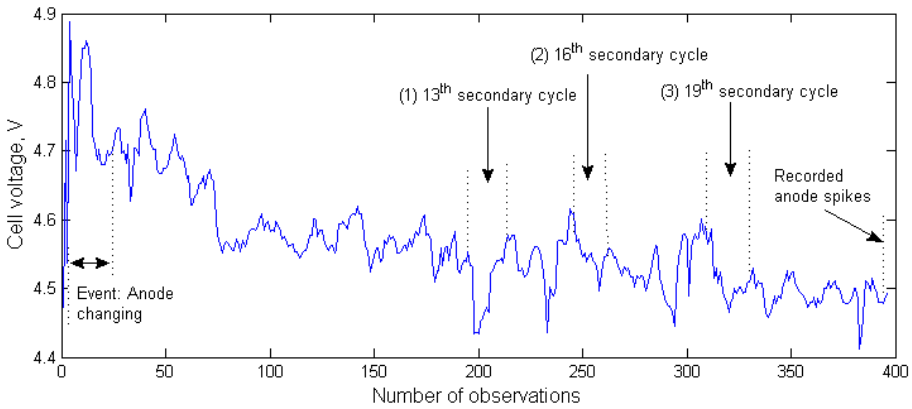

Figure 8.11: Samples for Anode Spike Detection in Example 1, indicating the Secondary Cycles that were involved in the Detection of the Anode Spike

(a)

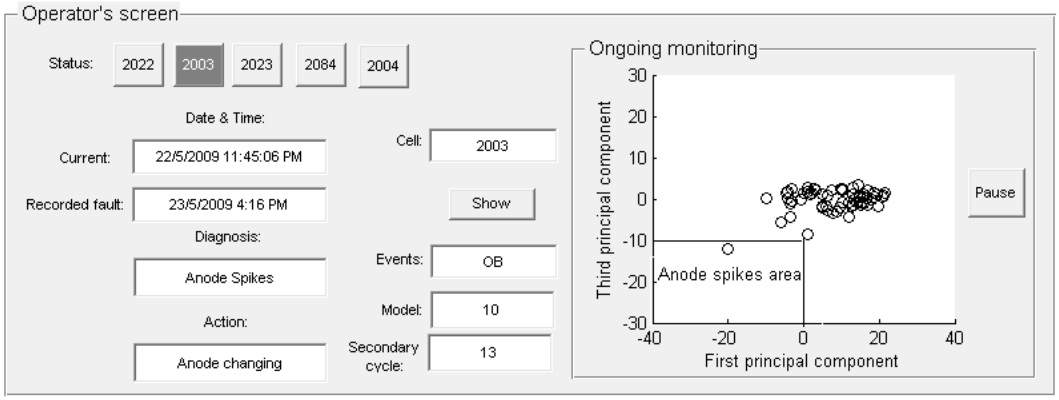

(b)

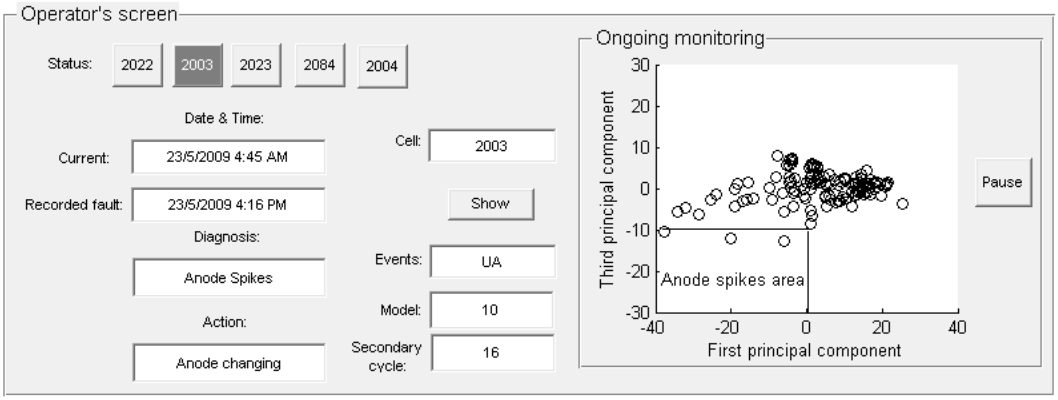

(c)

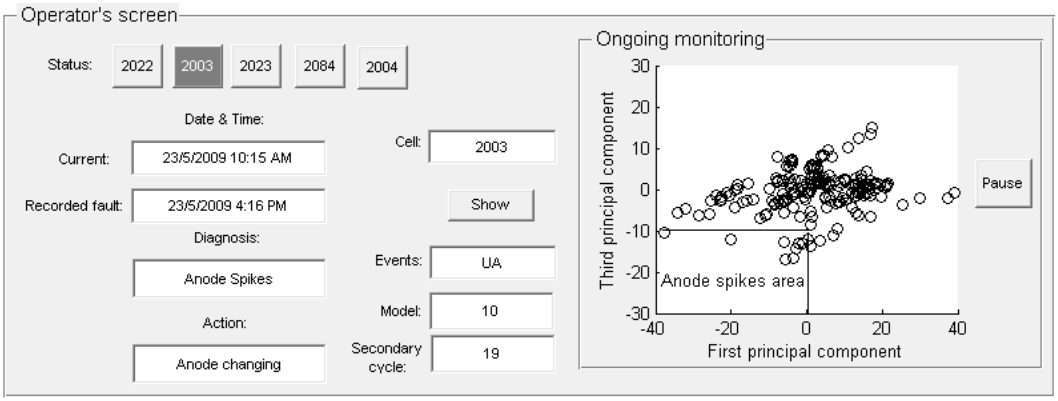

Figure 8.12: Anode Spike Detection in Example 1, indicating the Three Different Times when the Scores entered the Anode Spikes Area: (a) during the 13th Cycle, (b) during the 16th Cycle and (c) during the 19th Cycle

Firstly, the scores entered the 'problem area' at 11.45 p.m. on 22 May 2009 during the thirteenth secondary cycle in an anode changing event (Figure 8.12 (a)). Secondly, the scores entered the 'problem' area during the sixteenth secondary cycle, at 4.45 am on 23 May 2009

(Figure 8.12(b)). Thirdly, the scores again entered the 'problem area' at 10.15 am on 23 May 2009 (Figure 8.12 (c)). For this last (the nineteenth) secondary cycle, Figure 8.13 shows the deviation of cell voltage error data samples from the reference trajectory. The reason why the scores travelled in and out of the 'problem area' was due to the compensatory actions that had been taken by the operator to increase the low value of the total resistance of the cell whilst not realising a spike had developed. Since the anode spike protrusion still remained at the affected anode, the occurrence of the anode spike was once more detected, this time, by the Cascade fault detection system.

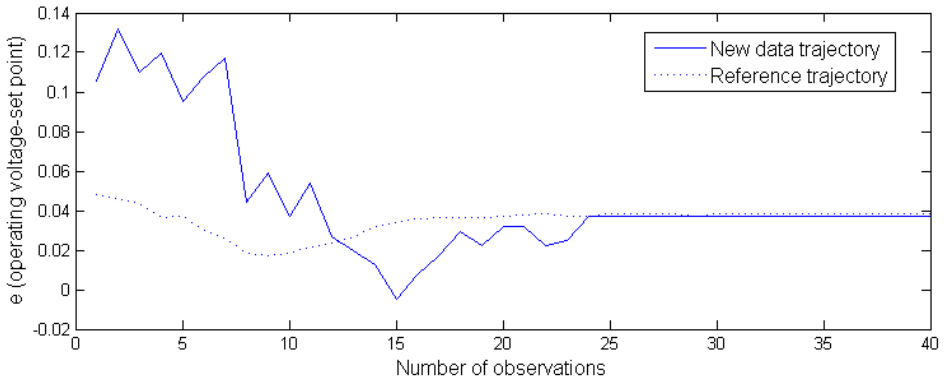

Figure 8.13: Deviations of Cell Voltage Error data samples during the 19th Secondary Cycle from the Reference Trajectory

Overall, this Cascade fault detection and diagnosis system, through its reference and fault models, appeared to detect the anodes spike at an earlier time, for example, before the anode spike was recorded by the operator in the aluminium smelter. The system proved to be faster than the current process used for the detection of anode spikes in three time instances: (1) 16 hours and 31 minutes earlier, (2) 11 hours and 31 minutes earlier, and (3) 6 hours and 1 minute earlier. In this particular case, an anode was changed due to the occurrence of the anode spike. If the anode spike can be detected early in the process, as in this particular instance of usage of the Cascade fault detection system, the operator can take corrective action earlier by going to the cell and either changing or cleaning the anode. This will stop

the short-circuiting that can increase the cell temperature to a level that could cause cell damage.

8.3.2. Example 2: Detection of an anode effect

For simulating the early detection of an anode effect, samples from cell 2004 were used. In this example, an anode effect was recorded at 8.45 am on 21 April 2009. In this example, the investigation was concerned with discovering exactly how early in the operating process the Cascade fault detection and diagnosis system would be able detect an anode effect.

The samples for detecting an anode effect were replayed from a Microsoft Excel spreadsheet file. The occasion when the scores entered the anode effect area was on the same day on which the actual anode effect occurred but approximately twenty minutes earlier, as can be seen in the reference model (Figure 8.14) and in the anode effect fault model (Figure 8.15).

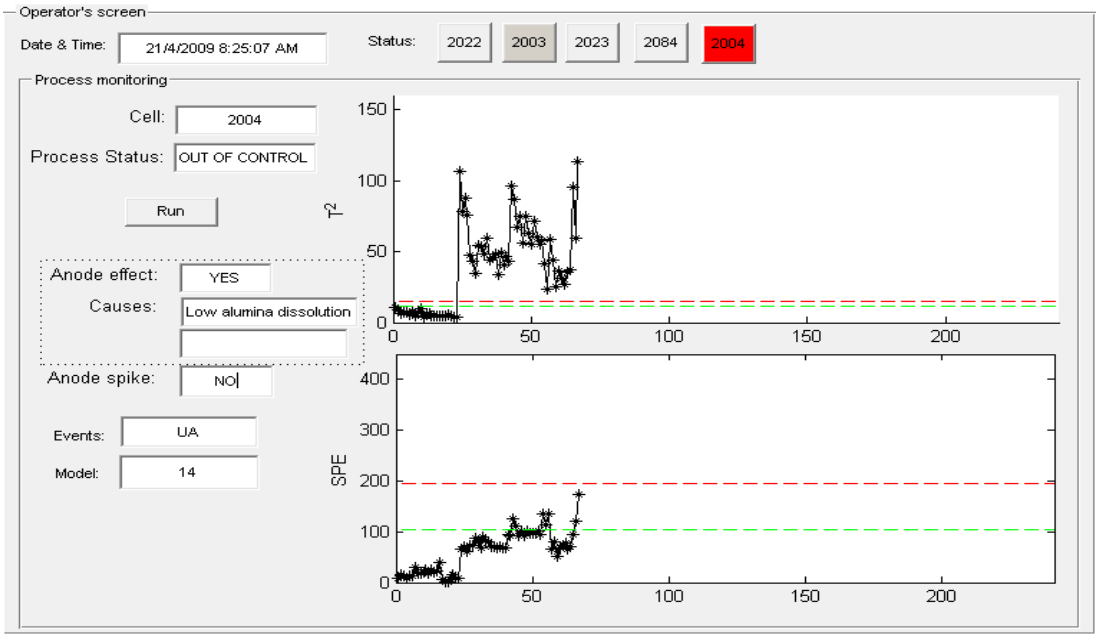

Figure 8.14 Operator Screen for Example 2 showing a Fault detected at 8:25 am was an indication of an Anode Effect

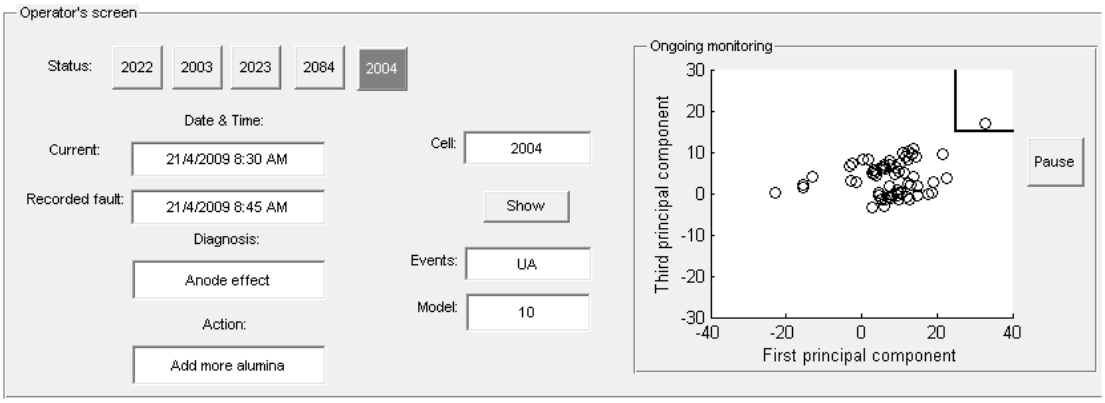

Figure 8.15: An Anode Effect detection in Example 2 where the Time of Detection was at 8:30 am, Fifteen Minutes earlier by the Fault Model than the Smelter Operation

In addition, during the period immediately prior to the anode effect, the alumina concentration in the cell was low so that the cell was feeding at a higher rate. Therefore, by predicting the occurrence of the anode effect a few minutes earlier, the cell could be fed earlier to increase the alumina concentration, or other action could have been taken to improve the rate at which alumina was dissolved in the bath. This would prevent the anode effect from occurring and also increase operational efficiency because not only do anode effects decrease current efficiency but they also emit greenhouse gas into the environment.

8.3.3. Detection of other faults

Before the system detected that the process was going to have an anode effect, there were many scores that violated the control limits of the monitoring charts. This shows that this system can detect other faults which were most probably the root cause of the anode effect. By using Module II in Cascade fault diagnosis, the root cause of the anode effect was identified as low alumina dissolution. Based on this information, the operator could go to the cell to check whether the cell temperature was low or whether there was a feeder blockage. This corrective action can prevent future re-occurrences of anode effects due to this particular root cause.

8.3.4. Severity of the detected abnormalities

Both abnormalities (anode effect and anode spike) cause complete disruption to the normal electrolysis process. They prevent metal production in the affected cell and the spike actually causes metal to revert back to alumina again (takes the cell backwards for a number of days). Both types of abnormality are frequent accompaniments to aluminium smelting even in the most modern of plants and they stand in the way of any further reduction in smelting energy consumption (M. Taylor, personal communication, July 21, 2010).

8.4. Conclusions

The two separate systems, fault detection and fault diagnosis were integrated using a method of tight coupling in order to enable interaction between the systems. The logic flows of the system were illustrated using data flow diagrams. These graphic visualisations describe in detail the interaction within and between the sub-systems. The interaction between the sub-systems in an integrated single system has been evaluated using real case studies. The result of the integration shows that the tight-coupling method works effectively as an integration method where the results were as expected when evaluating the sub-systems individually.

CHAPTER 9: CONCLUSIONS

For the purposes of this thesis, multivariate statistical techniques have been demonstrated to be effective in detecting and diagnosing faults in the aluminium smelting process. In this concluding chapter, firstly a brief summary of the thesis is given. This is followed by reference to the highlights in the literature used and the methodology employed. Next the research contributions and benefits are described. Finally, recommendations for possible future areas of research are given.

9.1. Summary of the thesis

A new multivariate Cascade fault detection and diagnosis system for the aluminium smelting process has been designed and developed in this thesis. Patterns related to known anode faults (spikes and anode effects) have also been extracted. The new system has been evaluated and simulated on-line using aluminium smelting data. These actions were taken due to the fact that the aluminium smelting industry urgently requires a new monitoring strategy in order to detect and diagnose faults in a timely and practical manner. This is because the operations of the smelters are currently beyond the capacity of their design; difficulties are experienced in process monitoring including: the need to process data which is both highly correlated and large in volume; the dynamic behaviour of the process, and lack of mathematical models for monitoring the process. The new Cascade system has been developed to address these problems using the multivariate statistical techniques of MPCA and MPLS. This is to allow for the building of multiple reference models based on the resistance versus alumina concentration curves for considering the dynamic behaviour during that occurs during alumina feeding and the cascade-like pattern that appears during the anode changing process. The evaluation of the newly designed system which has been presented in

this thesis indicates that it can successfully detect and diagnose anode faults within a reasonable timeframe. This implies that early fault detection and diagnosis can help to prevent undesirable outcomes in the industry such as the occurrence of unacceptably high temperatures or the emission of greenhouse gases.

9.2. Summary and highlights of the literature

The summary and highlights of the literature involve three main areas: (1) aluminium smelting process, (2) fault detection and diagnosis, and (3) multivariate statistical techniques.

1) In the area of the aluminium smelting process, understanding the variability pattern within an alumina feeding cycle throughout normal and abnormal events could lead to a breakthrough in fault detection and diagnosis. The changing patterns within normal and abnormal cycles are illustrated in Chapter 2 using real data in Figure 2.9 and Figure 2.10. Since, in this study, continuous alumina feeding cycles have been formed from the adopted strategy for alumina feeding of many smelters, the use of the variability pattern within these cycles to develop a fault detection and diagnosis system has been recommended (**Chapter 2**).
2) In the area of fault detection and diagnosis, extracting the key elements of systems that have been applied in detecting and diagnosing faults in the aluminium smelting process, could help in the comparison of the various elements of the systems. A taxonomy for a aluminium process fault detection and diagnosis system (Figure 3.1 in Chapter 3) is proposed based on the extracted key elements which include knowledge, techniques, usage frequency and mode of results (**Chapter 3**).
3) In the area of the multivariate statistical techniques, making a comparison between normal and abnormal patterns within an alumina feeding cycle using MPCA and MPLS methods, could be the ideal approach in using the multivariate statistical technique for fault detection and diagnosis. As shown in Figure 4.18 in Chapter 4, these methods have

superior abilities in terms of analysing variance from more than ten correlated variables, increasing detection efficiency by considering the dynamic component of data, and assisting in finding the causes of large variation. Furthermore, a classification between two main groups that complements a PCA-based detection system for fault diagnosis has been developed. This classification is shown in Figure 4.20 in Chapter 4 where one method from each group has been selected to develop the Cascade fault diagnosis system (**Chapter 4**).

The review of the literature pertaining to these three areas has helped to provide important information for addressing the two research questions:

1) The information found that has assisted in the answering of the first research question is that a fault detection system that considers the dynamic behaviour of the process (the resistance versus alumina concentration curves and the cascade-like pattern) can be developed using MPCA.
2) Information found that has assisted in the answering of the second research question is that a diagnostics system which complements the fault detection system can be developed using pre-identified abnormal regions and DPLS.

This information cited above has been useful in the navigation of the direction of the methodology of this thesis.

9.3. Summary and highlights of the methodology

The methodology applied in this thesis can be applied to other areas that have similar challenges in the controlling of a complex process. The challenges in this thesis are the operation of an aluminium smelter involving hundreds of reduction cells that are monitored simultaneously. Each cell engages with a complex aluminium smelting process that has a strong interrelationship between parameters including heat balance, bath chemistry and

energy balance. Thus, this research is of great interest to chemical engineers. The summary and highlights of the methodology applied in this thesis are described in the steps that follow.

1) Data from industry were processed and analysed

The process data for various time periods were received from the industry. Pre-processing and analysing data using statistical techniques showed that abnormal events could be observed in the data (section 5.1.1 in **Chapter 5**).

2) Knowledge from literature and operational experts was integrated

Based on the proposed fault detection and diagnosis system taxonomy (section 3.1, Chapter 3), knowledge from the literature and operational experts was integrated in terms of knowledge (overfeed-underfeed feeding control), techniques (MPCA/MPLS), usage frequency (continuous) and mode of results (text and graphics) (section 5.1.2 in **Chapter 5**).

3) Pilot studies were run

Two pilot studies were run in order to consider the two factors described in section 5.1.3. The first pilot study was concerned the use of MPCA for monitoring daily data for a number of cells (section 5.2) and the second pilot study concerned the use of MPCA for monitoring continuous data using a moving data window approach (section 5.3) (**Chapter 5**).

4) The new system was designed

The results of taking steps 1-3 revealed and confirmed the necessity for the following key factors: (1) the treatment of the overfeed/underfeed cycle as a batch using MPCA/MPLS, and (2) the incorporation of the behaviour of the aluminium reduction cell during anode changing. These factors led to the development of a new framework, Cascade fault detection and diagnosis for the aluminium smelting process (section 5.4 in **Chapter 5**).

5) Cascade fault detection was developed and evaluated

The system is based on six variables which are automatically measured and have an automatic control mode. The variables are related to resistance versus alumina concentration

curves that are typically used in the adopted strategy for alumina feeding control in many aluminium smelters. The task in this section was to arrange real data obtained from industry in a 3-D data array where the third dimension is number of feeding cycles. Also, multiple models were designed, using aluminium smelting data, to be developed based on the cascade-like pattern occurring during anode changing. Each step was addressed in the development of the system including the selection of process variables that have a high level of automation and knowledge, and aligning trajectories for the feeding cycles using two approaches. During the evaluation of the system using real data, the trajectory alignment using well defined alumina feeding cycles was shown to be an improvement on the use of artificially lengthened feeding cycles. The Cascade fault detection system was also compared with a one-time-instant approach and the proposed system was shown to be more effective in detecting faults (**Chapter 6**).

6) Abnormal patterns for some faults were extracted

During the evaluation of the fault detection system, KDD was used to differentiate abnormal patterns from real faults. These were: (1) a systematic pattern for an anode spike, (2) a 'large upward trend' for prediction of an anode effect, (3) an 'earlier upward trend during underfeeding' for low alumina dissolution and (4), an 'upward shift during overfeeding and underfeeding' for the occurrence of a blocked feeder (**Chapter 6**).

7) Cascade fault diagnosis was developed and evaluated

The abnormal patterns discovered were utilized in this part where abnormal data were also arranged in a 3-D data array in order to capture the variability patterns within an alumina feeding cycle. The modules for fault diagnosis were divided into two hierarchal modules so that simple faults could be diagnosed first using a pre-identified problem area approach. The boundaries for this problem area were identified in this thesis. Then, the more complex faults, or faults that had been misdiagnosed, were further diagnosed by DPLS. This system was

evaluated using real case studies and the results showed that this system was capable of diagnosing faults based on the identified abnormal patterns within an alumina feeding cycle (**Chapter 7**).

8) Functions of fault detection and diagnosis were integrated and simulated

After the separate development of a fault detection system and diagnosis, the functions of detection and diagnosis were integrated using MATLAB. The reason for this was to combine both different systems to make a complete unified real-time monitoring system which was called a Cascade Fault Detection and Diagnosis System. Through integration using a tight-coupling methodology, both the detection and diagnosis systems could interact effectively because of the high runtime performance. The difficulties in integrating both systems were solved by using subsystems based on the same approach as the data driven approaches. The integrated system was then simulated using real case studies (**Chapter 8**).

In this thesis, all the steps described in the methodology were taken to subsequently provide an answer to the main research question: The system presented in this thesis, based on the multivariate statistical techniques, PCA and PLS, effectively detects and diagnoses faults in the aluminium smelting process. The specific contributions of this thesis are described in the following section.

9.4. Research contributions

Designing, developing and evaluating a new multivariate Cascade fault detection and diagnosis system is an original contribution to the field of process control in the area of the aluminium smelting process. Five different aspects of this contribution are explained further below:

1) A new framework for fault detection has been developed and applied to the aluminium smelting data. This thesis contributes to the field of MPCA-based fault detection by

adding a new application to the previous work which was the treatment of a continuous process as a batch operation. Multiple fault models have been developed for both fault detection and systems diagnosis in order to address the dynamic behaviour of the process during anode changing. Furthermore, a new way to align the trajectory of an alumina feeding cycle has also been proposed by the use of well defined alumina feeding cycles. A pre-processing strategy to be employed prior to data training has also been developed. With this strategy, the proposed system can be used to monitor cells in the future with a minimum risk of compatibility problems. The development and evaluation of the new Cascade multivariate system has been published in this journal article: Abd Majid, N. A., et al. Multivariate statistical monitoring of the aluminium smelting process. *Computers and Chemical Engineering* (2011), doi:10.1016/j.compchemeng.2011.03.001.

2) A set of abnormal patterns has been discovered using the KDD approach. This set of patterns can be used as a future reference for detecting faults using other methods. These extracted patterns have also been discussed in the above-mentioned Computers and Chemical Engineering Journal.
3) A new framework for fault diagnosis has been developed and applied to the aluminium smelting data where an alumina feeding cycle was also treated as a batch operation using MPCA and MPLS. Part of this work, particularly on the use of the pre-identified abnormal area approach using MPCA as the fault diagnosis tool, has been published in this journal article: Abd Majid, N. A., Young, B., Taylor, M. P., Chen, J. J. J., Stam, M. A. & Mulder, A. (2011) Aluminium Process Fault Detection by Multiway Principal Component Analysis. *Control Engineering Practice*, 19, 367-379. Furthermore, research related to the use of DPLS and MPCA for fault diagnosis has been submitted to this journal article: Nazatul Aini Abd Majid, Mark P. Taylor, John J.J. Chen, Wei Yu & Brent

R. Young, Diagnosing faults in aluminium processing by using multivariate statistical approaches, *Journal of Materials Science* (2011).

4) Arising from the literature review, a taxonomy of fault detection and diagnosis has been developed. This taxonomy contributes to the field of process control of the aluminium smelting process where fault detection and diagnosis systems were classified according to their knowledge and abilities. A conference paper describing this taxonomy is: Abd Majid, N. A., Young, B., Taylor, M. P., Chen, J. J. J., (2011), *A Taxonomy of aluminium fault detection and diagnosis*, 10th Australasian Aluminium Smelting Technology Conference (to be submitted).

5) The application of PCA for monitoring daily data has been demonstrated because prior to designing the new system, a series of pilot studies had been run. Selected results of the pilot studies were published in the conference papers in the year of 2008:

   - ABD MAJID, N. A., YOUNG, B., TAYLOR, M. P. & CHEN, J. J. J. (2008a) PCA-based Process Monitoring and Fault Diagnosis for Aluminium Processing, *Proceedings of International Conference on Mechanical & Manufacturing Engineering (ICME2008)*, 21– 23 May 2008, Johor Bahru, Malaysia, IE_ID_0025
   - ABD MAJID, N. A., YOUNG, B. R., TAYLOR, M. P. & CHEN, J. J. J. (2008b) Real-time Process Monitoring and Fault Diagnosis for Aluminium Processing by Principal Component Analysis. *Foundations of Computer-Aided Process Operations (FOCAPO): Multi-Scale Integration of R&D, Manufacturing, and Optimization for Enterprise-Wide Operations*, June 29-July 2, Boston, USA.

   Furthermore, a series of pilot studies have also been run for investigating the use of PCA in diagnosing faults through pre-identified abnormal regions. Selected results were published in the following conference papers:

   - ABD MAJID, N. A., YOUNG, B., TAYLOR, M. P. & CHEN, J. J. J. (2009a) Detecting abnormalities in aluminium reduction cells based on process events using multi-way principal component analysis (MPCA). *Light Metals 2009*, *TMS (The Minerals, Metals and Materials Society)*, 589-593.
   - ABD MAJID, N. A., YOUNG, B., TAYLOR, M. P. & CHEN, J. J. J. (2009b) Principal component analysis (PCA) application for early detection of faults in

aluminium processing. *The 8th World Congress of Chemical Engineering (WCCE8),* August 23 - August 27, Montreal, Canada.

- ABD MAJID, N. A., YOUNG, B. R., TAYLOR, M. P. & CHEN, J. J. J. (2009c) Real-time system for monitoring aluminium reduction cells by using MPCA and dynamic Euclidean distances. *The 7th IEEE International Conference on Control & Automation (ICCA'09)*, December 9-December 11, Christchurch, New Zealand.
- ABD MAJID, N. A., YOUNG, B. R., TAYLOR, M. P. & CHEN, J. J. J. (2010) Fault diagnosis for the aluminum electrolysis process using principal component analysis and partial least square. *The 5th International Symposium on Design, Operation and Control of Chemical Processes, PSE ASIA 2010*, July 25- July 28, Singapore.

To our knowledge, this thesis initiated the study of the use of PCA and PLS for monitoring the aluminium smelting process with two conference papers published in the year of 2008. Later in 2009, there was a conference paper written by Tessier et al. (2009) using PCA for process monitoring but this thesis used an extension of PCA, MPCA, for monitoring the aluminium smelting process based on the established curves within an alumina feeding cycle

9.5. Benefits of the research

Six major benefits of the research for the aluminium smelting industry have been identified. They are: 1) better utilization of historically successful cells, 2) early detection of failure events, 3) quick identification/diagnosis of the cause of the failure events, 4) reduction of energy consumption and emission of greenhouse gases, 5) significant savings and 6) no additional cost.

9.5.1. Better utilization of historically successful cells

PCA offers beneficial solutions for the process control of aluminium reduction cells. Using PCA, a vast amount of data collected for each cell for every year can be utilized to form the reference distribution of normal cells for process monitoring. Obtaining reference cells from a vast amount of data in the database is much easier with the use of data-driven approaches.

The information contained in the database for each cell is summarised using MPCA which used a 3-D data array for better data organization. One of the functions of the successful cells is that they provide a mean-trajectory for every process variable. These trajectories can be used to detect future deviation of the data. Furthermore, the information extracted from this historical data is useful for identifying the related patterns or variability of abnormal events inside the cells.

9.5.2. Early detection of failure events

The occurrence of faults such as anode spikes and anode effects was detected by the Cascade monitoring system ahead of the detection time recorded by operators.

Abnormal events can be detected earlier in the process because the movements of the scores being observed are related to a combination of real and predicted data. Therefore, the prediction of the future data could help in detecting the problems that have occurred in the process in real time.

9.5.3. Quick identification/diagnosis of the cause of the failure events

The results from the use of the Cascade diagnostic tool can help the operator to focus immediately on the possible causes. The main contribution of this research is where past failure events in the database of aluminium reduction cells were utilized to provide useful information in terms of the trajectory of the faults for each selected variable. If the causes of the deviation of the process variables are not removed, this will lead to a re-occurrence of an anode effect. Therefore, by searching the cause earlier, inappropriate control action, which drives greater variation, can be prevented. This is one of the breakthrough areas listed by Taylor and Chen (2005) in improving the process control of aluminium reduction cells.

9.5.4. Reduction of energy consumption and emission of greenhouse gases

Energy diversion does occur during anode spikes and anode effects. The reduction of the frequency of these operating abnormalities not only reduces electricity consumption per tonne of aluminium but also improves process efficiency (Tabereaux, 2008). In fact, the reduction of the frequency of anode effects allows an aluminium smelter to attain sustainability by reducing the emission of perfluorocarbons (PFCs) which are harmful greenhouse gases produced during anode effects (Dando, 2003, Tabereaux, 2008). Therefore, the development of a fault diagnosis system that is able to detect anode spikes early in the aluminium smelting process in order to predict anode effects and to find the causes of an anode effect, can result in the reduction of energy consumption and the emission of greenhouse gas.

9.5.5. Significant savings

The system has been shown to detect the occurrence of the anode spike earlier than when detected by an operator. Hence, the system is expected to reduce the negative impacts of spiking problems, such as a reduction in current efficiency and a reduction in cell lifetime. The system has also been shown to detect an anode effect at an earlier time. If this system was implemented in real-time, the root cause of the anode effect could be found earlier in the process by investigating the T^2 and SPE values that have exceeded the control limits prior to the occurrence of the anode effect. The reduction of anode effects would be very beneficial to the smelter since anode effects cause a severe disturbance to the cell and can increase environmental problems. Therefore, based on these advantages, this Cascade fault detection and diagnosis system is expected to bring Aldel significant savings per year in its operating and maintenance costs.

9.5.6. No additional cost

There is no additional cost for implementing the Cascade detection system once the fundamental decision has been taken to build a process control system which focuses on detecting, diagnosing and removing abnormalities from the process – as part of everyday, routine, control. This decision does have a cost because detection with diagnosis and engineered or operational solutions will have to be followed up over time. However, when this is done more frequently, the benefit is increased, and the resulting process is more efficient (M. Taylor, personal communication, July 21, 2010).

In short, all the advantages of control charts based on PCA for monitoring aluminium reduction cells, lead to an improved process monitoring and fault diagnosis system which utilizes information stored in the database for both normal and abnormal aluminium reduction cells. In fact, the ultimate targets of the industry, which are to produce more aluminium with fewer impurities and less usage of energy which, in turn means less cost and better environmental safety, will be likely to be achieved.

9.6. Recommendations for future work

This thesis has opened up a number of possible fields for future work in the following areas:

1) On-line implementation

A future study investigating the on-line implementation of the Cascade fault detection and diagnosis system in an aluminium smelter would be very interesting. Many factors can be explored including: (a) the performance of the system throughout many years and the costs saved; and (b) the acceptance of operators in term of user interface, alarm strategy and data retrieval.

2) Improvement of the fault detection framework

Further research might investigate the integration of other signals (daily frequency data or more frequent data) into the new system. In order to speed the detection of an anode effect, for example, real raw-data (60 msec) values could be used.

3) Improvement of the fault diagnosis framework

A further study could investigate how to act like a learning system by using past experiences of the controlling actions employed for abnormal events that successfully removed the cause of the variation. A user interface could be developed to add a process engineer as an entity to the system so that the process of updating the model to identify new faults would be much easier.

4) Modelling quality variables/ process performance and process data

The same approach that was followed to model **Y**=class of faults to **X**=their process data within a feeding cycle for fault diagnosis may be used to develop a PLS based approach to aid other regression problems such as predicting quality variables, current efficiency and energy.

9.6.1. Limitations

The algorithm developed in this thesis is limited to the aluminium smelting process with a point-feed strategy for point-feed cells. This algorithm would require modification for bar-breaker cells that use demand feed. This algorithm is also limited to alumina smelting processes that have different patterns during anode changing. In this thesis, the pattern was a step increase in voltage, followed by a more gradual downward trend in cell voltage. The model developed for the phase when the downward trend ended can still be used for cells with different operating conditions for anode changing.

9.7. Conclusions

The challenges to the development of a fault detection and diagnosis system for the aluminium smelting process are not insignificant. However, the outcomes of the research which utilized knowledge from a breakthrough area (overfeed and underfeed strategy) using advanced statistical monitoring tools, MPCA and MPLS, in a Cascade environment that can continuously monitor the data in real-time and is easy to understand by operators, has produced a new fault detection and diagnosis system in the aluminium smelting process. This Cascade fault detection and diagnosis system will contribute to an aluminium smelting plant to operate at full capacity at its optimal productivity and energy efficiency levels.

REFERENCES

ABAFFY, C., AIQUEL, R., LAREZ, J. & GONZALEZ, J. (2006) CVG Venalum potline supervisory system. *Light Metals 2006***,** 301-305.

AGALGAONKAR, A. P., MUTTAQI, K. M. & PERERA, S. (2009) Open Loop Response Characterisation of an Aluminium Smelting Plant for Short Time Interval Feeding. *Power & Energy Society General Meeting, 2009. PES '09. IEEE* Calgary, AB.

AGUANDO, D. & ROSEN, C. (2008) Multivariate Statistical Monitoring of Continuous Wastewater Treatment Plants. *Engineering Applications of Artifial Intelligence,* 21**,** 1080-1091.

ANDREWS, R., DIEDERICH, J. & TICKLE, A. B. (1996) A survey and critique of techniques for extracting rules from trained artificial neural networks. *Knowledge-Based Systems* 8**,** 373–389.

BANTA, L., DAI, C. & BIEDLER, P. (2003) Noise classification in the aluminium reduction process. *Light Metal 2003***,** 431-435.

BEARNE, G. P. (1999) The Development of Aluminum Reduction Cell Process Control. *Aluminum Smelting (JOM)***,** 16-22.

BEREZIN, A. I., POLYAKOV, P. V., RODNOV, O. O., YASINSKI, V. L. & STONT, P. D. (2005) FMFA-Based expert system for electrolysis diagnosis. *Light Metals 2005***,** 429-434.

BOX, E. P. G., COLEMAN, E. D. & BAXLEY JR., R. V. (1997) A comparison of statistical process control and engineering process control. *Journal of Quality Technology,* 29**,** 128-130.

BRISK, M. (2005) Process control, advancing or retreating? *TCE,* July**,** 38-39.

CHEN, G. & MCAVOY, T. J. (1998) Predictive on-line monitoring of continuous processes. *Journal of Process Control,* 8**,** 409-420.

CHEN, J. J. J. (2008) Molten metal processing-aluminium smelting technology. Chemical and material engineering, University of Auckland (course notes).

CHEN, J. J. J. & TAYLOR, M. P. (2005) Control of temperature and aluminum fluoride in aluminum reduction. *Aluminium,* 81**,** 678-682.

CHIANG, H. L., RUSSELL, L. E. & BRAATZ, D. R. (2000) Fault Diagnosis in Chemical Processes using Fisher discriminant analysis, Discriminant Partial Least Squares, and Principal Component Analysis. *Chemometrics and Intelligent Laboratory Systems,* 50**,** 243-252.

CHIANG, H. L., RUSSELL, L. E. & BRAATZ, D. R. (2001) *Fault Detection and Diagnosis in Industrial Systems,* London, Great Britain, Springer.

CHO, H.-W. & KIM, K.-J. (2004) Fault diagnosis of batch processes using discriminant model. *International Journal of Production Research,* 42**,** 597 – 612.

DANDO, R. N. (2003) In-Plant PFC Monitoring: Technology Options And Performance Concerns. *Light Metals 2003* 205-210.

DASHA, S. & VENKATASUBRAMANIAN, V. (2000) Challenges in the industrial applications of fault diagnostic systems *Computers & Chemical Engineering,* 24**,** 785-791

DONG, D. & MCAVOY, T. J. (1996) Nonlinear principal component analysis--Based on principal curves and neural networks. *Computers & Chemical Engineering,* 20**,** 65-78.

DUCHESNE, C., KOURTI, T. & MACGREGOR, J. F. (2002) Multivariate SPC for startups and grade transitions. *AIChE Journal,* 48**,** 2890-2901.

DUFFUAA, S. O., KHURSHEED, S. N. & NOMAN, S. M. (2004) Integrating statistical process control,engineering process control and Taguchi's quality engineering. *International Journal of Production Research,* 42**,** 4109-4118.

FAYYAD, U. M., PIATETSKY-SHAPIRO, G., SMYTH, P. & UTHURUSAMY, R. (1996) *Advances in knowledge discovery and data mining*, American Association for Artificial Intelligence.

GADD, M. D. (2003) Aluminium smelter cell energy flow monitoring. *Chemical and Materials Engineering.* Auckland, The University of Auckland (MA-thesis).

GERTLER, J. J. (1998) *Fault detection and diagnosis in engineering systems*, Marcel Dekker, Inc, USA.

GRJOTHEIM, K. & WELCH, B. J. (1988) *Aluminium Smelter Technology*, Dusseldorf: Aluminium-Verlag.

GUH, R. S. (1999) On-line statistical process control : a hybrid intelligent approach. University of Nottingham (PhD-thesis).

HARRIS, D., GAO, Y., TAYLOR, M., CHEN, J. & HAUTUS, M. (2009) Operational Decision Making in Aluminium Smelters. *Engineering Psychology and Cognitive Ergonomics*. Springer Berlin / Heidelberg.

HEIME, A. & ESSER, K. (2001) Process control of aluminium reduction cells-a contribution to future developments. *European Metallurgical Conference EMC 2001,* 3**,** 213-220.

HESTETUN, K., HOVD, M. & PANTELIDES, W. M. A. C. (2006) Detection of abnormal alumina feed rate in aluminium electrolysis cells using state and parameter estimation. *Computer Aided Chemical Engineering,* Volume 21**,** 1557-1562.

HOLBREY, R. (2006) Dimension Reduction Algorithm for Data Mining and Visualization http://www.comp.leeds.ac.uk/richardh/astro/index.html.

HYLAND, M. M., PATTERSON, E. C., STEVENS-MCFADDEN, F. & WELCH, B. J. (2001) Aluminium fluoride consumption and control in smelting cells. *Scandinavian journal of metallurgy,* 30**,** 404-414.

JACKSON, J. E. (2003) *A user's guide to principal components,* New York, Wiley.

JANIKIRAM, M. & KEATS, B. (1998) Combining SPC & EPC in hybrid Industry. *Journal of Quality Technology,* 30**,** 189-200.

JIJI, R. D., HAMMOND, M. H., WILLIAMS, F. W. & ROSE-PEHRSSON, S. L. (2003) Multivariate statistical process control for continuous monitoring of networked early warning fire detection (EWFD) systems. *Sensors and Actuators B: Chemical,* 93**,** 107-116.

JOLLIFFE, P. (1986) *Principal component analysis,* New York, Springer-Verlag.

KANO, M. & NAKAGAWA, Y. (2006) Recent developments and industrial applications of data-based process monitoring and process control *Computer Aided Chemical Engineering,* 21**,** 57-62.

KASSIDAS, A., MACGREGOR, J. F. & TAYLOR, P. A. (1998) Synchronization of batch trajectories using dynamic time warping. *AIChE J.,* 44**,** 864-875.

KOURTI, T. (2002) Process analysis and abnormal situation detection: from theory to practice. *IEEE Control Systems Magazine***,** 10- 25.

KOURTI, T. (2003) Abnormal situation detection, three-way data and projection methods; robust data archiving and modeling for industrial applications. *Annual Reviews in Control,* 27**,** 131-139.

KOURTI, T. (2005) Application of latent variable methods to process control and multivariate statistical process control in industry. *International Journal of Adaptive Control and Signal Processing,* 19**,** 213-246.

KOURTI, T., LEE, J. & MACGREGOR, J. F. (1996) Experiences with industrial applications of projection methods for multivariate statistical process control. *Computers & Chemical Engineering,* 20**,** S745-S750.

KRAMER, M. A. (1991) Nonlinear principal component analysis using autoassociative neural networks. *AIChE Journal,* 37**,** 233-243.

KRZANOWSKI, W. J. (1987) Cross-Validation in Principal Component Analysis. *Biometrics,* 43**,** 575-584.

KU, W., STORER, R. H. & GEORGAKIS, C. (1995) Disturbance detection and isolation by dynamic principal component analysis. *Chemometrics and Intelligent Laboratory Systems,* 30**,** 179-196.

LENNOX, B., GOULDING, P. R. & SANDOZ, D. J. (1999) Analysis of multivariate statistical methods for continuous systems. *Computers & Chemical Engineering,* 23**,** S207-S210.

LENNOX, B., MONTAGUE, G. A. & HIDEN, H. G. (2001) Process Monitoring of an Industrial Fed-Batch Fermentation. *Biotechnology and Bioengineering,* 74**,** 125-135.

LU, S. P. (2002) Control and supervision of the aluminium electrolysis process with expert system *PhD Thesis.* Quebec University (PhD-thesis).

MACGREGOR, J. F. & KOURTI, T. (1995) Statistical process control of multivariate processes. *Control Engineering Practice,* 3**,** 403-414.

MACGREGOR, J. F., YU, H., GARCÍA MUÑOZ, S. & FLORES-CERRILLO, J. (2005) Data-based latent variable methods for process analysis, monitoring and control. *Computers & Chemical Engineering,* 29**,** 1217-1223.

MAURYAA, M. R., RENGASWAMY, R. & VENKATASUBRAMANIANA, V. (2004) Application of signed digraphs-based analysis for fault diagnosis of chemical process flowsheets *Engineering Applications of Artificial Intelligence* 17**,** 501-518.

MEGHLAOUI, A., THIBAULT, J., BUI, R. T., TIKASZ, L. & SANTERRE, R. (1998) Neural networks for the identification of the aluminium electrolysis process. *Computers & Chemical Engineering,* 22**,** 1419-1428.

MILETIC, I., QUINN, S., DUDZIC, M., VACULIK, V. & CHAMPAGNE, M. (2004) An industrial perspective on implementing on-line applications of multivariate statistics. *Journal of Process Control* 14**,** 821-836.

MONTGOMERY, D. C. (2005) *Introduction to Statistical Quality Control,* New York, NY, John Wiley & Sons.

MOORE & URATA, N. (2001) Multivariable Control of Aluminum Reduction Cells. *Light Metals 2001***,** 1243-1250.

NAGEM, N. F., DA FONSECA NETO, J. V. & BRAGA, C. A. (2009) Pattern Identification for Feed Control Strategy Using Fuzzy Neural Algorithm. *UKSIM '09. 11th International Conference on Computer Modelling and Simulation, 2009.*

NOMIKOS, P. & MACGREGOR, J. F. (1995a) Multi-way partial least squares in monitoring batch processes. *Chemometrics and Intelligent Laboratory Systems,* 30**,** 97-108.

NOMIKOS, P. & MACGREGOR, J. F. (1995b) Multivariate SPC Charts for Monitoring Batch Processes. *Technometrics,* 37**,** 41-59.

NOMIKOS, R. & MACGREGOR, J. F. (1994) Monitoring of batch processes using multi-way PCA. *AICheJ,* 40**,** 1361-1375.

PLETCHER, D. & WALSH, F. C. (1990) *Industrial Electrochemistry*, Chapman and Hall, New York, USA.

RAICH, A. & CINAR, A. (1996) Statistical process monitoring and disturbance diagnosis in multivariable continuous processes. *American Institute of Chemical Engineering Journal,* 42**,** 995–1009.

RENBIJUN, ZHAOWENDONG, DAISONGLING & CHENSHICHANG (2007) Research of fuzzy control for alumina in Henan HongKong Longquan Aluminium CO.LTD., China. *Light Metals 2007***,** 439-442.

ROLLAND, W. K., STEINSNES, A., LARSEN, A. S. & PAULSEN, K. A. (1991) Haldris-an expert system for process control and supervision of aluminium smelters. *Light Metals***,** 437-443.

ROMAGNOLI, J. A. & PALAZOGLU, A. (2006) *Introduction to Process Control*, CRC Press, Taylor & Francis Group.

SEGATZ, M. (2001) Process Control in Smelters. *Centre for electrochemistry and mineral processing certificate in aluminium smelting technology.* (course notes).

STAM, M. A., TAYLOR, M. P., CHEN, J. J. J. & DELLEN, S. V. (2007) Operational and Control Improvements in Reductions Lines at Aluminium Delfzijl. *Light Metals 2007* 1-5.

STAM, M. A., TAYLOR, M. P., CHEN, J. J. J., MULDER, A. & RODRIGO, R. (2008) Common Behaviour and Abnormalities in Aluminium Reduction Cells. *Light Metals 2008***,** 589-593

STEVENS MCFADDEN, F., BEARNE, G. P., AUSTIN, P. C. & WELCH, B. J. (2001) Application of advanced process control to aluminium reduction cells - a review. *Light Metal 2001***,** 1233-1242.

STEVENS MCFADDEN, F. J. (2005) The Multivariable Model-Based Control of the Non-Alumina Electrolyte Variables in Aluminum Smelting Cells. Chemical and Materials Engineering, The University of Auckland (PhD-thesis).

TABEREAUX, A. (2008) How to Achieve Sustainability by Reducing the Emission of PFCs at Aluminum Smelters. *LIGHT METAL AGE,* April**,** 30-40.

TAYLOR, M. P. (1997) Challenges in optimising and controlling the electrolyte in aluminium smelters. *Molten Slags, Fluxes and Salts '97 Conference.* Proceedings Molten Slags, Fluxes and Salts.

TAYLOR, M. P. & CHEN, J. J. J. (2005) Advances in Process Control for aluminum smelters. *Conference Plenary.* Bahrain.

TAYLOR, M. P. & CHEN, J. J. J. (2006) Smelting Operations and Technology Course. Auckland, University of Auckland, New Zealand (course notes).

TAYLOR, M. P. & CHEN, J. J. J. (2007) Advances in Process Control for aluminum smelters. *Materials and Manufacturing Processes,* 22**,** 947–957.

TESSIER, J., DUCHESNE, C., GAUTHIER, C. & DUFOUR, G. (2008a) Estimation of alumina content of anode cover materials using multivariate image analysis techniques. *Chemical Engineering Science,* 63**,** 1370-1380.

TESSIER, J., DUCHESNE, C., TARCY, G., GAUTHIER, C. & DUFOUR, G. (2010) Increasing Potlife of Hall–Héroult Reduction Cells Through Multivariate On-Line Monitoring of Preheating, Start-Up, and Early Operation. *Metallurgical and Materials Transactions B,* 41**,** 612-624.

TESSIER, J., DUCHESNE, C., TARCY, G. P., GAUTHIER, C. & DUFOUR, G. (2008b) Analysis of a potroom performance drift, from a multivariate point of view. *Light Metals 2008***,** 319-324.

TESSIER, J., ZWIRZ, T. G., TARCY, G. P. & MANZINI, R. A. (2009) Multivariate Statistical Process Monitoring of Reduction Cells. *Light Metals 2009***,** 305-310.

URAIKUL, V., CHAN, C. W. & TONTIWACHWUTHIKUL, P. (2007) Artificial intelligence for monitoring and supervisory control of process systems. *Engineering Applications of Artificial Intelligence*, 20**,** 115–131.

VAJTA, M. & TIKASZ, L. (1987) Adaptive prediction of anodeeffects in aluminium reduction cells. *Selected Papers from the IFAC Symposium. Pergamon.* Oxford, UK.

VEDAM, H. & VENKATASUBRAMANIAN, V. (1999) PCA – SDG based fault diagnosis methods using signed diagraphs for interpretation. *Control Engineering Practice* 7**,** 903-917.

VENKATASUBRAMANIAN, V., RENGASWAMY, R. & KAVURI, N. S. (2003a) A review of process fault detection and diagnosis part II: qualitative models and search strategies. *Computers & Chemical Engineering,* 27**,** 313–326.

VENKATASUBRAMANIAN, V., RENGASWAMY, R., KAVURI, S. N. & YIN, K. (2003b) A review of process fault detection and diagnosis: Part III: Process history based methods. *Computers & Chemical Engineering,* 27**,** 327-346.

VENKATASUBRAMANIAN, V., RENGASWAMY, R., YIN, K. & KAVURI, S. N. (2003c) A review of process fault detection and diagnosis: Part I: Quantitative model-based methods. *Computers & Chemical Engineering,* 27**,** 293-311.

WANG, X. Z. (1999) *Data mining and knowledge discovery for process monitoring and control*, Springer, London.

WESTERN ELECTRIC (1958) *Statistical Quality Control Handbook*, Western Electric Company, New York, NY, USA.

WIKSTRÖMA, C., ALBANOA, C., ERIKSSONA, L., FRIDÉNA, H., JOHANSSONA, E., NORDAHLA, Å., RÄNNARA, S., SANDBERGA, M., KETTANEH-WOLDB, N. & WOLD, S. (1998) Multivariate process and quality monitoring applied to an electrolysis process: Part I. Process supervision with multivariate control charts *Chemometrics and Intelligent Laboratory Systems,* 42**,** 221-231.

WISE, B. M. & GALLAGHER, N. B. (1996) The process chemometrics approach to process monitoring and fault detection. *Journal of Process Control,* 6**,** 329–348.

WOLD, S. (1978) Cross-validatory estimation of the number of components in factor and principal component models. *Technometrics,* 20**,** 397–405.

WOLD, S., SJO¨STRO¨M A, M. & ERIKSSON, L. (2001) PLS-regression: a basic tool of chemometrics. *Chemometrics and Intelligent Laboratory Systems* 58**,** 109–130.

YOON, S. & MACGREGOR, J. F. (2001) Fault diagnosis with multivariate staistical models part I: using steady sate fault signatures. *Journal of Process Control,* 11**,** 387-400.

YURKOV, V., MANN, V., NIKANDROV, K. & TREBUKH, O. (2004) Development of Aluminium Reduction Process Supervisory Control System. *Light Metal 2004***,** 263-267.

ZENG, S. P. & LI, J. L. (2006) Diagnosis system of the anode faults for alumina reduction cell. *Proceedings of the Sixth International Conference on Intelligent Systems Design and Applications (ISDA'06), IEEE.*

ZENG, S. P., LI, J. L. & Ding, L. (2007) Fault Diagnosis System for 350kA Pre-baked Aluminium Reduction Cell based on BP Neural Network. *Light Metals 2007***,** 583-587.

ZENG, S. P. & ZHANG, Q. (2003) A supervision system for aluminium reduction cell. *Light Metals 2003***,** 463-468.

ZHANG, Y. & DUDZIC, M. S. (2006) Industrial application of multivariate SPC to continuous caster start-up operations for breakout prevention. *Control Engineering Practice,* 14**,** 1357-1375.